

28 NOVEMBER 1975

MS C-16078
1-1152

3-8-76
new
LMSC-D462467
NASA CR-
147860

DESIGN, FABRICATION, AND TEST OF A TRACE CONTAMINANT CONTROL SYSTEM

JMK

(NASA-CR-147860) DESIGN, FABRICATION AND
TEST OF A TRACE CONTAMINANT CONTROL SYSTEM
(Lockheed Missiles and Space Co.) 356 p HC
\$10.50 CSCL 06K

N76-31908

Unclassified
G3/54 01745

BIOTECHNOLOGY ORGANIZATION
LOCKHEED MISSILES & SPACE COMPANY, INC.
SUNNYVALE, CALIFORNIA



28 NOVEMBER 1975

LMSC-D462467

**DESIGN, FABRICATION, AND TEST
OF A TRACE CONTAMINANT
CONTROL SYSTEM**

**PREPARED UNDER
CONTRACT NO. NAS-1-11526**

**BIOTECHNOLOGY ORGANIZATION
LOCKHEED MISSILES & SPACE COMPANY, INC.
SUNNYVALE, CALIFORNIA**

LIST OF CONTRIBUTORS

<u>Name</u>	<u>Area of Contribution</u>
<u>IMSC</u>	
T. Olcott	Project Direction
R. Lamparter	Analysis
B. Maine	Mechanical Design
A. Weitzmann	Mechanical Design
R. Luce	Electrical Design
G. Olivier	Reliability/Safety
E. Kawasaki	Analytical Chemistry
O. Masi	Analytical Chemistry
C. Richardi	Test Support
<u>Monsanto</u>	
J. Selle	Isotope Heat Source

NASA TECHNICAL MONITOR
Rex Martin
Crew Systems Division
Johnson Spacecraft Center

TABLE OF CONTENTS

<u>SECTION</u>		<u>PAGE</u>
	SUMMARY	1
1	INTRODUCTION	5
2	DESIGN REQUIREMENTS	8
2.1	CONTAMINANT MODELS	8
2.2	DESIGN CRITERIA	14
3	SYSTEM DEFINITION	24
3.1	COMPUTER ANALYSIS	24
3.1.1	Fixed Bed	34
3.1.2	Regenerable Bed	41
3.1.3	Contaminant Load Model Comparison	52
3.2	SYSTEM DESCRIPTION	54
3.2.1	Fixed Bed	57
3.2.2	Regenerable Bed Fan	57
3.2.3	Regenerable Bed	57
3.2.4	Pre-Sorbent	58
3.2.5	Catalytic Oxidizer	58
3.2.6	Post-Sorbent	60
4	COMPONENT OPTIMIZATION	61
4.1	FIXED CHARCOAL BED	61
4.2	REGENERABLE BED	64
4.2.1	Adsorption Cycle	64
4.2.2	Desorption Cycle	71
4.2.3	Final Regenerable Bed Selection	81
4.3	PRE-SORBENT	83
4.4	CATALYTIC OXIDIZER	86
4.4.1	Thermal Analysis Procedure	87
4.4.2	Thermal Analysis Results and Conclusions	93
4.4.3	Catalytic Oxidizer External Surface Thermal Control	96
4.4.4	Catalytic Oxidizer Pressure Drop	98
4.4.5	Radiation Dose Level	99
4.4.6	Impact of Revised Contaminant Load on the Catalytic Oxidizer Design	101

<u>SECTION</u>		<u>PAGE</u>
4.5	POST-SORBENT	102
4.6	CATALYTIC OXIDIZER AND REGENERABLE BED LINE AND VALVE SIZES	107
5	OPERATIONS ANALYSIS	111
5.1	FIXED CHARCOAL BED	114
5.2	REGENERABLE CHARCOAL BED	115
5.3	PRE AND POST SORBENT BEDS	117
5.4	CATALYST OXIDIZER	117
6	RELIABILITY ANALYSES	121
6.1	FAILURE MODE AND EFFECTS ANALYSIS	121
6.2	SAFETY HAZARD ANALYSIS	133
6.2.1	Cabin Leak to Vacuum	133
6.2.2	Generation of Toxic Gases	134
6.2.3	System High Surface Temperature	134
6.2.4	Radioactive Emissions	135
6.2.5	Flammability	136
6.3	FAULT DETECTION AND ISOLATION ANALYSIS	137
7	DESIGN	143
7.1	DESIGN REQUIREMENTS	143
7.2	DESIGN DESCRIPTION	144
7.2.1	Fixed Bed	154
7.2.2	Regenerable Bed	156
7.2.3	Pre-Sorbent Bed	157
7.2.4	Post-Sorbent Bed	160
7.2.5	Catalytic Oxidizer	160
7.3	COMPONENT DATA SHEETS	169
8	FABRICATION	188
8.1	GENERAL	188
8.2	FIXED BED	188
8.3	REGENERABLE BED	188
8.4	PRE-SORBENT AND POST-SORBENT BEDS	189
8.5	CATALYTIC OXIDIZER	189
9	TESTING	191
9.1	COMPONENT TESTING	191
9.1.1	Fixed Bed, Fan, and Δ P Sensor Test	191
9.1.2	Pre-and Post Sorbent Beds	193
9.1.3	Regenerable Bed Blower and Δ P Sensor Test	193
9.1.4	Catalytic Oxidizer	199

<u>SECTION</u>		<u>PAGE</u>
9.1.5	Regenerable Bed, Isolation Valves, Vacuum Valve and Bleed Valves	207
9.2	INTEGRATED SYSTEM TESTING	215
9.2.1	Apparatus and Procedures	215
9.2.2	Test Results	220
9.2.3	Analysis of Results	286
10	CONTAMINANT VENTING SYSTEM	290
10.1	INVESTIGATION OF NON-VENTING TECHNIQUES	290
10.1.2	Catalyst Poisoning Investigation	291
10.1.3	Post-sorbent Evaluations	296
10.2	VACUUM VENTING ANALYSIS	314
10.2.1	Contaminant Gas Vent Rate	315
10.2.2	Contaminant Gas Exhaust Plume Analysis	327
10.2.3	Contaminant Evaporation Rate	334
10.2.4	Other Vented Materials	335
11	SPACE CONTAMINANT CONTROL SYSTEM CONCEPTUAL DESIGN	338
11.1	CONTAMINANT LOAD MODEL	338
11.2	DESIGN ANALYSIS	341
12	CONCLUSIONS	342

LIST OF FIGURES

<u>FIGURE</u>		<u>PAGE</u>
1	REGENERABLE BED SIZE vs NUMBER OF CONTAMINANTS CONTROLLED	51
2	TRACE CONTAMINANT CONTROL SYSTEM SCHEMATIC	56
3	TRACE CONTAMINANT CONTROL SYSTEM OPERATIONAL MODES	59
4	SORBENT BED PRESSURE LOSS CORRELATION	63
5	WATER ADSORPTION ISOTHERM FOR BARNEBEY CHENEY ACTIVATED CHARCOAL TYPE BD	66
6	REGENERABLE CHARCOAL BED TEMPERATURE EFFECT ON MASS AND WATER LOSS	67
7	REGENERABLE ACTIVATED CHARCOAL OPTIMIZATION	69
8	DESORPTION CYCLE - ANALYSIS SYSTEM SCHEMATICS STUDIED	72
9	DESORPTION TEMPERATURES FOR FIG. 2	76
10	REGENERABLE ACTIVATED CHARCOAL BED - SELECTED CONFIGURATION	77
11	PRE AND POST SORBENT BEDS LiOH CONTAMINANT REMOVAL CHARACTERISTICS	85
12	CATALYTIC OXIDIZER THERMAL CONFIGURATION	88
13	CATALYTIC OXIDIZER SURFACE TEMPERATURE	94
14	CATALYTIC OXIDIZER THERMAL CHARACTERISTICS	95
15	LINE SIZE OPTIMIZATION	110
16	TRACE CONTAMINANT CONTROL SYSTEM INSTRUMENTATION	139
17	MOCKUP - FRONT VIEW	145
18	MOCKUP - REAR VIEW	146
19	MOCKUP - LEFT FACE	147
20	T.C.C.S. FRONT VIEW	149
21	T.C.C.S FRONT VIEW	150
22	T.C.C.S REAR VIEW	151
23	T.C.C.S. REAR VIEW	152
24	T.C.C.S. - VIEW OF LEFT SIDE	153
25	FIXED BED CANISTER	155

<u>FIGURE</u>		<u>PAGE</u>
26	REGENERABLE BED	158
27	PRE-SORBENT BED CANISTER AND MOUNTING BRACKET	159
28	POST-SORBENT BED	161
29	HEAT EXCHANGER	162
30	HEAT EXCHANGER	163
31	CATALYST BED CONTAINER	166
32	CATALYTIC OXIDIZER	167
33	FIXED BED VANE AXIAL FAN AND REGENERABLE BED CENTRIFUGAL BLOWER	176
34	SOLENOID VALVES	179
35	FIXED BED FAN AND REGENERABLE BED BLOWER DIFFERENTIAL PRESSURE SENSORS AND VACUUM LINE PRESSURE SENSOR	185
36	FIXED BED & BLOWER TEST	192
37	FIXED BED & FAN CHARACTERISTICS	194
38	PRE & POST SORBENT BED TESTS	195
39	PRE AND POST-SORBENT CANISTER PRESSURE DROP CHARACTERISTICS	196
40	REGENERABLE BED BLOWER & Δ P SENSOR TEST	197
41	REGENERABLE BED BLOWER PERFORMANCE MFGR.: DYNAMIC AIR ENGRG. CO50 K	198
42	ELECTRICALLY HEATED CATALYTIC OXIDIZER COMPONENT TEST	200
43	CATALYTIC OXIDIZER TEMPS.	204
44	CATALYTIC OXIDIZER METHANE CONVERSION PERFORMANCE	205
45	CATALYTIC OXIDIZER COMPONENT TEST APPARATUS AT MONSANTO - MOUND LAB	206
46	CATALYTIC OXIDIZER COMPONENT TEST APPARATUS AT IMSC WITH THE ISOTOPE HEAT SOURCE	209
47	TESTING OF REGENERABLE BED COMPONENTS	210
48	REGENERABLE BED WITH 14x20 MESH CHARCOAL EXCEPT FOR 1 1/2 INCH LAYER OF 8x14 MESH AT EACH END	212
49	TOLUENE - DAILY CONCENTRATION DATA	225
50	BENZENE - DAILY CONCENTRATION DATA	225

<u>FIGURE</u>		<u>PAGE</u>
51	AMMONIA - DAILY CONCENTRATION DATA	226
52	METHYL ETHYL KETONE - DAILY CONCENTRATION DATA	226
53	METHYL ACETATE - DAILY CONCENTRATION DATA	227
54	FREON 11 - DAILY CONCENTRATION DATA	227
55	ACETONE - DAILY CONCENTRATION DATA	228
56	FREON 12 - DAILY CONCENTRATION DATA	228
57	PROPYLENE - DAILY CONCENTRATION DATA	229
58	PROPANE - DAILY CONCENTRATION DATA	230
59	FREON 22 - DAILY CONCENTRATION DATA	231
60	METHYL ALCOHOL - DAILY CONCENTRATION DATA	232
61	ACETYLENE - DAILY CONCENTRATION DATA	232
62	CARBON MONOXIDE - DAILY CONCENTRATION DATA	233
63	ETHANE - DAILY CONCENTRATION DATA	233
64	ETHYLENE - DAILY CONCENTRATION DATA	234
65	METHANE - DAILY CONCENTRATION DATA	234
66	SULFUR DIOXIDE - DAILY CONCENTRATION DATA	235
67	CABIN METHANE CONCENTRATION COMPLETE CYCLE PERFORMANCE	237
68	CABIN CARBON MONOXIDE CONCENTRATION COMPLETE CYCLE PERFORMANCE	238
69	DAILY HUMIDITY	239
70	DAILY TEMPERATURE	239
71	POTENTIAL PLOT DATA - BARNEBEY CHENEY BD CARBON	258
72	ADSORPTION ZONE LENGTH - BARNEBEY CHENEY BD CARBON AT 1.3 FT/MIN	259
73	EFFECT OF LONG TERM DESORPTION - PROPYLENE CONTROL	279
74	CORRECTED POTENTIAL PLOT - BARNEBEY CHENEY BD CARBON	282
75	CATALYST CANNISTER TEMPERATURE PROFILE	284
76	CATALYTIC OXIDIZER AFTER COMPLETION OF TEST PROGRAM	287
77	INTERIOR OF CATALYTIC OXIDIZER	288
82	CONTAMINANT VENTING - CONSTANT MASS FLUX CONTOURS	330
83	CONTAMINANT VENTING - CONSTANT MACH NO. CONTOURS	331
84	CONTAMINANT VENTING - CONSTANT PRESSURE CONTOURS	332
85	CONTAMINANT VENTING - CONSTANT HEATING CONTOURS	333
86	VAPOR PRESSURES	336
87	SPACELAB TRACE CONTAMINANT CONTROL SYSTEM LAYOUT	339

LIST OF TABLES

<u>TABLE</u>		<u>PAGE</u>
1	MAXIMUM CONCENTRATION AND PRODUCTION RATE OF TRACE CONTAMINANTS	9
2	MAXIMUM ALLOWABLE CONCENTRATIONS AND PRODUCTION RATES OF AIRBORNE TRACE CONTAMINANTS	12
3	SYSTEM DESIGN CRITERIA	23
4	SYSTEM PERFORMANCE SUMMARY	25
5	FIXED SORBENT BED - SHORT TERM COMPUTER ANALYSIS RESULTS	35
6	FIXED SORBENT BED - LONG TERM COMPUTER ANALYSIS RESULTS	38
7	REGENERABLE SORBENT BED - SHORT TERM COMPUTER ANALYSIS RESULTS	42
8	REGENERABLE SORBENT BED - LONG TERM COMPUTER ANALYSIS RESULTS	47
9	POTENTIAL SOURCES OF CONTAMINANTS REQUIRING EXCESSIVE CHARCOAL FOR CONTROL	53
10	SYSTEM CONFIGURATION COMPARISON BETWEEN CONTAMINANT LOAD MODELS	55
11	VARIATION IN FIXED BED PARAMETERS WITH DIAMETER	62
12	INFLUENCE OF BED DIAMETER ON DESIGN PARAMETERS	71
13	ASSUMPTIONS AND REQUIREMENTS FOR REGENERABLE CHARCOAL BED ANALYSIS	82
14	FINAL SELECTED REGENERABLE BED CONFIGURATION	81
15	CONTAMINANTS REMOVED BY THE PRE-SORBENT BED	83
16	PRE-SORBENT CANISTER PRESSURE LOSS CHARACTERISTICS	86
17	PRESSURE DROP LOSSES WITHIN THE CATALYTIC OXIDIZER	100
18	CONTAMINANTS YIELDING TOXIC MATERIALS IN A CATALYTIC OXIDIZER AND POST-SORBENT REQUIREMENTS	103
19	POST-SORBENT CANISTER PRESSURE LOSS CHARACTERISTICS	106
20	FIXED BED CONTAMINANTS REQUIRING MORE THAN 4 CFM FLOW	114
21	REGENERABLE BED CONTAMINANTS REQUIRING GREATER THAN 0.5 CFM	116

<u>TABLE</u>		<u>PAGE</u>
22	CATALYTIC OXIDIZER AVAILABLE ENERGY FROM COMBUSTION	118
23	FAILURE MODE AND EFFECTS ANALYSIS	123
24	SYSTEM COMPONENTS AND INSTRUMENTATION	138
25	FAULT DETECTION SUMMARY	141
26	CATALYTIC OXIDIZER COMPONENT TEST RESULTS WITH ELECTRIC HEATER AT IMSC	
27	CATALYTIC OXIDIZER COMPONENT TEST RESULTS WITH ELECTRIC HEATER AND ISOTOPE HEAT SOURCES AT MONSANTO-MOUND LAB	203
28	GAMMA & NEUTRON LEVELS AT VARIOUS LOCATIONS FROM THE CATALYTIC OXIDIZER	208
29	REGENERABLE BED DESORPTION CHARACTERISTICS	214
30	CONTAMINANTS USED IN THE SYSTEM LEVEL TEST	216
31	ANALYTICAL TECHNIQUES USED	219
32	GAS CHROMATOGRAPH OPERATIONAL PARAMETERS	221
33	TRACE CONTAMINANT CONTROL SYSTEM DESIGN VERIFICATION TESTS SIGNIFICANT EVENTS	222
34	LOCATION OF DATA BY CONTAMINANT	224
35	COMPARISON OF CALCULATED AND EXPERIMENTAL CONTAMINANT EQUILIBRIUM LEVELS	240
36	POST SORBENT BED PERFORMANCE DATA FOR HYDROGEN CHLORIDE AND HYDROGEN FLUORIDE	249
37	IDENTIFICATION BY INFRARED SPECTROPHOTOMETRIC, MASS SPECTROMETRIC AND OTHER ANALYSES METHODS OF CONTAMINANTS SPECIES OTHER THAN THOSE ROUTINELY ANALYZED	251
38	IDENTIFICATION BY MASS SPECTROMETRY OF OTHER CONTAMINANTS BESIDES THOSE KNOWN TO BE INTRODUCED INTO THE SYSTEM	254
39	CONTAMINANTS UNIDENTIFIED ON GAS CHROMATOGRAMS OBTAINED FROM ROUTINE ANALYSIS OF MAJOR TRACE CONTAMINANTS INTRODUCED INTO THE SYSTEM	255
40	FIXED BED TIME TO BREAKTHROUGH (DAYS) CALCULATED VS TIME RESULTS	265
41	SHORT TERM RATE CALCULATIONS	267
42	LONG TERM RATE CALCULATIONS	269
43	REGENERABLE BED - COMPARISON OF COMPUTED RESULTS	274
44	VARIATION IN REGENERABLE BED REMOVAL EFFICIENCY WITH CYCLE TIME	277
45	CATALYTIC OXIDIZER REMOVAL EFFICIENCY	281

<u>TABLE</u>		<u>PAGE</u>
46	CATALYST POISONING TEST CONDITIONS	291
47	POST-SORBENT BED TESTING	297
48	CATALYST EVALUATIONS - SIGNIFICANT EVENTS	298
49	CHEMICAL ANALYSIS RESULTS - BED 1	300
50	CHEMICAL ANALYSIS RESULTS - BED 1 AND 2	301
51	BED 3 - CHLORIDE DATA (mg/m ³)	303
52	BACKGROUND CONTAMINANT DATA OXIDIZER OUTLET	305
53	SUMMARY OF CHLORIDE AND FLUORIDE DATA	306
54	BED 5 - SUMMARY OF CHLORIDE AND FLUORIDE DATA	308
55	BED 6 - SUMMARY OF SO ₂ DATA	309
56	BED 6 - SUMMARY OF CHLORIDE DATA	311
57	CONTAMINANT INPUT DATA	323
58	SATURATED ZONE MASS (SUM) OUTPUT SUMMARY	325
59	VAPOR PRESSURE CONSTANTS	326
60	180 DAY TEST SYSTEM DESORPTION ANALYSIS	328
61	CONTAMINANT GAS FLOW RATES	329
62	CONTAMINANT EVAPORATION RATE	334
63	SPACE CONTAMINANT CONTROL SYSTEM/SUMMARY DATA	340

DESIGN FABRICATION AND TEST OF A
TRACE CONTAMINANT CONTROL SYSTEM

By Thomas M. Olcott
Bioengineering
Lockheed Missiles & Space Co.

SUMMARY

A program was conducted which resulted in the design, fabrication and experimental evaluation of a trace contaminant control system to determine suitability of the system concept for application to future manned spacecraft. The system was designed utilizing methodology developed during previous phases of this technology development effort. The results of this program have served to validate and refine this methodology.

During the course of the program two different contaminant models were considered. The load model initially required by the contract was based on the Space Station Prototype (SSP) general specification SVSK HS4655. Other performance and design criteria were also based on the requirements of this specification. The contaminant load model presented in this specification was an adaptation, reflecting a change from a 9 man crew to a 6 man crew, of the model developed in previous phases of this effort and reported in NASA CR 66346. Trade studies and a system preliminary design were accomplished based on this contaminant load. The trade study and preliminary design tasks included computer analyses to define the optimum system configuration in terms of component arrangements, flow rates and component sizing. These computer analyses were conducted utilizing a computer program developed during previous phases of the contaminant control system development effort.

Subsequent to the system definition task analyses of individual components were conducted to optimize component configuration. These component analyses were conducted for all of the major system elements including valves and plumbing. In addition to the performance analyses, reliability analyses were conducted which included a failure mode and effects analysis, a safety hazards analysis, and a fault detection and isolation analysis. These analyses supported the system design activities including selection of instrumentation and control techniques. The preliminary design was documented in a trade study and preliminary design report.

At the completion of the preliminary design effort a revised contaminant load model was developed by NASA for the SSP program. Additional analyses were then conducted to define the impact of this new contaminant load model on the system configuration. This new model is reproduced as Table 2 of this report. To assess the impact of the new contaminant load model, additional computer analyses were conducted to define system flowrates and component sizing. The component designs were not reoptimized; however, new component configurations were defined based on the trends established in the previous optimization. These trends related to maintaining L/D ratios and component pressure drops. This approach was considered entirely valid since no major change in component sizing occurred as a result of the revised contaminant load. Included in the preliminary design effort was the fabrication of a full scale foam-core mock-up with the appropriate SSP system interfaces. This mock-up included the IMSC developed Trace Contaminant Control System and the Emergency Carbon Dioxide Removal System; and the Mass Spectrometer and the Data Acquisition Unit that were planned to be included in the contaminant control module of the SSP system.

The full scale mock-up served to facilitate system layout, augment integration progress reviews, and demonstrate the system maintainability concept. The mock-up was documented photographically.

At the completion of the preliminary design effort detailed design of the system was carried out. The system was designed to utilize either radioisotope heat sources or electrical heaters to provide thermal energy for the catalytic

oxidizer. The system was designed in accordance with the Design Criteria Handbook SSP document No. 9 and the SSP general specification SVSK HS 4655.

Fabrication of the system was accomplished in the IMSC research shop and at selected vendors. All structure and canisters were fabricated at IMSC with the exception of the catalytic oxidizer heat exchanger and catalyst canister. All solenoid valves were specially fabricated to meet the design requirements by various valve suppliers. The electronics assembly and wiring was conducted in the IMSC electronics shop. Circuit board wiring was accomplished with a wire wrap process. All other system components were purchased parts.

At the conclusion of the component fabrication phase, checkout and performance tests were conducted on the individual system components. The component level tests were conducted on the catalytic oxidizer, regenerable bed, fixed bed, pre and post-sorbent beds, electronics and instrumentation. The catalytic oxidizer testing was conducted at IMSC with electrical heaters, then at the AEC with both electrical and isotope heaters. Thermal, pressure drop, radiation dose level, and contaminant removal performance was determined during these tests. The regenerable bed was tested to establish thermal, vacuum desorption, pressure drop and contaminant removal characteristics. The fixed bed and pre- and post-sorbent beds were all tested to establish pressure drop characteristics. All electrical equipment was checked out and all instrumentation calibrated. After component performance was verified the system was assembled and system level testing was initiated.

During the system level testing the contaminant removal system was operated for a period of approximately 240 days with a simulated contaminant load designed to stress each of the system components. Isotope heaters were used in the catalytic oxidizer during the first 190 days of testing. During the final phase of testing electric heaters were utilized in the catalytic oxidizer to gain experience on this mode of operation. The system operated continuously and satisfactorily throughout the design verification test period with only two equipment malfunctions. These were failures of solid state relays that were easily replaceable. The system maintained the contaminant levels well

below the maximum allowable concentration throughout the test period with the exception of carbon monoxide and methyl alcohol which only slightly exceeded the allowable level during the initial two week high rate period.

After the completion of the design verification test an additional study was undertaken to more precisely define the need for and risks involved with venting contaminants to space from the regenerable charcoal bed. This task involved additional testing to ascertain whether the catalytic oxidizer could function without poisoning with the regenerable charcoal bed not providing upstream protection and whether a suitable post-sorbent existed that would control the undesirable products of oxidation that would be generated by allowing the contaminants normally removed by the regenerable bed to enter the catalytic oxidizer. These tests were conducted continuously over a period of approximately one year. During this period the catalyst temperature was elevated to approximately 867 K (1100 F). Compounds containing halogens, sulphur and nitrogen were continuously introduced into the oxidizer. Catalyst activity as measured by methane removal efficiency was maintained through the test period. The potential catalyst poisons being introduced were also oxidized. Several candidate post-sorbent materials were evaluated during the test period including lithium hydroxide, base-treated charcoal and Purafil. The results indicated that a composite sorbent could be effectively utilized to control undesirable products of oxidation. In addition to the laboratory investigation of non venting techniques, analytical studies were conducted to assess the impact of venting. A computer program was developed which defined the rate of contaminant evolution during the desorption process as well as the dispersion characteristic on the vehicle wall. The conclusion of this study indicated that contaminant venting by the regenerable bed would not present a contamination problem to critical spacecraft surfaces.

The final task conducted during the program was a conceptual design of a contaminant control system suitable for use in Spacelab. Since insufficient data existed from which an assessment of a new contaminant load model could be made, the design was developed parametrically based on various fractions of the SSP load model.

Section 1
INTRODUCTION

The development of a system design for trace contaminant control for long duration manned spacecraft missions was initiated in 1966 under Contract NAS 1-6256. That contract with Lockheed Missiles and Space Company (IMSC), with TRW Systems as a major subcontractor, and NASA resulted in engineering layout drawings of the selected design approach and the long-term testing of a model system. The results of this effort are described in NASA CR 66346, NASA CR 66347 and NASA CR 66497. The tasks accomplished under NAS 1-6256 included the following:

- o Mission definition
- o Contaminant load definition
- o Isotope selection
- o Catalyst selection
- o Catalyst performance tests
- o Analysis and optimization
- o Design layout drawings
- o Development plan

Following the above effort the trace contaminant system development was continued under Contract NAS 1-7433 with TRW Systems a major subcontractor to IMSC. This phase dealt with the development of the isotope-heated catalytic oxidizer system including detailed design of a resistively heated simulated isotope, and development and detailed design of pre- and post-sorbent beds. The tasks involved in this program were:

- o Contaminant load definition for a pre- and post-sorbent bed
- o Design and fabrication of a model pre-sorbent bed
- o Long term sorbent bed evaluation
- o Design and fabrication of a model post-sorbent bed

- o Detailed design of full scale pre- and post-sorbent beds
- o Specifications for the isotope heat source materials of construction
- o Joining and fabrication tests on the isotope heat source materials of construction
- o Fabrication and evaluation of the test heater to be used in the simulated isotope heat source
- o Compatibility tests to determine the extent of interdiffusion between the graphite re-entry aid and the noble metal cladding
- o Fabrication and evaluation of the thermal insulation to be used in the isotope-heated catalytic oxidizer
- o Detailed design of the isotope-heated catalytic oxidizer including the resistively heated simulated isotope heat source.

The results of the above phase of development are reported in NAS CR 66739.

The program was continued under contract NAS 1-9242, and was directed towards the remaining elements of the spacecraft contaminant control system including regenerable and non-regenerable charcoal sorbent beds. MSA was a major subcontractor during this program. The tasks involved in this phase of the program were:

- o Contaminant load review and refinement
- o Establishing charcoal performance characteristics
- o Developing a design methodology for multi-contaminant adsorption
- o System analysis and optimization
- o Long-term testing of a system scaled-down model
- o Full-scale system preliminary design

The results of the above phase of development are reported in NASA CR 2027.

Following the initial development of all system elements, NASA proceeded with the fabrication and design verification testing of an engineering prototype system. This effort was carried out under contract NAS 1-11526 for the NASA Johnson Spacecraft Center. The program was initiated in 1972 and major support

was provided by the Atomic Energy Commission through the Monsanto Research Corporation at Mound Laboratory. The tasks involved in this phase of the program are shown below and are discussed in this report.

- o Component sizing and optimization
- o AEC coordination and licensing
- o Operational analyses including, failure modes and effects analysis, safety hazards analysis, fault detection and isolation analysis and design performance analyses
- o Mock-up studies to demonstrate maintainability provisions
- o Detailed hardware design
- o Hardware procurement and fabrication
- o Component level checkout testing
- o System level design verification testing
- o Investigation of non-venting techniques
- o Vacuum venting analysis
- o Spacelab contaminant control system conceptual design

Section 2

DESIGN REQUIREMENTS

The following section presents the design requirements for the trace contaminant removal system developed during this program. During the course of the program the contaminant load model was changed. This change impacted the system configuration in terms of component sizing and flow rates. Since the component optimization studies had been conducted based on the earlier model and it was not feasible to redo the optimization, the final component configurations were developed using trends established from the initial optimization study. This approach was dictated by cost and was felt to be valid for development purposes since the component sizing was not significantly affected by the change in contaminant load.

2.1 CONTAMINANT MODELS

The initial contaminant load model selected for use in this program is presented in Table 1. This model was taken from the space station prototype life support system (SSP) program and is listed in the SSP General Specification SVSK HS4655. This model is identical to the contaminant model generated by IMSC under Contract NAS 1-6256; however, the original load has been revised to reflect a drop in metabolic generation rates from the original 9-man crew to the new 6-man-crew. Details on the development of this contaminant model are presented in NASA CR-66346. A minor variation is observed between Table 1 and the original listing. In the case of ethyl mercaptan, methyl mercaptan, and propyl mercaptan, the new listing shows non-biological sources for these materials. This appears to be in error as the literature and NASA CR-66346 cites these materials as known biological contaminants. As no generation rate was given for these materials, a rate consistent with the prediction rate of similar materials as defined by R. A. Dora (ref. 1) is suggested. This would result in an adjusted value of about 0.01 gm/day for each of the mercaptans.

TABLE 1
MAXIMUM CONCENTRATION AND PRODUCTION RATE OF TRACE CONTAMINANTS

Contaminant	Production Rates			Maximum** Allowable Concentration (mg/m ³)
	Non-Biological (gm/day)	Biological * (gm/day)	Total (gm/day)	
Acetone	10.20	0.003	10.20	240
Acetaldehyde	2.50	0.0012	2.50	36
Acetic Acid	0.25		0.25	2.5
Acetylene	2.50		2.50	180
Acetonitrile	0.25		0.25	7
Acrolein	0.25		0.25	0.25
Allyl Alcohol	0.25		0.25	0.5
Ammonia	2.50	6.0	8.5	3.5
Amyl Acetate	0.25		0.25	53
Amyl Alcohol	0.25		0.25	36
Benzene	2.50		2.50	8
n-Butene	2.50		2.50	180
iso-Butene	0.25		0.25	180
Butene-1	2.50		2.50	180
cis-Butene-2	0.25		0.25	180
trans-Butene-2	2.50		2.50	180
1, 3 Butadiene	2.50		2.50	220
iso-Butylene	0.25		0.25	180
n-Butyl Alcohol	2.50	0.018	2.52	30
iso Butyl Alcohol	0.25		0.25	30
sec-Butyl Alcohol	0.25		0.25	30
tert-Butyl Alcohol	0.25		0.25	30
Butyl Acetate	0.25		0.25	71
Butraldehydes	0.25		0.25	70
Butyric Acid	0.25		0.25	14
Carbon Disulfide	0.25		0.25	6
Carbon Monoxide	2.50	0.2	2.7	29
Carbon Tetrachloride	0.25		0.25	6.5
Carbonyl Sulfide	0.25		0.25	25

TABLE 1 (Cont'd)

IMSC-D462467

Contaminant	Production Rates			Maximum** Allowable Concentration (mg/m ³)
	Non-Biological (gm/day)	Biological * (gm/day)	Total (gm/day)	
Chlorine	0.25		0.25	1.5
Chloroacetone	0.25		0.25	100
Chlorobenzene	0.25		0.25	35
Chlorofluoromethane	0.25		0.25	24
Chloroform	2.50		2.50	24
Chloropropane	0.25		0.25	84
Caprylic Acid	0.25		0.25	155
Cumene	0.25		0.25	25
Cyclohexane	2.50		2.50	100
Cyclohexene	0.25		0.25	100
Cyclohexanol	0.25		0.25	20
Cyclopentane	0.25		0.25	100
Cyclopropane	0.25		0.25	100
Cyanamide	0.25		0.25	45
Decalin	0.25		0.25	5.0
1, 1 Dimethyl cyclohexane	0.25		0.25	120
trans 1, 2 Dimethyl Cyclohexane	0.25		0.25	120
2,2 Dimethyl butane	0.25		0.25	93
Dimethyl Sulfide	0.25		0.25	15
1, 1 Dichloroethane	2.50		2.50	40
Di iso Butyl Ketone	0.25		0.25	29
1, 4 Dioxene	2.50		2.50	36
Dimethyl Furan	0.25		0.25	3.0
Dimethyl Hydrazine	0.25		0.25	0.1
Ethane	2.50		2.50	180
Ethyl Alcohol	2.50	0.6	2.56	190
Ethyl Acetate	2.50		2.50	140
Ethyl Acetylene	0.25		0.25	180
Ethyl Benzene	0.25		0.25	44
Ethylene Dichloride	0.25		0.25	40
Ethyl Ether	2.50		2.50	120
Ethyl Butyl Ether	0.25		0.25	200

TABLE 1 (Cont'd)

Contaminant	Production Rates			Maximum** Allowable Concentration (mg/m ³)
	Non-Biological (gm/day)	Biological * (gm/day)	Total (gm/day)	
Ethyl Formate	2.50		2.50	30
Ethylene	2.50		2.50	180
Ethylene Glycol	0.25		0.25	114
trans 1, Methyl 3 Ethyl Cyclohexane	0.25		0.25	117
Ethyl Sulfide	0.25		0.25	97
Ethyl Mercaptan	0.25		0.25	2.5
Freon 11	2.50		2.50	560
Freon 12	2.50		2.50	500
Freon 21	0.25		0.25	420
Freon 22	0.25		0.25	350
Freon 23	0.25		0.25	12
Freon 113	0.25		0.25	700
Freon 114	2.50		2.50	700
Freon 114 unsym	0.25		0.25	700
Freon 125	0.25		0.25	25
Formaldehyde	0.25		0.25	0.6
Furan	0.25		0.25	3
Furfural	0.25		0.25	2
Hydrogen	2.50	0.3	2.8	215
Hydrogen Chloride	0.25		0.25	0.15
Hydrogen Fluoride	0.25		0.25	0.08
Hydrogen Sulfide	0	0.0005	0.0005	1.5
Heptane	0.25		0.25	200
Hexene-1	0.25		0.25	180
n-Hexane	2.50		2.50	180
Hexamethylcyclotrisihexane	0.25		0.25	240
Indole	0.25	0.6	0.85	126
Isoprene	0.25		0.25	140
Methylene Chloride	2.50		2.50	21
Methyl Acetate	2.50		2.50	61
Methyl Butyrate	0.25		0.25	30
Methyl Chloride	0.25		0.25	21

TABLE 1 (Cont'd)

Contaminant	Production Rates			Maximum ** Allowable Concentration (mg/m ³)
	Non-Biological (gm/day)	Biological * (gm/day)	Total (gm/day)	
2-Methyl-1 Butene	0.25		0.25	1430
Methyl Chloroform	2.50		2.50	190
Methyl Furan	0.25		0.25	3
Methyl Ethyl Ketone	2.50		2.50	59
Methyl Isobutyl Ketone	0.25		0.25	14
Methyl Isopropyl Ketone	2.50		2.50	70
Methyl Cyclohexane	0.25		0.25	200
Methyl Acetylene	0.25		0.25	165
Methyl Alcohol	2.50	0.06	2.56	26
3-Methyl Pentane	0.25		0.25	295
Methyl Methacrylate	0.25		0.25	41
Methane	29.5	3.6	33.1	1720
Mesitylene	0.25		0.25	2.5
mono Methyl Hydrazine	0.25		0.25	0.055
Methyl Mercaptan		0.01	0.01	2
Naphthalene	0.25		0.25	5.0
Nitric Oxide	0.25		0.25	32
Nitrogen Tetroxide	0.25		0.25	1.8
Nitrogen Dioxide	0.25		0.25	0.9
Nitrous Oxide	0.25		0.25	47
Octane	0.25		0.25	255
Propylene	2.50		2.50	180
iso-Pentane	2.50		2.50	295
n-Pentane	2.50		2.50	295
Pentene-1	0.25		0.25	180
Pentene-2	0.25		0.25	180
Propane	2.50		2.50	180
n-Propyl Acetate	0.25		0.25	84
n-Propyl Alcohol	2.50		2.50	75
iso-Propyl Alcohol	2.50		2.50	98
n-Propyl Benzene	0.25		0.25	44
iso-Propyl Chloride	0.25		0.25	260

TABLE 1 (Cont'd)

Contaminant	Production Rates			Maximum** Allowable Concentration (mg/m ³)
	Non-Biological (gm/day)	Biological * (gm/day)	Total (gm/day)	
iso-Propyl Ether	0.25		0.25	120
Propionaldehyde	0.25		0.25	30
Propionic Acid	0.25		0.25	15
Propyl Mercaptan	0.25		0.25	82
Propylene Aldehyde	0.25		0.25	10
Pyruvic Acid		2.27	2.27	0.9
Phenol	0.25	2.27	2.52	1.9
Skatol		0.25	0.25	141
Sulfur Dioxide	0.25		0.25	0.8
Styrene	0.25		0.25	42
Tetrachloroethylene	0.25		0.25	67
Tetrafluoroethylene	0.25		0.25	205
Tetrahydrofuran	0.25		0.25	59
Toluene	2.50		2.50	75
Trichloroethylene	0		0	*
1, 2, 4 Trimethyl Benzene	0.25		0.25	49
1, 1, 5 Thrimethyl cyclohexane	0.25		0.25	140
Valeraldehyde		0.25	0.25	70
Valeric Acid		0.25	0.25	110
Vinyl Chloride	2.50		2.50	130
Vinyl Methyl Ether	0.25		0.25	60
Vinyldene Chloride	0.25		0.25	20
O-Xylene	2.50		2.50	44
m-Xylene	2.50		2.50	44
p-Xylene	2.50		2.50	44

* For six crewmen.

** This applies to nominal operational levels, reduced and emergency levels are to be determined.

During the course of the program NASA revised the SSP contaminant load model adjusting both generation rates and allowable concentrations. The revised model also reflected the change in contaminant generation rate with time and provided for an initial high rate for the first two weeks of the mission and a reduced rate for the balance of the mission. These variable rates were for the non-metabolic loads only. The revised contaminant load model that the final system design was based on is presented in Table 2.

2.2 DESIGN CRITERIA

In addition to the contaminant load model other system design criteria were utilized to establish the optimum configuration. These criteria listed in Table 3 were taken from the SSP General Specification SVSK HS 4655 and were used through the program for the trade studies. The design studies were based on the optimum use of electrical power and hence peak power operation occurred during the daylight portion of the orbit cycle to take advantage of the lower penalty solar cell power. To simplify overall system integration it was later decided to use only 400 Hz power.

TABLE 2 - MAXIMUM ALLOWABLE CONCENTRATIONS AND PRODUCTION RATES OF AIRBORNE TRACE CONTAMINANTS

	MOLE WT.	PRODUCTION RATES			MAXIMUM ALLOWABLE CONCENTRATION		
		NONBIOLOGICAL Initial (gm/day)	Nominal (gm/day)	BIOLOGICAL 6 Men (gm/day)	14 days mg/1 *PPM	long term mg/1 *PPM	
1. Alcohols							
Allyl Alcohol	58.08	0.25	0.025			0.005	0.2
Amyl Alcohol	88.15	0.25	0.025			0.036	10.
Iso-Butyl Alcohol	74.12	0.25	0.025			0.03	10.
N-Butyl Alcohol	74.12	2.50	0.25	0.008	0.076	25	0.03
Sec-Butyl Alcohol	74.12	0.25	0.025		0.076	25	0.03
Tert-Butyl Alcohol	74.12	0.25	0.025			0.03	10.
Cyclohexanol	100.16	0.25	0.025			0.02	5.
Ethyl Alcohol	46.07	2.50	0.25	0.024	0.19	100	0.19
Ethylene Glycol	62.07	0.25	0.025			0.114	45.
Methyl Alcohol	32.04	2.50	0.25	0.0085	0.013	10	0.0039
Phenol	94.11	0.25	0.025	0.57		0.0019	0.5
N-Propyl Alcohol	60.09	2.50	0.25			0.075	30.
Iso-Propyl Alcohol	60.09	2.50	0.25		0.12	50	0.098
2. Aldehydes							
Acetaldehyde	44.05	2.50	0.25	0.0005	0.09	50	0.09
Acrolein	56.06	0.25	0.025			0.0012	0.05
Butyraldehyde	72.10	0.25	0.025			0.15	50
Crotonaldehyde	70.09	0.25	0.025			0.001	0.35
Formaldehyde	30.03	0.25	0.025			0.00012	0.1
Furfural	96.08	0.25	0.025			0.002	0.5
Propionaldehyde	58.08	0.25	0.025			0.118	50.
Valeraldehyde	86.13			0.005		0.175	50.
3. Aromatic Hydrocarbons							
Benzene	78.11	0.90	0.09		0.003	1	0.003
Cumene	120.19	0.25	0.025			0.025	1.0
Decalin	138.24	0.25	0.025			0.005	5.
Ethyl Benzene	106.16	0.25	0.025	0.087	20	0.087	20.
Mesatylene	120.19	0.25	0.025	0.1	20	0.05	10.

IMSC-D462467

TABLE 2 - MAXIMUM ALLOWABLE CONCENTRATIONS AND PRODUCTION RATES OF AIRBORNE TRACE CONTAMINANTS

	PRODUCTION RATES			MAXIMUM ALLOWABLE CONCENTRATION		
	MOLE WT.	NONBIOLOGICAL Initial (gm/day)	BIOLOGICAL Nominal (gm/day)	6 Men (gm/day)	14 days mg/1 *PPM	long term mg/1 *PPM
3. Aromatic Hydrocarbons (continued)						
Naphthalene	128.16	0.25	0.025		0.005	1.
n-Propyl Benzene	120.19	0.25	0.025		0.044	9.
Styrene	104.14	0.25	0.025	0.1	0.085	20.
Toluene	92.13	2.50	0.25	0.19	0.075	20.
1,2,4 Trimethyl Benzene	120.19	0.25	0.025		0.044	10.
M-Xylene	106.16	2.50	0.25		0.044	10.
O-Xylene	106.16	2.50	0.25		0.044	10.
P-Xylene	106.16	2.50	0.25		0.044	10.
4. Esters						
Amyl Acetate	130.18	0.25	0.025		0.053	10.
Butyl Acetate	116.16	0.25	0.025	0.12	0.12	25.
Ethyl Acetate	88.10	2.50	0.25	0.14	0.14	40.
Ethyl Formate	74.08	2.50	0.25		0.03	10.
Methyl Acetate	74.08	2.50	0.25		0.03	10.
Methyl Butyrate	102.13	0.25	0.025		0.03	7.
Methyl Methacrylate	100.12	0.25	0.025		0.041	10.
n-Propyl Acetate	102.13	0.25	0.025		0.084	20.
5. Ether						
Dimethyl Furan (2,5)	96.12	0.25	0.025		0.003	0.8
1,4 Dioxane	88.11	2.50	0.25		0.007	2.
Ethyl Butyl Ether	102.17	0.25	0.025		0.2	50.
Ethyl Ether	74.12	2.50	0.25		0.12	40.
Furan	68.07	0.25	0.025		0.003	1.
Methyl Furan	82.10	0.25	0.025		0.03	9.
Methyl Vinyl Ether	58.00	0.25	0.025		0.06	29.
iso-Propyl Ether	102.17	0.25	0.025		0.12	30.
Tetrahydrofuran	72.10	0.25	0.025		0.059	20.

TABLE 2 - MAXIMUM ALLOWABLE CONCENTRATIONS AND PRODUCTION RATES OF AIRBORNE TRACE CONTAMINANTS

	PRODUCTION RATES				MAXIMUM ALLOWABLE CONCENTRATION			
	MOLE WT.	NONBIOLOGICAL Initial (gm/day)	Nominal (gm/day)	BIOLOGICAL 6 Men (gm/day)	14 days mg/1 *PPM	long term mg/1 *PPM	long term mg/1 *PPM	
6. Chlorocarbons								
*Carbon Tetrachloride	153.84	0.25	0.025		0.	0.00016	0.04	
Chloroacetone	92.53	0.25	0.025		0.046	10	0.035	7.5
Chlorobenzene	112.56	0.25	0.025					
*Chloroform	119.30	0.25	0.025		0.03	5	0.084	26.
Chloropropane	78.54	0.25	0.025					
Dichlorobenzene	147.01	0.25	0.025					
1,1-Dichloroethane	93.97	2.50	0.25					
1,2-Dichloroethane	98.97	0.25	0.025					
Methyl Chloride	50.49	0.25	0.025					
*Methyl Chloroform	133.41	0.25	0.025					
Methyl Chloride	84.94	2.50	0.25		0.087	25	0.035	10.
Iso-Propyl Chloride	78.54	0.25	0.025					
Tetrachloroethylene	165.83	0.25	0.025		0.136	20	0.067	81.
*Trichloroethylene	131.39	0.25	0.025					
Vinyl Chloride	62.50	2.50	0.25		0.26	100	0.127	50
Vinyldene Chloride	96.95	0.25	0.025		0.008	2	0.004	1.
7. Chlorofluorocarbons								
Chlorofluoromethane	68.48	0.25	0.025					
Chlorotrifluoroethane	116.47	0.25	0.025					
Freon 11	137.38	2.50	0.25		0.028	5	0.028	100.
Freon 12	120.92	2.50	0.25					
Freon 21	102.93	0.25	0.025					
Freon 22	86.47	0.25	0.025					
Freon 113	187.39	0.25	0.025					
Freon 114 (sym)	170.92	2.50	0.25					
Freon 112 (unsym)	170.92	0.25	0.025					
Freon 124	136.48	0.25	0.025					
Trifluorochloroethylene	116.48	0.25	0.025					

*Contaminants not allowed on space station

TABLE 2 - MAXIMUM ALLOWABLE CONCENTRATIONS AND PRODUCTION RATES OF AIRBORNE TRACE CONTAMINANTS

	PRODUCTION RATES				MAXIMUM ALLOWABLE CONCENTRATION			
	MOLE WT.	INITIAL (gm/day)	NONBIOLOGICAL Nominal (gm/day)	BIOLOGICAL 6 Men (gm/day)	14 days mg/1 *PPM	long term mg/1 *PPM	long term *PPM	
8. Fluorocarbons								
Freon 23	70.01	0.25	0.025			0.012	4.	
Freon 125	120.02	0.25	0.025			0.025	5.	
Tetrafluoroethylene	100.02	0.25	0.025			0.205	50.	
9. Hydrocarbons								
Acetylene	26.04	2.50	0.25			0.18	170	
Iso-Butane	58.12	0.25	0.025			0.18	75	
n-Butane	58.12	2.50	0.25			0.18	75	
Butene-1	56.10	2.50	0.25			1.15	500	
cis-Butene-2	56.10	0.25	0.025			0.18	80	
Trans-Butene-2	56.10	2.50	0.25			0.18	80	
1,3 Butadiene	54.00	2.50	0.25			0.22	100	
Iso-Butylene	56.10	0.25	0.025			0.18	80	
Cyclohexane	84.16	2.50	0.25			0.68	200	
Cyclohexene	82.14	0.25	0.025			1.0	300	
Cyclopentane	70.13	0.25	0.025			0.1	35	
Cyclopropane	42.08	0.25	0.025			0.1	60	
1,1 Dimethylcyclohexane	112.21	0.25	0.025			0.12	25	
Trans 1,2-Dimethyl-1-cyclohexane	112.21	0.25	0.025			0.12	25	
2,2 Dimethylbutane	86.18	0.25	0.025			0.093	25	
Ethane	30.07	2.50	0.25			0.18	150	
Ethyl Acetylene	54.09	0.25	0.025			0.18	80	
Trans 1, Methyl 3, Ethyl - cyclohexane	126.24	0.25	0.025			0.117	23	
Ethylene	28.05	2.50	0.25			0.18	100	
Heptane	100.20	0.25	0.025			0.2	50	

TABLE 2 - MAXIMUM ALLOWABLE CONCENTRATIONS AND PRODUCTION RATES OF AIRBORNE TRACE CONTAMINANTS

	PRODUCTION RATES				MAXIMUM ALLOWABLE CONCENTRATION			
	MOLE WT.	NONBIOLOGICAL Initial (gm/day)	BIOLOGICAL Nominal (gm/day)	6 Men (gm/day)	14 days mg/1 *PPM	mg/1 *PPM	long term mg/1 *PPM	
9. Hydrocarbons (cont.)								
Hexane-1	84.16	0.25	0.025			0.0034	1	
n-Hexane	86.17	2.50	0.25			0.7	200	
Isoprene	68.11	0.25	0.025			0.56	200	
Methane	16.04	29.5	2.95	3.6		1.72	2620	
Methyl Acetylene	40.06	0.25	0.025			0.165	100	
2 Methyl - 1 - Butene	70.13	0.25	0.025			1.43	500	
Methyl Cyclohexane	98.18	0.25	0.025			0.2	50	
3-Methyl Pentane	86.17	0.25	0.025			3.5	1000	
Octane	114.22	0.25	0.025			0.235	50	
Iso-Pentane	72.15	2.50	0.25			0.295	100	
n-Pentane	72.15	2.50	0.25			0.6	200	
Pentane-1	70.13	0.25	0.025			0.18	60	
Pentane-2	70.13	0.25	0.025			0.18	60	
Propane	44.09	2.50	0.25			0.18	100	
Propylene	42.08	2.50	0.25			0.86	500	
1,1,5-Trimethylcyclotrihexane	126.24	0.25	0.025			0.14	27.	
10. Inorganic Acids								
Chlorine	70.91	0.25	0.025			0.0015	0.5	
Hydrogen Chloride	36.47	0.25	0.025			0.00015	0.1	
Hydrogen Fluoride	20.01	0.25	0.025			0.00008	0.1	
11. Ketones								
Acetone	58.08	10.20	1.02	0.0008	0.71	300	300	
Di isobutyl Ketone	142.23	0.25	0.025			0.029	5.	
Methyl Ethyl Ketone	72.10	2.50	0.25			0.059	20.	
Methyl Isobutyl Ketone	100.16	0.25	0.025			0.082	20.	
Methyl Isopropyl Ketone	86.13	2.50	0.25			0.07	20.	

TABLE 2 - MAXIMUM ALLOWABLE CONCENTRATIONS AND PRODUCTION RATES OF AIRBORNE TRACE CONTAMINANTS

	PRODUCTION RATES				MAXIMUM ALLOWABLE CONCENTRATION			
	MOLE WT.	Initial (gm/day)	Nominal (gm/day)	BIOLOGICAL (gm/day)	14 days mg/1	*PPM	long term mg/1	*PPM
12. <u>Mercaptans</u>								
Ethyl Mercaptan	62.13			0.005			0.004	1.5
Methyl Mercaptan	48.10			0.005			0.002	1.
Propyl Mercaptan	76.15			0.005			0.082	26.
13. <u>Miscellaneous</u>								
Ammonia	17.03	2.50	0.25	1.5	0.017	25	0.017	25
Carbon Monoxide	28.01	2.50	0.25	0.2	0.017	15	0.017	15
Hexamethylcyclotri-siloxane	222.38	0.25	0.025				0.24	3
Hydrogen	2.016	2.50	0.25	0.3			0.215	2600.
Hydrogen Sulfide	34.08	0.08	0.00045				0.0015	1.
Sulfur Dioxide	64.07	0.25	0.025		0.0026	1	0.0026	1.
14. <u>Nitrogen Oxides</u>								
Nitric Oxide	30.01	0.25	0.025				0.0012	1.0
Nitrogen Dioxide	46.01	0.25	0.025				0.0009	0.5
Nitrogen Tetroxide	92.02	0.25	0.025				0.0009	0.25
Nitrous Oxide	44.01	0.25	0.025				0.047	26.
15. <u>Organic Acids</u>								
Acetic Acid	60.05	0.25	0.025				0.005	2.
Butyric Acid	88.10	0.25	0.025				0.018	5.
Caprylic Acid	144.21						0.155	26.
Propionic Acid	74.08	0.25	0.025				0.015	5.
Pyruvic Acid	88.06				1.26		0.0009	0.25
Valeric Acid	102.13				0.005		0.11	26.

TABLE 2- MAXIMUM ALLOWABLE CONCENTRATIONS AND PRODUCTION RATES OF AIRBORNE TRACE CONTAMINANTS

	PRODUCTION RATES				MAXIMUM ALLOWABLE CONCENTRATION			
	NONBIOLOGICAL		BIOLOGICAL		14 days mg/l	*PPM	mg/l	long term *PPM
	MOLE WT.	Initial (gm/day)	Nominal (gm/day)	6 Men (gm/day)				
16. <u>Organic Nitrogens</u>								
Acetonitrile	41.05	0.25	0.025		0.003	2	0.003	2
Cyanamide	42.04	0.25	0.025			0.045	0.045	26
Dimethyl Hydrazine	60.10	0.25	0.025			0.0001	0.0001	0.04
Indole	117.14			0.15		0.0024	0.0024	0.5
Monomethyl Hydrazine	46.07	0.25	0.025			0.000035	0.000035	0.02
Skatole	131.17			0.15		0.0025	0.0025	0.5
17. <u>Organic Sulfides</u>								
Carbon Disulfide	76.13	0.25	0.025			0.006	0.006	2.
Carbonyl Sulfide	60.07	0.25	0.025			0.005	0.005	2.
Dimethyl Hydrazine	90.18	0.25	0.025			0.00037	0.00037	0.1
Dimethyl Sulfide	62.13	0.25	0.025		0.0025	1	0.0025	1

Conversion of PPM to mg/liter (by volume)

$$X \text{ mg/liter} = \frac{(\text{PPM})(P_T)(n_c)}{RT \text{ (10}^3\text{)}}$$

where:
 P_T = parts per million
 P_T = total pressure of mixture (atmospheres)
 n_c = Molecular weight of contaminant (mole)
 R = gas constant, 0.08205 liter-atmos.
 $\frac{RT}{P_K}$ gm-mole

$$T = 77^{\circ}\text{F}, 25^{\circ}\text{C}, 298^{\circ}\text{K}$$

TABLE 2 MAXIMUM ALLOWABLE CONCENTRATIONS AND PRODUCTION RATES
OF AIRBORNE TRACE CONTAMINANTS (continued)

isobutanol = iso-Butyl Alcohol
 n-Butanol - n-Butyl Alcohol
 2-Butanone = Methyl Ethyl Ketone
 Butyl Ethyl Ether = Ethyl Butyl Ether
 Chlorodifluoromethane = Freon 22
 Chlorotetrafluoroethane = Freon 124
 Propylene Aldehyde = Crotonaldehyde = Trans-2-Butenal - Crotonic Aldehyde =
 - Methylacrolein
 Decahydronaphthalene = Decalin
 1,1-Dichloroethene = Vinylidene Chloride
 1,2-Dichloroethane = Ethylene Chloride = Ethylene
 Dichlorodifluoromethane = Freon 12
 Dichlorofluoromethane = Freon 21
 Dichlorotetrafluoroethane = Freon 114
 Diethyl Sulfide = Ethyl Sulfide = Thicethyl Ether
 Ethanol = Ethyl Alcohol
 p-Dioxane = 1, 4-Dioxane = Dioxan
 Methanol = Methyl Alcohol
 2-Methyl Butanone-3= 3-Methyl-2-Butanone = Methyl Isopropyl Ketone
 Methoxyethene = Methyl Vinyl Ether = Ethenyl Methyl Ether
 Pentanal = Valoral = n-Valeric Aldehyde = Valderaldehyde
 Propanal = Propional = Propionic Aldehyde = Propionaldehyde
 Propone = Propylene
 Propyne = Propine = Methyl Acetylene = Allylene
 Pentafluoroethane = Freon 125
 Perchloroethylene = Tetrachloroethylene
 Propanthiol = Propyl Mercaptan
 isopropanol = iso=Propyl Alcohol
 Propyl Chloride = Chloropropane
 Trichlorodifluoromethane = Freon 11
 Trichlorotrifluoroethane = Freon 23
 1,3,5-Trimethyl Benzene = Mesitylene
 Valerone = Diisobutylketone

TABLE 3
SYSTEM DESIGN CRITERIA

Orbit Data	<ul style="list-style-type: none"> - Total orbital cycle (minutes) 94 - Available power (minutes) 54 - Dark time (minutes) 39
Cabin Pressure	<ul style="list-style-type: none"> - Variable (psia) 5 to 14.7 - Normal Design (psia) 14.7
Electrical Power Source	<ul style="list-style-type: none"> - Type: Photovoltaic and batteries - Weight penalty for continuous regulated 591 50V \pm 5% dc power (1b/kw) - Weight penalty for continuous regulated 115 vac, 3 phase (1b/kw) <ul style="list-style-type: none"> - 60 cycle 725 - 400 cycle 710 - Weight penalty for unregulated 56 V \pm 10% dc power on sunlit side (1b/kw) 154
Heat rejection weight penalties	<ul style="list-style-type: none"> - For heat rejected directly to the coolant (1b/BTU/hr) 0.054 - Increment to be added for heat rejected to the cabin air (1b/BTU/hr) 0.074

Section 3

SYSTEM DEFINITION

The contaminant load that the Trace Contaminant Control System is designed to control has a wide variety of chemical and physical characteristics. The system must therefore be composed of several components. Each component will remove groups of compounds having similar characteristics. Previous development effort (ref. 2) has shown that trace contaminant control can be achieved by a system having non-regenerable and regenerable activated carbon sorption beds; lithium hydroxide catalytic oxidizer pre- and post-sorbent beds; and a catalytic oxidizer.

In the generation of the final selected system, a number of computer runs were made with the contaminant control system design program. This program established the required flow for each contaminant and calculated the quantities of charcoal required to remove the contaminants. This data was then analyzed to determine the final schematic, charcoal quantities, and contaminants controlled by each of the system components. Computer analyses were conducted for both the initial and the revised contaminant loads. Results are presented for the final load; however, a comparison of system configuration is given for both contaminant load models.

3.1 COMPUTER ANALYSIS

The first step in the analysis was the definition of system flow required to control each contaminant within its maximum allowable concentration. Assumptions were made at this time as to the removal efficiency of the system for each contaminant. Calculations were then made using the contaminant control computer program. Initially, runs were made at both the high and low generation rates to find the flow required for control of each contaminant. This data is presented in Table 4. Several contaminants in the revised contaminant load model did not have short-term allowable concentration data. The short-term allowable level

TABLE 4 - SYSTEM PERFORMANCE SUMMARY

CONTAMINANT & CLASS	Short Term - 14 Days				Long Term - 166 Days			
	Removal Technique (1)	Required Flow CFM	Conc. (5) Ci/m ³	MAC mg/m ³	Removal Technique	Required Flow CFM	Conc (5) Ci/m ³	MAC mg/m ³
1. ALCOHOLS								
Allyl Alcohol	F	13.6	.17	.50	R	1.53	.153	.5
Amyl Alcohol	F	.19	.17	36.0	F	.02	.017	36.
Iso-Butyl Alcohol	F	.09	.17	76.0	F	.02	.017	30.
N-Butyl Alcohol	F	.90	1.71	76.0	F	.23	.176	30.
Sec-Butyl Alcohol	F	.23	.17	30.0	F	.02	.017	30.
Tert-Butyl Alcohol	F	.23	.17	300.0	F	.02	.017	30.
Cyclohexanol	F	.34	.17	20.0	F	.03	.017	20.
Ethyl Alcohol	R	.41	15.5	190.	R	.04	.168	190.
Ethylene Glycol	F	.06	.17	114.	F	.005	.017	144
Methyl Alcohol	R	4.72	13.3	13.	R	1.97	1.54	3.9
Phenol	F	11.7	.56	1.9	F	8.53	.405	1.9
N-Propyl Alcohol	F	.91	1.70	75.	R	.10	.153	75.
Iso-Propyl Alcohol	R	.64	15.3	120.	R	.08	.153	98
2. ALDEHYDES								
Acetaldehyde	R	.85	15.3	90.	R	.09	1.53	90
(2) Acrolein	M	5.67	.17	1.2	M	6.38	.153	.12
Butyraldehyde	F	.05	.17	150.	F	.01	.017	150.
Crotonaldehyde	F	6.81	.17	1.0	R	.77	.153	1.0
(2) Formaldehyde	M	5.1	.15	1.2	M	5.1	.015	.12
Furfural	F	3.4	.17	2.0	F	.34	.017	2.0
Propionaldehyde	R	.01	1.53	11800	R	.01	.153	11800
Valeraldehyde	F	.001	.003	175	F	.01	.0306	175.

TABLE 4 (Cont'd)

CONTAMINANT & CLASS	Short Term - 14 Days				Long Term - 166 Days			
	Removal Technique (1)	Required Flow CFM	Conc. (5) C ₁ mg/m ³	MAC mg/m ³	Removal Technique	Required Flow CFM	Conc. (5) C ₁ mg/m ³	MAC mg/m ³
3. AROMATIC HYDROCARBONS								
Benzene	F	.17	.61	3.0	R	.92	.55	3.0
Cumene	F	.27	.17	25.	F	.03	.017	25.0
Decalin	F	1.36	.17	5.0	F	.14	.017	5.0
Ethyl Benzene	F	.08	.17	87	F	.008	.017	87.0
Mesatylene	F	.07	.17	100.	F	.01	.017	50.
Naphthalene	F	1.36	.17	5.0	F	.14	.017	5.0
n-Propyl Benzene	F	.16	.17	44.	F	.02	.017	44.
Styrene	F	.07	.17	100.	F	.01	.017	85.
Toluene	F	.36	1.7	190.	F	.09	.17	75.
1,2,4 Trimethyl Benzene	F	.14	.17	49.	F	.014	.017	49.
M-Xylene	F	1.55	1.7	44.	F	.16	.17	44.
O-Xylene	F	1.55	1.7	44.	F	.16	.17	44.
P-Xylene	F	1.55	1.7	44.	F	.16	.17	44.
4. ESTERS								
Amyl Acetate	F	.13	.17	53	F	.01	.017	53.
Butyl Acetate	F	.06	.17	120	F	.01	.017	120.
Ethyl Acetate	R	.55	15.3	140	R	.06	1.53	140.
Ethyl Formate	R	2.55	15.3	30.	R	.26	1.53	30.
Methyl Acetate	F	1.12	1.7	61.	R	.26	1.53	30.
Methyl Butyrate	F	.23	.17	30	F	.02	.017	30.
Methyl Methacrylate	F	.17	.17	41.	F	.02	.017	41.
n-Propyl Acetate	F	.08	.17	84	F	.01	.017	84.
5. ETHER								
Dimethyl Furan (2,5)	F	2.27	.17	3.0	R	.26	.153	3.0
1,4 Dioxane	F	1.89	1.7	36	R	1.09	1.53	7.0
Ethyl Butyl Ether	F	.03	.17	200	F	.01	.017	200

CONTAMINANT & CLASS	Short Term - 14 Days				Long Term - 166 Days			
	Removal Technique (1)	Required Flow CFM	Conc. (5) C ₁ mg/m ³	Conc. (5) MAC mg/m ³	Removal Technique	Required Flow CFM	Conc. (5) C ₁ mg/m ³	Conc. (5) MAC mg/m ³
5. ETHER (Cont'd)								
Ethyl Ether	R	.64	15.3	120.	R	.06	1.53	120.
Furan	R	2.55	1.53	3.0	R	.26	.153	3.0
Methyl Furan	F	.23	.17	30.	F	.02	.017	30.
Methyl Vinyl Ether	F	.12	.17	59.	R	.01	.153	59.
iso-Propyl Ether	F	.06	.17	120.	R	.01	.153	120.
Tetrahydrofuran	R	.12	.17	59	R	.01	.153	59
6. CHLOROCARBONS								
(3) Carbon tetrachloride	-	4.25	-.17	1.6	-	4.25	-.017	.16
(2) Chloroacetone	F	.15	.17	46	F	.02	.017	35.
Chlorobenzene	F	-	-	-	-	-	-	-
(3) Chloroform	F	.08	.17	84.	R	.01	.153	84.
Chloropropane	F	1.70	.17	46	F	.02	.02	35.
Dichlorobenzene	F	.34	15.3	40	R	.19	1.53	40.
1,1 Dichloroethane	R	.38	1.53	20	R	.04	.153	20.
1,2 Dichloroethane	R	.29	-	21	N	.04	.1	21.
Methyl Chloride	N	-	-	-	-	-	-	-
(3) Methyl Chloroform	-	.88	15.3	87.0	R	.22	1.53	35.
Methylene Chloride	R	.03	.17	260	R	.01	.153	260.
iso-Propyl Chloride	F	.05	.17	136	F	.01	.017	67
Tetrachloroethylene	F	-	-	-	R	-	-	-
(3) Trichloroethylene	R	.29	15.3	260	R	.06	1.53	127.
Vinyl Chloride	R	.96	1.53	8.0	R	.19	.153	4.0

TABLE 4. (Cont'd.)

CONTAMINANT & CLASS	Short Term - 14 Days				Long Term - 166 Days			
	Removal Technique (1)	Required Flow CFM	Conc. (5) C ₁ mg/m ³	MAC mg/m ³	Removal Technique	Required Flow CFM	Conc. (5) C ₁ mg/m ³	MAC mg/m ³
7. CHLOROFLUOROCARBONS								
Chlorotrifluoroethane	N	.25	-	24.	N	.03	-	24
Freon 11	R	.016	1.53	480.	R	.01	.153	480
Freon 12	R	2.73	15.3	28.	R	.27	1.53	28
Freon 21	R	.15	15.3	500	R	.02	1.53	500
Freon 22	R	.02	1.53	420	R	.01	.153	420
Freon 113	N	.017	-	350	R	.01	.153	350
Freon 114 (Sym)	F	.002	.17	3830	R	.01	.153	150
Freon 114 (Unsym)	F	.01	.17	700	R	.01	.153	700
(4) Freon 124	-	.01	.17	700	R	.01	.153	700
Trifluorochloroethylene	R	.01	1.53	2790	-	.01	.153	1670
				2380	R	.01	.153	2380
8. FLUOROCARBONS								
Freon 23	N	.52	-	12	N	.06	-	12
Freon 125	R	.31	1.53	25	R	.03	.153	25
Tetrafluoroethylene	R	.04	1.53	205	R	.01	.153	205
9. HYDROCARBONS								
Acetylene	CO	.34	15.5	180	CO	.034	15.5	180
iso-Butane	F	.04	.17	180	R	.01	.153	180
n-Butane	R	.43	15.3	180	R	.04	1.53	180
Butene-1	R	.07	15.3	1150	R	.01	1.53	1150
cis-Butene-2	R	.04	1.53	180	R	.01	.153	180
Trans-Butene-2	R	.43	15.3	180	R	.04	1.53	180
1,3 Butadiene	R	.35	15.3	220	R	.04	1.53	220
iso-Butylene	R	.04	1.53	180	R	.01	.153	180

TABLE 4 (Cont'd)

IMSC-D462467

CONTAMINANT & CLASS	Short Term - 14 Days				Long Term - 166 Days			
	Removal Technique (1)	Required Flow CFM	Conc C ₁ mg/m ³	Conc (5) MAC mg/m ³	Removal Technique	Required Flow CFM	Conc C ₁ mg/m ³	MAC mg/m ³
9. HYDROCARBONS (Cont'd)								
Cyclohexane	F	.07	1.7	1000	F	.01	.17	680
Cyclohexene	R	.08	1.53	100	R	.01	.153	100
Cyclopentane	F	.07	.17	100	R	.01	.153	100
Cyclopropane	CO	.061	.155	-	CO	.01	.155	100
1,1 Dimethylcyclohexane	F	.06	.17	120	F	.01	.017	120
Trans 1,2-Dimethylcyclohexane	F	.06	.17	120	F	.01	.017	120
2,2 Dimethylbutane	CO	.07	.17	93	CO	.01	.017	93
Ethane	CO	.332	15.5	180	R	.01	.155	180
Ethyl Acetylene	R	.04	1.53	180	R	.01	.153	180
Trans 1, Methyl 3, Ethyl - cyclohexane	F	.06	.17	117	F	.01	.017	117
Ethylene	CO	.332	15.5	180	CO	.034	1.55	180
Heptane	F	.03	.17	200	F	.01	.017	200
Hexane-1	F	2.00	.17	3.4	F	.20	.017	3.4
n-Hexane	F	.07	1.7	1000	F	.01	.17	700
Isoprene	F	.01	.17	560	F	.01	.017	560
Methane	CO	1.57	693	1720	CO	.31	136	1720
Methyl Acetylene	CO	.037	1.55	165	CO	.004	.13	165
2 Methyl - 1 - Butene	F	.005	.17	1430	R	.01	.155	1430
Methyl Cyclohexane	F	.03	.17	200=	F	.01	.017	200
3 Methyl Pentane	F	.002	.17	3500	F	.01	.017	3500
Octane	F	.03	.17	235	R	.03	1.53	235
iso-Pentane	F	.23	1.7	295	F	.01	.17	295
n-Pentane	F	.05	1.7	1480	R	.01	.153	600
Pentene-1	F	.04	1.7	180	F	.01	.153	180
Pentene-2	F	.04	1.7	180	R	.01	.017	180
Propane	R	.43	15.3	180	R	.04	1.53	180
Propylene	CO	.071	15.5	860	R	.01	1.55	860
1,1,5-Trimethylcyclohexane	F	.05	.17	140	F	.017	.017	140

TABLE 4 (Cont. a)

CONTAMINANT & CLASS	Short Term - 14 Days				Long Term - 166 Days			
	Removal Technique (1)	Required Flow CFM	Conc. (5) C ₁ mg/m ³	MAC mg/m ³	Removal Technique	Required Flow CFM	Conc (5) C ₁ mg/m ³	MAC mg/m ³
10. INORGANIC ACIDS								
Chlorine	PS	4.1	1.34	1.5	PS	.41	1.34	1.5
(2) hydrogen chloride	PS	4.1	1.34	1.5	PS	4.1	1.34	.15
(2) hydrogen fluoride	M	7.7	.156	0.8	M	7.35	.156	.08
11. KETONES								
Acetone	R	.14	62.5	710	R	.04	6.25	710
Di isobutyl Ketone	F	.24	.17	29	F	.02	.017	29
Methyl Ethyl Ketone	F	1.15	1.70	59	R	.13	1.53	59
Methyl Isobutyl Ketone	F	.08	.17	82	F	.02	.017	41
Methyl Isopropyl Ketone	F	.98	1.7	70	F	.10	.17	70
12. MERCAPTANS								
Ethyl Mercaptan	R	.04	.036	4.0	R	.04	.031	4.0
Methyl Mercaptan	R	.061	.0034	2.0	R	.08	.031	2.0
Propyl Mercaptan	F	.002	.0034	82	F	.002	.0031	82.
13: MISCELLANEOUS								
Ammonia	PA	5.77	2.5	17	PA	2.5	1.1	17
Carbon Monoxide	CO	3.88	17.0	17	CO	.65	2.84	17
Hexamethylcyclotrisiloxane	F	.28	1.7	240	F	.01	.017	240
Hydrogen	CO	.32	17.7	215	CO	.063	3.4	215
Hydrogen Sulfide	M	.0072	.0024	1.5	M	.0072	.0024	1.5
Sulfur Dioxide	PS	2.52	1.42	2.6	PS	.25	.142	2.6

TABLE 4 (Cont'd)

CONTAMINANT & CLASS	Short Term - 14 Days				Long Term - 166 Days			
	Removal Technique (1)	Required Flow CFM	Conc (5) Ci/m ³	MAC mg/m ³	Removal Technique	Required Flow CFM	Conc (5) Ci/m ³	MAC mg/m ³
14. NITROGEN OXIDES								
Nitric Oxide	N PS	1.3 .68	- 1.33	4.7 9.0	N FS	.51 .68	- .133	1.2 .9
(2) Nitrogen Dioxide	R M	.85 1.3	1.53 .15	9.0 4.7	R P5	.85 .13	.153 .015	.90 4.7
(2) Nitrogen Tetraoxide								
Nitrous Oxide								
15. ORGANIC ACIDS								
Acetic Acid	F	1.36	.17	5	R	.15	.153	5
Butyric Acid	F	.38	.17	18	R	.04	.153	18
Caprylic Acid	F	.001	.0034	155	F	.01	.0034	155
Propionic Acid	F	.45	.17	150	F	.05	.017	150
Pyruvic Acid	F	38.1	.858	900	F	.11	.858	.900
Valeric Acid	F	.001	.034	111	F	.01	.0034	110
16. ORGANIC NITROGENS								
Acetonitrile	R	2.55	1.53	3.0	R	.26	.153	3
Cyanamide	R	.17	1.53	45.0	R	.02	.153	45
Dimethyl Hydrazine	S	6.81	-	.1	S	7.66	-	10
Indole	S	1.70	.102	2.4	F	1.70	.102	2.4
Monomethyl Hydrazine	F	-	-	-	S	21.8	.153	.035
Skatole	F	1.63	.102	2.5	F	1.63	.102	2.5
17. ORGANIC SULFIDES								
Carbon Disulfide	R	1.27	1.53	6.0	R	.13	.153	6.0
Carbonyl Sulfide	M	1.22	-	5.0	M	.12	.014	5.0
Diethyl Sulfide	F	18.4	.17	.37	F	1.84	.017	.37
Dimethyl Sulfide	R	3.06	1.53	2.5	R	.31	.153	2.5

TABLE 4 (Completed)

NOTES:	(1) Removal Techniques
	F Fixed Activated Charcoal Bed
	R Regenerable Activated Charcoal Bed
	CO Catalytic Oxidizer
	M Sorption by Moisture
	PA Sorption by Phosphoric Acid
	PS Sorption by Presorbent LiOH
	S Must be controlled at source
	N Controlled by high temperature catalytic oxidizer and improved post-sorbent bed materials (see Section 10.1)
(2)	No short term MAC given - assumed as 10 x long term
(3)	Restricted from use with materials, equipment to be used on spacecraft by NASA directive.
(4)	Unknown material.
(5)	C _i based on 1133 l/min (40 CFM) for F, M, PA; 141.6 l/min (5 CFM) for R, PS; 120.3 l/min (4.25 CFM) for CO.

was assumed to be the same as the long-term level, except for those contaminants that would dictate design flow rates. For these contaminants, an allowable short-term level of 10 times the long-term level was assumed in order to utilize the same flow for both long and short-term conditions. This assumption enables the power, control and overall design of the low flow loop to be common for the entire mission. These contaminants are noted with (2) in Table 4.

Inspection of Table 4 indicates that relative to flow rate, two general groupings of contaminants can be made. One group requires flow rates below 141.6 l/min (5 CFM), and the second group includes contaminants that require a much greater flow than 141.6 l/min (5 CFM). Fortunately the contaminants in the high flow group are relatively better adsorbed on charcoal and so can be controlled in a flow loop having a non-regenerable charcoal bed. The contaminants in the grouping requiring only low flow for control are, also, poorly adsorbed on charcoal which can be accomplished best with a regenerable charcoal bed, or they are best controlled by reaction in a catalytic oxidizer. These observations typify the system analysis that was required, accomplished and resulted in a system configured to include both fixed and regenerable charcoal beds. The data in Table 4 indicates that the fixed-bed design flow rate is dictated by pyruvic acid which requires a flow rate of 1079 l/min (38.1 CFM). To provide a design margin the fixed bed flow was then set at 1133 l/min (40 CFM). The regenerable bed maximum flow requirement is 133.7 l/min (4.72 CFM) for control of methyl alcohol. The flow rate requirement of 120.3 l/min (4.25 CFM) for carbon monoxide control established the maximum flow of the catalytic oxidizer. When desorption time is considered, the flow required of the regenerable bed size is 114.6 l/min (5.0 CFM). The computer program was then run for a flow rate of 113.3 l/min (40 CFM) with phosphoric acid and 114.6 l/min (5.0 CFM) without phosphoric-acid impregnated charcoal for both the high (14 day) and low (long-term) contaminant generation rates. This data was then used to establish the bed sizes.

3.1.1 Fixed Bed

The fixed bed flow, i.e. the high flow segment of the system, was set by the pyruvic acid removal requirement. The bed was considered as being composed of 3 segments: 14-day saturated zone, 166-day saturated zone, and an adsorption zone. The adsorption zone length was based upon pyruvic acid since it not only determined the flow rate, but is the poorest adsorbed of the contaminants to be controlled by the fixed bed charcoal. The computer analysis was based on a 90% removal efficiency with an inlet air temperature of 294 K (70°F). A section-by-section analysis is presented in Tables 5 and 6, for the fixed bed at the short- and long-term production rates, respectively. As can be seen, the short-term saturated zone requirement is 56.2 gm/day (Table 5, Section 9). The requirements for long-term saturated zone requirement is 34.8 gm/day (Table 6, Section 11). These rates give a total for the short term and the long term phases of the design mission of 0.77 kg (1.7 lb), 5.76 kg (12.7 lb), and a total of 6.53 kg (14.4 lb) for the non-regenerative or fixed charcoal weight.

The adsorption zone length is primarily dependent on the flow rate, (Ref. 2), and the adsorption zone length at 39.6 cm/min (1.3 ft/min) is 0.5 cm (0.2 in). This results in an adsorption zone size of 6.99 kg (15.4 lb). The total bed size required is thus 13.52 kg (29.8 lb), or 15.4 kg (34.0 lb) with a 15 percent safety factor.

The above untreated charcoal will not control ammonia, and in the absence of test experience to quantify the ammonia removal rate in the humidity control system, it was judged necessary to provide for ammonia exclusively by a method previously researched at Lockheed. Lockheed demonstrated in the previous contract (Ref. 2), that ammonia can be removed by sorption on activated charcoal which has been treated with phosphoric acid. Those tests showed that this treatment is effective at an acid loading of 2 millimoles of acid per gram of charcoal. The above loading of phosphoric acid on the fixed charcoal bed would achieve ammonia removal, even if the reaction takes place only to the monobasic level.

TABLE 5
FIXED SORBENT BED - SHORT TERM
COMPUTER ANALYSIS RESULTS

<u>Section 1</u>	Mass of Section gms/day	Cumulative Mass of Section gms/day	
			.858
Decalin			
Caprylic Acid			
Indole			
Skatole			
Valeric Acid			
<u>Section 2</u>	6.40	7.26	
Hexamethylcyclotrisiloxane			
Naphthalene			
Octane			
1.1.5 Trimethyl Cyclohexane			
2.2-Dimethyl Butane			
Mesitylene			
Butyl Acetate			
Cyclo hexanol			
Ethyl Benzene			
3-Methyl Pentane			
N-Propylacetate			
Amyl Alcohol			
Ethyl Butylether			
Chlorobenzene			
D. Chlorobenzene			
Methyl Cyclohexane			
1.2.4-Trimethyl Benzene			
Methyl Butyrate			
N-Propyl Benzene			
Cumene			
Ethylene Glycol			
<u>Section 3</u>	9.34	16.6	
O-Xylene			
TiXylene			
Di-Isobutyl Ketone			
Phenol			
Trans-1 methyl - 3 ethyl cyclohexane			
Amyl Acetate			
Methyl Isobutyl Ketone			
Furfural			
Methyl Methacrylate			
Diethyl Sulfide			
Iso-Butyl Alcohol			
Propionic Acid			
Propyl Mercaptan			

TABLE 5. (Cont'd)

	Mass of Section gms/day	Cumulative Mass of Sections gms/day
<u>Section 4</u>	1.81	18.4
M-Xylene		
Methyl furan		
<u>Section 5</u>	4.33	22.7
N-hexane		
Hexene-1		
Trans 1,2 Dimethylcyclohexane		
1,1-Dimethylcyclohexane		
<u>Section 6</u>	12.5	35.3
N-Butyl Alcohol		
Toluene		
Heptane		
Tetrachloroethylene		
Styrene		
Isoprene		
Tert-Butyl Alcohol		
Sec-Butyl Alcohol		
Valeraldehyde		
<u>Section 7</u>	9.45	44.7
n-Pentene		
Butyraldehyde		
<u>Section 8</u>	.45	45.2
Methyl Isopropyl Ketone		
<u>Section 9</u>	11.0	56.2
Cyclohexane		
Pyruvic Acid		
Pentene-2		

TABLE 5 (Cont'd)

	Mass of Section gms/day	Cumulative Mass of Sections gms/day
<u>Section 10</u>	85.52	141.7
Isopentane		
1-4 Dioxane		
n-Propyl Alcohol		
Methyl Ethyl Ketone		
Benzene		
Iso Butane		
Chloropropane		
Pentene 1		
2 Methyl-1 Butene		
Cyclopentane		
Dimethyl 1 Furane		
Freon 11 ⁴ (unsymmetrical)		
Freon 11 ⁴ (symmetrical)		
Dimethyl Hydrazine		
Allyl Alcohol		
Methyl Vinyl Ether		
Iso-propyl ether		
Butyric Acid		
<u>Section 11</u>	115.1	256.8
Methyl Acetate		
Iso-Propyl Chloride		
Freon 113		
Crotonaldehyde		
Acetic Acid		
Acrolein		
Chloroacetone		

TABLE 6

FIXED SORBENT BED - LONG TERM

	COMPUTER ANALYSIS RESULTS	Cumulative Mass of Sections gms/day
<u>Section 1</u>	Mass of Section gms/day	.02
Caprylic Acid		
Indole		
Skatole		
<u>Section 2</u>	.08	.10
Decalin		
Valeric Acid		
<u>Section 3</u>	.04	.14
Hexamethylcyclotrisiloxene		
<u>Section 4</u>	.14	.29
Octane		
Naphthalene		
<u>Section 5</u>	2.08	2.37
o-Xylene		
p-Xylene		
Di Isobutyl Ketone		
2,2-Dimethylbutane		
Mesitylene		
Butyl Acetate		
Ethyl Benzene		
Cyclohexanol		
3-Methyl Pentane		
Ethyl Butyl Ether		
N-Propyl Acetate		
Amyl Alcohol		
1,2,4 - Trimethyl Benzene		
Chlorobenzene		
Di Chlorobenzene		
Methyl Cyclohexane		
Trans-1, Methyl-1-3-Ethyl Cyclohexane		
N-Propyl Benzene		

TABLE 6 (Cont'd)

	Mass of Section gms/day	Cumulative Mass of Sections gms/day
<u>Section 5 (Cont'd)</u>		
Cumene		
Methyl Butyrate		
Amyl Acetate		
Methyl Isobutyl Ketone		
Methyl Methacrylate		
Furfural		
Diethyl Sulfide		
Ethylene Glycol		
<u>Section 6</u>	.27	2.64
m-xylene		
<u>Section 7</u>	2.55	5.19
Phenol		
Hexane-1		
N-Hexane		
Trans 1,2 - Dimethylcyclohexane		
1,1 Dimethylcyclohexane		
methyl Furan		
Heptane		
iso Butyl Alcohol		
Propionic Acid		
Propyl Mercaptan		
<u>Section 8</u>	3.95	9.14
Toluene		
Styrene		
Tetrachloroethylene		
Sec-Butyl Alcohol		
Tert-Butyl Alcohol		
<u>Section 9</u>	.547	9.69
N-Butyl Alcohol		

TABLE 6 (Cont'd)

	Mass of Section gms/day	Cumulative Mass of Sections gms/day
<u>Section 10</u>	3.87	13.6
N-Pentane		
Methyl Isopropyl Ketone		
Butyraldehyde		
Chloroacetone		
Valeraldehyde		
<u>Section 11</u>	21.22	34.78
Pyruvic Acid		
Cyclohexane		
Isoprene		
Pentene-2		

During the short (14 day) term when contaminant generation rates are high, the total saturated zone is available for contaminant removal. This corresponds to 411 gm/day. This provides control with the charcoal quantity included through Section 11 of Table 5 for the short term. This is reflected in the data presented in Table 4. The contaminants controlled for the long-term are presented in Table 6 through pyruvic acid (Section 11).

The total capacity of the fixed bed being available through the initial short-term high production rate period is fortunate, as it allows control of croton-aldehyde and benzene. These are ultimately displaced from the fixed bed and removed by the regenerable bed in the long-term, but require above 141.6 l/min (5 CFM) flow rate for the short-term situation.

3.1.2 Regenerable Bed

The results of the regenerable bed analysis for the short- and long-term rates are represented in Tables 7 and 8, respectively. As this bed has a one day cycle time, the sizing criteria is based upon the short-term, maximum generation rates. The regenerable-bed computer analyses were based on an 80% removal efficiency with an inlet air temperature of 311K (100°F). Inlet air temperature was selected in a trade-off of the adsorption capacity vs water loss in the desorption cycle as will be discussed in a later section. As previously mentioned, the flow requirement of 142 l/min (5 CFM) for this bed is established by the requirement for control of methyl alcohol. Utilizing this flow rate a computer analysis was conducted to establish the charcoal requirements for the regenerable bed. The mass of charcoal required in the regenerable bed vs the number of contaminants removed is plotted in Figure 1. As can be seen from Table 7 and Figure 1, the required weight of charcoal begins to increase quite rapidly after Section 22. It is also clear that the weight of charcoal required to remove all possible contaminants would be prohibitive. Thus, a bed size cut off corresponding to tetrafluoroethylene was chosen.

TABLE 7
 REGENERABLE SORBENT BED - SHORT TERM
 COMPUTER ANALYSIS RESULTS

	Mass of Section gm/day	Cumulative Mass of Sections gm/day
<u>Section 1</u>	.76	.76
Decalin		
Caprylic Acid		
Indole		
Skatole		
Valeric Acid		
<u>Section 2</u>	5.57	6.34
Hexamethylcyclotrisiloxane		
Naphthalene		
Octane		
1,1,5 Trimethylcyclohexane		
2,2 - Dimethyl Butane		
Phenol		
Di-isobutyl Ketone		
Cyclohexanol		
Mesitylene		
Butylacetate		
Ethyl Benzene		
n-Propyl Acetate		
Valeric Acid		
Amyl Alcohol		
Chlorobenzene		
3-Methyl Pentane		
Ethylene Glycol		
Ethyl Butyl Ether		
Methylcyclohexane		
Methyl Butyrate		
Furfural		
1-2,4-Trimethyl Benzene		
n-Propyl Benzene		
Cumene		
Methyl Isobutyl Ketone		
Trans-1 Methyl 3 Ethyl Cyclohexane		
Amyl Acetate		
Methyl Methacrylate		
Propyl Mercaptain		

TABLE 7 (Cont'd)

	Mass of Section gm/day	Cumulative Mass of Section gm/day
<u>Section 3</u>	6.52	12.85
o-Xylene		
Hexene - 1		
iso-Butyl Alcohol		
Methyl Furan		
Diethyl Sulfide		
Propionic Acid		
<u>Section 4</u>	1.38	14.23
m-Xylene		
<u>Section 5</u>	3.31	17.5
n-Hexane		
Trans 1,2-Dimethylcyclohexane		
1,1-Dimethylcyclohexane		
<u>Section 6</u>	5.73	23.3
N-Butyl Alcohol		
Pyruvic Acid		
Isoprene		
Heptane		
Tetrachloroethylene		
Styrene		
Tert-Butyl Alcohol		
Sec-Butyl Alcohol		
<u>Section 7</u>	.98	24.3
Toluene		
<u>Section 8</u>	7.1	31.4
n - Pentane		
Chloropropane		
Butyraldehyde		
Valeraldehyde		

TABLE 7 (Cont 'd)

	Mass of Section /day	Cumulative Mass of Sections /day
<u>Section 9</u>	3.94	35.3
Cyclohexane		
Pentane-2		
iso-Butane		
Pentene-1		
<u>Section 10</u>	4.77	40.1
1,4 Dioxane		
2 Methyl 1 Butane		
<u>Section 11</u>	7.88	47.9
n-Propyl Alcohol		
Cyclopentane		
<u>Section 12</u>	16.6	64.6
Isopentane		
Freon 11 ⁴ (unsymmetrical)		
Freon 11 ⁴ (symmetrical)		
<u>Section 13</u>	49.7	11 ⁴ .3
Methyl Acetate		
Dimethyl Furan		
Allyl Alcohol		
Dimethyl Hydrazine		
iso-Propyl Chloride		
iso-Propyl Ether		
Methyl Vinyl Ether		
Butyric Acid		
Acetic Acid		
Freon 113		
<u>Section 14</u>	308	422.3
Acetone		
1,1 Dichloroethane		
Ethyl Formate		
n-Butane		
Methylene Chloride		
Freon 11		
cis-Butene-2		
Crotonaldehyde		
Acrolein		

TABLE 7 (Cont'd)

	Mass of Section gm/day	Cumulative Mass of Sections gm/day
Section 14 (Cont'd)		
Vinylidene Chloride		
Chlorotrifluoro ethane		
Monomethylhydrazine		
1,2, Dichloroethane		
Chloroacetone		
Ethyl Mercaptan		
<u>Section 15</u>	3.35	425.6
trans-Butene-2		
<u>Section 16</u>	33.0	458.6
Butene-1		
Ethyl Alcohol		
<u>Section 17</u>	26.23	484.8
Ethyl Ether		
Ethyl Acetylene		
<u>Section 18</u>	55.8	540.7
iso-Propyl Alcohol		
Propionaldehyde		
<u>Section 19</u>	211.8	752.5
1,3 Butadiene		
Ethyl Acetate		
iso-Butylene		
Dimethyl Sulfide		
Trifluorochloroethylene		
<u>Section 20</u>	1852.	2604.
Propane		
Freon 12		
Tetrahydrofuran		
Cyclohexene		
Carbon disulfide		
Freon 21		
Freon 125		
Furane		
Acetonitrile		
Nitrogen Tetroxide		

TABLE 7 (Cont'd)

	Mass of Section gm/day	Cumulative Mass of Sections gm/day
<u>Section 21</u>	1259.	3863.
Methyl Alcohol		
Acetaldehyde		
Vinyl Chloride		
<u>Section 22</u>	369	4232.
Tetrafluoroethylene		
Methyl Mercaptan		
Cyanamide		

TABLE 8
 REGENERABLE SORBENT BED - LONG TERM
 COMPUTER ANALYSIS RESULTS

	Mass of Section gm/day	Cumulative Mass of Sections gm/day
<u>Section 1</u>	.02	.02
Caprylic Acid		
Indole		
Skatol		
<u>Section 2</u>	.07	.09
Decalin		
Valeric Acid		
<u>Section 3</u>	.03	.12
Hexamethylcyclotrisiloxane		
<u>Section 4</u>	3.26	3.38
Phenol		
Naphthalene		
Octane		
o-Xylene		
p-Xylene		
m-Xylene		
n-Hexane		
1,1,5 Trimethylcyclohexane		
Di-isobutyl Ketone		
2,2 - Dimethyl butane		
Mesitylene		
Butyl Acetate		
Cyclahexanol		
Ethyl Benzene		
3-Methyl Pentane		
n-Propyl Acetate		
Ethyl Butyl Ether		
Amyl Alcohol		
Chlorobenzene		
Methylcyclohexane		
1,2,4-Trimethyl Benzene		
Methyl Butyrate		
n-Propyl Benzene		
Cumene		
TransMethyl-1-3 Ethyl Cyclohexane		
Amyl Acetate		
Methyl Isobutyl Ketone		
Furfural		
Ethylene Glycol		

TABLE 8 (Cont'd)

	Mass of Section gm/day	Cumulative Mass of Sections gm/day
<u>Section 4 (Cont'd)</u>		
Methyl Methacrylate		
Hexene-1		
Diethyl Sulfide		
trans 1,2 Dimethylcyclohexane		
Methyl Furan		
iso-Butyl Alcohol		
1,1 - Dimethylcyclohexane		
Propionic Acid		
Propyl Mercaptan		
<u>Section 5</u>	1.15	4.53
N-Butyl Alcohol		
Toluene		
Heptane		
Tetrachloroethylene		
Styrene		
Isoprene		
<u>Section 6</u>	1.42	5.95
n-Pentane		
tert-Butyl Alcohol		
sec-Butyl Alcohol		
Chloroacetone		
<u>Section 7</u>	9.48	15.4
Pyruvic Acid		
Methyl isopropyl Ketone		
Cyclohexane		
1,4 Dioxane		
Benzene		
Pentane -2		
iso-Butane		
Pentane -1		
Chloropropane		
Butyraldehyde		
2 Methyl -1 Butane		
Cyclopentane		
Dimethyl Furan		
Freon 114 (unsymmetrical)		
Freon 114 (symmetrical)		
Valeraldehyde		

TABLE 8 (Cont'd)

	Mass of Section gm/day	Cumulative Mass of Sections gm/day
<u>Section 8</u>	135	16.8
Isopentane n-Propyl Alcohol		
<u>Section 9</u>	.46	17.2
Methyl Ethyl Ketone		
<u>Section 10</u>	21.14	38.4
Methyl Acetate Isopropylether Methyl Vinyl Ether Tetrahydrofuran Dimethylhydrazine isopropyl Chloride Allyl Alchol Butyric Acid Freon 113		
<u>Section 11</u>	108.	147.
Acetone 1,1 Dichloroethane Ethyl Formate n-Butane trans-Butane -2 Butene-1 Ethyl Ether Freon 11 Methylene Chloride cis-Butene-2 Crotonaldehyde Acetic Acid Vinylidene chloride Ethyl Acetylene Chlorotrifluoroethane 1,2 Dichloroethane Acrolein Ethyl Mercaptan		
<u>Section 12</u>	14.7	162
Ethyl Alcohol Monomethyl Hydrazine		

Table 8 . (Cont'd)

	Mass of Section gm/day	Cumulative Mass of Sections gm/day
<u>Section 13</u>	2.94	164.
iso-Propyl Alcohol		
<u>Section 14</u>	96.	260.
1,3 Butadiene		
Ethyl Acetate		
Freon 12		
Cyclohexene		
Propionaldehyde		
Dimethyl Sulfide		
Trifluoro Chloroethylene		
<u>Section 15</u>	545.	805.
Propane		
iso-Butylene		
Freon 21		
Carbon disulfide		
Furan		
Freon 125		
Nitrogen Tetroxide		
Acetonitrile		
<u>Section 16</u>	1093	1899
Propylene		
Acetaldehyde		
Vinyl Chloride		
Tetrafluoroethylene		
<u>Section 17</u>	2086.	3984.
Methyl Alcohol		
Freon 22		
Cyanamide		
Methyl Mercaptan		

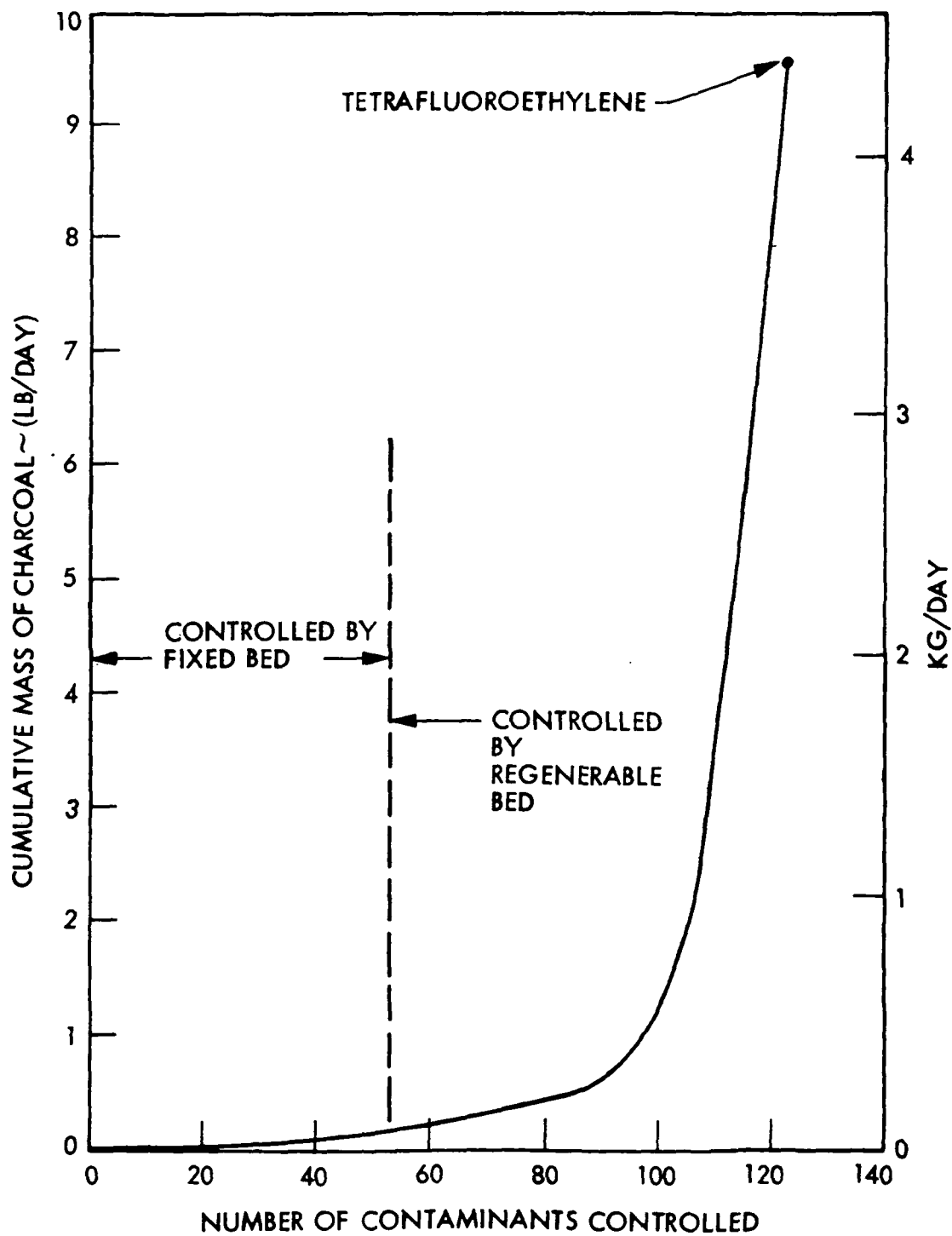


Figure 1 Regenerable Bed Size vs Number of Contaminants Controlled

Table 9 presents a list of all of the contaminants requiring more charcoal for control than tetrafluoroethylene (thru Section 22). This design point was chosen for investigation because (1) it represented a point where the weight for a regenerable charcoal removal technique increased significantly as additional contaminants were considered, (2) fair justification existed for the presence of vinyl chloride and tetrafluoroethylene, and (3) all contaminants requiring more charcoal than this were only produced by equipment off-gassing and had relatively unsubstantiated production rates; that is, the contaminant hasn't been found in any manned spacecraft or manned simulator test. Also listed on this table are (1) potential sources, where they are known, (2) whether or not these sources could be controlled, and (3) whether or not the contaminant has been found in either the LEM or Apollo ground simulation tests since the Apollo fire.

This last item is of particular significance, since a great deal of material changes have taken place since that time, and therefore, contaminants that were identified in manned systems prior to that time, but have not been identified since, are probably not potential space station contaminants. Selecting tetrafluoroethylene as the cut-off point to limit bed size to practical limits, the size of the regenerative bed saturated zone is 4232 grams/day (9.3 lb/day), as can be seen in Table 7. For this saturated zone size and 146 l/min (5 CFM), flow rate the adsorption zone size is 1.55 kg (3.4 lbs) giving a total bed size of 5.8 kg (12.7 lb).

As the generation rate of contaminants drop, the regenerable bed can remove additional materials. Thus, although Freon 22 will not be controlled at the allowable level for the first 14 days, it will be controlled at the long-term rate.

3.1.3 Contaminant Load Model Comparison

As indicated previously, computer studies were made to establish flow rate and charcoal quantity for the fixed and regenerable charcoal beds for both the initial and revised contaminant load model. Flow rate requirements for the catalytic oxidizer and pre- and post-sorbent beds were also defined. The

TABLE 9 - POTENTIAL SOURCES OF CONTAMINANTS REQUIRING EXCESSIVE CHARCOAL FOR CONTROL

Contaminant	Potential Source	Is Source Controllable	Identified In Any Manned System	Identification in Apollo 101, 103 & LEM-3
Nitric Oxide	Not known	Yes	Yes	No
Freon 23	Refrigerant; Intermediate in organic synthesis	Yes Not known	Yes	No
Chlorofluoro-methane	Not known	Not known	Yes	No
Methyl Chloride	Refrigeration, Butyl rubber catalyst solvent. Petroleum refining; Foaming agent in Styrofoam mfg. Reagent in silicon production.	Yes Yes Yes Yes No	Yes	No

previous sections of this report describe the results of these analyses for the revised contaminant load model and Table 10 presents a comparison of these results for both contaminant load models. As can be seen from Table 10 the most significant change occurred with the fixed bed. Another significant change that occurred was the increase in flow rate required by the catalytic oxidizer. This flow rate increase was caused by a change in the carbon monoxide allowable concentration in the revised contaminant load. To achieve the required thermal performance in the catalytic oxidizer regenerative heat exchanger in a reasonable size it is necessary to accept a fairly high pressure drop. Since this heat exchanger was a relatively long-lead-time item it had been ordered prior to the contaminant load change. Thus the impact of changing system flow rate had a significant impact on the catalytic oxidizer pressure drop. In comparing the overall system pressure drop (i.e. power), cost, and the integration and control of the regenerable bed and the catalytic oxidizer with different ideal flow rate requirements it was arbitrarily decided to reduce the regenerable bed flow rate to be the same as for the catalytic oxidizer, since the only consequence would be that methyl alcohol would exceed the maximum allowable level by approximately 20% during the short-term period.

3.2 SYSTEM DESCRIPTION

Based upon the results of the computer analyses a contaminant control system concept and schematic was evolved. The schematic is discussed in this section and the analysis and optimization of individual components is presented in subsequent sections.

The trace contaminant control system consists of a high flow through a fixed charcoal bed, and a low flow through a regenerable charcoal bed, pre-sorbent bed, catalytic oxidizer, and post-sorbent bed. There are also fans, valves, instrumentation and controls. A schematic of the system is presented in Figure 2. A discussion of the system elements follows.

TABLE 10
SYSTEM CONFIGURATION COMPARISON BETWEEN
CONTAMINANT LOAD MODELS

Contaminant Load Models		
	Initial	Revised
Fixed Bed:		
Flow Rate l/min (CFM)	1980 (70)	1130 (40)
Charcoal Quantity kg (lb)	40 (88)	15.4 (34)
Regenerable Bed:		
Flow Rate l/min (CFM)	113 (4)	120 (4.25)
Charcoal Quantity kgm (lb)	4.7 (10.3)	5.8 (12.7)
Catalytic Oxidizer/Pre- and Post-Sorbent		
Flow Rate l/min (CFM)	93 (3.3)	120 (4.25)

quantity figure includes
saturation plus adsorption zones

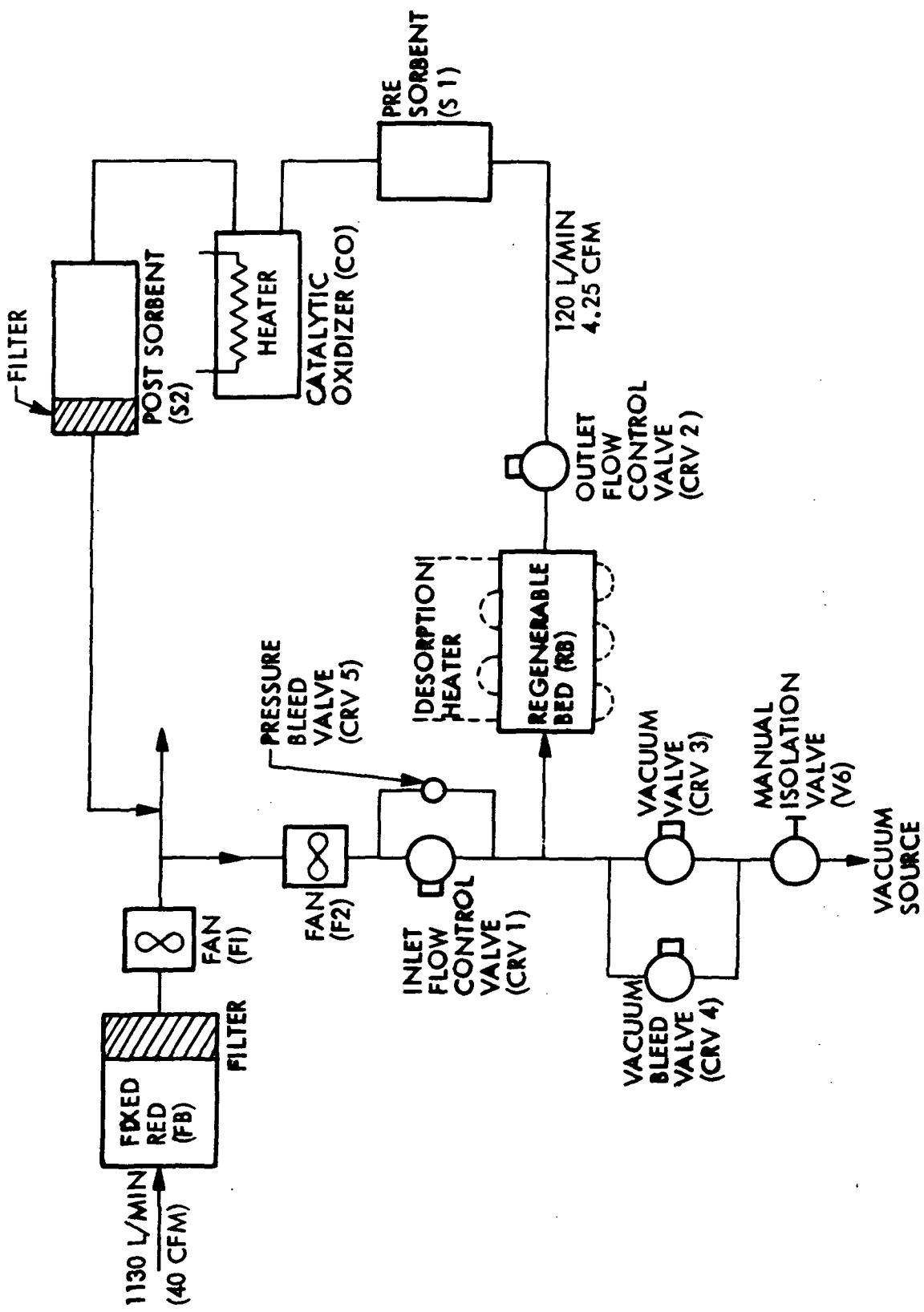


Figure 2 Trace Contaminant Control System Schematic

3.2.1 Fixed Bed

The fixed bed is designed for control of well-adsorbed contaminants, ammonia, and other highly water soluble contaminants. The fixed bed flow rate is 1130 l/min (40 SCFM), which is supplied by an in-line vane axial fan. A filter is located on the downstream side of the fixed bed which prevents particulate matter from entering other parts of the system.

3.2.2 Regenerable Bed Fan

A small portion of the fixed-bed effluent is delivered to the regenerable bed, pre-sorbent bed, catalytic oxidizer, and post-sorbent beds by a centrifugal fan. Air from the fan passes into the regenerable bed during the adsorption portion of the cycle. The temperature rise across this fan corresponds to the rise required as defined by the regenerable bed optimization.

3.2.3 Regenerable Bed

The regenerable charcoal bed will control the less well adsorbed contaminants including some of the contaminants that would tend to poison the catalyst. During the regenerable bed adsorption cycle 120 l/min (4.25 SCFM) of air leaving the fan passes through the inlet flow control valve and into the regenerable bed. The air entering the regenerable bed is at a maximum temperature of 311 K (100 F). This temperature has been selected to minimize the net system weight penalty.

The air then leaves the regenerable bed and passes through the exit filter and outlet valve. The 120 l/min (4.25 SCFM) then passes to the pre-sorbent bed and the catalytic oxidizer.

During the desorption cycle of the regenerable bed, operation of the system is as follows: The regenerable bed fan shuts down, the inlet and exit flow control valves close and the vacuum bleed valve opens. An external electric heater which is located on the periphery of the regenerable bed is energized to heat the bed. The desorption cycle is initiated once every 24 hours at the beginning of the daylight portion of the orbit. After the vacuum bleed

valve has been open 30 minutes, to allow the bed to reduce in pressure slowly, the vacuum valve is opened and the vacuum bleed valve is closed. Prior to the completion of the daylight portion of the orbit, the regenerable bed will be heated to temperature. At this point in the cycle, the heater power is reduced to maintain bed temperature.

When the desorption cycle is complete, after a total time of 195 minutes, the vacuum valve is closed, the guard heater is turned off and the pressure bleed valve opens to allow gas to bleed back into the canister. When this has been accomplished, at time 200 minutes, the inlet and outlet flow control valves are opened and the adsorption cycle is resumed. A diagram indicating the time phasing of the various functions and the status of individual components is presented in Figure 3.

3.2.4 Pre-Sorbent

A basic pre-sorbent bed (lithium hydroxide) is located upstream of the catalytic oxidizer to minimize the exposure of acid gases to the catalyst. Previous tests indicated that acid gases are primarily removed in the fixed charcoal bed. However, the exposure of the catalyst to acid gases even in very low concentrations will eventually result in catalyst poisoning. Consequently, extra precaution is warranted in protecting the catalyst against poisoning and particularly at the relatively moderate temperature in this application.

3.2.5 Catalytic Oxidizer

Air from the pre-sorbent canister flows into the catalytic oxidizer whose purpose is to oxidize hydrocarbons, CO and H_2 into less noxious substances. The canister contains a plate fin regenerative heat exchanger, two isotope heat sources and .74 l (45 in^3) of catalyst. The entire unit is insulated with approximately 2.5 cm (1 in) of Min-K 1301 insulation. An external 0.6 cm (1/4 in) blanket of Min-K is placed around the unit to maintain an acceptable touch temperature. The regenerative heat exchanger is a stainless steel plate fin unit with a 5 x 7.5 cm (2 x 3 in) cross section and flow length of 17.8 cm (7 in).

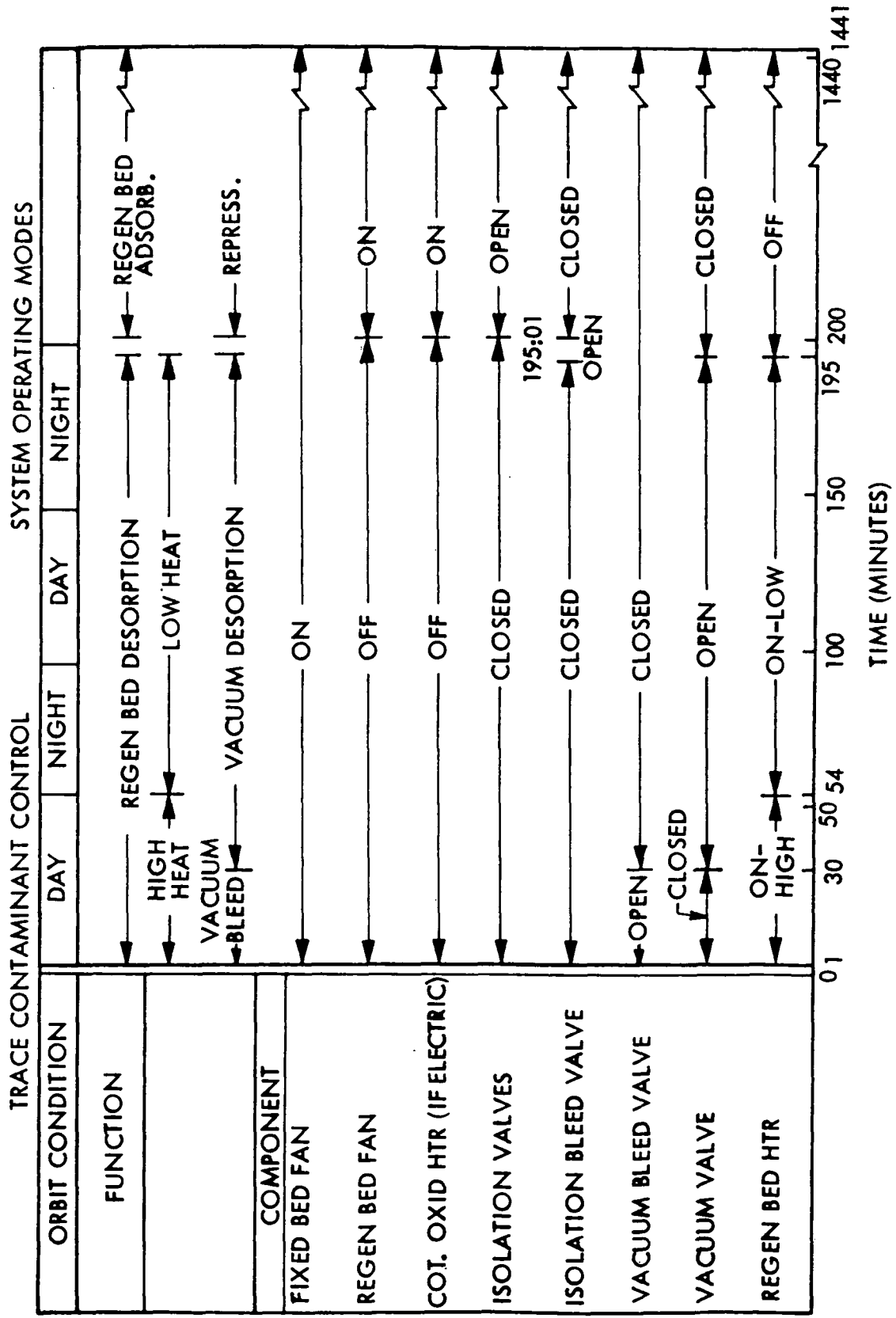


Figure 3 Trace Contaminant Control System Operational Modes

Inlet gas leaving the heat exchanger passes over the isotope heat sources and then into the catalyst bed. The gas from the catalyst bed then exits through the regenerative heat exchanger. The catalyst bed temperature is approximately 733 K (680 F) with 120 l/min (4.25 SCFM) of flow and 811 K (1000 F) during the no-flow conditions. The regenerative heat exchanger outlet temperature is approximately 344 K (160 F) during flow conditions. The downstream post-sorbent bed is insulated to maintain acceptable touch temperatures.

3.2.6 Post-Sorbent

A basic post-sorbent bed (lithium hydroxide) is located downstream of the catalytic oxidizer to remove any potential undesirable acidic products of oxidation. It is not anticipated that any significant quantity of compounds such as the halogenated compounds reach the catalytic oxidizer since these could be reacted to acidic oxidiation products. The post-sorbent bed is provided as a safeguard should this occur.

SECTION 4

COMPONENT OPTIMIZATION

This section of the report describes the results of the individual component optimization studies based on the initial contaminant load model, and the final component configuration selected which was based on the final contaminant load model. During the course of this program two contaminant load models were considered. The first load model selected for the program was based on the Space Station Prototype (SSP) General Specification SVSK H54655. Trade studies and computer analyses were conducted to define the system configuration in terms of component arrangement, system flow rates, and component sizing. Following the system definition the individual component optimizations were conducted. These results constituted the initial preliminary design. After the completion of the preliminary design effort a revised contaminant load model was developed by NASA for the SSP program. The trade studies were revised to include the impact of the new contaminant load model on the system configuration and component sizing and flow rates. The component designs were not reoptimized; however, new component configurations were defined based on criteria established in the previous optimization. These criteria included maintaining L/D ratios or component pressure drop characteristics wherever possible. This approach was considered valid since no major change in component sizing occurred as a result of the revised contaminant load.

4.1 FIXED CHARCOAL BED

In the analysis conducted to define the system flow schematic, with the initial contaminant load, the mass of the saturated zone was estimated to be 28.9 kg (63.7 lb). A complete definition of the bed also requires an estimation of the adsorption zone required for the bed. In NASA CR 2027, Figure 12, the adsorption zone length for benzene, which is one of the design contaminants for this bed, is shown to be 0.46 cm or 0.18 inches at a velocity of 33 cm/min 1.3 (ft/min). Further, this zone length has been shown to scale directly with

superficial velocity. In order to help assure good bed distribution and assure validity of the adsorption zone length, a minimum L/D of 1.0 should be maintained. The minimum pressure drop and bed penalty will occur when the largest possible particle size is used. Thus, a 4 x 6 mesh activated charcoal was selected. The relation of the diameter, (L/D), adsorption zone length, total length, pressure loss, and fan penalty are indicated in Table 11.

TABLE 11
VARIATION IN FIXED BED PARAMETERS
WITH DIAMETER

Diameter, cm(in)	40.6(16)	43.2(17)	45.6(18)	48.2(19)	50.8(20)
Adsorption Zone cm(in)	17.8(7.0)	15.5(6.1)	14 (5.5)	12.5(4.9)	11.4(4.5)
Total Length cm(in)	64.2(25.3)	56.6(22.3)	50.8(20.0)	15.5(17.9)	41.1(16.2)
L/D	1.58	1.30	1.1	0.94	0.81
Pressure Loss N/m ² in H ₂ O	1320(5.32)	976(3.92)	732(2.94)	568(2.28)	446(1.79)
Fan Penalty, kg (lb)	40(88)	30(65)	22(49)	17(38)	14(30)

The fan penalty is based on an assumed efficiency of 29 percent and continuous AC regulated power. Pressure drop data is plotted in Figure 4, which presents pressure loss and flow for activated charcoal of three mesh grades.

All of the above beds have the same volume, which corresponds to a total bed weight of 40 kg (88 lb). It is clear that the fan power is a considerable portion of the total penalty and that significant savings in total equivalent weight can be realized by selecting the largest diameter possible. Consistent with the desire to maintain L/D at 1.0 or larger, the 45.6 cm (18 in) bed diameter was selected.

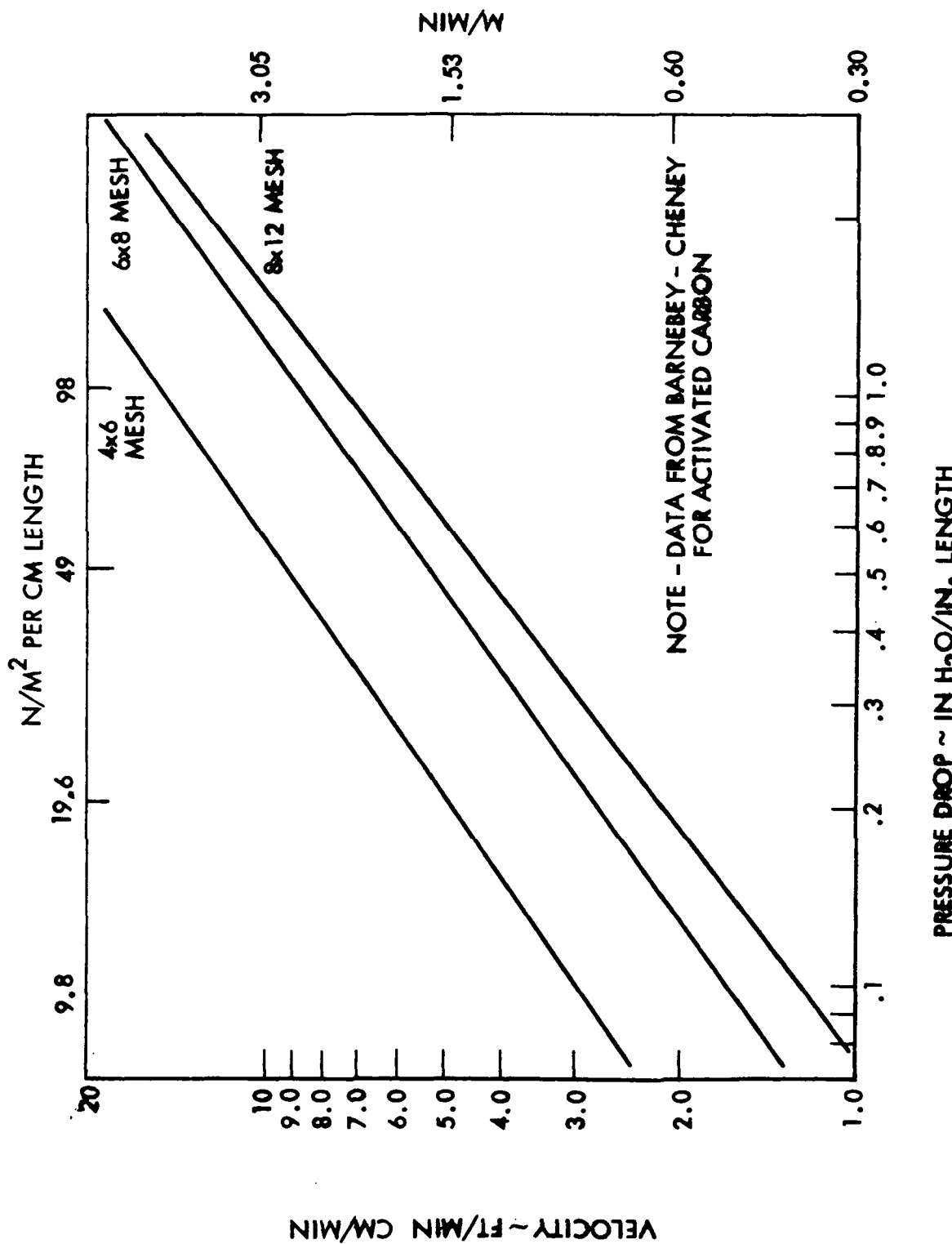


Figure 4 Sorbent Bed Pressure Loss Correlation

In summary, the fixed charcoal bed, for the initial contaminant bed, has a 45.6 cm (18 in) diameter, is 51 cm (20 in) long, and has a fixed weight of 40 kg (88 lb). The bed is capable of controlling all contaminants having an A value less than the value for benzene for up to 180 days. The charcoal is treated with 2 millimoles per gram of phosphoric acid for ammonia removal.

The selected fixed bed for the final contaminant load was chosen on the basis of maintaining the same L/D and resulted in a final bed design of 33 cm (13 in) in diameter, 38 cm (15 in) long with 15.5 kg (34 lb) of activated charcoal having a pressure loss of 6.4 cm (2.5 in) of water at the design flow rate.

4.2 REGENERABLE BED

The following section describes the analyses conducted to define the configuration and operating conditions for the regenerable bed, for the initial contaminant load.

4.2.1 Adsorption Cycle

The process of contaminant adsorption by a regenerable bed involves several design criteria. The greatest influences on bed design are the contaminant load or removal requirements, process air flow, pressure drop and fan power, adsorption temperature, and regeneration frequency and temperature. Each affects system weight so it is necessary that the fan size, pressure drop, and bed size be optimized for net weight while meeting the removal requirements for this bed. The weight factors considered in the optimization are listed below:

1. Vehicle heat rejection penalty
2. Vehicle power penalty
3. Regenerative bed weight
4. Desorbed water vapor vented

Vehicle heat rejection penalty is the weight required to radiate heat from the vehicle. It was assumed that the heat would be added directly to the cabin atmosphere. This heat primarily results from fan power. The vehicle power penalty for this analysis also results from the fan.

The regenerative bed weight is included in the optimization because its adsorption capacity, and consequently bed size, is strongly influenced by inlet air temperature, which is a function of air heating by the fan.

Desorbed water vapor vented overboard is a variable because the total amount vented overboard is dependent upon bed size and relative humidity of the air passing through the bed. Air temperature is, in turn, a function of the fan power.

Assumptions made are shown below:

1. System flowrate - 113 l/min (4 SCFM)
2. Cabin air temperature - 292 to 297 K (65 F to 75 F)
3. Dew point - 284 K (57 F) nominal
4. Overall fan efficiency - 25%
5. Heat rejection penalty - 0.032 gm per joule/hr (0.074 lb per BTU/hr)
6. Power penalty - continuous regulated DC, 268 kg/kw (591 lb/kW)
7. Water loading for the selected charcoal is shown in Figure 5.

Maximum cabin dew point at minimum cabin air temperature was used for process air conditions. This was done because relative humidity is maximum under those conditions, which results in the maximum water adsorption to be expected. The relation between water adsorbed by the charcoal and inlet relative humidity is shown in Figure 6.

It is important to note the degree to which water adsorption increases with increasing relative humidity of air entering the regenerative bed. It is evident that the process air could be heated upstream of the charcoal bed in

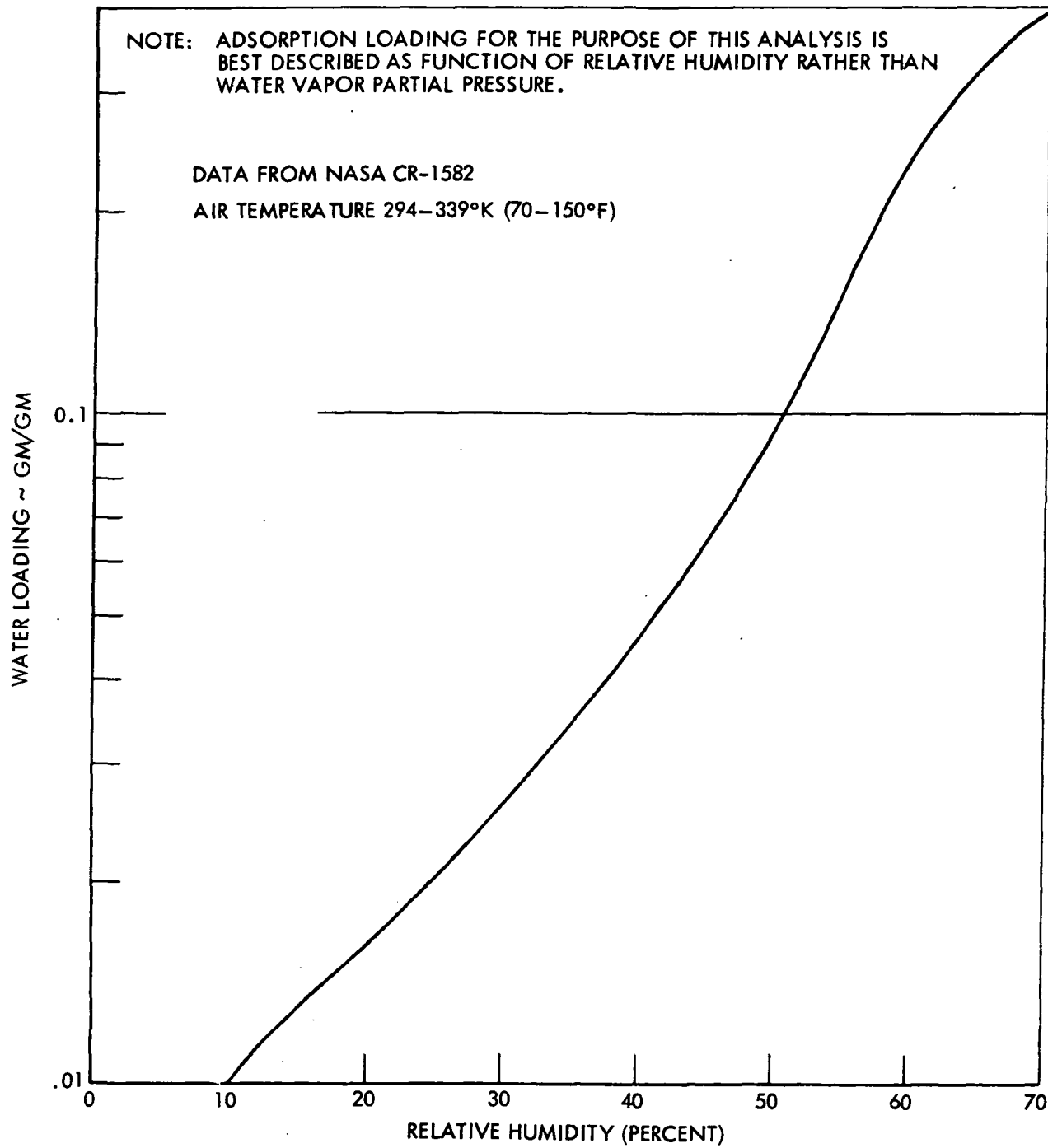


Figure 5 Water Absorption Isotherm for Barnebey Cheney Activated Charcol Type BD

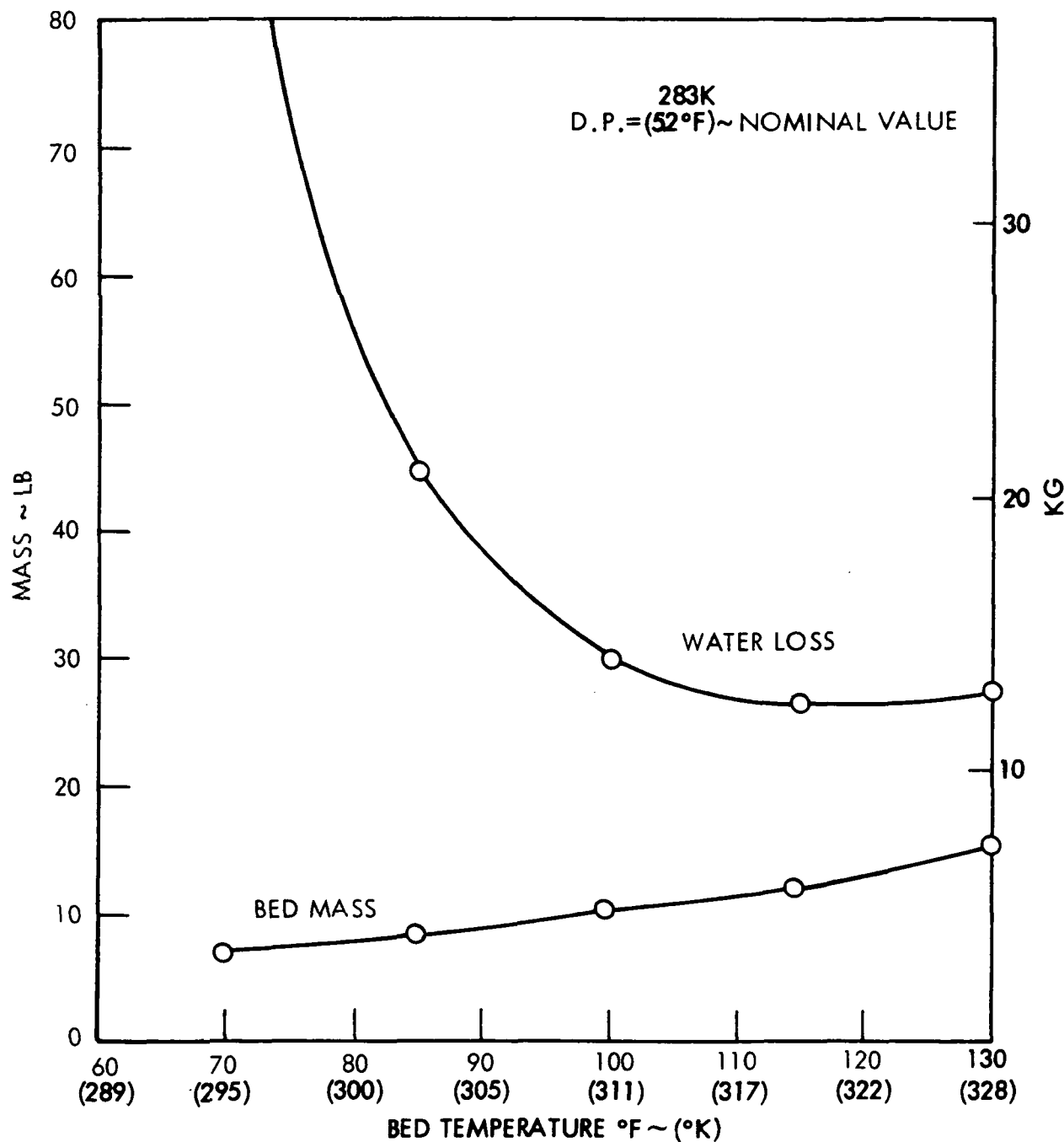


Figure 6 Regenerable Charcoal Bed Temperature Effect on Mass and Water Loss

order to reduce the water dump penalty. This may be accomplished by fan heating or by fan heating plus a heater. Both approaches were considered in the optimization. The effect of bed inlet temperature on the water lost during desorption is shown in Figure 6. As can be seen, the effect is pronounced.

Bed size is based upon a process temperature equal to the temperature rise due to the fan and/or heater plus an initial cabin temperature of 297 K (75 F). This results in the maximum bed size necessary for normal operating conditions. As shown in Figure 6, the bed size is also a function of temperature.

The analytical procedure used to define the regenerable bed was to (1) calculate air temperature rise due to the fan and/or heater power for a given system pressure drop, (2) calculate bed size and weight based upon air temperature, (3) calculate water adsorbed based upon relative humidity of the heated air, (4) compute power and heat rejection penalties based upon fan and heater power, (5) system total weights, and (6) repeat for other system pressure drops.

The results of the optimization are presented in Figure 7. The bed inlet temperature and the bed total equivalent weight is plotted as a function of system ΔP or regenerable bed fan head rise. It can be seen from this figure that the minimum total equivalent weight occurs at a system ΔP of 36 cm (14 in) of water with a bed temperature of 302 K (85 F). The fan provides sufficient temperature rise to create this inlet air temperature. Below 36 cm (14 in) of water head rise, if no additional heating is provided, the bed inlet temperature will fall and the total equivalent weight will rise drastically due to the increase in water loss during desorption at the higher inlet relative humidities.

A separate inlet heater could be provided to maintain the inlet temperature; however, this does not cause a reduction in total equivalent weight as can be seen by the dashed lines on Figure 7. Thus, the optimum operating condition is to provide all of the heat required with the regenerable fan and to operate at the desired bed inlet temperature.

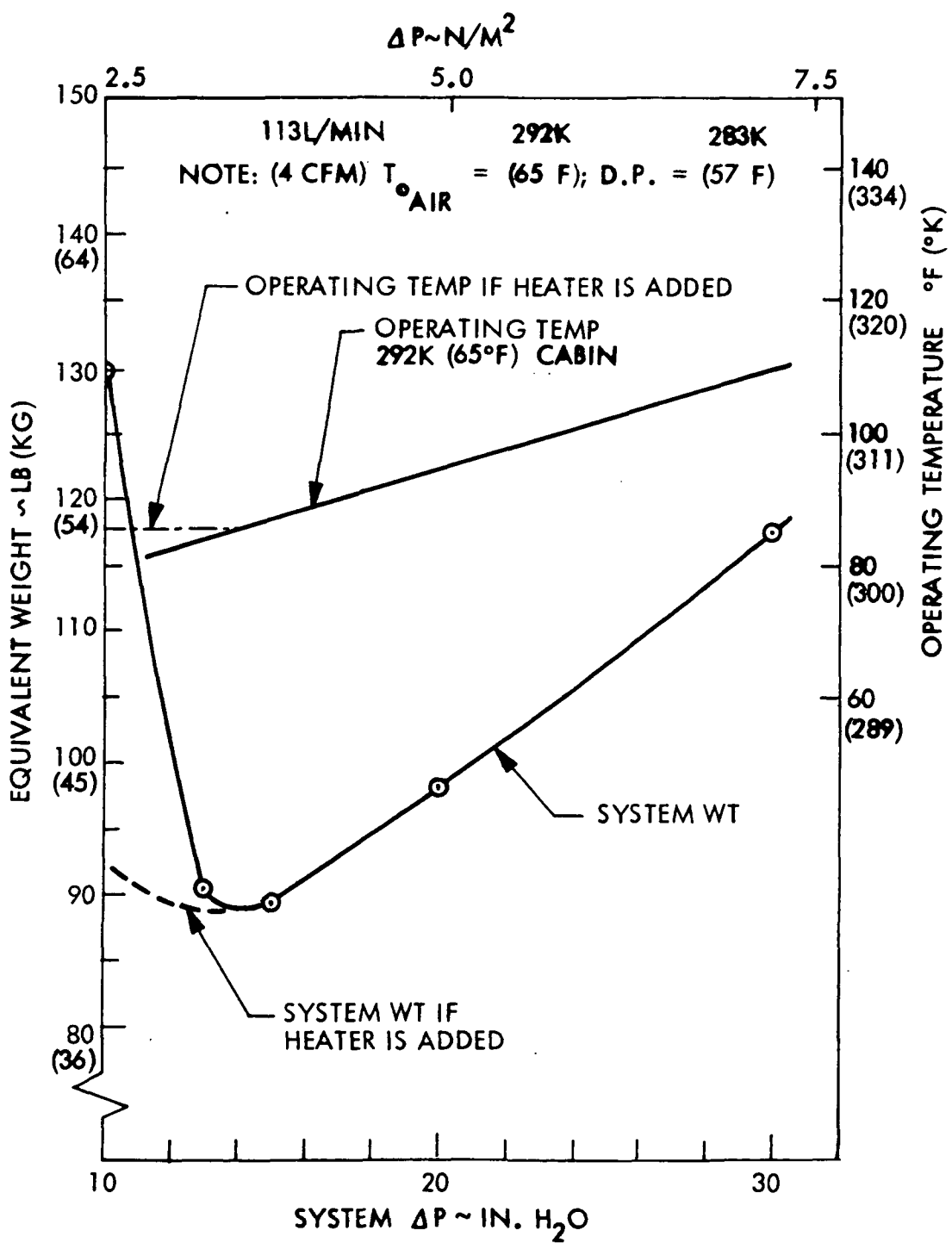


Figure 7 Regenerable Activated Charcoal Optimization

In summary, the optimum operating temperature is for a bed temperature of 302 K (85 F) for a 291 K (65 F) cabin. The low cabin temperature was assumed for the optimization as it represents a conservative approach to the design. Also, because of the severe penalty due to water loss, a 2-3 K (5 F) margin was assumed which raises the normal bed temperature to 305 K (90 F) with a 291 K (65 F) cabin. As the cabin temperature can rise as high as 297 K (75 F) under normal operating conditions, the bed sizing is based upon a 311 K (100 F) operating temperatures which represents the maximum normal operating temperature with a fixed air temperature rise.

The charcoal requirements for the saturated zone were established in Section 3.1 as 4.2 kg (9.3 lb) for a 311 K (100 F) operating temperature. The adsorption zone length was based on an "A" value of 34.7 which corresponds with tetra-fluoroethylene, the final contaminant controlled by the regenerable bed. For this "A" value, the adsorption zone length for a linear velocity of 33 cm/min (1.3 ft/min) is 0.97 cm, as given in Figure 12 of NASA CR-2027.

Selection of a one-day adsorption cycle was based upon studies made in a previous NASA contract reported in CR-2027, which showed a reduction in total equivalent weight as the cycle time is reduced. No reversal of this trend is observed down to periods less than 0.5 day. A one-day cycle was established, however, to minimize valve cycling which would improve system reliability. An additional consideration is the desire to establish an easy-to-monitor pattern during the development and to have a period that matches with an integral number of orbits, which is 16 orbits for the 24-hour cycle time.

The charcoal chosen for the preliminary design was an 8-12 mesh size. This selection is based upon an anticipation of the selected finned canister with 2.5 cm (1 in) fin spacing and a desire to maintain at least 10 particle diameters between the fins. A finer mesh would only serve to increase ΔP without apparent benefits; as the saturated zone and adsorption zone length data is based upon a similar mesh material. Table 12 presents the relation of several bed design parameters to the bed diameter. The pressure loss is based upon data presented in Figure 4.

TABLE 12
INFLUENCE OF BED DIAMETER ON DESIGN PARAMETERS

Diameter cm (in)	12.7(5)	15.3(6)	17.8(7)	20.3(8)	22.8(9)
Length cm (in)	76.2(30)	52.8(20.8)	38.6(15.3)	29.8(11.75)	23.6(9.3)
L/D	6	3.47	2.19	1.47	1.03
Pressure Loss N/m ² in H ₂ O	2460(9.9)	1060(4.25)	526 (2.11)	290(1.16)	169(0.68)

To achieve the desired regenerable bed inlet temperature, a total fan pressure rise of 3.5 kN/m^2 (14 in) of water is required. The regenerable bed pressure drop must be in the neighborhood of 0.5 kN/m^2 (2 in) of water to achieve the desired system pressure drop of 3.5 kN/m^2 (14 in) of water. Based upon the desire to have a bed pressure drop of approximately 0.5 kN/m^2 (2 in) of water, the 17.8 cm (7 in) diameter bed was selected. The L/D of 2.11 will assure good performance and uniform flow distribution.

This bed was then utilized as the base line for further investigations to define the optimum approach to desorption.

4.2.2 Desorption Cycle

The regenerable charcoal bed is subjected to vacuum while at elevated temperatures during the adsorption cycle. Temperature and vacuum requirements are discussed in NASA CR 2027. The purpose of this analysis is to establish the heating mode and heater requirements.

There are several methods of heating the charcoal bed, each with variations in operational sequences. The methods considered in this analysis are:

1. Heat during evacuation with heater
2. Closed loop circulated air, heater and/or fan heat
3. Closed loop circulated air, waste heat plus fan heat
4. Heat before evacuation with heater, no air flow

These approaches are shown schematically in Figure 8.

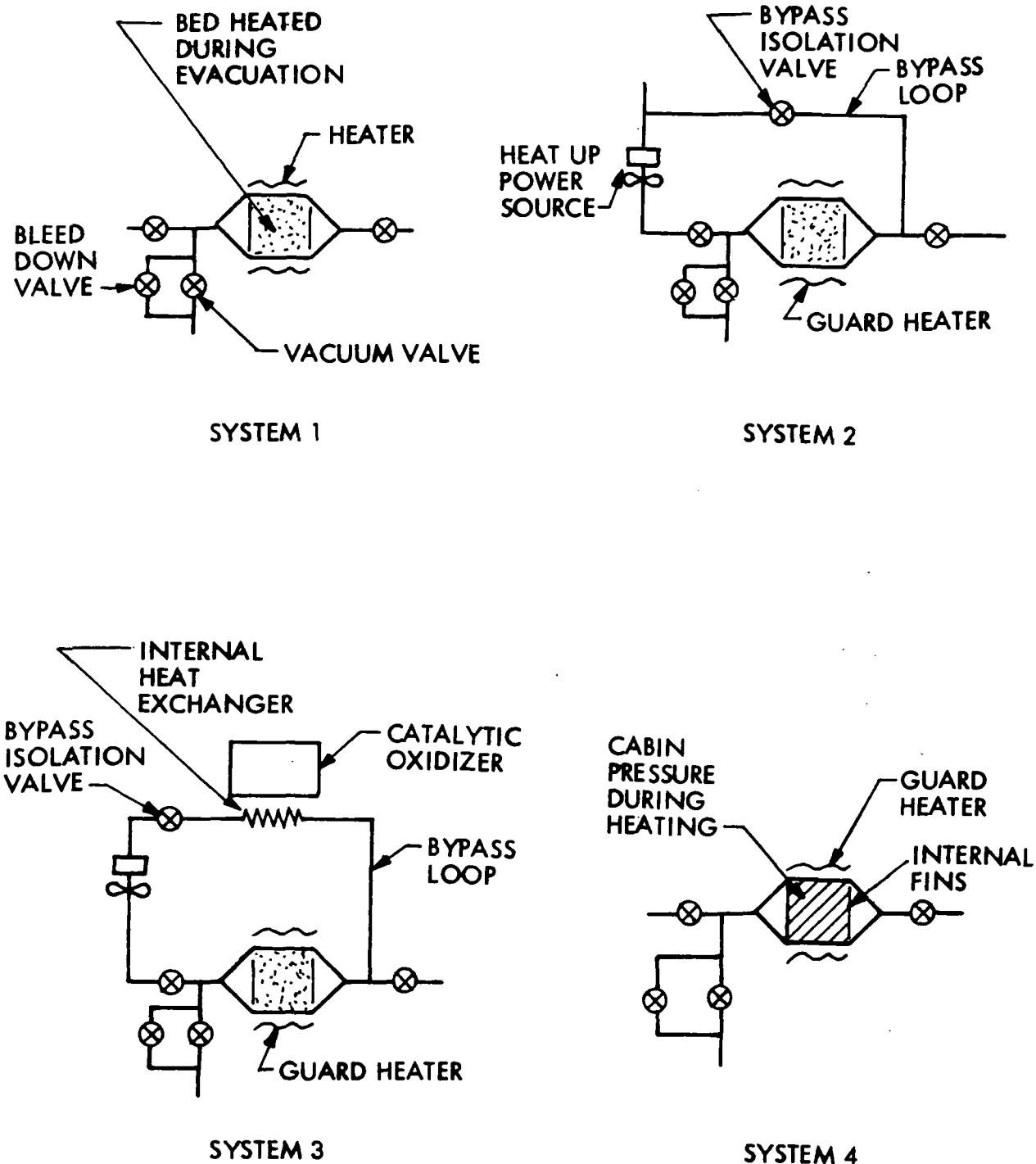


Figure 8 Desorption Cycle-Analysis System Schematics Studied

Heating of system 1 takes place during bed evacuation. Radiation through the bed is the primary mechanism for heat transfer. This configuration is similar to system 4, except that heat up times are longer. A potential advantage of this system is that the total desorption cycle duration may be reduced since heating and desorption takes place simultaneously.

System 2 essentially utilizes convective air to heat up the bed. A bypass loop and isolation valve are added to the basic system to provide closed loop circulation. The fan, bed, plumbing, and circulating air heat up together. This system has the advantage of relatively uniform bed heating.

System 3 is similar to system 2 in concept, but uses waste heat from the catalytic oxidizer as the heat source. The advantage of this system is that power and heat rejection penalties may be reduced when compared to any of the other systems.

System 4 utilizes air as a conductor during the heating process. The heaters may be placed within the charcoal, around the outside of the bed canister, or both. A disadvantage of this system is that if heaters are not strategically placed, then the heat up time will be excessive, the required heater temperature will be excessive, or both. However, the bypass loop of system 2 or 3 is not required.

The analyses of these systems were performed in two levels. The first level was a cursory look at the advantages and disadvantages of each. Systems 1 and 3 were eliminated in this manner. Systems 2 and 4 were then analyzed in more depth. The analysis and results of each system will now be discussed.

4.2.2.1 System 1 - Both heating and evacuation are begun together by powering up the heater, closing the inlet and outlet flow control valves, and opening the bleed down valve. Pressure within the bed will rapidly fall to low vacuum conditions. Simultaneously, water will be desorbed and dumped overboard.

The latent heat of vaporization will, however, lower the bed temperature to the freezing point of the water. The bed will then remain at the freezing point until the remaining ice sublimes. Enough heat must therefore be added to the bed to vaporize the ice and raise the temperature of the bed to the required desorption temperature of the bed to the required desorption temperature of 373 K (212 F).

The means of transferring heat into the bed became the primary concern for this system, since heating takes place at very low pressure and radiation is the primary means for heat transfer. Heat-up time was therefore estimated. The assumptions made are:

1. Heaters located around canister
2. Bed diameter 17.8 cm (7 in)
3. Maximum heater temperature, 477 K (400 F)
4. Bed desorption temperature, 372 K (212 F)
5. Charcoal emissivity, 0.95
6. Heat transfer from one granule to the next is:

$$q = \frac{\sigma A \epsilon}{2} (T_h^4 - T_c^4)$$

7. One dimensional heat transfer
8. Granule size, 0.19 cm (0.075 in) diameter
9. Conduction through granule neglected

The heat-up time to vaporize the water and raise the mean bed temperature to 373 K (212 F) was calculated to be in excess of 10 hours. This is a conservatively short time, since granule internal conduction, which was neglected in the calculations, will further increase the temperature drop from one granule to the next. The ten hour heat-up time is quite excessive and the system was dropped from further contention.

4.2.2.2 System 2 - This system was the leading candidate for regenerable bed heating until all of the practical hardware characteristics were considered.

The original concept, shown in Figure 9, had a 2.5 cm (1 in) bypass line and valve. The circulation fan was a centrifugal type. The method of heating was to close the bed outlet flow control valve, open the bypass valve, (and the dump valve in the prototype case), turn on the heat-up heater, and maintain fan flow. A continuous closed loop flow of air was thereby formed.

Flow resistance of the continuous loop was less than the adsorption circuit. Volumetric flowrate was, therefore, increased during bypass flow and a new high flow equilibrium was established. The bed flowrate increased from the adsorption rate of 113 l/min (4 CFM) to the heat-up rate of 385 l/min (13.6 CFM). The increased flow resulted in fan power increase and more significantly, decreased bed temperature drop from inlet to outlet. The temperatures in the loop are shown in Figure 9 for the heated condition just before evacuation. These data show that the bed can be heated with moderate temperature air. Valving is available that can withstand these temperatures. However, in reviewing the fan selection, it appeared that an optimum flight fan with the desired head rise and flow characteristics would probably be a positive displacement type as opposed to centrifugal. Thus, for a flight situation increased flow in the recirculation mode would not occur, and the flowrate would be 113 l/min (4 CFM) for both adsorption and desorption heat up. With this reduced flowrate, the temperature drop between the inlet and outlet of the bed increased considerably, since nearly the same quantity of energy had to be transferred in the same time period. The amount of heat transferred with the low flow is greater because the bed has to be heated to a higher average temperature and because the leak rate is greater at the higher bed temperature. These temperatures are shown in the Figure 9 sketch below. Because of the excessive temperatures shown, this configuration was eliminated.

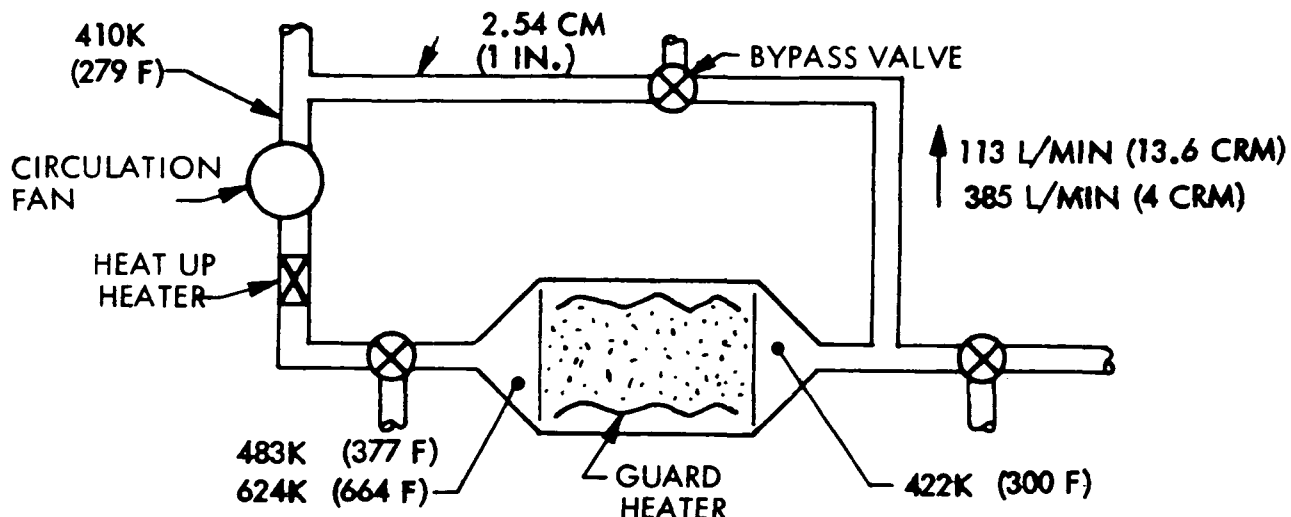


Figure 9 Desorption Temperatures for System 2

4.2.2.3 System 3 - This system was eliminated early during the cursory analysis because the weight savings by using waste isotope heat were considered insufficient to justify the additional complexity, cost, and thermal balancing required. The additional equipment required could be a built-in shell heat exchanger within the catalytic oxidizer. It would be located between the insulation and the catalyst canister. The practical weight savings over System 2, considering additional hardware and power penalty, is approximately 7.25 kg (16 lb).

4.2.2.4 System 4 - Figure 10 illustrates the configuration analyzed. A heater is placed on the outside surface of the canister. Heaters located within the charcoal would have improved heat transfer characteristics

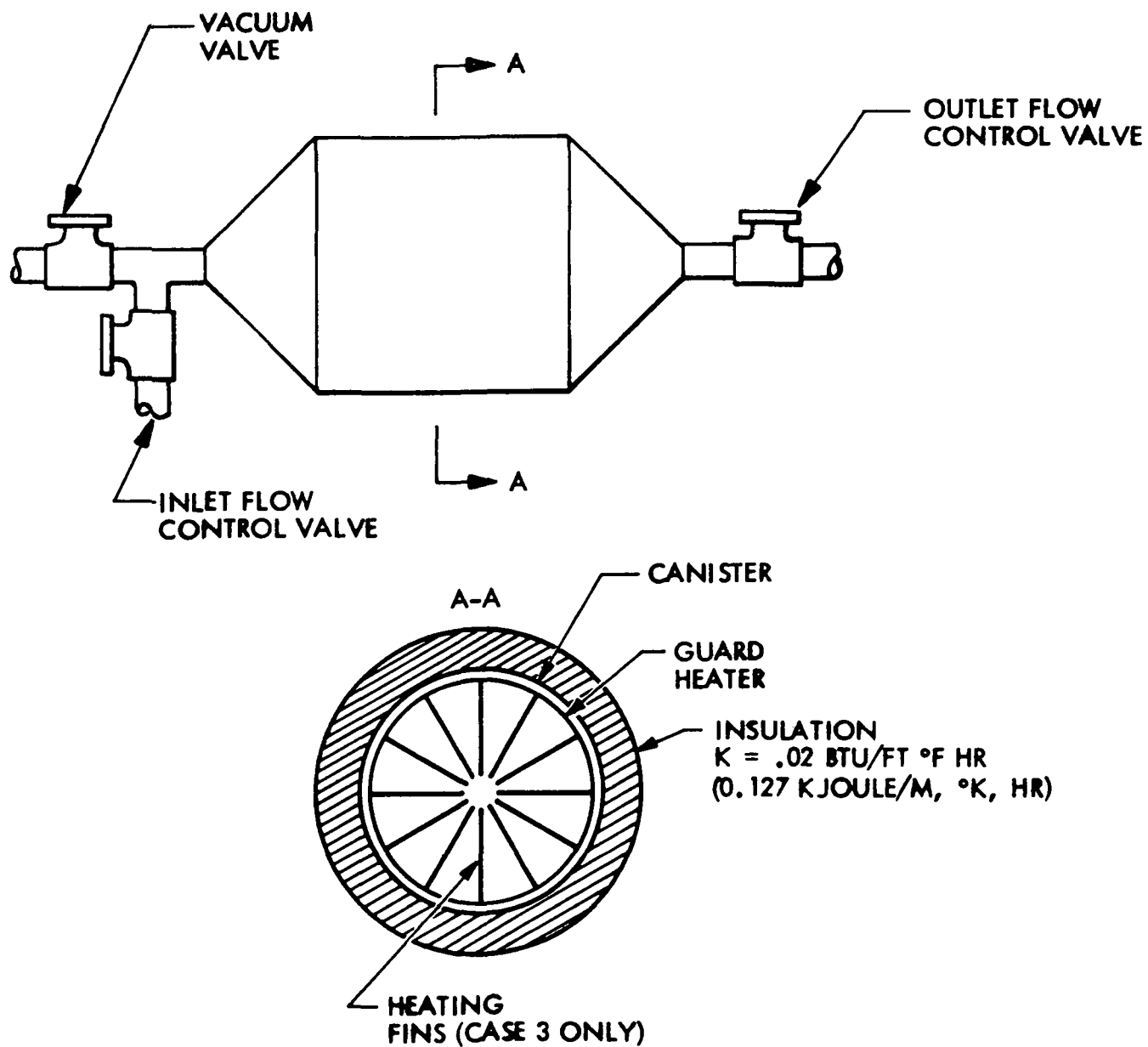


Figure 10 Regenerable Activated Charcoal Bed - Selected Configuration

but would require an electrical feed-through that must penetrate the pressure shell, and so they were eliminated from the analysis. Insulation surrounding the canister reduces heater power and the power and heat rejection penalties.

The desorption cycle for this system consists of first heating up the bed to 422 K (300 F) with the guard heater at a high power level prior to evacuation, and then evacuating the bed. The desorption temperature then rapidly falls to a minimum of 373 K (212 F) due to water evaporation during evacuation. This temperature is maintained with the guard heater at a low power level. The initial heat-up temperature is based upon maximum evaporative cooling with a 5 K (10 F) temperature margin.

Three heating cases were examined. The first case was to restrict the maximum heater temperature to 450 K (350 F) without the fins that are shown in Figure 10. This temperature limitation represents a safe maximum temperature to preclude charcoal degradation. The second case was to restrict the heat-up time to the time that the spacecraft is in the sunlight during one orbit, 54 minutes. Fins also were not used with this case. The time limitation permits a reduced power penalty since heating can be done entirely in sunlight.

No fins were used with either of these cases so that the performance of the least complex configurations could be determined. The results are listed below:

	Case 1 450 K (350 F) Maximum Heater Temp.	Case 2 54 Minutes Max. Heat-up Time
Heat-up time to 422 K (300 F)	10 hrs.	54 min
Maximum heater temp, K (F)	450(350)	644(700)
Heater Power (watt)	41	234
Insulation Thickness cm (in)	2.5(1)	6.3(2.5)
Adsorption Time (hrs)	13	22

It can be seen that either a very long heat-up period is required or that a very high temperature is required. Case 1 is not weight competitive because the adsorption period is considerably shortened by the long duration desorption period and the system size and weight would have to be significantly increased over Case 2. (approx: 27.3 kg (60 lb)). In case 2 the temperature gradient in the bed is excessive and degradation may occur.

Case 3 reduces both the temperature and time problem by including fins within the bed to enhance heat transfer. These fins are aluminum sheets spaced approximately 2.5 cm apart which are aligned with the canister longitudinal axis. The spacing is the minimum whereby a high degree of confidence exists that there will be no air channeling at the fin surface.

System characteristics for the selected configuration are summarized below:

Heat-up time	54 minutes
Maximum heater temperature	470 K (386 F)
Heater power	213 watt
Insulation thickness	3 cm (1.25 inch)
Adsorption time	22 hours

The bed was thermally modeled by calculating the temperature profile for the charcoal between the two center fins, assuming that convection and radiation from the fins to charcoal would be negligible. This was done from the relation;

$$q_x = q_{\text{fin}} (L - x)$$

where L = half of distance between fins 1.25 cm (0.5 in)

q_{fin} = heat flux at fin surface

x = distance from fin surface

which states that, after the temperature of charcoal at the mid-point between the fins begins to rise, the temperature gradient, dT/dx is constant at any point. The temperature at any point x was derived from the above relation and is,

$$T_x = \left(\frac{dT}{dx} \right)_{fin} \quad (LX = \frac{x^2}{2}) \quad + T_{fin}$$

where

$\frac{dT}{dx}_{fin}$ is the charcoal temperature gradient at the fin surface.

and the mean temperature is

$$T_{mean} = T_{fin} - \frac{(dT)}{(dx)_{fin}} \frac{(L)}{(3)}$$

The charcoal temperature gradient was found from,

$$\frac{dT}{dx}_{fin} = \frac{q_{fin}}{K_{charcoal} A_{fin}}$$

Assumptions and requirements are listed in Table 13.

The spread between the charcoal mid-point and fin surface was calculated to be 57K (102 F) for a heat-up time of 54 minutes.

The mean temperature of the charcoal was calculated to be 38 K (68 F) lower than the fin temperature. The fin temperature is, therefore, 460 K (368 F) when the mean charcoal temperature is 422 K (300 F). The charcoal mid-point temperature between the fins is 403 K (266 F). Although the mid-point temperature is less than 422 K (300 F), it was assumed that during the evacuation process and subsequent guard heating, the temperature in the bed would rapidly become uniform.

The minimum temperature in the bed is only found on the longitudinal axis of the canister. The temperature between the center fins near the canister surface is higher because of the gradient of the fins. This gradient was calculated by the same method as the charcoal gradient. The resulting temperature rise from the fin center to canister surface is 7 K (13 F) for a 0.13 cm (.05 in)

TABLE 13
ASSUMPTIONS AND REQUIREMENTS FOR
REGENERABLE CHARCOAL BED ANALYSIS

Fin spacing	2.54 cm (1 in)
Fin dimensions	39.7 cm by 0.13 cm (15.6 in by 0.05 in)
Fin material	Aluminum
Mean charcoal temperature between fins	422 K (300 F) (at bed center)
Guard heater power	44 watt
Insulation thickness	3.2 cm (1.25 in)
Desorption temperature	373 K (212 F)
Heat-up time	54 minutes
Heat-up power penalty (daylight)	70 kg/KW (154 lb/KW)
Heat rejection penalty (directly to cabin air)	0.0318 gm per joule/hr (0.074 lb/BTU/hr)
Insulation conductivity	.133 k joule/m, K, hr (0.021 BTU/hr ft F)
Cabin air temperature	291 K (65 F)
Initial bed temperature	311 K (100 F)
No air circulation outside canister	
Heater power is constant during heat-up	
Charcoal conductivity	.127 k joule/m, K, hr (0.02 BTU/hr ft F)
Charcoal mass	4.6 kg (10.05 lb)
Charcoal specific heat (BC-BD)	1.04 joule/gm K (0.24 BTU/lb F)
Bed size	17.8 cm dia. by 39.7 cm (7 in. dia. by 15.6 in.)

aluminum fin. The fin/canister junction temperature is therefore 467 K (381 F) for the two center fins. The 0.13 cm (.05 in) thickness was selected because of ease of fabrication and structural stiffness, even though the weight optimum thickness is approximately 0.07 cm (.03 in). The optimum is based upon increased power penalty and reduced fin weight for thinner fins. The overall penalty of 0.13 cm (0.05 in) fins is 0.36 kg (0.8 lb).

Since Concept 4 provided the desired desorption conditions without excessive charcoal temperatures, as in the case of Concepts 1 and 2, it was selected as the preferred approach.

4.2.3 Final Regenerable Bed Selection

The final configuration of the regenerable bed based on the revised contaminant load utilized the same L/D and resulted in the configuration shown in Table 14.

TABLE 14
FINAL SELECTED REGENERABLE BED CONFIGURATION

Length	-	41.9 cm (16.5 inches)
Diameter	-	19.1 cm (7.5 inches)
Sorbent	-	5.8 kg (12.7 lbs) 8 x 12 mesh Barnebey Cheney BD charcoal
Desorption Power*	-	150 watts during heat up 50 watts during guard with approximately 1 inch insulation
Inlet Temperature	-	311°K (100°F)
Differential Pressure	-	522 N/m ² (2.1 inches water)
Flow Rate	-	120 l/min (4.25 SCFM)
Inlet & Outlet Duct Diameter	-	2.5 cm approx (1 in)
Weight	-	9.1 kg approx (20 lbs)

*Altered during checkout test phase

4.3 PRE-SORBENT

The primary function of the pre-sorbent bed is to protect the catalytic oxidizer from potential poisons. Test experience has shown that chemical compounds which contain halogens, sulfur, and nitrogen are likely to deactivate the catalyst material. As previously discussed, the total contaminant load is controlled with a combination of beds. A survey of the total contaminant list shows that the bulk of potential poison materials are removed in the fixed and regenerable activated charcoal sorption beds. The primary nitrogen source, NH_3 , and all contaminants requiring high removal flows are removed in the fixed charcoal bed. The design of the regenerable bed is established to allow the maximum removal of poison materials within practical bed size limitations as discussed in the previous section.

After matching the total contaminant list with those contaminants controlled in the charcoal beds, the following table of contaminants which are catalyst poisons and must be controlled by the pre-sorbent canister, results:

TABLE 15
CONTAMINANTS REMOVED BY THE PRE-SORBENT BED

Contaminant	Formula	Gen. Rate gm/day	LiOH Required mols/day $\times 10^{-2}$
Chlorine	Cl_2	.25	.706
Hydrogen Chloride	HCl	.25	.686
Hydrogen Fluoride	HF	.25	1.250
Nitrogen Dioxide	NO_2	.25	.540
Nitrogen Tetraoxide	N_2O_4	.25	.540
Sulfure Dioxide	SO_2	.25	.375

Table 15 lists the contaminants to be removed by the pre-sorbent bed, the design generation rate (or required removal rate), and the moles of LiOH sorbent required for control, assuming complete reaction. It can be seen that less than 0.23 kg (0.5 lb) for a 180-day mission is required if complete reaction is assumed. Assuming that a 90% contaminant removal efficiency is desired, a bed design was generated.

Since each of the above contaminants is removed by the charcoal beds at their MAC levels, the use of the design generation rate is setting the LiOH requirement is conservative. The primary function of this bed is as a back-up to the charcoal beds and to reduce the level of these potential catalyst poisons to the lowest possible level.

In operation, the lithium hydroxide will be converted to lithium carbonate by a high level of carbon dioxide in the circulating process air. Each of the contaminant materials listing in Table 15 is more strongly adsorbed than the carbonate and thus will displace CO_2 and be adsorbed by the bed forming lithium salts. The final bed size was established after reviewing the sorption characteristics of carbon dioxide on lithium hydroxide. Previous testing at IMSC under NASA contract of an integrated contaminant control system has demonstrated the validity of using the CO_2 data for pre- and post-sorbent bed calculations (Ref. 3).

In Figure 11, the relationship between contact time and chemical utilization is presented for a removal efficiency of 90 percent. The contact time is the total LiOH volume divided by the gas flow rate. The bed volume is based on a lithium hydroxide density of 480 kg/m^3 (30 lb/ft^3).

A total of 0.041 g moles per day or 0.177 kg (0.39 lb) per 180-day mission are required for complete reaction (see Table 15). Using Figure 11, we see that 0.91 kg (2 lb) are required to achieve the desired 90 percent removal of these materials. The resultant bed volume is 1.9 l (0.067 ft^3). Using this bed volume, the bed pressure loss was then calculated as a function of diameter using the data for 6 x 8 mesh shown in Figure 4. Table 16 shows the result of these calculations. The finally selected bed diameter of 12.7 cm (5 in) was selected. This dimension maintains L/D over the desired minimum of 1.0 and is consistent with a minimum pressure loss penalty. Checks with other pressure loss data for lithium hydroxide indicates that the pressure loss might be less than the 250 N/m^2 (1.03 in water) calculated using the charcoal data. However, the selected approach was accepted as a conservative value.

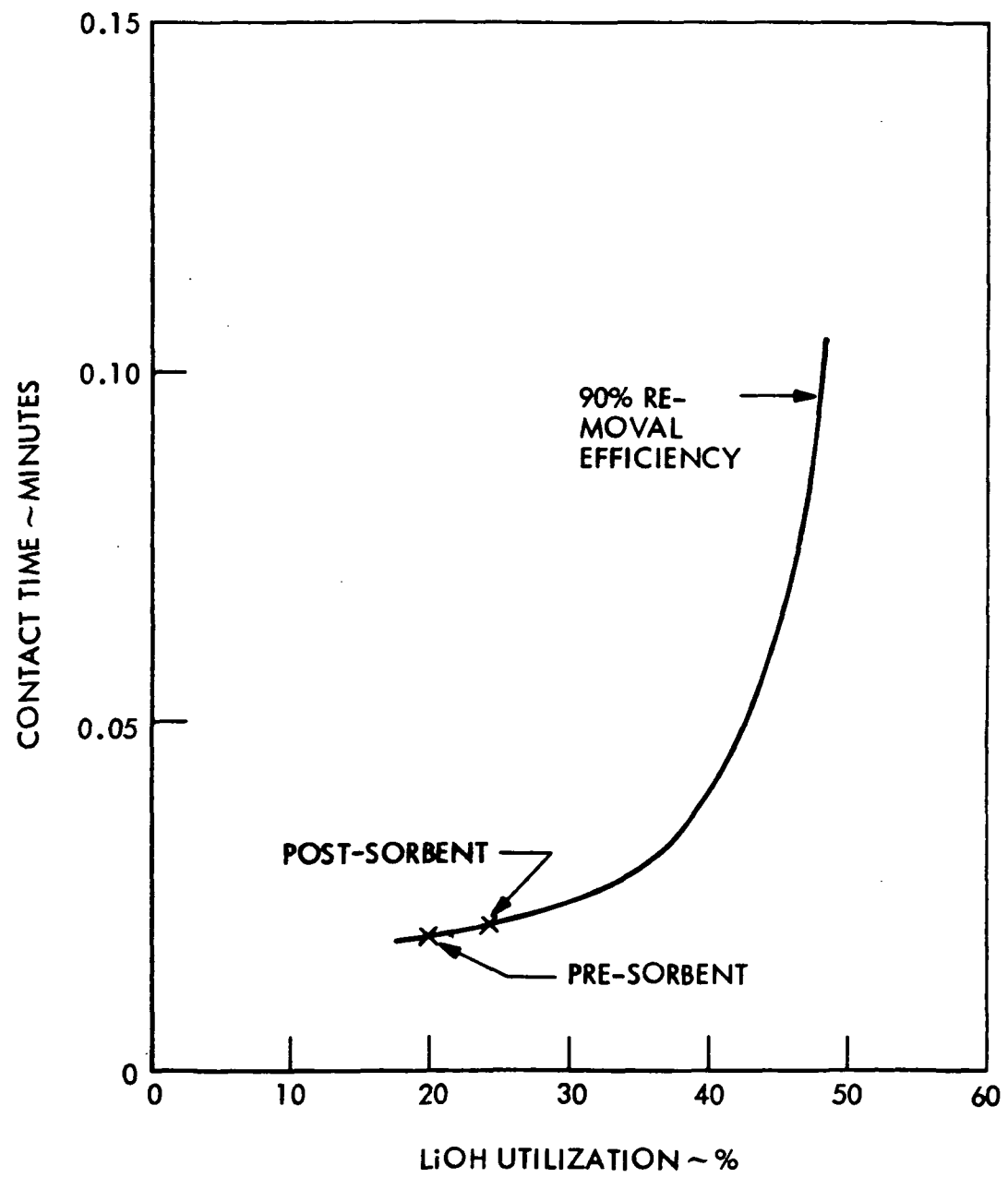


Figure 11 Pre and Post Sorbent Beds LiOH Contaminant Removal Characteristics

The final bed dimensions are 12.7 cm (5 in) diameter and 15.3 cm (6 in) length with a total chemical weight of 0.9 kg (2 lb). The anticipated pressure loss is 250 N/m² (1.03 in water).

TABLE 16
PRE-SORBENT CANISTER PRESSURE LOSS CHARACTERISTICS

Bed Diameter cm (inches)	L/D	Pressure Loss N/m ² (in. H ₂ O)
10.2 (4.0)	2.23	710 (2.85)
11.5 (4.5)	1.51	405 (1.62)
12.7 (5.0)	1.12	257 (1.03)
14 (5.5)	0.85	156 (0.625)
15.3 (6.0)	0.66	98 (0.395)

The size of the pre- and post-sorbent LiOH beds required for the revised contaminant load will be somewhat less than that required for the original contaminant load since the total integrated load was reduced. The bed designs however were not altered as little savings could be realized with these small beds. Instead the added safety factor was accepted.

4.4 CATALYTIC OXIDIZER

The catalytic oxidizer provides control of carbon monoxide, hydrogen, methane, and other low modular weight hydrocarbons. Previous NASA contract work at IMSC has resulted in the design of an isotope heated catalytic oxidizer operating under conditions similar to the ones of this study. Test data taken on oxidation efficiency has confirmed the selected operating points. Thus, this former work serves as a basis for the assumptions and design approach taken in this study. The results of this analysis were used to establish the final design requirements.

The catalytic oxidizer has two operational modes which must be thermally analyzed. These are the flow and no-flow modes. The flow condition is normal operation whereby throughput air is heated to contaminant oxidation temperatures. The no-flow

condition is representative of shutdown for regenerable bed desorption or other non-operational periods. However, during any condition whereby the oxidizer is intact, the isotope provides continuous constant heat that must be rejected to the surroundings. Some of this heat is removed by the throughput air during operation, but not during the no-flow condition. The problem is, therefore, to provide a thermal design which will satisfy two heating requirements within boundary temperature limits.

It is desirable to have the least complex system practical, which is a passive system. Based upon previous investigations, it was established that it is possible to design an isotope heated catalytic oxidizer without an active thermal control system. This analysis provides thermal design data by which such a system may be defined.

The approach to the analysis was to parametrically define the key design variables so that sensitivities could be determined and also so that limits could be more easily established.

4.4.1 Thermal Analysis Procedure

The following section describes the procedure used in the catalytic oxidizer thermal analysis. A diagram of the thermal model is shown in Figure 12.

There are three temperature limits imposed upon the design. These are the maximum outside touch temperature, catalytic bed operational temperature, and maximum catalytic bed temperature during no-flow conditions. These temperatures, along with other requirements and assumptions are listed below.

Maximum outside touch temperature, T_o	$322^{\circ}\text{K}(120^{\circ}\text{F})$
Catalytic bed operating temperature, $T_{i\text{nom}}$	$633^{\circ}\text{K}(680^{\circ}\text{F})$
Catalytic bed max temperature, $T_{i\text{max}}$	$811^{\circ}\text{K}(1000^{\circ}\text{F})$
Ambient temperature, T_{∞}	$291-297^{\circ}\text{K}(65-75^{\circ}\text{F})$
Emissivity of oxidizer exterior surface	0.95
Emissivity of surroundings	0.80
Negligible convection to surrounding air	
Oxidizer flow rate	93.3 l/min (3.3 SCFM)
Insulation conductivity (Min-K 1301)	$130 \text{ k joule/hr, m}^2, ^{\circ}\text{K/cm}$ ($0.25 \text{ BTU/hr ft}^2 ^{\circ}\text{F/in}$)

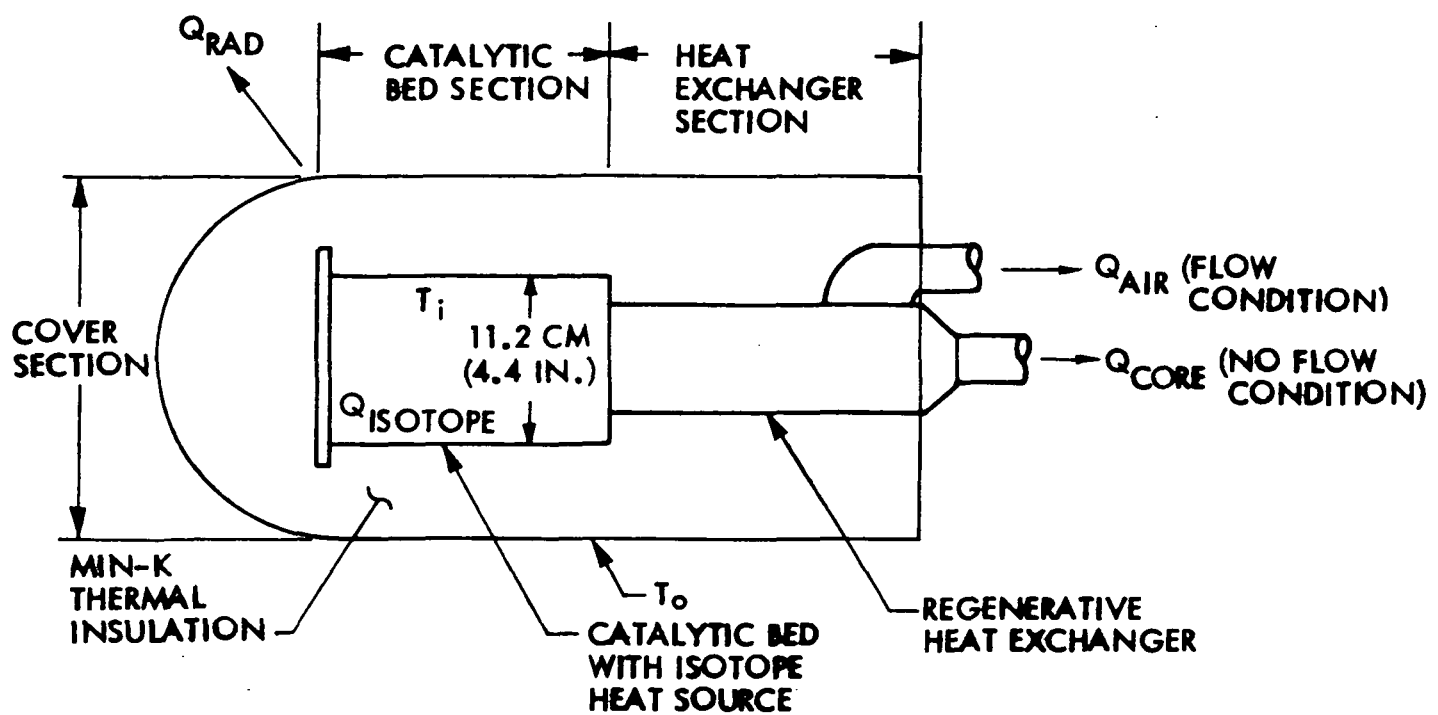


Figure 12 Catalytic Oxidizer Thermal Configuration

Counterflow heat exchanger	
Heat rejection power penalty	.032 kg per joule/hr (0.074 lb/BTU/hr)
Insulation density	320 kg/m ³ (20 lb/ft ³)

In the above list, the catalyst operating temperature and no-flow shutdown temperature bear further discussion. In former studies at Lockheed, a 633 K (680 F) operating temperature was required for the removal of methane. Extensive long-duration testing at 633 K (680 F) has also demonstrated satisfactory removal of the other oxidizer controlled contaminants.

Data taken and presented in NASA CR-66346 indicates that at the 20% removal efficiency required for methane in this program, a temperature of only 611 K (640 F) is required for the humid inlet gas. As little significant penalty results from this increase in temperature, 633 K (680 F) was selected as the catalytic oxidizer design temperature on the basis of extensive heat background. The maximum no-flow temperature of 811 K (1000 F) is based upon potential catalyst degradation above this operating temperature. Tests at Lockheed have been performed at up to 811 K (1000 F) with good catalyst performance. Lack of test data above this level would involve design risk which is neither necessary or desirable. Thus, 811 K (1000 F) was set as the upper limit of the oxidizer canister temperature.

During the no-flow operating condition, the temperature of the isotopic heat source will rise to its highest level. The catalyst canister incorporates radial nickel fins which transport the thermal energy from the interior to the surface. The fins are sized to limit the radial gradient to about 17 K (30 F). The isotope operating temperature can then be calculated using an emissivity of 0.8 for the surface and the interior of the catalyst canister. This results in a maximum isotope temperature of 922 K (1200 F).

The design variables which significantly affect the thermal balance of the oxidizer are insulation thickness, heat exchanger effectiveness, and isotope power. Although the maximum catalytic bed temperature has been specified, it is of interest to know its effect upon isotope power and external touch temperature. Hence, it was included as a variable in the analysis.

An overall heat balance was described which included these variables. For the flow condition this is,

$$Q_{\text{isotope}} = Q_{\text{rad}} + Q_{\text{air}}$$

where:

Q_{isotope} is isotope power

Q_{rad} is the total heat transfer out through the insulation during flow

Q_{air} is the heat leaving the oxidizer via the flowing air

For the no-flow condition, the heat balance is,

$$Q_{\text{isotope}} = Q_{\text{rad}} + Q_{\text{core}}$$

where:

Q_{core} is the conduction through the heat exchanger core to ducting and end plates during no-flow conditions.

The expressions for each of these terms will now be defined.

- o Q_{air} - The loss of heat due to inefficiency of the regenerative heat exchanger is,

$$Q_{\text{air}} = m C_p \Delta T$$

where:

ΔT = temperature difference of air between heat exchanger outlet and inlet.

For the counterflow type heat exchanger, the thermal effectiveness is,

$$\epsilon = \frac{T_i - T_{\text{outlet}}}{T_i - T_{\text{inlet}}}$$

The air heat loss then becomes

$$Q_{\text{air}} = m C_p [1 - \epsilon] (T_i - T_{\text{inlet}})$$

- o Core conduction heat loss, Q_{core} (during no flow).

Core conduction was calculated according to,

$$Q_{\text{core}} = \frac{T_{\text{core}}}{R_{\text{core}}}$$

Although the above relation assumes linear temperature gradient during the no-flow condition, the error with this approach is small. The gradient is not quite linear because a small portion of heat is conducted radially outward from the heat exchanger through the insulation to the surroundings. The amount of heat loss is only approximately six percent of the core conduction. A more precise analysis would consider the heat exchanger as a short fin whereby the core conduction is a loss from the fin end and insulation loss is fin side loss. This is more complicated and does not readily permit the analysis to be changed to different configurations.

- o Loss through Insulation, Q_{rad}

Heat loss through insulation was calculated in three parts; heat exchanger section, catalytic bed section, and end cover section. This is expressed as,

$$Q_{rad} = Q_{hx} + Q_{cb} + Q_c$$

The insulation thickness for each section was interrelated, which permits the total heat loss to be a function of catalytic bed insulation thickness. This was accomplished by making the outside diameter of the insulation of the heat exchanger section and catalytic bed section equal. This was done to simplify fabrication. Also, the cover insulation thickness was made equal to the catalytic bed insulation for analytical simplicity. It was recognized that the cover insulation thickness would probably be slightly different from the catalytic bed insulation thickness but the weight variation and outside touch temperature (T_o) variation will be small. A revised calculation will be made later to assure that the touch temperature limitations is not exceeded.

The heat loss through any of the sections is,

$$Q = \frac{T}{R_{insul} + R_{rad}}$$

where

$$T = T_i - T$$

For the catalytic beds and heat exchanger sections this becomes,

$$Q_{hx} \text{ or } Q_{cb} = \frac{T_i - T_\infty}{\frac{1}{2\pi l} \left(\frac{\ln R_o/R_i}{k} + \frac{T_o - T_\infty}{\sigma F R_o (T_o^4 - T_\infty^4)} \right)}$$

for the cover,

$$Q_c = \frac{T_i - T_\infty}{\frac{L}{\pi R_i^2 k} + \frac{T_o - T_\infty}{\pi R^2 \sigma F (T_o^4 - T_\infty^4)}}$$

where R_o = catalytic bed and heat exchanger section insulation outside radius

R_i = inside radius of insulation

5.6 cm (2.2 in) for catalytic bed section

3.8 cm (1.5 in) for heat exchanger section

l = insulation section length

17.9 (7.0 in) for catalytic bed section

14.5 (5.7 in) for heat exchanger section

L = cover thickness, $R_o - 5.6$ cm (2.2 in)

F = gray body shape factor - 0.74

The procedure of analysis was to:

- 1) Select outside cylindrical radius, R_o
- 2) Calculate insulation resistance
- 3) Select catalytic bed temperature, T_i
- 4) Estimate touch temperature, T_o , and calculate radiation resistance
- 5) Calculate insulation heat loss and outside touch temperature
- 6) Iterate if calculated touch temperature is significantly different from estimate in step 4.
- 7) Repeat for various catalytic bed temperature, T_i .
- 8) Calculate difference in heat loss between flow ($T_i = 633^\circ\text{K}, 680^\circ\text{F}$) and no-flow ($T_i > 633^\circ\text{K}, 680^\circ\text{F}$)
- 9) Calculate core conduction heat loss based upon $T_i > 633^\circ\text{K}, 680^\circ\text{F}$
- 10) Determine air heat loss
- 11) Determine heat exchanger effectiveness

After the thermal analysis was completed, a weight analysis was performed. Weight considered included heat rejection penalty and insulation weight. Although the weight of the heat exchanger is a variable, it has only secondary influence upon the total effective weight. Its weight does not become significant until the effectiveness exceeds 0.9 (weight is approx. 0.9 kg (2 lb) at $\epsilon = 0.9$).

It was assumed that all isotope heated air would be returned to the cabin air and the heat rejection penalty would be 0.032 kg per joule/hr (0.074 lb per BTU/hr).

4.4.2 Thermal Analysis Results and Conclusions

The results of the thermal analysis are shown in Figure 13 and 14. Figure 13 presents the catalytic oxidizer surface temperature as a function of isotope power, insulation thickness and no-flow bed temperature. Figure 14 presents the catalytic oxidizer weight penalty as a function of the various operating parameters. Referring to Figure 13, one can see that if the touch temperature is to be less than 322 K (120 F) and the maximum no-flow temperature is to be 811 K (1000 F), then the insulation thickness must be 7.6 cm (3 in). Referring to Figure 14, it can be seen that this operating point requires a heat exchanger effectiveness of 0.92 and is not optimum from a total equivalent weight point of view. Consulting with various heat exchanger manufacturers, it was concluded that an effectiveness of 0.92 could not be realized with this type of heat exchanger without resorting to an extensive development program and even then, this high performance could not be guaranteed. Therefore, it was necessary to allow the external surface temperature to rise above 322 K(120 F). This, however, presented no problem since protection against contact with the hot surfaces could be provided.

Returning to Figure 14, it can be seen that the optimum operating condition in terms of total equivalent weight is at an isotope power of 316.8 k joules/hr (300 BTU/hr), with an insulation thickness of 3.8 cm (1.5 lb). This condition, however, again requires an excessive heat exchanger effectiveness.

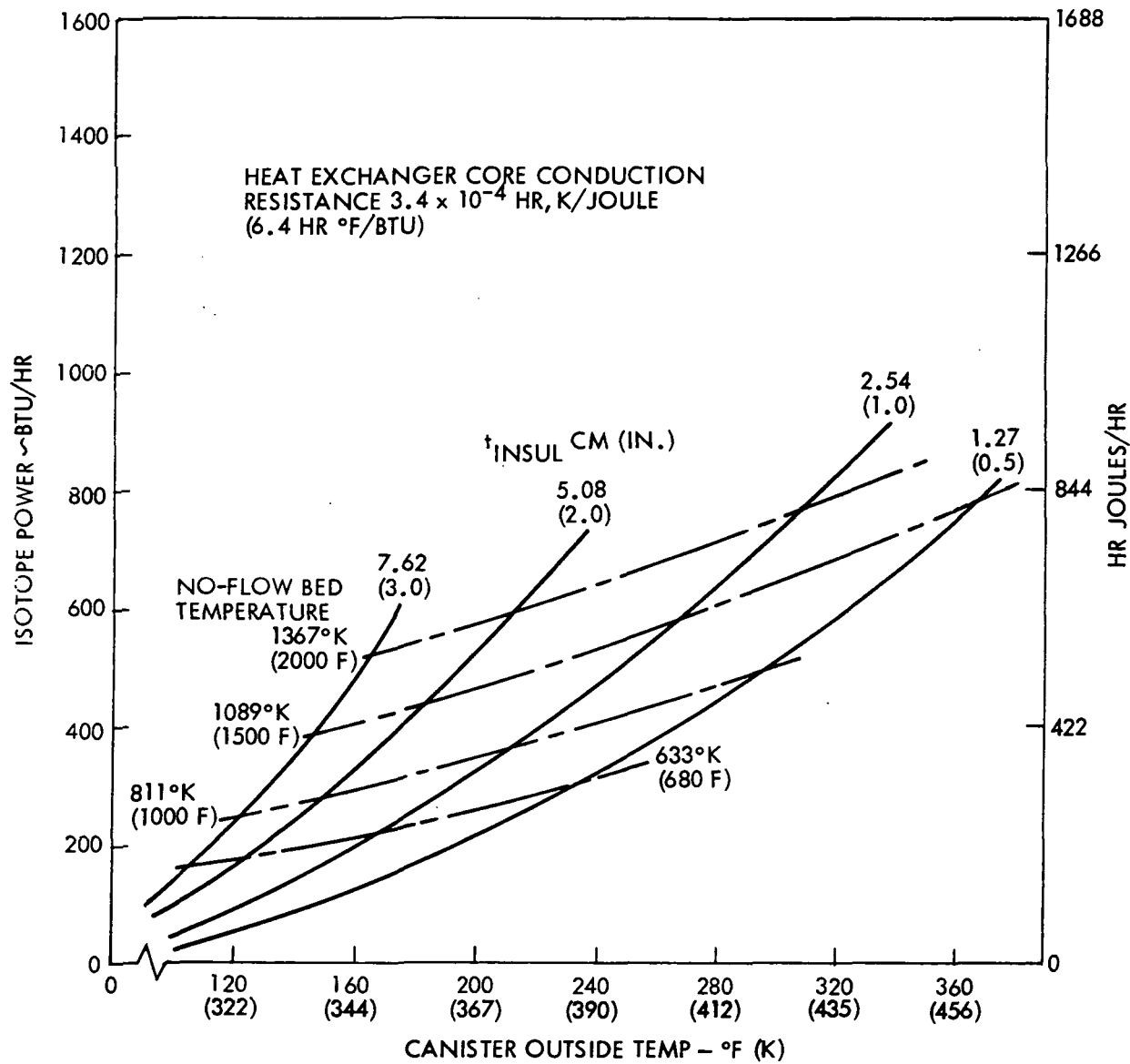


Figure 13 Catalytic Oxidizer Surface Temperature

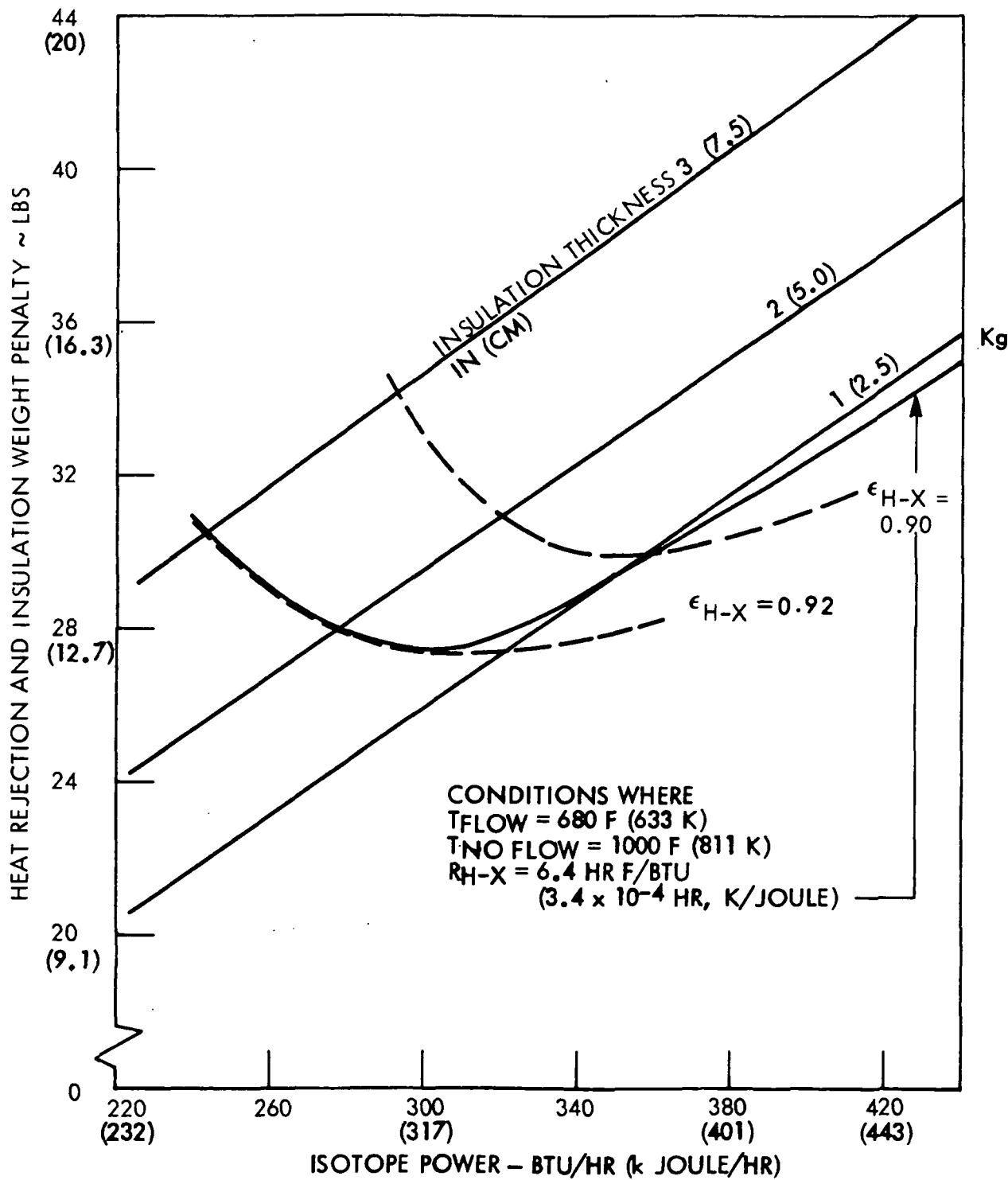


Figure 14 Catalytic Oxidizer Thermal Characteristics

The operating point that results with a 90% effective heat exchanger requires 380.2 k joules/hr (360 BTU/hr) of isotope power and an insulation thickness of approximately 2.5 cm (1 in). This operating point is only 1.1 kg (2.5 lb) heavier in total equivalent weight than the ideal point (which is not considered a significant penalty). The required isotope power of 380.2 k joule/hr (360 BTU/hr) or 106 watts is slightly less than two of the AEC isotope heat sources built for the Life Support II Program. These capsules are described in AEC Report MLM-1757. The use of one of the 70-watt sources and the one 46-watt source would result in a total power of 116 watts, which is only 9% in excess of the desired power level. These power levels are based on the output as of early 1973.

4.4.3 Catalytic Oxidizer External Surface Thermal Control

A thermal evaluation of the catalytic oxidizer shows that the outside surface temperature of the unit will reach 394 K (250 F) under the no-air-flow condition. As this item is heated by an isotope heat source which has a steady heat output, provision must be made to prevent possible burns through contact with this item during maintenance operations where crew members may come into contact with the unit. Two concepts were studied which can meet the requirement of safe handling. These are (1) installation of a properly designed screen which prevents contact with the hot surface and will not reach dangerously high temperatures, and (2) use of an external insulation that minimizes the rate of energy transfer to some portion of the body to such an extent that no discomfort is felt.

4.4.3.1 Heat Shield - The purpose of the heat shield is to prevent skin burns or discomfort arising from contact with the hot surface of the catalytic oxidizer. The screen must, therefore, be in close proximity to the hot surface, but not heat up to a level that could produce a burn or discomfort. It should also impose minimal radiation restriction to the oxidizer surface. This is necessary because any increase of the resistance to heat transfer will result in an increase of both the isotope temperature and canister temperature. The effect of shield percent open area and emissivities were, therefore, examined so that a shield configuration could be selected. This was done for no air flow conditions when the isotope and canister temperatures are at a maximum.

The range of shield openness (area of holes divided by total shield area) considered was from 0.50 to 0.78. The upper limit is representative of the maximum openness anticipated to be available in perforated sheet assuming straight aligned square holes.

The first case analyzed was for a shield with gold ($\epsilon = 0.018$) on the inside surface and paint ($\epsilon = 0.95$) on the outside surface, and 78 percent openness. This resulted in a shield temperature of 301 K (82 F) for zero gravity, no-convection conditions and a cabin temperature of 297 K (75 F). This is an unnecessarily low temperature, and it was concluded that an extremely low emissivity inner surface is not required. The inner surface emissivity corresponding to a shield temperature of 322 K (120 F) for the above conditions was then calculated for 78 percent openness and the resultant value was 0.17. A review of the materials then led to the selection of aluminum perforated sheet as the leading candidate shield. In the oxidized state, its emissivity is approximately 0.11. However, perforated aluminum sheet of the type desired is not readily available at 78 percent openness so a 50 percent open shield was analyzed. The screen temperature is 323 K (122 F) for these conditions, which is acceptable. However, the isotope temperature is increased 44 K (80 F) due to the radiative restriction imposed upon the canister surface by the 50% shield. It is, therefore, recommended that the openness be as large as commercial availability and structural strength will permit.

The distance between the shield and canister, however, must be greater than natural convective boundary layer during normal gravity operation. The boundary layer thickness at the bottom of the canister was calculated to be 0.56 cm (0.21 in), which increased gradually to approximately 1.28 cm (0.5 in) near the top. This would require a separation distance of greater than 1.28 cm (0.5 in) which would increase the diameter of the catalytic oxidizer by more than 2.5 cm (1 in). This was felt to be undesirable, so an alternate approach was selected.

4.4.3.2 External Insulation Blanket - The selected approach for surface thermal protection was to encase the unit in a blanket of material which can be safely handled at temperatures of up to the 394 K (250 F) which are predicted by the thermal analysis.

Evaluations were made at IMSC of 0.63 cm (0.25 in) thick blanket of flexible Min-K which was heated to achieve a surface temperature of 394 K (250 F). When handled, this material, although initially warm to the touch, presents no discomfort and can be safely touched without danger of burn. A mechanism is postulated for this observation as follows. Min-K is a low density, low specific heat material having a very low thermal conductivity. Because of these properties, little thermal energy is available which could cause burns at the site of contact. Furthermore, the low conductivity prevents the rapid transfer of heat to the point of contact required for discomfort or burning. The selected design has a 0.63 cm (0.25 in) thick blanket of this material over the entire surface of the oxidizer, allowing safe handling at any anticipated surface temperature.

4.4.4 Catalytic Oxidizer Pressure Drop

The primary source of pressure drop in the catalytic oxidizer is the regenerative heat exchanger. Discussions with potential heat exchanger manufacturers have indicated that a heat exchanger that satisfies the system requirements and has an effectiveness of 0.90 will have a pressure drop of approximately 1750 N/m^2 (7.0 in water). The next largest element of pressure drop in the system is the catalyst bed. The configuration of this bed is essentially defined by the length of the isotope heat sources and the volume of catalyst required. The pressure drop of the catalyst bed is approximately 523 N/m^2 (2.1 in water). The remaining elements of pressure drop are the internal turns and passages within the oxidizer. These are quite small and are estimated to be approximately 50 N/m^2 (0.2 in water).

Table 17 presents a summary of the total catalytic oxidizer pressure drop losses. As can be seen from this table, the total loss is approximately 2320 N/m^2 (9.3 in water) at a flow rate of 93 l/min (3.3 SCFM) and an operating temperature of 633 K (680 F).

4.4.5 Radiation Dose Level

The following section describes the analyses conducted to define the radiation dose levels of the selected isotope heat sources.

The experimental radiation dose data contained in AEC report MIM-1757 has been evaluated to obtain the radiation dose at various distances from a 70-watt plus a 46-watt source. The radiation from the source is mainly fast neutrons. Mound Laboratory personnel point out that the conversion factor used to obtain rem dose in the reference report is high, as it applies to a different neutron spectrum. Using the measured spectrum and the rem dose-neutron fluence factors in NCRP Report 38 for whole body irradiation, the factor is 3.4×10^{-5} millirem per neutron/cm² rather than the 4.3×10^{-5} factor used in the AEC report. As mentioned in the AEC report, the dose at points on the cylindrical axis of the heat source is lower than at the sides, which is the measurement point reported. Dose in the handling-knob direction is 59% of the side dose. As it is reasonable to install the catalytic oxidizer with the handling-knob direction toward the volume occupied by personnel, this reduced dose direction was assumed for the analysis.

Radiation dose constraints have been circulated by NASA-MSC (letter, R. G. Rose, Radiation Constraints for Skylab, and Space Station, 1/15/71). For the isotope heat source, the eye dose can be assumed to set the allowable distances, as other targets have a greater ratio of attenuation in reaching the target at its reference body depth divided by the decreased allowable dose factor. (A possible exception is the testes, but a slight change in body orientation or a seated position affords greater attenuation in reaching the target than the 3 cm effective depth designated by the reference letter). The quarterly maximum allowable eye dose is 52 rem, and this dose is allowed for two consecutive quarters,

TABLE 17

PRESSURE DROP LOSSES WITHIN THE CATALYTIC OXIDIZER
 AT FLOW 93 l/min (3.3 SCFM) AND TEMPERATURE 633 K (680 F)

	<u>N/m² (in water)</u>
Entry after first HX pass	6 (0.024)
Across first heat source support	6 (0.024)
Across second heat source support	6 (0.024)
Through cylindrical ring	3.7(0.015)
Due to 180° flow reversal	5 (0.02)
Circumferential Annulus (after passing thru catalyst)	7.5(0.03)
Exit (entering HX for second pass)	6 (0.024)
Through catalyst bed	523 (2.1)
Through regenerative heat exchanger	<u>1750</u> <u>(7.0)</u>
Total	2313 9.26

if followed by six months of removal from exposure, in other words, 10^4 rem is the allowed total eye dose in a 180-day period. This is somewhat less than the 185 rem level used in previous studies described in NASA CR-66346.

As suggested in the reference letter, a trade-off between man-made and natural radiation sources is required with adequate allowance for unexpected exposure. It is suggested that the catalytic oxidizer dose be maintained at 10% of the total allowable dose. Ten percent is somewhat higher than the previous design level of 5%. This is, in the most part, attributable to the lower allowable dose rate (10^4 rem vs 185 rem) and the fact that the currently available heat sources do not utilize the lower emission fuel form that would be available for a flight capsule. This means that the current heat sources have approximately four times the dose level of future heat sources. Using 10% for the allowable level leads to a required average separation distance of 125 cm from the 70 ± 46 watt isotope sources. Average in this case refers to a geometrically weighted distance-time relationship as dose vs distance follows the reciprocal distance squared relationship. Reducing the level to 5% will have the effect of increasing the above continuous values to 175 cm. This should be acceptable in a vehicle the size of a space station.

To account for maintenance operations, it was assumed that during the 180 days, a total of 20 operations at 50 cm distance from the source was performed. The dose accumulated during those operations is 1.1 rem. Required average separation distances to not exceed the 10% allocation, then becomes 130 cm.

4.4.6 Impact of Revised Contaminant Load on the Catalytic Oxidizer Design
The revised contaminant load model required that the catalytic oxidizer flow rate be increased from 93 l/min to 120 l/min (3.3 to 4.25 CFM). This requires the use of two 70 watt isotope heat sources in lieu of the one 70 watt and one 46 watt source originally planned. The final catalytic oxidizer unit as specified by the analysis has the following characteristics.

Catalyst Bed Length	9.5 cm (3.75 in)
Catalyst Volume	0.74 l (45 in ³)
Flow	120 l/min (4.25 CFM)
Differential Pressure	2491 N/m ² (10 in H ₂ O)
Catalyst	0.9 kg (2 lb) Englehard 1/2% Pd on Alumina
Isotope Power	Two 70 watt sources
Insulation	Approximately 2.5 cm (1 in) of Min-K 1301 with a 0.6 cm (0.25 in) outer blanket of Min-K 1301
Catalyst Operating Temp.	633 K (680 F)
Catalyst Temp During Shutdown	811 K (1000 F)
Heat Exchanger	Plate Fin, Effectiveness 90% Size 5 x 7.5 x 18 cm (2 x 3 x 7 in)
Weight	Approximately 9.1 kg (20 lb)

4.5 POST-SORBENT

The design philosophy of the contaminant control system states that wherever possible, contaminant materials will be controlled at their source and not discharged into the cabin atmosphere. This criterion was applied to the catalytic oxidizer product gases to evaluate the requirement for, and establish the design point of the post-sorbent bed. It should be noted at this point that toxic materials formed in the catalytic oxidizer will be controlled below the allowable levels in the absence of the post-sorbent bed. Thus, this component is redundant and only provided in accordance with the design philosophy, which is to control contaminants at their source.

A complete review of the contaminant list shows that there are a large number of contaminants which have toxic decomposition products if allowed to enter the catalytic oxidizer. These contaminants are listed in Table 18. The contaminant name, formula, generation rate, and moles of LiOH required to control (assuming complete reaction), are presented. It is evident from a review of the list that each of the materials are potential catalyst poisons. Prior testing of catalyst beds indicates that these materials will not poison

TABLE 18
CONTAMINANTS YIELDING TOXIC MATERIALS
IN A CATALYTIC OXIDIZER AND POST-SORBENT REQUIREMENTS

Contaminant	Formula	Generation Rate gm/day	LiOH Required gm/day
Ammonia	NH ₃	8.5	500
Carbon disulfide	CS ₂	.25	3.3
Carbonyl sulfide	COS	.25	4.16
Chlorine	Cl ₂	.25	3.52
Chloroacetone	C ₃ H ₅ ClO	.25	2.72
Chlorobenzene	C ₆ H ₅ Cl	.25	2.23
Chlorofluoromethane	CH ₂ ClF	.25	3.68
Chloropropane	C ₃ H ₆ Cl	.25	3.21
Cyanamide	CH ₂ N ₂	.25	5.95
Dimethyl Sulfide	(CH ₃) ₂ S	.25	3.78
1, 1 Dichloroethane	C ₂ H ₄ Cl ₂	.25	2.52
Dimethylhydrazine	(CH ₃) ₂ N ₂ H ₂	.25	4.17
Ethylene Dichloride	C ₂ H ₂ Cl ₂	.25	2.58
Ethyl sulfide	(C ₂ H ₅) ₂ S	.25	2.78
Ethyl Mercaptan	C ₂ H ₆ S	.25	4.04
Freon 11	CFCl ₃	.25	1.84
Freon 12	CF ₂ Cl ₂	.25	2.08
Freon 21	CH F Cl ₂	.25	2.42
Freon 22	CH F ₂ Cl	.25	3.73
Freon 23	CH F ₃	.25	4.38
Freon 113	C ₂ H ₂ F Cl ₃	.25	1.65
Freon 114	C ₂ F ₄ Cl ₂	.25	1.46
Freon 114	C ₂ F ₂ Cl ₂	.25	1.46
Freon 125	C ₂ F ₅ H	.25	2.08
Hydrogen chloride	H Cl	.25	6.76
Hydrogen fluoride	HF	.25	12.5
Hydrogen sulfide	H ₂ S	.0005	.03
Methylene chloride	CH ₂ Cl ₂	.25	2.94
Methyl chloride	CH ₃ Cl	.25	5.00

TABLE 18 (Cont'd)

Contaminant	Formula	Generation Rate gm/day	LiOH Required gm/day
Mono-methyl hydrazine	$\text{CH}_3\text{N}_2\text{H}_4$.25	5.31
Methyl mercaptan	CH_3SH	.25	5.21
Nitric oxide	NO	.25	8.35
Nitrogen tetroxide	N_2O_4	.25	2.72
Nitrogen dioxide	NO_2	.25	5.44
Iso-propyl chloride	$\text{C}_3\text{H}_7\text{Cl}$.25	3.20
Propyl mercaptan	$\text{C}_3\text{H}_7\text{SH}$.25	3.28
Sulfur dioxide	SO_2	.25	3.90
Tetrochloroethylene	C_2Cl_4	.25	1.51
Tetrafluoroethylene	C_2F_4	.25	2.50

the catalyst at low concentration levels. If concentration levels into the oxidizer are maintained at a level of 10% of MAC or less, no poisoning will occur. However, the contaminants will be reacted forming toxic materials such as HCl, Cl₂, SO₂, NO₂, HF, and COCl₂. The LiOH post-sorbent will directly remove these products.

The design point for the post-sorbent bed considers that one-tenth of the contaminants generated enter the catalytic oxidizer. This assumption is consistent with the design criteria for the fixed and regenerable charcoal beds and pre-sorbent canister. By summing the total moles required for control, a LiOH requirement of 0.33 kg (0.725 lb) is established for a 180-day mission. As in the case of the pre-sorbent bed, the requirement for 90% removal per pass and bed removal characteristics sets the total quantity. The design procedure is identical to that for the pre-sorbent canister. Using Figure 11, a total post-sorbent weight of 1.36 kg (3 lb) is set. A pressure loss summary appears in Table 19. This table shows that a canister of greater than 12.7 cm (5 in) will exceed the L/D criteria of 1.0. Further, the selection of a 12.7 cm (5 in) diameter identical to the pre-sorbent canister results in design savings as the beds will differ only in length. The air leaving the catalytic oxidizer will be at a temperature of 344 K (160 F). With an air flow of 93 l/min (3.3 SCFM) at this temperature, the possibility of the surface temperature exceeding 120 F was evaluated. If a surface temperature of 322 K (120 F) and a surroundings of 300 K (80 F) is considered, 58 k joule/hr (55 BTU/hr) can be dissipated from the surface of the post-sorbent canister if the outside surface has an emissivity of 0.9 and no allowance is made for convection. Looking at the inside surface, the heat available from the gas at 344 K (160 F), with an assumed value of $h = 1040 \text{ k joule/m}^2 \text{ K hr/cm}^2$ (2 BTU/hr ft² F), will be 105.5 k joule/hr (100 BTU/hr) to the same 322 K (120 F) surface. Thus, we see, due to the imbalance, that the surface temperature will exceed 322 K (120 F) for an unprotected surface. If a layer of 0.6 cm (0.25 in) of Min-k is placed around the unit, the surface temperature will be maintained below 322 K (120 F). The post-sorbent bed will be 12.7 cm (5 in) in diameter, 22.3 cm (8.75 in) long, and contain 1.4 kg (3 lb) of LiOH. It will be wrapped with a blanket of Min-K

TABLE 19
POST-SORBENT CANISTER PRESSURE LOSS CHARACTERISTICS

Bed Diameter cm (in)	L/D	Pressure Loss N/m ² (in. H ₂ O)
10.1 (4.0)	3.34	1075 (4.3)
11.5 (4.5)	2.36	597 (2.4)
12.7 (5.0)	1.68	398 (1.6)
14.0 (5.5)	1.28	235 (0.94)
15.3 (6.0)	0.99	147 (0.59)

which is 0.6 cm (0.25 in) thick to maintain the surface temperature below 322 K (120 F). The pressure loss will be 398 N/m^2 (1.6 in) water).

4.6 CATALYTIC OXIDIZER AND REGENERABLE BED LINE AND VALVE SIZES

The following section describes the analyses required to define the line and valve sizes for the catalytic oxidizer and regenerable bed plumbing. This analysis is based on the design calculations presented in the previous sections but includes the effect of line and valve weights. Thus, this represents a refinement in these calculations and results in a slightly higher total system pressure drop.

The analysis deals with all of the plumbing between the regenerable bed fan and the outlet to the cabin. This equipment was optimized together on a weight basis. The weights considered are:

1. Lines and valves
2. Fan power penalty
3. Heat rejection penalty
4. Regenerable bed weight
5. Regenerable bed water dump

Fan power and heat rejection penalties were included because fan power and heat rejection to the cabin are affected by the line pressure drop. The influence of system pressure drop, whether due in part to lines or major components, is discussed in the regenerable bed adsorption analysis. The weight of the catalytic oxidizer and post-sorbent bed was assumed to be a constant and was not included as part of the analysis. The pressure drop through these units was included, however, since fan power and operating temperatures are a function of the total system pressure drop.

Flow data generated in the adsorption analysis was used as the basis for determining all the weights listed above with the exception of line and valve weight. Figure 6 is a summary of this data.

Line and valve pressure drops and weights were calculated as a function of line size. These calculations are considered to be preliminary since the precise component configuration and line installation have not been determined. They are reasonable preliminary design estimates of the system, which were firmed up during detail design.

Valve and line scaling equations were derived based upon flight type hardware weight for the application. The valves are low pressure loss, solenoid operated vacuum valves. The line was assumed to be thin wall aluminum tubing. The equations used are:

$$W_{line} = 1.7 D_{line} \text{ (kg)} \quad 3.8 K_{line} \text{ (lb)}$$

$$W_{valve} = 0.77 D^{1.5} \text{ (kg)} \quad 1.7 D_{line}^{1.5} \text{ (lb)}$$

With these data and scaling equations, the analysis was performed.

Pressure drop calculations were made from the incompressible flow relations,

$$P = \frac{f(L/D)}{2g} \frac{V^2}{}$$

which is sufficiently accurate for gas flow with a small pressure drop relative to total pressure. The equivalent L/D assumed for the components is listed below:

<u>Component</u>	<u>L/D</u>	<u>or</u>	<u>f L/D</u>	<u>No. Required</u>
90° Bends	20			10
Line	50			
Sudden Expansions			1	3
Valves	150			2

The analytical procedure used was:

1. Calculate line and valve pressure drop for a given line size.
2. Calculate line and valve weight.
3. Determine total system pressure drop, which is the major component ΔP , plus the line and valve ΔP .
4. Determine power penalty, heat rejection penalty, regenerable bed weight, regenerable bed water dump from adsorption analysis data.
5. Sum steps 2 and 4 to find the total weight.
6. Repeat for other given line sizes and find optimum line size.

The results are shown in Figure 15. For the assumptions made, the curve shows that a 2.5 cm (1 in) line and valves is optimum. Also, it can be seen that a variation of size by plus or minus 0.64 cm (0.25 in) only results in a penalty of 0.91 kg to 1.36 kg (2 to 3 lb), even though there is a large percentage change in the line pressure drop.

The resulting head rise required for the regenerable fan is approximately 3.74 kN/m^2 (15 in water) with a flow rate of 11.3 l/min (4 SCFM). The 3.74 kN/m^2 (15 in water) is based on the 3.5 kN/m^2 (14 in water) previously defined for the major components (Regenerable Bed - 0.522 kN/m^2 (2.1 in water); Catalytic Oxidizer - 2.3 kN/m^2 (9.3 in water); Pre-sorbent Bed - 0.25 kN/m^2 (1.0 in water), Post-sorbent Bed - 0.4 kN/m^2 (1.6 in water) plus the 0.25 kN/m^2 (1.0 in water) for lines and valves defined by Figure 15.

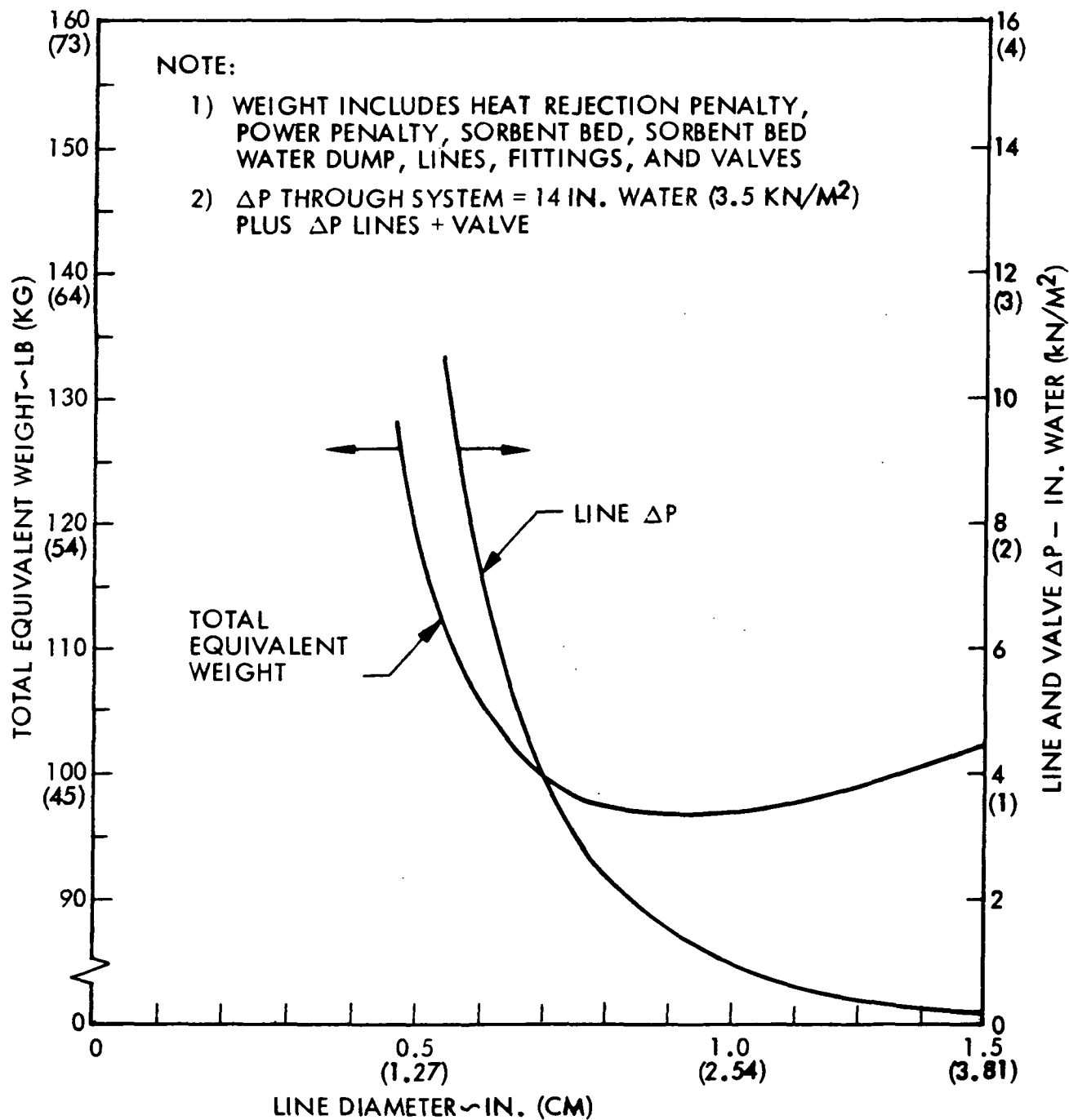


Figure 15 Line Size Optimization

SECTION 5

OPERATIONS ANALYSIS

The following section presents a discussion of the impact of off-design contaminant load increases or upsets. The analyses conducted to support this study were based on the revised contaminant load model.

Any increase in contaminant rate will first show up as an increase in the cabin concentration for that contaminant. What should be considered is the limit to which any concentration will rise and the ability of the Trace Contaminant Control System to restore the concentration or maintain it at some new level.

Two types of upsets will be considered. These are a single incident instantaneous release of some material (type 1), or a step increase in production rate, (type 2). Depending upon which of these types is considered differing control mechanisms operate.

With a type 1 upset the concentration in the cabin can be considered to rise instantaneously. If there is no increase in the steady state rate for that contaminant, the concentration level will drop rapidly to the normal steady state value. The rate of decay will depend upon cabin volume. However, if one considers a cabin volume of about 142 m^3 (5000 ft 3) and flowrates of 1130 l/min (40 CFM) through the fixed bed and 142 l/min (4 CFM) through the other control components, it is apparent the approach to equilibrium will be rapid.

The next consideration must be the concentration level which results from a type 1 release of a contaminant. The total quantity of release which can be safely tolerated is set by the short term allowable level of the contaminant liberated and the decay rate due to processing. No short-term, levels, e.g. less than 24 hours, have been specified by NASA. However, referring to the

industrial TLV standards, examples of potential storage can be estimated. The 1⁴ day level for methanol and carbon monoxide are 13 and 17 mg/m³. The industrial TLVs are 260 and 55 mg/m³. These differing values can be interpreted as potential cabin storage values of 35 and 5.38 grams. Thus, we see that the cabin can serve as a contaminant storage volume which is brought under control by air processing through the Trace Contaminant Control System. From the point of view of cabin storage, TLV could be used to represent the limit which is associated with crew safety. Much higher levels are possible as the TLV values are still conservative. This type of consideration should only be made in special cases where material selection alternatives are limited.

The quantity of a definable upset will depend upon the specific contaminants involved. If the upset exceeds the allowable maximum short term level, alternate methods are indicated. Examples might include a cabin gas purge of about 182 kg (400 lb) of gas, interim gas masks, a special control system, or special care in preventing upsets of specific contaminants. Indeed, special care is indicated in the SSP specification which states:

"Materials selected for use shall not produce toxic or noxious environmental degradation products measured in terms of total organic (as pentane equivalents) CO, CO₂ or NH₃. In addition, these materials shall be capable of functioning in an atmosphere of pure (100%) oxygen at 3.5 to 5.0 psi or a mixture of oxygen-nitrogen (75/25% by volume at 14.7 psi) before, during, or after exposure to all environmental conditions without contributing to a potential fire or explosion hazard."

If the increase in rate of release of a contaminant is sustained over a long period, a type 2 release, the cabin concentration will rise to a new steady state level. That level will depend upon the flow rate through the controlling component.

The trace contaminant control system (TCSS) is composed of five sorbent beds in series each of which selectively removes some group of contaminants. These beds are listed below along with the design flow for each bed as dictated by the listed contaminant.

<u>TCCS Component</u>	<u>Flow</u>	<u>Contaminant</u>
Fixed Charcoal Bed	1130 l/min (40 CFM)	Pyruvic Acid
Regenerable Charcoal Bed	1200 l/min (4.25 CFM)	Methyl Alcohol
LiOH Pre-sorbent	" " " "	Chlorine & Hydrogen Chloride
Catalytic Oxidizer	" " " "	Carbon Monoxide
LiOH Post-sorbent	" " " "	Oxidizer Products

In all of the designs the flow requirement is established by the short-term postulated contaminant generation rates. As the only source of pyruvic acid is the crew, the flow requirement through the fixed charcoal bed is the same for the long term rate, i.e. a constant 113 l/min (40 CFM) throughout the mission. In all other cases, the short-term generation rates are the determining factor for the design flow rate. A review of the revised NASA contaminant load shows that the short-term rates for equipment contaminant loadings are, in general, an order of magnitude greater than the long-term rates. This results in a high initial concentration level and the anticipated lower steady state concentration level. Thus, we see that any load increases in the long-term contaminant production rates of less than a factor of 10 are provided for in the basic design, as the system flow rates are maintained at the levels required for the short-term contaminant production rates throughout the mission.

The following sections describe the capabilities of the various system components to control increased loads.

5.1 FIXED CHARCOAL BED

The fixed activated charcoal bed is the first component of the TCCS which the contaminated gas stream encounters. The design point of this bed is established by two major criteria: flow rate; and charcoal quantity. For the fixed bed both the flow and quantity are set by the requirement for pyruvic acid at 1079 l/min (38.11 CFM). Of the other contaminants controlled in the fixed bed, only those listed in Table 20 require greater than 113 l/min (4.0 CFM) for control at the maximum allowable levels.

TABLE 20
CONTAMINANTS CONTROLLED LONG-TERM BY THE FIXED BED REQUIRING
MORE THAN 11.3 l/min (4 CFM) FLOW

Contaminant	Mission Phase	Flow l/min	CFM	Source*
Allyl Alcohol	Short	385	(13.6)	E
Phenol	Short	331	(11.7)	E&B
	Long	242	(8.53)	E&B
Benzene	Short	231	(8.17)	E
Acrolein	Short	161	(5.67)	E
	Long	181	(6.38)	E
Formaldehyde	Short	144	(5.1)	E
	Long	144	(5.1)	E
Chloroacetone	Short	120	(4.25)	E
	Long	120	(4.25)	E
Ammonia	Short	163	(5.77)	E&B
Pyruvic Acid	Short	1080	(38.1)	B
	Long	1080	(38.1)	B
Di-ethyl Sulfide	Short	521	(18.4)	E

*E - Equipment

B - Biological

Thus, for most of the contaminants in the contaminant listing, a safety factor in fixed-bed flow of greater than ten already exists. Another way of looking at this is that a ten-fold increase in production rate of any given contaminant not listed in Table 20 can be controlled without exceeding the allowable limits.

Among those contaminants listed in Table 20, phenol, ammonia and pyruvic acid have as the primary source biological sources, i.e. the crew members. These materials are not likely to undergo large upsets. Looking at equipment upsets only for these contaminants a ten-fold safety factor exists.

This leaves only allyl alcohol, benzene, acrolein, formaldehyde, chloroacetone, and diethyl sulfide as possible fixed-bed controlled contaminants which present a major upset problem. Referring to the basic SSP materials philosophy, special emphasis should be placed upon controlling the source of these contaminants, especially relative to potential upset conditions.

The charcoal requirement for the fixed bed is the sum of the short-term and long-term requirements. The major factor in the sizing of this bed is the long-term control of pyruvic acid which requires 35 grams of charcoal per day for control. All other fixed-bed contaminants are controlled over the long term by less than 15 grams per day of charcoal. Thus, even a large contaminant load increase of 30 times the normal daily rate, would require only an additional 450 grams of charcoal in the fixed bed. In view of the fact that co-existence is possible and that the design assumes that all contaminants are generated at these maximum rates, the design as it stands is conservative. Any reduction in the load of contaminants will make available sites for adsorption of materials generated in an upset.

5.2 REGENERABLE CHARCOAL BED

In a manner similar to the fixed bed study, the contaminants controlled by the regenerable charcoal bed were examined and a listing has been made of those contaminants for which a safety factor of ten in flow rate does not exist. The flow rate through this bed initially was to be 142 l/min (5 CFM). Table 21 shows the contaminants which require greater than 14.2 l/min (0.5 CFM) for control.

TABLE 21

CONTAMINANTS CONTROLLED BY THE REGENERABLE BED AND REQUIRING
GREATER THAN 14.2 l/min (0.5 CFM)

Contaminant	Mission Phase	Req. Flow l/min (CFM)	Source*
Allyl Alcohol	Long	433 (1.53)	E
Methyl Alcohol	Short	134 (4.72)	E&B
	Long	568 (1.97)	E&B
isopropyl alcohol	Short	18.1 (.64)	E
Acetaldehyde	Short	24.1 (.85)	E&B
Crotonaldehyde	Long	21.8 (.77)	E
Benzene	Long	26 (.92)	E
Ethyl Acetate	Short	15.6 (.55)	E
Ethyl Formate	Short	72 (2.55)	E
1,4 Dioxane	Long	30.9 (1.09)	E
Ethyl Ether	Short	18.1 (.64)	E
Furan	Short	72 (2.55)	E
Methylene Chloride	Short	24.9 (.88)	E
Vinylidene Chloride	Short	27.2 (.96)	E
Freon 11	Short	77.2 (2.73)	E
Nitrogen Tetroxide	Short	24.1 (.85)	E
	Long	24.1 (.85)	E
Acetonitrile	Short	72 (2.55)	E
Carbon disulfide	Short	36 (1.27)	E
Dimethyl sulfide	Short	86.5 (3.06)	E

*E - Equipment

B - Biological

As was the case with the fixed bed, most of the contaminants can sustain generation rates much higher than normal without exceeding the allowable levels. Only six contaminants: allyl alcohol, methyl alcohol, crotonaldehyde, benzene, 1, 4 dioxane, and nitrogen tetroxide present a potential flow problem in the long term if a large load increase occurs. Each of these contaminants has cabin equipment as its listed source. Thus, careful screening of materials could eliminate any problems with these few materials.

The primary function of the regenerable bed is to remove material which could poison the catalytic oxidizer. The regenerable bed size is quite sensitive to halocarbon, nitrogen and sulfur compounds; thus providing for increased bed size for a postulated upset conditions does not seem desirable. However, contaminant spikes of brief occurrence do not result in a condition of permanent catalyst poisoning and no long-term problem should exist.

5.3 PRE- AND POST-SORBENT BEDS

Each of these beds has been designed with a significant over-capacity and no problems should arise due to load increases. Further, materials removed by them, such as hydrogen chloride, hydrogen fluoride and chlorine will also be partially removed by reaction and sorption in subsystems outside of the Trace contaminant Control System. No credit has been taken for these effects, which increase the design safety factor.

5.4 CATALYTIC OXIDIZER

The catalytic oxidizer oxidizes those hydrocarbon materials not removed in the activated carbon beds. The contaminants removed by the catalytic oxidizer and the required flow rates are presented below:

CATALYTIC OXIDIZER CONTAMINANTS - FLOW REQUIREMENTS

Contaminant	Mission Phase			
	Short		Long	
	l/min	CFM	l/min	CFM
Methyl Alcohol	13 ⁴	4.72	55.8	1.97
Acetylene	9.6	.34	0.96	0.034
Cyclopropane	1.7	.061	0.28	0.01
Ethane	9.4	.332	0.96	0.034
Ethylene	9.4	.332	0.96	0.034
Methane	44.5	1.57	8.7	0.31
Methyl Acetylene	1.05	.037	0.28	0.01
Carbon Monoxide	110	3.88	1.8	0.65
Hydrogen	9.05	.32	0.18	0.063

Considering a safety factor of ten on flow as was the case with the other beds, methyl alcohol, methane, and carbon monoxide are shown potential problems. Each of these contaminants are primarily generated by equipment. Thus, a possibility of control at the source seems possible. Further, carbon monoxide, which would be generated in considerable quantities in a fire, could be controlled by a special low-temperature oxidizer provided for such an emergency.

A potentially more dangerous problem exists if a radioisotope heat source is used in the catalytic oxidizer. The heat released by combustion of contaminants could result in an over-temperature condition leading to an radioisotope capsule rupture and a subsequent radiation hazard.

Table 22 shows the energy of combustion attributable to the normal specified contaminant load.

TABLE 22
CATALYTIC OXIDIZER AVAILABLE ENERGY FROM COMBUSTION

Contaminant	Heat Value		m short gm/day	m long gm/day	Q short watts	Q long watts
	joule/gm	BTU/lb				
Methyl Alcohol	2220	9,550	2.50	.258	.641	.066
Acetylene	4990	21,460	2.50	.25	1.45	.145
Cyclopropane	4900	21,032	.25	.025	.14	.014
Ethane	5090	22,304	2.50	.25	1.50	.150
Ethylene	5015	21,625	2.50	.25	1.46	.146
Methane	5540	23,861	33.1	6.55	21.28	4.210
Methyl Acetylene	4650	20,000	.25	.025	.13	.013
Carbon Monoxide	1010	44,344	2.70	.45	.32	.053
Hydrogen	14190	60,958	2.80	.55	4.60	.903
Total Energy (Watts)						5.700

The current design of the radioisotope-heated catalytic oxidizer uses a 140-watt heat source. With this source, the temperature at the long-term contaminant level is 705 K (810 F). This can be scaled with energy to provide a table of temperature with variations in contaminant load as follows:

<u>Load</u>	<u>Isotope Energy</u> watts	<u>Total Energy</u> watts	<u>Temperature</u>
Zero contaminant	140	140	689 K (780 F)
Long-term rates	140	146	705 K (810 F)
Short-term rates	140	172	775 K (936 F)

The short-term contaminant introduction rates result in a temperature that is at the design limit for the current heat source and any additional energy made available from an upset would only cause an even greater thermal problem.

Three subsystems in the environmental control system provide examples of failures which could cause an increased load which could result in a catalytic oxidizer over-temperature.

A failure of the regenerable bed desorption controls would result in a significant increase in combustion energy until catalyst poisoning occurred.

Both the electrolysis and carbon dioxide reclamation subsystem pose a potential leakage problem. Depending upon the specific subsystem concept chosen, and the nature of a failure, leakage could result in available power from hydrogen or methane combustion of over 100 watts if a leak of only 10 percent of the processed quantities is considered. Even for a short duration, until detection, this could prove hazardous.

In summary, the catalytic oxidizer seems capable of handling most foreseeable upsets, especially if combined with a low-temperature carbon monoxide burner. However, the prospect of a significant overheat condition makes use of an isotope heat source undesirable. An electrically heated unit could compensate for energy of combustion by reducing the available electrical energy. An isotope heat source cannot. One possible compromise might be a combination of an

isotope heat source and an electrical heater for control. Later testing has shown that an electrically heated catalytic oxidizer can, in fact, operate for long periods of time at 867 K (1100 F).

SECTION 6

RELIABILITY ANALYSES

The following sections describe the reliability analyses conducted to support the system design. These analyses include 1) failure mode and effects analysis (2) safety hazards analysis and (3) fault detection and isolation analysis.

6.1 FAILURE MODE AND EFFECTS ANALYSIS

The Failure Mode and Effects Analysis (FMEA) is primarily directed to examination of the failure modes that could occur during operation of a flight model in a manned space vehicle. However, where the current ground system differs from the future flight model (the former includes removable end plates on the sorbent canisters) and thereby introduces additional failure modes, these also are indicated.

The following definitions will apply:

- (a) Failure: The inability of an item to perform its required function within previously specified limits.
- (b) Failure Mode: The particular way in which a failure can occur independent of why the contributing failure phenomena are present.

The EMEA is based on the following assumptions:

- (a) Each basic failure mode is an independent and separate occurrence. Entries shown in the "Failure Effect on Component/Functional Assembly" column are primary effects only. The entries in the "Failure Effect on System" column may be either primary or secondary failure effects.
- (b) Each failure is permanent and not intermittent.
- (c) Inputs to the system are normal.
- (d) The system is in operation and in its normal environment.

This analysis has categorized the criticality of each failure into one of the following:

- I: A hardware failure which could adversely affect the safety of the crew.
- II: A hardware failure which could result in not achieving a primary mission objective or result in premature cessation of a mission.
- III: A hardware failure which interrupts a secondary mission function but which can be corrected before mission operation or crew safety is affected.
- IV: A hardware failure which could not result in loss of primary or secondary mission objectives nor adversely affect crew safety before it can be corrected.

As indicated in the FMEA presented in Table 23, no Criticality I or II failures are foreseen.

It should be noted that the failure mode and effects analysis presumes the use of redundant O-rings in the gas connections. This feature was not provided in the current hardware since commercially available hardware utilizing redundant O-ring seals could not be obtained.

The schematic of the system with the component identification used in the FMEA is shown in Figure 16.

ANNUAL STATUS
OF POOR QUALITY

System: Space Contaminant Control System
Equipment: Cabin Air Filter
Mission Phase: Orbit (Except where indicated otherwise)

Table 23
FAILURE MODE AND EFFECT ANALYSIS

Ident. No.	Name	Function	Failure Mode and Cause	Failure Effect on System	Criticality	Failure Detection Method	Crew Action Req.	Req. / Avail.
FB	Fixed Bed (High flow fixed charcoal bed)	Charcoal bed for adsorption of high molar volume contaminants in cabin air; charcoal-impregnated with phosphoric acid for specific control of ammonia.	External leakage (at end plate sealing ring). Note: This is a failure mode for ground model only. Flight model will have end plate welded in place to preclude failure mode.	Pan draws air into system bypassing fixed bed (Ground model only).	High molar volume contaminants not removed from cabin air, (a) these contaminants inactivate regenerable bed, and (b) NO_x enters oxidizer, forms NO_2 , poison catalyst. (Ground model only).	III	Mass spectrometer and leak detector (Ground model only).	Replace fixed bed end plate seal. (Ground model only)
PI	Fixed Bed Fan	Draw cabin air over fixed charcoal bed at 70 CFM flow rate.	Electrical outage.	Pan rotor stops.	High molar volume contam. not removed from cabin air; regenerable bed fan draws "contaminated" air thru regenerable bed and catalytic oxidizer.	III	Mass spectrometer and differential pressure sensors (Ground model only).	Clean input screen, if clogging continues, replace filter seal (on ground model) or replace fixed bed (on flight model).
RS	Regenerable Bed (Low flow regenerative charcoal bed)	Charcoal bed for adsorption of low molar volume contam in cabin air with periodic desorption of bed by reducing total pressure below 1000 mbars. Flight model will have end plate welded in place to preclude failure.	Mechanical (bearing) failure.	During adsorption cycle: No effect on regenerable bed. During desorption cycle: Provides cabin leak to vacuum. (Ground model only)	Some of the contaminants requiring catalytic oxidation not removed from cabin air. (Ground model only) Gradual loss of cabin air. (Ground model only)	III	Mass spectrometer and leak detector (Ground model only)	Replace regenerable bed and plate seal. (Ground model only) Vacuum pressure reading above normal & leak detector. (Ground model only)

Table 23
FAILURE MODE AND EFFECTS ANALYSIS
Systems _____
Subsystems _____
Equipment _____
Mission Phases _____

Ident. No.	Rel. Ab. Logic No.	Function	Failure Mode and Cause	Failure Effect on Component/Functional Int'l.	Criticality	Failure Detection Method	Time Req./Avail.
	<u>Regenerable Bed</u>		Internal leakage (at connector O-ring)	Double (redundant) O-rings prevent any failure effect.	No effect	--	--
	<u>Cont.</u>		Channeling through sorbent or saturated zone reaches equilibrium corresponding to MAC.	Contaminants not removed by sorbent at required rate.	Low molar volume contam. not removed from cabin air; eventually, oxidizer catalyst will be poisoned.	III Mass spectrometer	Perform a desorption cycle; if failure mode continues, replace charcoal (ground model) or replace regenerable bed (flight model).
			Heating elements fail off (open electrical circuit)	During adsorption cycle; no effect.	No effect.	--	--
				During desorption cycle, evaporation drops air temperature preventing further desorption.	Low molar volume contam. not removed from cabin air during next adsorption cycle - catalyst poisoned.	III Meter current; regenerable bed exit air temp. monitor.	Replace regenerable bed heaters.
				During adsorption cycle; higher than normal temperature prevents adequate adsorption.	Low molar volume contam. not removed from cabin air; eventually, catalyst will be poisoned.	III Meter voltage; bed exit air temp-monitor.	Check and repair electronics.
				Fan rotor stops.	Contaminants normally processed by regenerable bed or catalytic oxidizer not removed from cabin air.	III Regenerable bed fan differential pressure sensors at zero differential.	If power available at differential pressure, replace fan; otherwise check power source.
	<u>Regenerable Bed Fan</u>		Draw air from fixed bed fan outlet at 4 CFM for processing thru regenerable bed and catalytic oxidizer.	Mechanical (bearing) failure.	Decreased flow rate reduces effectiveness of regenerable bed, prevents catalytic oxidation, catalyst eventually poisoned as in Fixed Bed "external leakage" failure mode.	III Regenerable bed fan differential pressure sensors between zero and normal.	--

Table 23
FAILURES MODE AND EFFECTS ANALYSIS

System	Subsystems	Equipment	Mission Phase	Page _____ of _____	Revision _____ Date _____	By _____	Due _____	Time Req./ avail.
Ident. No.	Failure Logic No.	Failure Punction	Failure Mode and Cause	Failure Effect on Component/functional 3972.	Failure Effect on System	Criticality	Failure Detection Method	crew Action Req.
81	Pre-Sorbent	Lithium hydroxide sorbent to remove acid gases from air sample prior to its entering catalytic oxidizer.	External plate sealing (at end plate sealing ring). Note: This is a failure mode for ground model only. Flight model will have end plate welded in place to preclude failure mode.	Air flow to catalytic oxidizer reduced; contaminants requiring oxidation not removed from cabin air at required rate. (Ground model only).	III	Mass spectrometer (See Note 1).	Replace end plate seal. (Ground model only).	
82	Catalytic Oxidizer	Oxidize trace contaminant removed by charcoal beds by passing air sample over catalyst heated to operating temperature of 600°F.	Channelling thru sorbent or saturated zone reaches equilibrium corresponding to MAC.	Acid gases not removed from air sample (See Note 2)	Gradual poisoning of catalyst in catalytic oxidizer.	III	(See Note 2)	Replace sorbent (ground model)
				No effect.	Double (redundant) O-rings prevent any failure effect.	--	--	
				External air leakage (at input or output connector O-rings)	The small pressure differential (less than 10" H ₂ O) across the seal reduces the effect of a minor leak to an insignificant level. A major leak could eventually develop, the effect of the reduced flow being the same as catalyst channeling or poisoning (see below). However, the latter failure mode would occur first and since the associated maintenance action will include replacement of the seal, the major seal leakage is prevented.	--	--	
				External leakage at back plate sealing ring.	Approx. 1 inch Min-K-1301 insulation will hold radiating heat losses within design tolerance. Temperature requirements also consider the normal heat losses conducted to the end ports. There are no operating failure modes that could increase thermal leakage beyond the design parameters.	--	--	

Table 23
FAILURES MODE AND EFFECTS ANALYSIS

System	Page _____ of _____	Revision _____ Date _____	By _____	Doc. _____	Time Req./Avail.		
Subsystems	Failure Log No.	Function	Failure Mode and Cause	Failure Effect on System	Criticality	Failure Detection Method	Correct Action Req.
Equipment	Ident. No.	Failure Log No.	Component/Functional Area	Failure Effect on System	Criticality	Failure Detection Method	Correct Action Req.
Mission Phase	82	<u>Post-Sorbent</u>	Lithium hydroxide sorbent to remove potential undesirable products of oxidation from catalytic oxidizer.	No effect on post-sorbent. (at end plate sealing ring) Note: This is a failure mode for ground model only. Flight model will have end plate welded in place to preclude failure mode.	No effect on primary system function, however "contol-at-source" criteria (undesirable products removed from cabin atmosphere at their source) is lost but personnel are protected by other system elements.	III	(See Note 3) Replace sorbent (ground model).
	CR1	<u>Inlet Flow Control Valve</u>	Remote shut-off of air at regenerator bed input; isolates cabin air from vacuum source; two-way N. O. valve.	External leakage (at connector O-rings) Internal leakage (clogging at seat) (See Note 4)	Double (redundant O-rings) prevent any failure effect. Applicable during desorption cycle only; provides cabin leak to vacuum. (See Note 5)	No effect. Gradual loss of cabin air.	III Vacuum pressure higher than normal level during deorption cycle; valve indicator shows closed.
				Electronics fail open (valve open)	Applicable during desorption cycle only; provides open valve cabin air to vacuum.	Loss of cabin air.	III Valve position select indicator shows open
				Electronics fail short (valve closed)	Applicable during adsorption cycle only; air flow ceases downstream of valve.	Low molar volume contaminants not removed from cabin air.	III Regenerable bed fan repair electronics or replace valve.

Table 23
FAILURE MODE AND EFFECTS ANALYSIS

System	Subsystem	Equipment	Mission Phase	Page <u>6</u> of <u>6</u>	Revised <u>10/10/85</u> Date <u>10/10/85</u>	By <u>DRG</u> Due <u>10/10/85</u>	
Ident. No.	Func.	Failure Mode and Cause	Failure Effect on System	Criticality	Failure Detection Method	Crew Action Req.	Line Req./Avail.
CRV4	<u>Vacuum Bleed Valve</u>	With flow valves and vacuum valve closed, enables pressure in regenerable bed to be gradually bled to vacuum before vacuum valve is opened; two-way, N.C. valve.	Double (redundant) O-rings prevent any failure effect.	No effect.	--	--	--
		Internal leakage (at connector O-rings), (clogging at seat) (See Note 4).	Same as effect from "internal leakage" failure mode of vacuum valve.	III	Same as detection of "internal leakage".	See maintenance for vacuum valve "internal leakage".	
		Electronics fail open (valve closed)	Unable to bleed air from regenerable bed.	III	Valve Indicator shows closed (Opening of vacuum valve will be prevented).	Repair electronics or replace valve.	
		Electronics fail short (valve open)	Same as effect from "electronics fail short" failure mode of vacuum valve.	III	Same as "electronics fail short" of vacuum valve except that bleed valve indicator shows open.	Repair electronics or replace valve.	
MV1	<u>Isolation Valve</u>	Isolation of trace contamination control system from vacuum source; manual valve, closed only for maintenance actions on vacuum and bleed valves.	External leakage (at connector O-rings), Internal leakage (clogging at seat)	No effect.	--	--	--
			Double (redundant) O-rings prevent any failure effect.	IV	Vacuum pressure gauge during preventive maintenance check.	Close downstream valve at vacuum source; replace system isolation valve.	
			Valve ineffective.	Non except maintenance of upstream valves prevented.	--	--	--
			Double (redundant) O-rings prevent any failure effect.	IV	Same as detection of "internal leakage".	See maintenance for inlet flow control valve "internal leakage".	
CRV5	<u>Pressure Bleed Valve</u>	With flow valves and vacuum valves closed, enables pressure in regenerable bed to be gradually raised from vacuum before flow valves are opened; two-way N.C. valve.	External leakage (at connector O-rings), Internal leakage (clogging at seat) (See Note 4).	No effect.	--	--	--
			Same as effect from "internal leakage" failure mode of inlet flow control valve.	III	Valve Indicator shows closed.	Repair electronics or replace valve. (See Note 7).	
		Electronics fail open (valve closed)	Unable to bleed air into regenerable bed.	III	Same as "internal leakage" above except valve indicator shows open.	Repair electronics or replace valve.	
		Electronics fail short (valve open)	Applicable during desorption cycle only: provides cabin leak to vacuum.				

System Space Station Prototype
 Subsystem Trace Contaminant Control System
 Equipment Orbit (Manned, Test Bed)
 Mission Phase Orbit

Table 23
 FAILURE MODE AND EFFECTS ANALYSIS

Ident. No.	Name	Module, Logic No.	Function	Failure Mode and Cause	Component/Functional Asy.	Failure Effect on System	Criticality	Failure Detection Method	Corrective Action Seq.	Time Req'd./Avail.
E 1	400 Hz Panel	Subsystem Terminal Blocks	Convert 115V, 600 Hz input to +5V DC, single power output.	5V output high or low (electronics failure).	Panel Inoperative	No effect.	N/A	At SSP Power Supply Panel	Not Applicable to Subsystem Analysis	
E 2	5 Volt Power Supply		Convert 115V, 600 Hz input to +5V DC, dual tracking power outputs.	+15V or -15V outputs high or low (electronics failure)	Degradation of subsystem electronics, potential loss of subsystem.	No effect.	III	Indicator (LED) at subsystem, failure signal available to DMS.	Replace power supply.	
E 3	15 Volt Power Supply		Furnish timing base for subsystem operations	Loss of output (timing) signal (electronics failure)	Degradation of subsystem electronics, potential loss of subsystem.	No effect	III	Indicators (LED's) show failure of either output at subsystem; failure signals available to DMS.	Replace power supply.	
E 4	Digital Clock			Clock output inaccurate, i.e., incorrect time readouts (electronics failure).	Loss of automatic operation (manual operation not affected).	No effect	III	Circuit in electronics package detects this failure mode; failure signal available to DMS.	Replace clock.	
E 5	High Voltage Power Supply and Vacuum Sensors		Convert 115V, 400Hz input to 240V AC (rectified output); 330V DC for use with Penning type gauge circuit used to sense and measure vacuum in exhaust line.	Three identical circuits are used in voting arrangement; hence, there is no effect from any one sensor/circuit failure.	No effect.	III	System effect indicated will be detected at SSP main power panel.	Indicators (LED's) at subsystem; Green: three sensors/circuits in operation. Yellow: one of three failed. Red: Second circuit failed. Analog output from non-failed sensors available to DMS.	Assume indication at main panel will also indicate specific subsystem drawing the abnormal load. Troubleshooting subsystem will show "out-of-sync" operation. Replace clock.	

Table 23
FAULT MODE AND EFFECTS ANALYSIS

System: Space Station Prototype
Subsystems: Trace Contaminant Control System
Equipment:
Mission Phase: Orbit (Manned, Test Bed)

Ident. No.	Name	Relab. Logic No.	Function	Failure Mode and Cause	Failure Effect on Component/Functional Area	Failure Effect on System	Criticality	Failure Detection Method	Line	Line Req./Area.	Crus Action Seq.
8 5	(Continued)			Technician subjected to electrical shock during maintenance action on this equipment (H.V. circuit carries static potential after line circuit breaker is open).	Warning labels on equipment and instructions in maintenance procedures will require that H.V. circuit be grounded before maintenance actions are started in order to preclude this failure mode.	No effect (except Crit. III becomes crit. if indicated precautions are not taken).	III	Not applicable.	None		
8 6	Electronics Package			Technician subjected to electrical shock during maintenance action elsewhere in subsystem (H.V. circuit energized and accessible to technician).	Metallic (grounded shielding) surrounding high voltage circuits and maintenance instructions requiring disconnect of input to high voltage circuits will preclude this failure mode.	No effect.	III	Not applicable.	None.		
				Includes electronic circuitry (logic) for (a) operation of subsystem in either auto or manual modes and (b) failure isolation of subsystem.	Loss (degradation) of one or more logic circuits in electronics package.	No effect.	III	DNS will isolate failure to: (a) specific control function circuitry in electronics package.	(1) Troubleshoot, replace indicated portion of package or replace package.		
								(b) Specific control function (valve, fan, etc.) or associated circuitry in electronics package.	(2) replace both failed control function and electronic package.		
								(c) Specific sensor or associated circuitry in electronics package.	(Same as above, except sensor in lieu of control function.)		

NOTES:

- (1) Failure detection of leakage at the end plate sealing ring of the (ground model) pre-sorbent is identical to detection of a catalyst failure in the catalytic oxidizer. However, the probability of the pre-sorbent leak developing in this low pressure system is insignificant compared to the catalyst failure. On the ground, the leakage failure would be differentiated from the catalyst failure by a leak detector. As noted, the leakage failure mode does not occur in the flight model.
- (2) As indicated in the technical analyses of the pre-sorbent, most of the gas components that could poison the catalytic oxidizer will have been already removed by the charcoal beds before they reach the pre-sorbent. Hence, it is improbable that the saturated zone of the pre-sorbent will be reached. Correct packaging also reduces the probability of channeling to insignificance. Special instrumentation (in addition to the mass spectrometer) will be used during ground model testing to confirm these hypotheses.
- (3) Conservative design of the post-sorbent provides that probability of the failure mode is essentially insignificant. As indicated for the pre-sorbent, special instrumentation will be used during ground testing to confirm the design.
- (4) Filter at the outlet of the fixed bed should prevent any particles entering and clogging the input flow control valve or vacuum valve. Filter at the outlet of the regenerable bed similarly protects the output flow control valve. Ground testing confirmed that additional filtering was not required at the inlet of the regenerable bed to further protect the vacuum valve during desorption. Hence, the probability of internal leakage by clogging is very low. Leakage increase due to normal wear-out of the valve seat is very slow and is not considered a failure mode.

- (5) The failure mode will occur when the valve is closed at the beginning of desorb preheat. Hence, its immediate effect is to leak gases (mainly water vapor) from the regenerable bed into the cabin during the initial heating period. This loss of heat (through the restricted opening of a clogged valve seat) is not sufficient to affect the required temperature rise in the regenerable bed. The effect of any contaminants released from the bed into the cabin will not be significant. Failure effects of the valve leakage become significant only when the vacuum valve is opened at which time the air leakage would be detected as indicated.
- (6) An additional effect of the leakage failure mode at the outlet flow control valve is that gases will be drawn from the catalytic oxidizer when the vacuum valve is opened. The immediate effect is to pass hot gases over the outlet flow control valve seat. This may accentuate the initial failure mode, although the heat exchanger will cool the back-flowing gases. The vacuum pressure sensor will detect the failure and shut down the system and prevent further failure effects.
- (7) If electronics can be repaired without removing valve from system, the system failure effect shown will be prevented. If the valve must be removed, the regeneration sequence will be manually overruled. It is not anticipated that a one-time occurrence of this failure will damage the system; however, if ground testing indicates otherwise, a manual override may be provided for the pressure bleed function.

6.2 SAFETY HAZARD ANALYSIS

The following section will examine inherent safety hazards that are potentially incorporated in a system of this nature and will discuss the precautions that have been included to prevent or mitigate the effects of such hazards.

6.2.1 Cabin Leak to Vacuum

Since the system piping is connected to a vacuum source, there exists a potential leak path from the cabin "shirt-sleeve" environment to vacuum. As indicated in the FMEA, external leakage of flight components is prevented by the redundant O-rings at connectors. This however was not implemented in the prototype system. All other mechanical closures of piping or components will be brazed or welded. Hence, the only path possible is internally through the vacuum valve and either flow control valve. (For purposes of this discussion, the vacuum bleed valve is considered to be included as part of the vacuum valve and the pressure bleed valve is considered to be part of the inlet flow control valve). Under normal operating conditions, the vacuum valve and flow valves are not open to the regenerable bed at the same time, so that a cabin leak can occur only if one of these valves should fail. The system's electronics will continually monitor each valve position indicator and compare this signal to the expected valve position at any point in the adsorb/desorb cycle. An error signal will cause all valves to close until reset after completion of maintenance actions. The system will also be fail-safe in that the normally closed vacuum valve will close mechanically in event of power failure. Should the valve failure be a slightly open valve due to clogging (not revealed by the valve indicator), failure will be detected by the vacuum pressure sensors in the exhaust line. These sensors will normally "read" vacuum during adsorption and slightly higher during desorption (after vacuum bleed). If a leak occurs, the outflow of cabin air will indicate a higher pressure commensurate with the flow rate. The pressure sensors would then command a shutdown of all valves. These sensors are themselves fail-safe in that three sensors will be incorporated in a voting circuit. Should one sensor fail, the other two will constitute the prevailing command but an alarm will indicate this condition in order that this set of three sensors can be replaced when convenient. The concept of redundant voting sensors was not implemented in the prototype system. Although a small amount of cabin air

will be lost before the failure detection devices are activated, the size of the cabin is such that this loss will not affect the safety of the personnel.

6.2.2 Generation of Toxic Gases

The oxidation of contaminants in the catalytic oxidizer will result in the production of certain toxic substances. The identification of these substances, their anticipated levels in the oxidizer exhaust, and the function of the post-sorbent in removing them from the air stream is discussed in a previous section. As indicated therein, the sorbents in the system ahead of the oxidizer act to maintain the level of toxic products below their allowable levels even in the absence of the post-sorbent. Hence, failure of the post-sorbent function would not directly affect the safety of personnel.

6.2.3 System High Surface Temperature

The catalytic oxidizer operates at a catalyst temperature of 633 K (680 F) with normal air flow and 811 K (1000 F) with no flow. The air stream leaving the oxidizer is at a temperature of 344 K (160 F). Hence, precautions should be taken to protect personnel. Design of the oxidizer and associated piping is based on a maximum safe "touch" temperature of 322 K (120 F). It is anticipated that with a one-inch blanket of Min-K 1301 insulation, together with an outer insulation blanket the outside surface of the catalytic oxidizer will not present a burn hazard. Present analysis indicates that the heat sink provided by the attaching structural members at the outlet of the oxidizer will be sufficient to protect personnel during maintenance activities are included in the maintenance procedures.

6.2.4 Radioactive Emissions

The AEC has certified the safety of the isotope capsule container utilized for the prototype system. On this basis, safety hazards created by structural damage of the container are precluded. The precautions required by AEC, NASA, or local regulations for handling and operating an isotope heat source are included in the written procedures. Hence, this discussion is limited to the radiation dose levels that can be anticipated during test and operation of the present ground system.

AEC Research and Development Report MIM-1757 (Ref. 3) indicates that the two units to be furnished are from a lot previously used on the Life Support II Program during 90-day manned chamber tests at McDonnell Douglas. The two units were approximately 73 watts and 48 watts as of April 1969, and December 1969, respectively. The radiation from the source consists principally of fast neutrons. Discussions with Mound Laboratory (AEC) personnel note that the conversion factor used to obtain rem dose in the above report is high, since it applies to a different neutron spectrum. Using the measured spectrum and the rem dose-neutron fluence factors in NCRP Report 38 (Ref. 4) for whole body irradiation, the factor is 3.4×10^{-5} millirem for neutron/cm^2 rather than the 4.3×10^{-5} factor used in the report. As stated in the reference, the dose at points on the cylindrical axes of the heat source is lower than at the sides, which is the measurement point reported. Dose in the handling-knob direction is 59% of the side dose. The capsules are mounted with the handling-knob toward the space occupied by personnel so that the lower dose level can be assumed.

The radiation dose constraints used in the design of the Trace Contaminant Control System are those indicated by NASA-MSC (letter, R. G. Rose, Radiation Constraints for Skylab, Shuttle, and Space Station, dated 1/15/71) (Ref. 5). For the isotope heat source, eye dose can be assumed to set the allowable distances, since other targets have a greater ratio of attenuation considering the reference body depth of the target associated with its allowable dose factor. (A possible exception is the testes, but a slight change in body orientation

such as a seated position provides greater attenuation than the 3 cm effective depth designated by the reference letter.) The quarterly maximum allowable eye dose is 52 rem, and this dose is allowed for two consecutive quarters, if followed by six months of removal from exposure. This indicates a 10^4 rem allowable total eye dose in a 180-day mission.

Based on the above, the present system is designed to maintain the radiation dose at 10 percent of the allowable dose. This provides sufficient margin to safeguard against additional man-made and natural radiation sources as well as any unexpected exposure. This corresponds to a required average separation distance of 125 cm from the center of the heat source. Average in this case refers to a geometrically weighted distance-time relationship since dose varies inversely as the square of the distance. In allowing for maintenance operation it was assumed that in a 180-day mission, there would be 20 such operations at 50 cm distance from the source. The dose accumulated would be 1.1 rem. In order to maintain the 10 percent allocation, the average separation distance for these personnel would increase to 130 cm. The above separation distances should present no problem in a vehicle the size of a space station. It has also been noted (Section 4.4.5) that the isotope power source that would be used on a flight model would produce less than 5 percent of the allowable dose at the above average separation distances.

6.2.5 Flammability

Present indications show that there are no materials in the system that would fail to meet spacecraft flash point and fire point requirements. A non-metallic materials list for the complete system is presented in Appendix A. Available data on the activated charcoal flammability is not conclusive, but this material appears to be satisfactory. It should be noted that for the flight models, the charcoal sorbent will be entirely contained in a welded canister.

Available data on activated charcoal (Barnebey Cheney AC-4) flammability indicate that the material tested is rather resistant to ignition. The COMAT printout for May 8, 1972 indicates that in a standard flash and fire point test at 42.7 kN/m^2 (6.2 psia) pure oxygen, the flash and fire points were greater than 589 K (600 F). Also, of two upward flame propagation rate tests in 42.7 kN/m^2 (6.2 psia) pure oxygen, one showed no evidence of ignition and one showed smoldering combustion only, at a rate of 0.025 mm/sec (.001 in/sec). A downward propagation rate test at the same oxygen condition showed no evidence of ignition. Only for the 114 kN/m^2 (16.5 psia) pure oxygen condition was active combustion achieved. The upward rate was .28 mm/sec (0.011 in/sec).

Without consulting the test reports to determine how the presumably granular material was handled or formed to the standard 5 x 25 cm (2 x 5 in) sample, it is difficult to evaluate this data. However, compared to the 478 K (400 F) flash point or 505 K (450 F) fire point requirements for Category B spacecraft materials, charcoal appears to meet requirements. It also appears to meet the Category A requirement of zero upward propagation rate for anticipated oxygen contents of the atmosphere.

6.3 FAULT DETECTION AND ISOLATION ANALYSIS

System components and instrumentation are identified in this analysis (and in the FMEA) as shown in Table 24 and Figure 16. The FMEA indicated the failure modes that can exist during operation of the system. It was determined that instrumentation should be provided that would (a) detect each potential failure, (b) isolate the failure to a maintainable unit, and (c) direct system shutdown, if necessary. The analysis was based on a flight model and assumes the existence of an OCS (onboard computer system) external from the Trace Contaminant Control System. In general, the system's instrumentation will send analog or digital signals to control logic in the OCS. These signals, either individually or in combination, together with operating standards programmed in the OCS software, will enable the OCS to direct a system shutdown in event of failure. The failed component would be identified by indicator lights at the OCS control console. The need for redundant logic that would provide shutdown capability within the

TABLE 24
SYSTEM COMPONENTS AND INSTRUMENTATION

Code	Item	Quantity
FB	Fixed Bed	1
RB	Regenerable Bed	1
S1	Pre-Sorbent	1
S2	Post-Sorbent	1
CO	Catalytic Oxidizer	1
F1	Fixed Bed Fan	1
F2	Regenerable Bed Fan	1
CRV1	Inlet Flow Control Valve	1
CRV2	Outlet Flow Control Valve	1
CRV3	Vacuum Valve	1
CRV4	Vacuum Bleed Valve	1
CRV5	Pressure Bleed Valve	1
V6	Vacuum Isolation Valve (Manual)	1
* P1	Fixed Bed Fan Diff. Pressure Sensor	3
* P2	Regenerable Bed Fan Diff. Pressure Sensor	3
* P3	Vacuum Line Pressure Sensor	3
* V1	Regenerable Bed Heater Voltage Detector	1
* I1	Regenerable Bed Heater Current Detector	1
* T1	Regenerable Bed Temperature Sensor	1
T2	Catalytic Oxidizer Temperature Sensor	1
* M/S	Mass Spectrometer	#
FM1	Regenerable Bed Bleed Flow Sensor	1
FM2	Catalytic Oxidizer Flow Sensor	1
-	Valve Position Indicators	1 per valve

* Fault detection instrumentation.

Mass spectrometer (GFE) at remote location; ports for sensor provided in piping at sorbent beds and oxidizer.

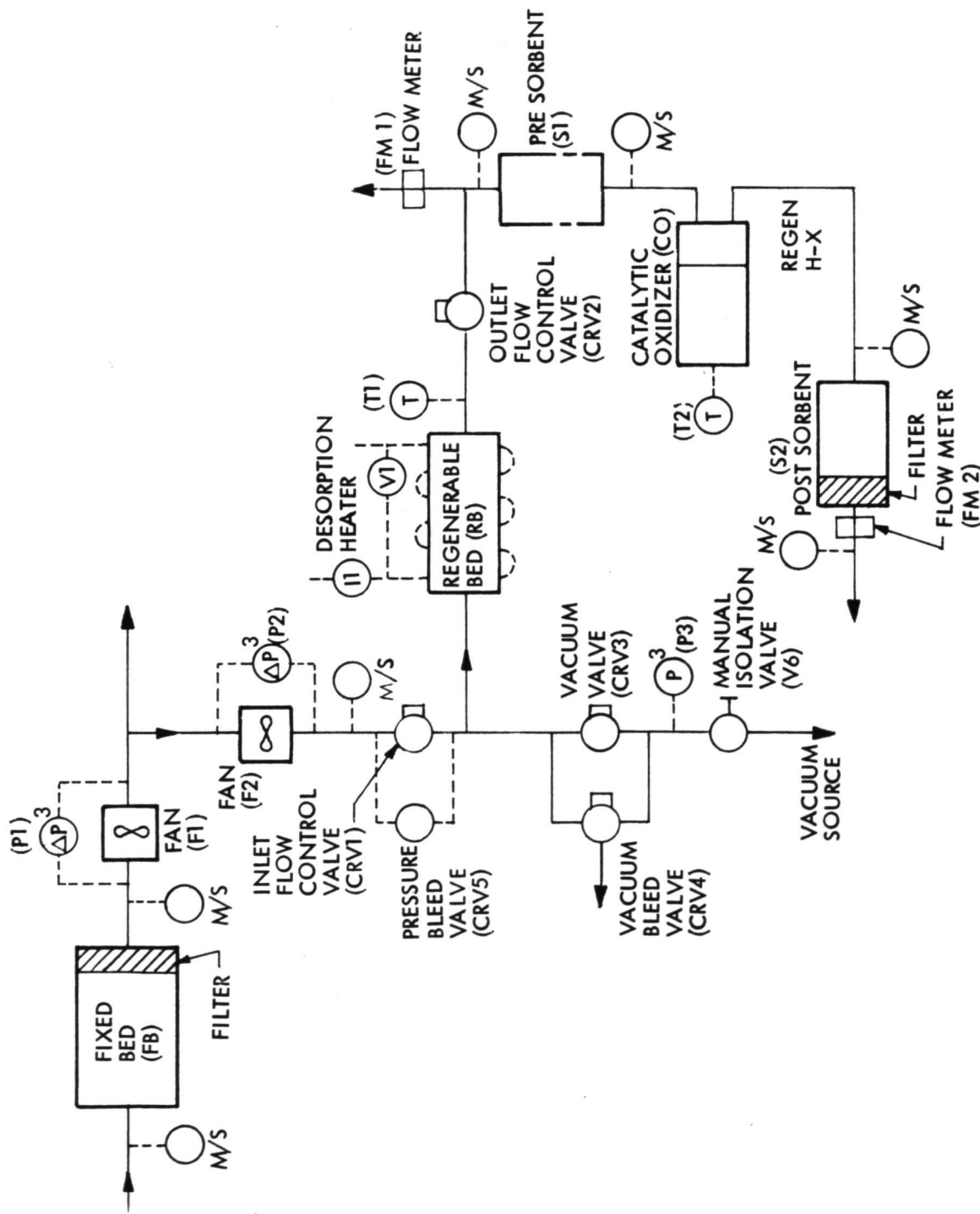


Figure 16 Trace Contaminant Control System Instrumentation

Contaminant Control System itself was also examined. However, there are no Criticality I or Criticality II failure modes in the system and the internal shutdown capability is not considered necessary for this hardware phase.

A summary of the fault detection required for the system is shown in Table 25. The fault-detection instrumentation is identified by the asterisk in Table 24. In order to eliminate a single point of failure, three sensors are provided for each of the pressure measurements P1, P2 and P3. These voting circuits were not implemented in the prototype system. The analog signals from the three sensors would be routed through a voting circuit which will recognize that a fault exists in one of the sensors when their outputs are not the same. The signal lines to the OCS will carry (a) the analog of the majority pressure sensors, and (b) the status of the sensors themselves. When a sensor fault is indicated, the maintenance action will be to replace the set of three sensors. The pressure measurement analog will be compared to standards that have been established in the OCS software in order to determine when a pressure fault exists. The action indicated in the Fault Detection Summary will be directed by the OCS. The analogs of the temperature measurement (T1) and the electrical measurements (V1 and I1) will be individual signals to the OCS. Voting circuits are not required since either of the two regenerable bed heater faults affect two separate measurements. The software in the OCS will detect a measurement fault as well as a sensor fault. The mass spectrometer sensors in the system will send individual signals to the OCS. The differentials of these signals at various points throughout the system will enable the mass spectrometer and OCS software to identify a failure in any of the sorbent beds or catalytic oxidizer. The valve position indicators will be individual signals to the OCS.

As indicated, the instrumentation has been designed for a flight model. For initial ground testing, this instrumentation will be employed without an OCS. Instead of directing the instrumentation output signals to an OCS, they will be sent to pressure, temperature, and electrical recorders/indicators and pilot lights on the test console. Faults throughout the testing will be recognized by visual monitoring of these devices. In addition voting sensors were not utilized in the prototype system.

TABLE 25
FAULT DETECTION SUMMARY

Fault	FMEA Ref.	Detected By	System Action	Ref. Note
Fixed Bed Sorbent ineffective	FB	M/S*	Alarm and manual shutdown	(1)
Fixed Bed Filter/Screen clogged	FB	P1 at $>797 \text{ N/m}^2$ (3.2 in water)	Alarm and manual shutdown	(1)
Fixed Bed Fan stopped	F1	P1 at zero	System automatic shutdown	(2)
Fixed Bed Fan low speed	F1	P1 at $<548 \text{ N/m}^2$ (2.2 in water)	Alarm and manual shutdown	(1)
Regen. Bed Sorbent ineffective	M/S		Alarm and manual shutdown	(1)
Regen. Bed Heater open circuit	RB	T1 zero during pre-heat and desorption T1 380 F during pre-heat and desorption. T1 212 F during desorption.	Partial automatic shutdown	(3)
Regen. Bed Heater short circuit	RB	V1 zero except during desorption T1 150 F during adsorption	Partial automatic shutdown	(3)
Regen. Bed Fan stopped	F2	P2 at zero.	Partial automatic shutdown	(3)
Regen. Bed Fan low speed	F2	P2 at $<3.98 \text{ kN/m}^2$ (in water)	Alarm and manual shutdown	(1)
Pre-Sorbent ineffective	S1	M/S	Alarm and manual shutdown	(1)
Catalytic Oxidizer ineffective	CO	M/S	Alarm and manual shutdown	(1)
Post-Sorbent ineffective	S2	M/S	Alarm and manual shutdown	(1)
Flow Control Valves/Pressure Bleed Valve internal leakage	CRV1 CRV2 CRV5	P3 $>5.3 \times 10^{-2} \text{ N/m}^2$ (4×10^{-4} torr) and valve indicators closed during desorption.	Partial automatic shutdown	(3)
Flow Control Valves elect. Controls open circuit	CRV1	P3 $>5.3 \times 10^{-2} \text{ N/m}^2$ (4×10^{-4} torr) and failed valve indicator open during desorption	Partial automatic shutdown	(3)
Flow Control Valves elect. Controls short circuit	CRV2	P2 at $>4.73 \text{ kN/m}^2$ (19 in water) and failed valve indicator closed during adsorption.	Partial automatic shutdown	(3)

IMSC-D462467

TABLE 25 (continued)

FAULT DETECTION SUMMARY				Ref. Note
Fault	FMEA Ref.	Detected By	System Action	
Vacuum Valve/Vacuum Bleed Valve internal leakage	CRV3 CRV4	P3>5.3 x 10 ⁻² N/m ² (4 x 10 ⁻⁴ torr) and valve indicators closed during adsorption	De-energize F2, CRV3, CRV4 CRV5; energize CRV1, CRV2	(4)
Vacuum Valve/Vacuum Bleed Valve elect. controls short circuit	CRV3 CRV4	P3>5.3 x 10 ⁻² N/m ² (4 x 10 ⁻⁴ torr) and failed valve indicator open during adsorption.	De-energize F2, CRV3, CRV4 CRV5; energize CRV1, CRV2	(4)
Vacuum Valve elect. controls open circuit	CRV3	P3 at (vacuum) during desorption	Partial automatic shutdown	(3)
Vacuum Bleed Valve elect. controls open circuit	CRV4	Valve indicator closed during vacuum bleed	Partial automatic shutdown	(3)
Pressure Bleed Valve elect. controls open circuit	CRV5	Valve indicator closed during pressure bleed.	De-energize F2, CRV3, CRV4, CRV5; energize CRV1, CRV2	(4)
Pressure Bleed Valve elect. controls short circuit	CRV5	P3 > 5.3 x 10 ⁻² N/m ² (4 x 10 ⁻⁴ torr) and valve indicator open during desorption	Partial automatic shutdown	(3)
Main circuit Breaker Open	E1	All Indicators "OFF"	System Automatic Shutdown (requires manual start after fault correction)	(2)
5 Volt Power Supply, output out of tolerance.	E2	Power Supply Indicator Lamp	As above.	(2)
15 Volt Power Supply, output out of tolerance.	E3 E4	Power Supply Indicator Lamp Clock Indicator Lamp	As above.	(2)
Loss of Clock Timing Signal	E3	Reference FMEA	Alarm and Manual Shutdown	(1)
Failure (open, short or degradation) of electronic circuits in electronics package.	E6		Reference FMEA	(2)

NOTES:

- (1) System continues in operation until shutdown manually when convenient to perform maintenance action.
- (2) All elements of system are de-energized.
- (3) F1 remains energized; balance of system is de-energized.
- (4) F1, CRV1, and CRV2 are energized (or remain energized); balance of system is de-energized.

* Mass Spectrometer, GFE and not a part of this system.

Section 7

DESIGN

The following sections of this report describe the Trace Contaminant Control System (TCCS) design characteristics. Included in this discussion are the system and component design requirements and detailed design descriptions of the individual system components. Detailed engineering drawings for the entire system are presented in Appendix B and a listing of all non-metallic materials is presented in Appendix A. In performing detailed design, the use of commercially available stock (such as tubing) was employed, in cases where substantial cost savings would accrue to the program. This resulted in some cases in slight changes in component sizes for the as-built system compared to the design optimization described in Sections 3 and 4.

7.1 DESIGN REQUIREMENTS

The Trace Contaminant Control System initial design was optimized to somewhat different criteria than the Space Station Prototype. Prior to completing the final design it became necessary to adapt the hardware design to the requirements of the Hamilton Standard General Space Station Prototype System Specification SVHS 4655 and the Design Criteria Handbook SSP document number 9. The major system-level design requirements are as follows:

- Operate in a normal air environment at a pressure of 101.4 kN/m^2 (14.7 psia).
- Withstand explosive decompression of cabin with internal pressure at 101.5 kN/m^2 (14.7 psia).
- Undergo no appreciable corrosion due to lack of protection or having dissimilar metals in contact in the presence of moisture or fumes.
- Avoid selection of materials which are toxic or which create a flammability hazard.
- Provide touch protection where required on the surface of components having high operating temperature.

The overall system packaging requirements are as follows:

- o Size: Maximum envelope 86 x 86 x 127 cm (34 x 34 x 50 in). The system was originally laid out to include a Data Acquisition Unit and certain components identified on Hamilton Standard drawing SSP #SVSK 84477 (e.g. - The Emergency Carbon Dioxide Removal System). However, after completing the layout and full scale mockup. IMSC was informed that these items would not be included. Consequently there are some large unoccupied spaces in the TCCS.
- o Interfaces: Vehicle-to-TCCS interfaces are based on the requirements of Hamilton Standard General Spec SV HS 4655F. Cabin air inlet, vacuum source connection and electrical power connection are located on the left face. The vehicle electrical power source was specified as 400 Hertz, 3 phase Y, 120/208 volt. The air discharge duct is on the top surface, near the right edge.
- o Access: Each maintainable component is to be readily accessible. Access into the TCCS is to be from the front, rear, right and left sides (not top or bottom).
- o Captive Fasteners: All side panels and maintainable components to be installed using captive fasteners.

The individual component design requirements were defined by the analyses and trade studies and are presented in the component data sheets. These data sheets are presented in section 7.3.

7.2 DESIGN DESCRIPTION

Within the constraints described in the design requirements, a Trace Contaminant Control System configuration was developed. Paper studies were followed with a full-scale Foamcore mockup, shown in Figure 17, 18, and 19. Figure 17 presents a front view of the system viewed from the aisle of the spacecraft. Figure 18 presents the rear view and Figure 17 a side view. At the time this mockup was constructed, it was believed that 3 sets of differential pressure sensors and vacuum sensors would be required for reasons of reliability, but because of the curtailment of the SSP project only one of each sensor was included. The Hamilton Standard Data Acquisition Unit, emergency CO₂ removal canister, blower and two control valves can be seen in the photographs of the mockup. These items were originally intended to be installed into the system after its delivery to NASA. This requirement however was eventually deleted.

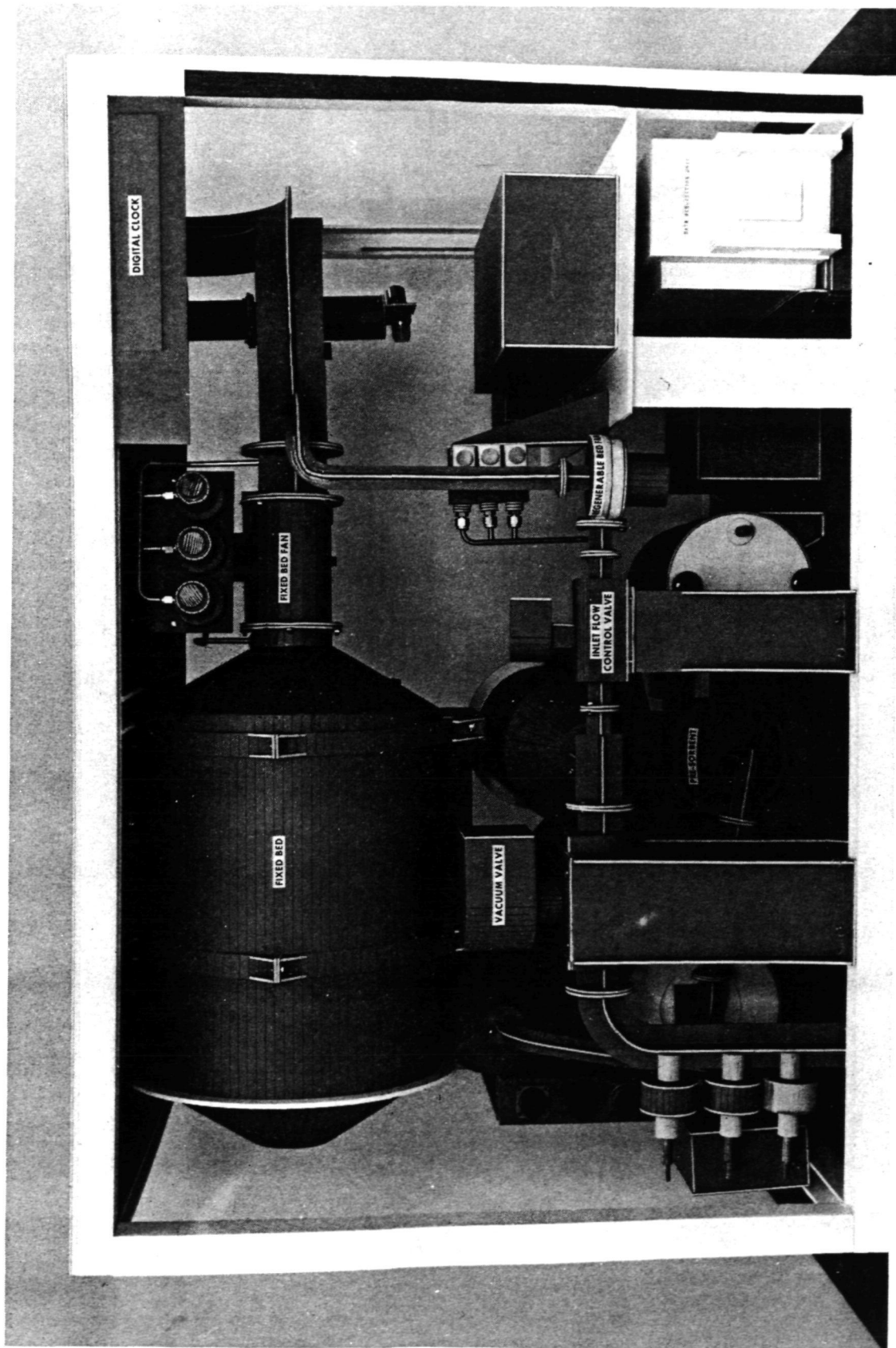


Figure 17 Mockup - Front View

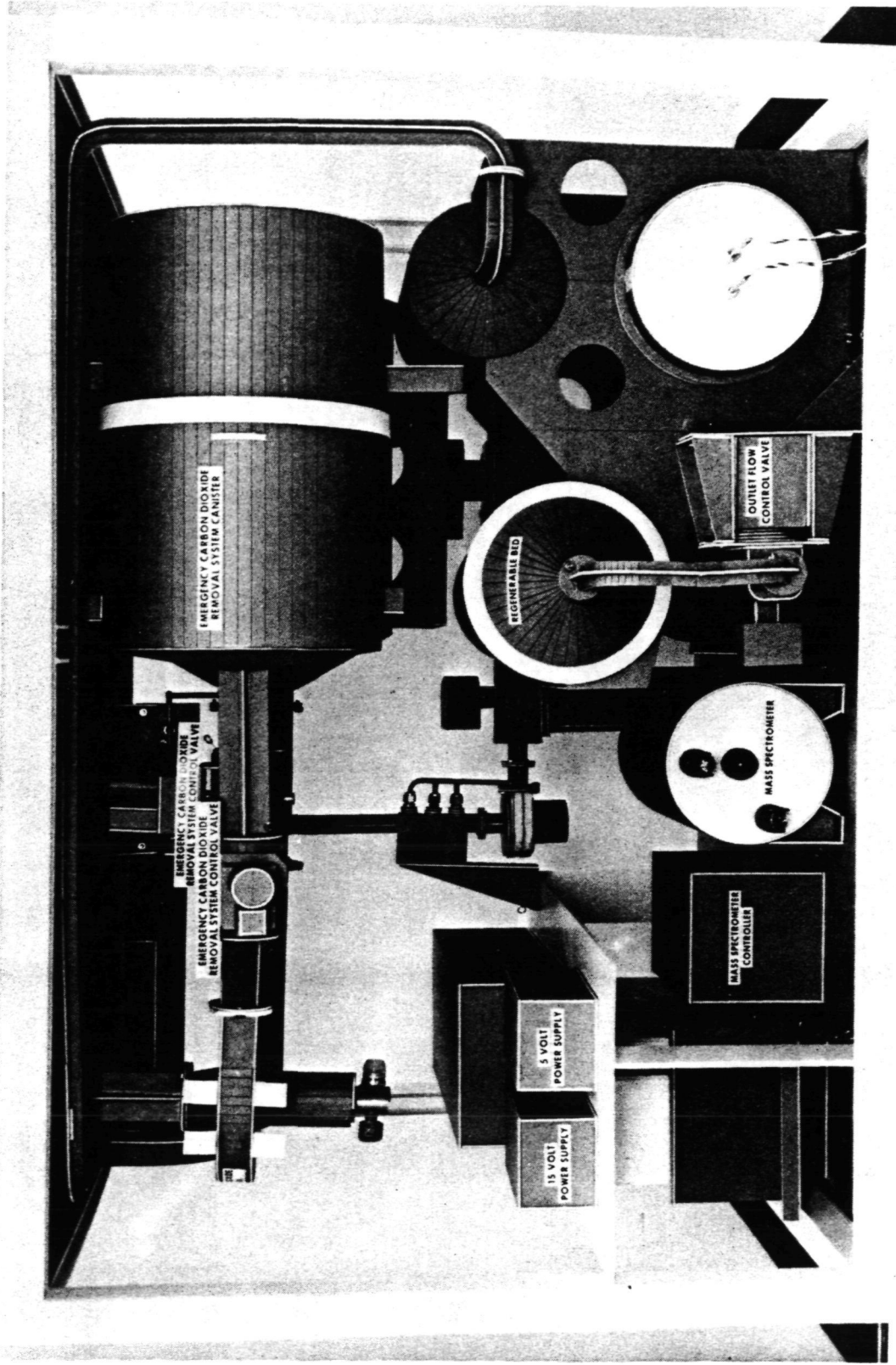


Figure 18 Mockup - Rear View

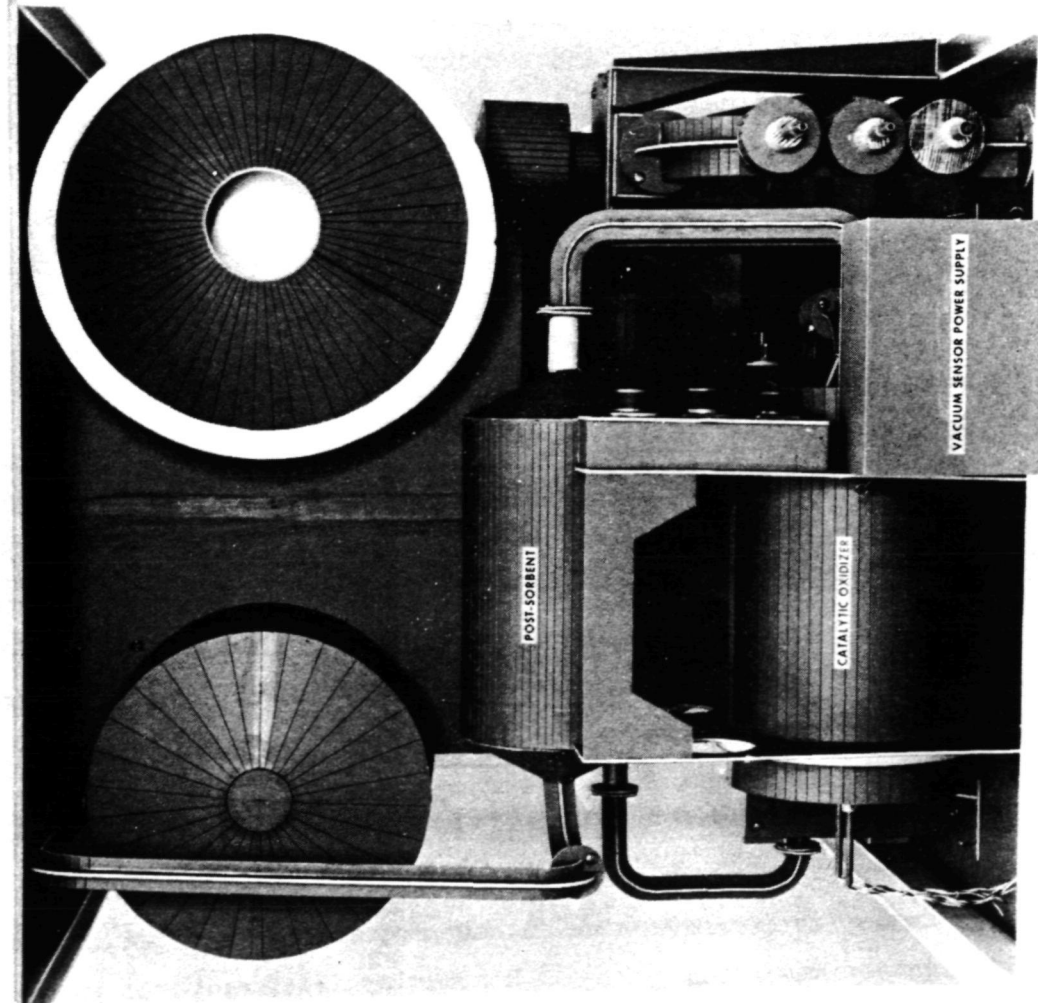


Figure 19 Mockup - Left Face

All of the maintainable components were located so as to provide accessibility from the front, rear, or the two sides. This meant that all four of these vertical panels would have to be removable. This required all components to be supported from the structural frame, the top plate, or the bottom plate. It was decided to construct the frame primarily of extruded aluminum Unistrut, with welded joints and gussets for reinforcement. The control panel and the digital clock are attached to the front of the frame. The fixed bed, and fixed-bed fan and the delivery duct are supported from the top plate by appropriate brackets. All of the remaining components are supported from the bottom plate. See Figures 20 to 24 for outline drawings and photographs of the system. One large bracket supports the catalytic oxidizer, the regenerable bed, and the post-sorbent bed. Each of these components can be shifted longitudinally on its cradle within the bracket. In addition, a small amount of lateral and vertical adjustment is possible for each of these three canisters to its cradle.

A system of ducts interconnects the various mechanical components. The connectors for these ducts must be capable of easy disconnection, and must be leak tight. In addition there are problems associated with accommodating thermal expansion/contraction, as well as manufacturing tolerances in the location of the components and the dimensions of the ducts. One of the possible solutions considered was inclusion of bellows as an integral part of certain ducts. However, this would have resulted in higher pressure drops. Part of the Trace Contaminant Control System is periodically subjected to high internal vacuum. This requires rigid connectors; Aeroquip-Marman flanged O-ring connectors were selected for the high-vacuum portions of the Trace Contaminant Control System. However the remainder of the system experiences only small differential pressures. This makes it feasible to employ connectors which can accommodate both longitudinal and angular misalignment. Accordingly, Gamah (Stanley Aviation Corp) connectors were used thruout the non-vacuum ducting. Viton is the elastometer selected for nearly all O-rings in the Trace Contaminant Control System.

Corrosion posed a potential problem in certain areas for two reasons: extremely high temperatures in the catalytic oxidizer, and presence of a corrosive

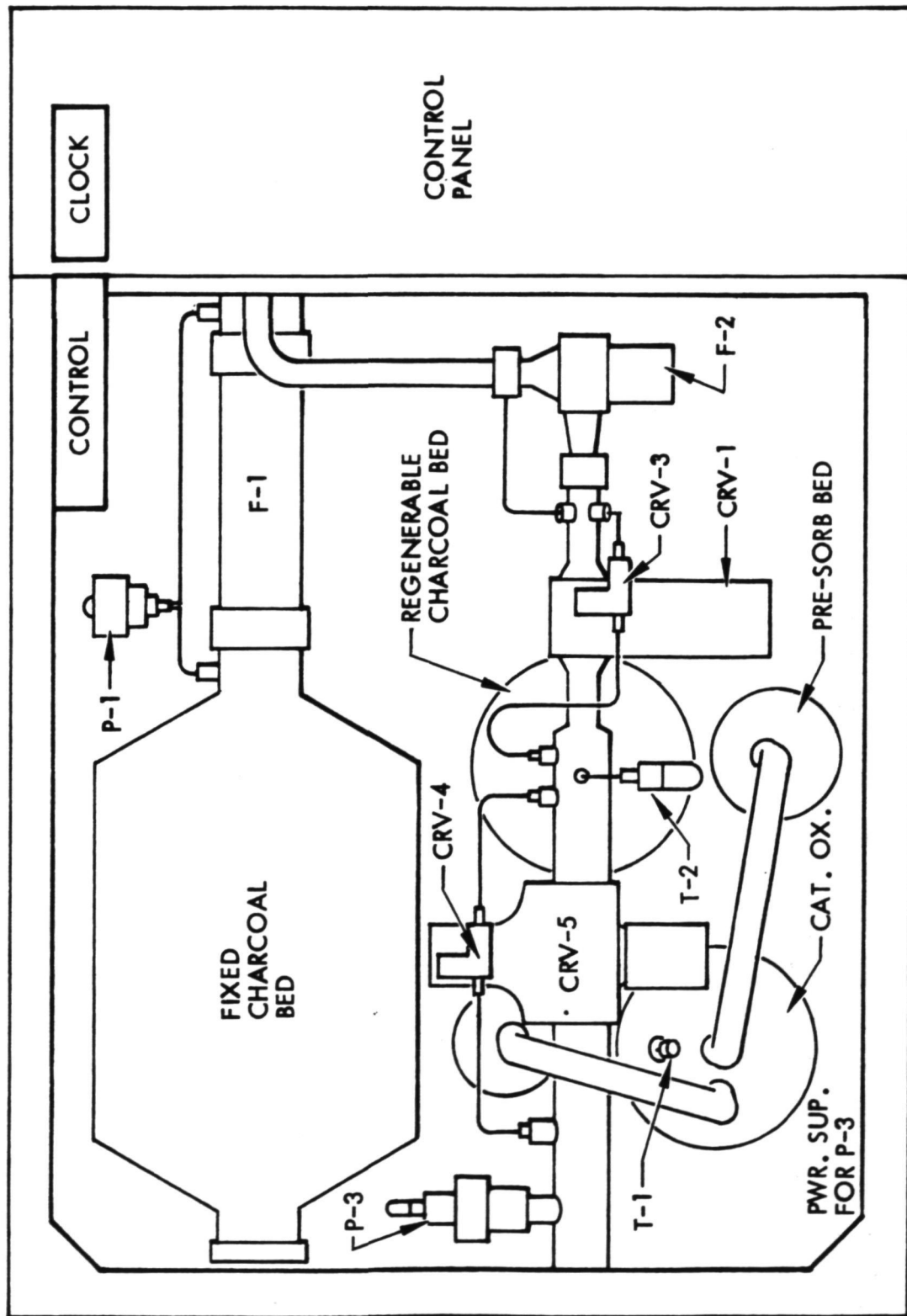


Figure 20 Trace Contaminant Control System Front View

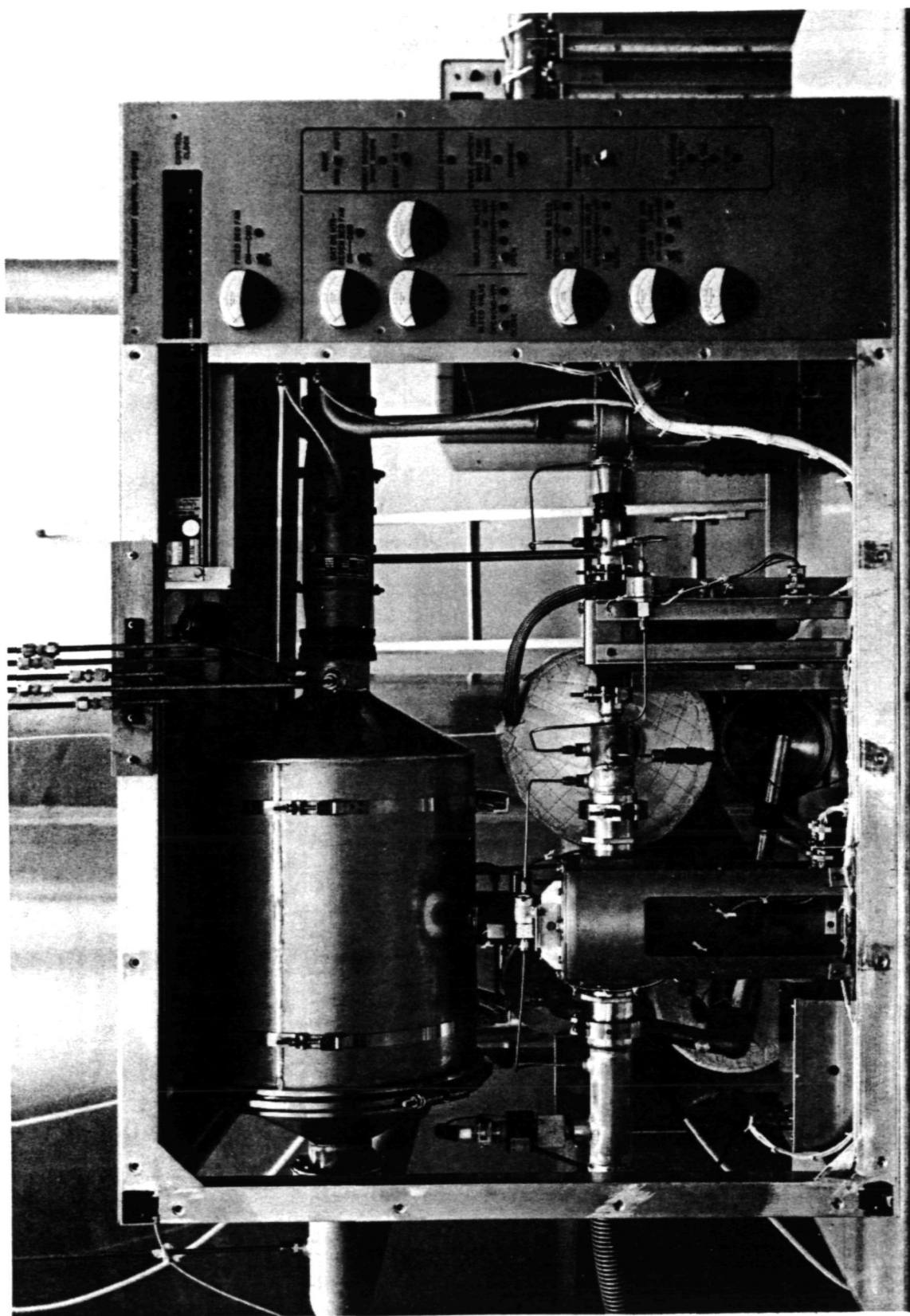


Figure 21 TCCS - Front View

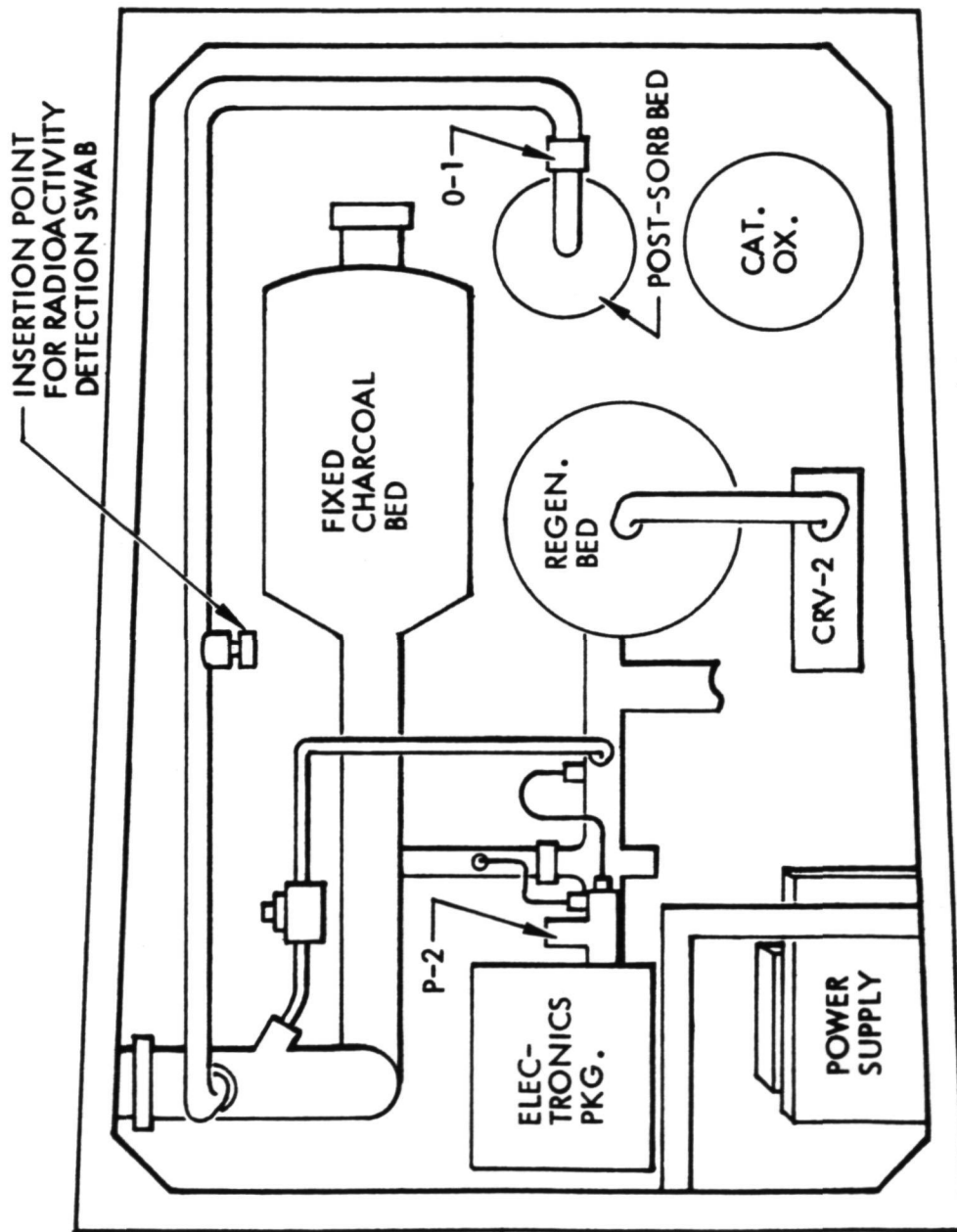


Figure 22 Trace Contaminant Control System Rear View

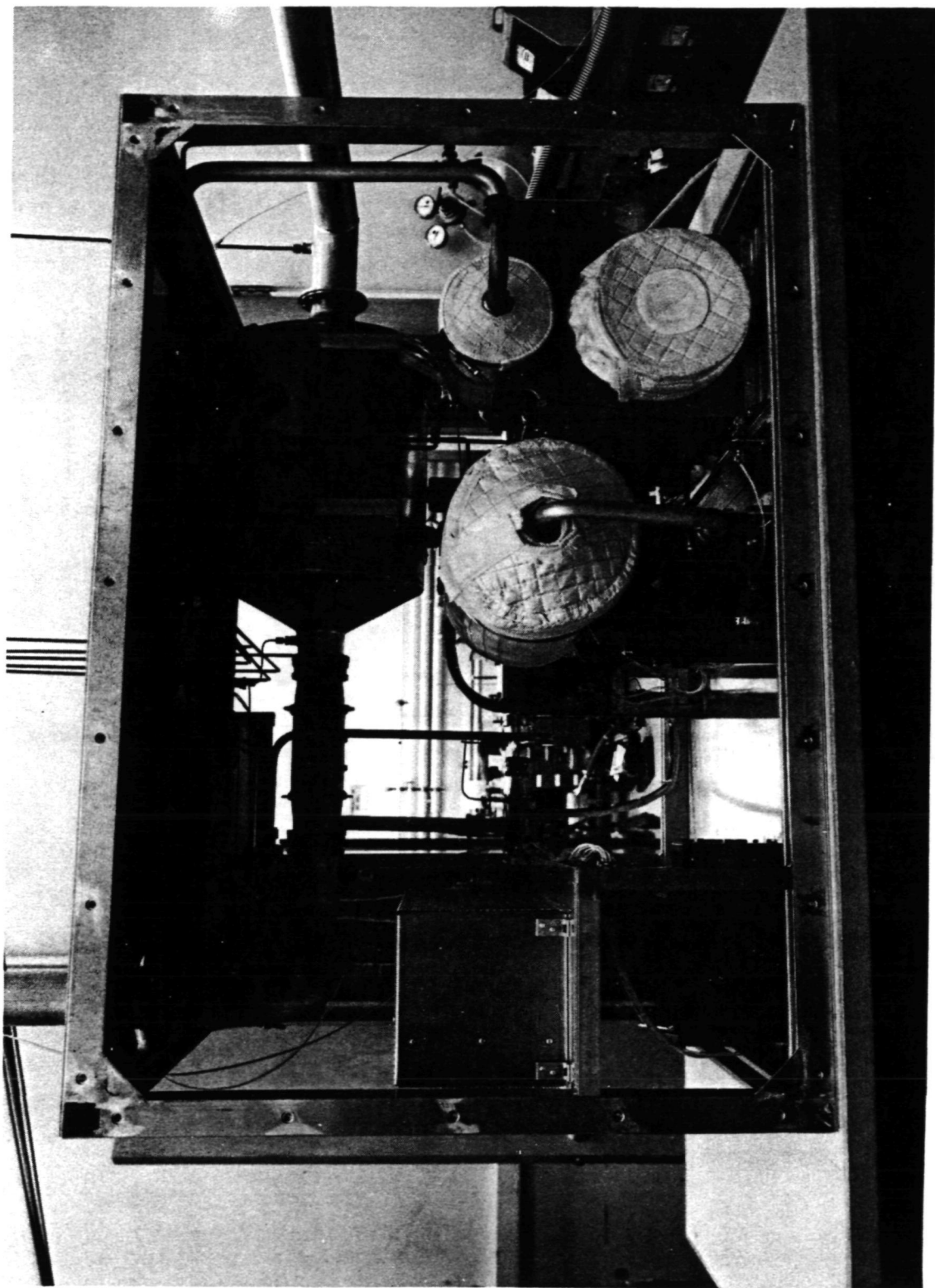


Figure 23 TCCS - Rear View

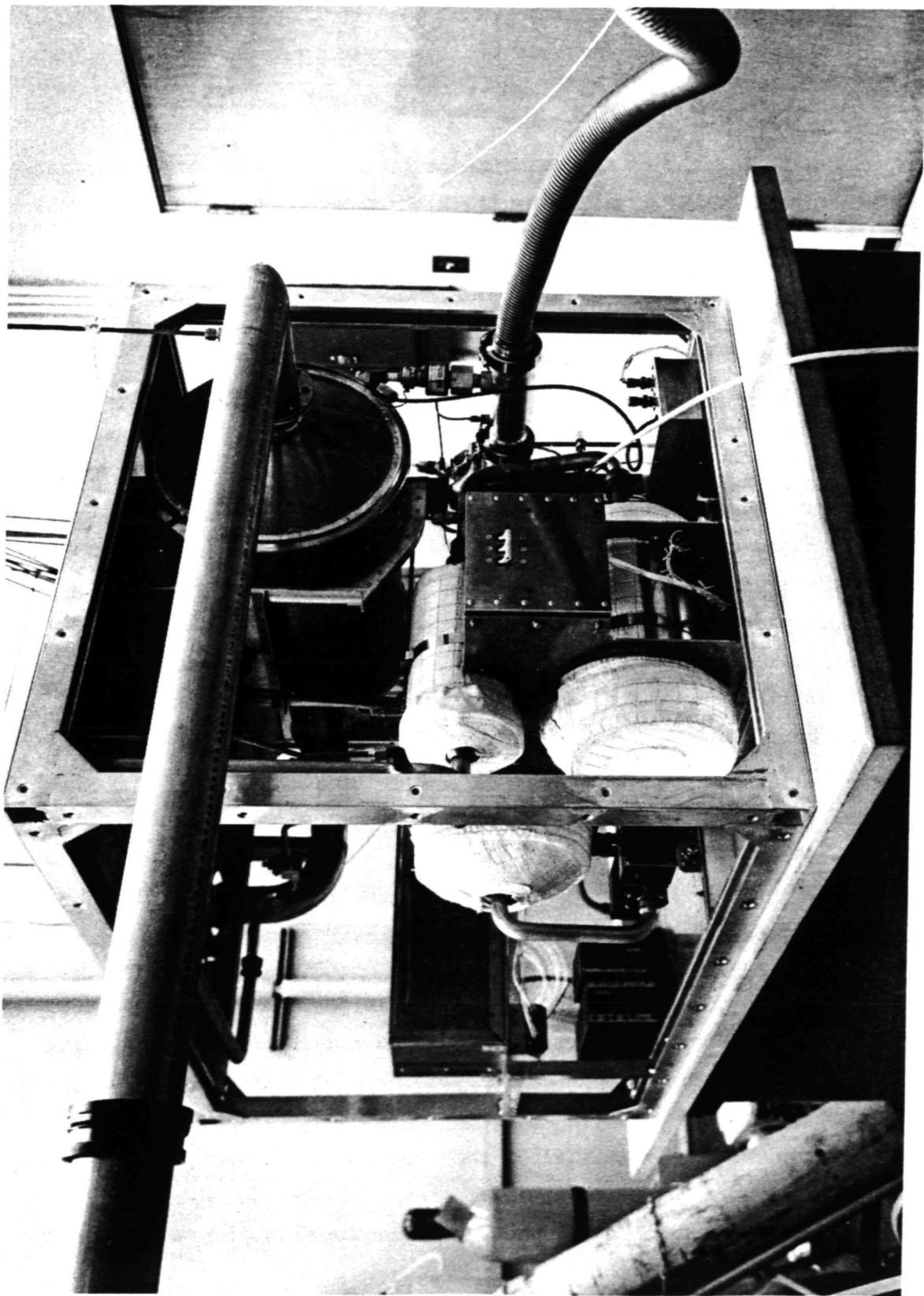


Figure 24 TCCS - View of Left Side

chemical, lithium hydroxide, in the pre- and post-sorbent beds. Consequently, stainless steel was chosen as the material for these components and the ducting between them.

A number of small diameter tubes are connected to the Trace Contaminant Control System and lead vertically upward (Figure 21). These are gas sampling lines needed for testing only.

A considerable amount of information relating to the design and operation of the Trace Contaminant Control System and the individual components is included in the Operating and Maintenance Manual. For a more complete understanding of the system this manual may be consulted.

After the Trace Contaminant Control System was assembled a 1 cm (0.39 in) orifice was inserted in the ducting to trim the catalytic oxidizer loop approximately 120 l/min (4.25 CFM). This orifice is located in the first Gamah coupler downstream from the post-sorbent bed. The following sections describe the major system components fabricated by IMSC. Figures are presented for each of these components. The purchased components such as fans and valves are described in the component data sheets (Section 7.3). Figures are presented for the purchased components with the component data sheets.

7.2.1 Fixed Bed

The fixed bed configuration is defined in IMSC dwg. CC-117 presented in Appendix B and in Figure 25. The design of this canister is typical of several others in the Trace Contaminant Control System. Its general shape is cylindrical, with a cone at each end. The cone at one end terminates in an inlet duct connector and at the opposite end, an exit duct connector. The charcoal is restricted to the cylindrical portion by a flat disc of wire mesh screen at each end. Each of these is supported by a rigid retainer which resembles a spoked wheel. The retainer at the exit end is located up against the exit cone, which is welded to the cylinder. However the entrance cone is removable to enable charcoal to be loaded or unloaded. The entrance cone and



Figure 25 Fixed Bed Canister

the cylinder are both equipped with flanges, and these flanges are clamped together with Aeroquip - Marman clamps. To ensure a positive compressive force on the charcoal, a coil spring is compressed to apply approximately 623 N (140 lb) of force. The canister and duct connectors are made of aluminum. A Fiberglas filter is placed on the screen at the exit end to prevent the release of solid particles. The bracket (Ref. IMSC dwg. CC-130) which supports the fixed bed is designed to enable vertical, lateral and longitudinal adjustments in the location of this unit.

7.2.2 Regenerable Bed

This bed contains 6.1 kg (13.5 lb) of charcoal. However, unlike the Fixed Bed described above, it has to meet these special requirements:

- o The inlet end is a tee, with connections to a 2.5 cm (1 in) duct and a 5.1 cm (2 in) duct.
- o Internal-to-external differential pressures vary from -101.5 to 69 kN/m² (-14.7 to 10 psid).
- o The canister must be vacuum tight.
- o Electrical band heaters are strapped around the canister and raise its temperature to approximately 383 K (230 F)
- o Internal vanes or plates are required to conduct heat to all of the charcoal. Since this heating must be accomplished while there is an internal vacuum, there is no air convection. Consequently to enhance heat conduction and radiation it was deemed necessary that every piece of charcoal be not further than 1.25 cm (0.5 in) from an internal vane.

Because of the heat conduction requirements as well as weight minimization, aluminum was selected as the material. Internal fin thickness was determined by thermal calculations. The fin configuration selected was radially inward from the inner surface of the canister (Ref. IMSC dwg. CC-113). Canister thickness was dictated by the stresses of differential pressure together with the weakening experienced by aluminum at elevated temperatures. Strength values of aluminum at a temperature of 533 K (500 F) were used to assure a safe, conservative design. Stresses were analyzed for several failure modes: buckling of a tube under external pressure loading; combined shear stress; and combined tensile stress.

In order to monitor the temperature of the charcoal at the central axis of this bed, a sheathed thermocouple is inserted from the tee end, through the end-screen disc. The penetration of this thermocouple through the wall is via a vacuum-tight fitting employing O-ring seals. The two duct connections at the inlet-end tee and the duct connection at the exit end are aluminum Aeroquip-Marman flanged connectors of the O-ring-in-groove type, secured with Marman clamps. This same type of joint is used at the junction between the canister cylinder and exit cone. The boil spring which holds the screen disc and retainer against the charcoal at the outlet end is designed to exert a nominal force of 10N (20 lb).

The heating of this unit is accomplished by clamping 3 electrical band heaters, each 7.6 cm (3 in) wide, around the outside of the canister. Each band has a series resistance of 360 ohms, and consumes 120 watts at 208 V.A.C. during high-rate heating. To minimize heat loss, three layers of Johns-Manville flexible Min-K blanket are applied to completely cover the canister and electric band heaters. This insulation can easily be removed and re-installed since the edges are fitted with Velcro. The regenerable bed without the end cap insulation, and the charcoal support screen, is shown in Figure 26.

7.2.3 Pre-Sorbent Bed

The configuration of the pre-sorbent bed is shown in IMSC drawing CC-111 (presented in Appendix B) and in Figure 27. Since this bed contains lithium hydroxide, a caustic chemical, the canister is made of annealed type 321 Cres steel. A sheet thickness of 0.064 cm (0.025 in) was sufficient to withstand the hoop stress which could result from sudden loss of cabin pressure. The general configuration of this unit is similar to that of the fixed bed which was previously described. The coil spring was designed to exert a force of 44 N (10 lb) on a nominal load of lithium hydroxide. The O-ring which seals the end-bell-to-canister flanges is made of a type of silicone rubber which is resistant to caustic chemicals.

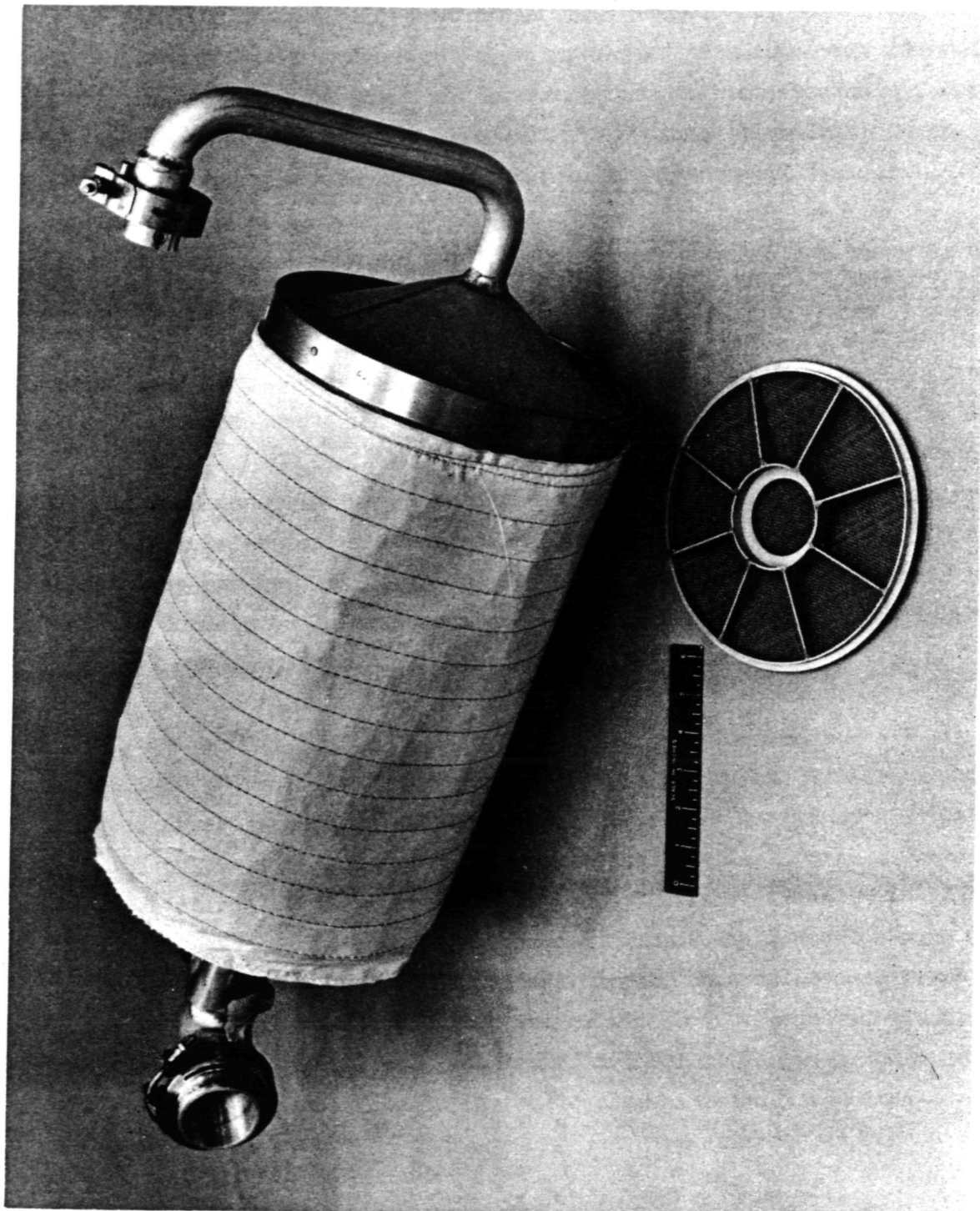


Figure 26 Regenerable Bed

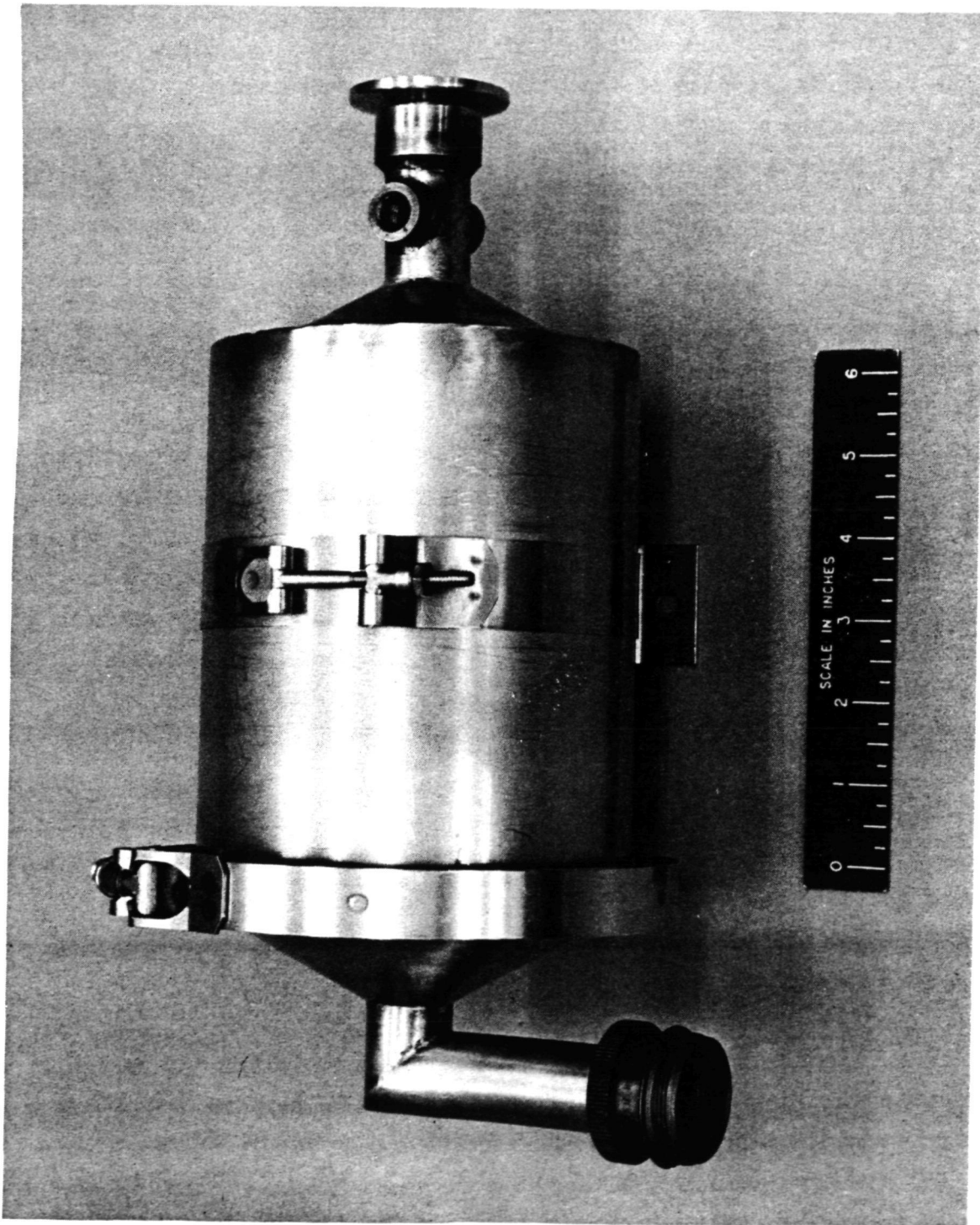


Figure 27 Pre-Sorbent Bed Canister and Mounting Bracket

7.2.4 Post-Sorbent Bed

This unit is very similar to the pre-sorbent bed, except for the duct connections at the two ends, and the fact that it is 7 cm (2.75 in) longer. Also, a Fiberglas filter is provided at the outlet end to trap particles. Since the hot air discharged from the Catalytic Oxidizer passes into the post-sorbent bed, this unit is insulated with a Min-K blanket which is retained by Velcro edge bindings. The post-sorbent bed is depicted in Figure 28.

7.2.5. Catalytic Oxidizer

To perform its function this unit must pass an airstream of 120 l/min (4.25 SCFM) through approximately 0.9 l (55 in³) of catalytic-coated alumina pellets about 1 kg (2 lb) - at a temperature of 644 K to 700 K (700 to 800 F). To perform this efficiently, and to discharge the processed air at a temperature of 344 K (160 F) rather than 644 K (700 F), a heat exchanger is incorporated in this unit. Air enters the heat exchanger first, and is warmed as it passes through. It next passes over 811 K (1000 F) heaters which warm the air to approximately 700 K (800 F). The air then passes counter-flow thru the heat exchanger where its temperature is lowered to 344 K (160 F) before being discharged. The heat exchanger is shown in IMSC dwg. CC-101 in appendix B, and in Figures 29 and 30. It is made of stainless steel.

There is a requirement to provide alternate heat sources: electrical or radio-isotope (decay of radioactive plutonium isotope compounds). The source of the latter units is the Mound Research Laboratory of Monsanto Corp., under contract to the AEC. It was decided to use 2 heaters of one of the existing designs, each of which produce 71.4 watts of heat.

Since the Trace Contaminant Control System is intended to be a prototype of a system suitable for manned spacecraft, it was deemed necessary to orient the catalytic oxidizer for minimum radiation directed toward the front face. Gamma radiation and neutron flux are minimal along the central axis of the cylindrical heater units, therefore, this axis was placed perpendicular to the front face.

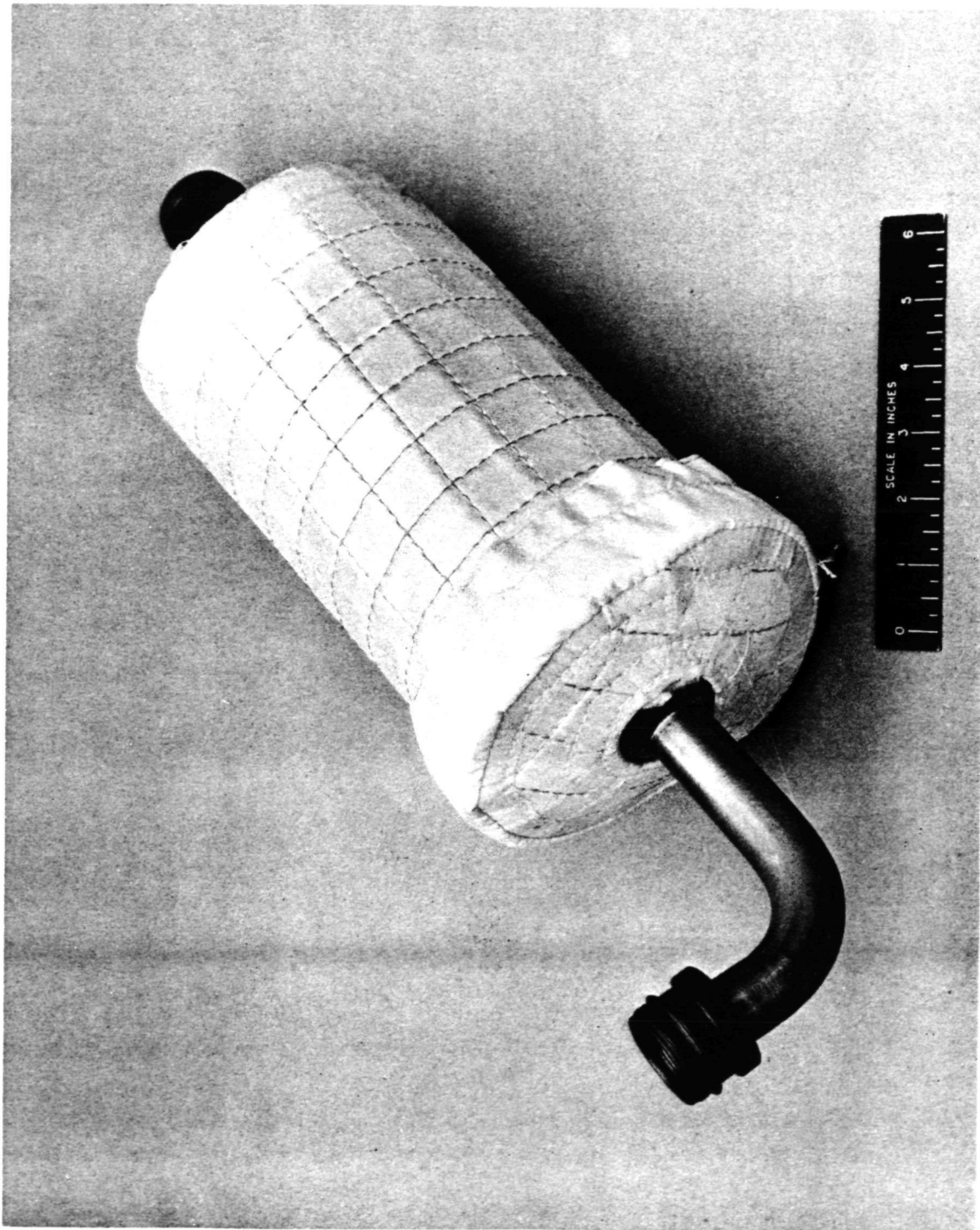


Figure 28 Post-Sorbent Bed

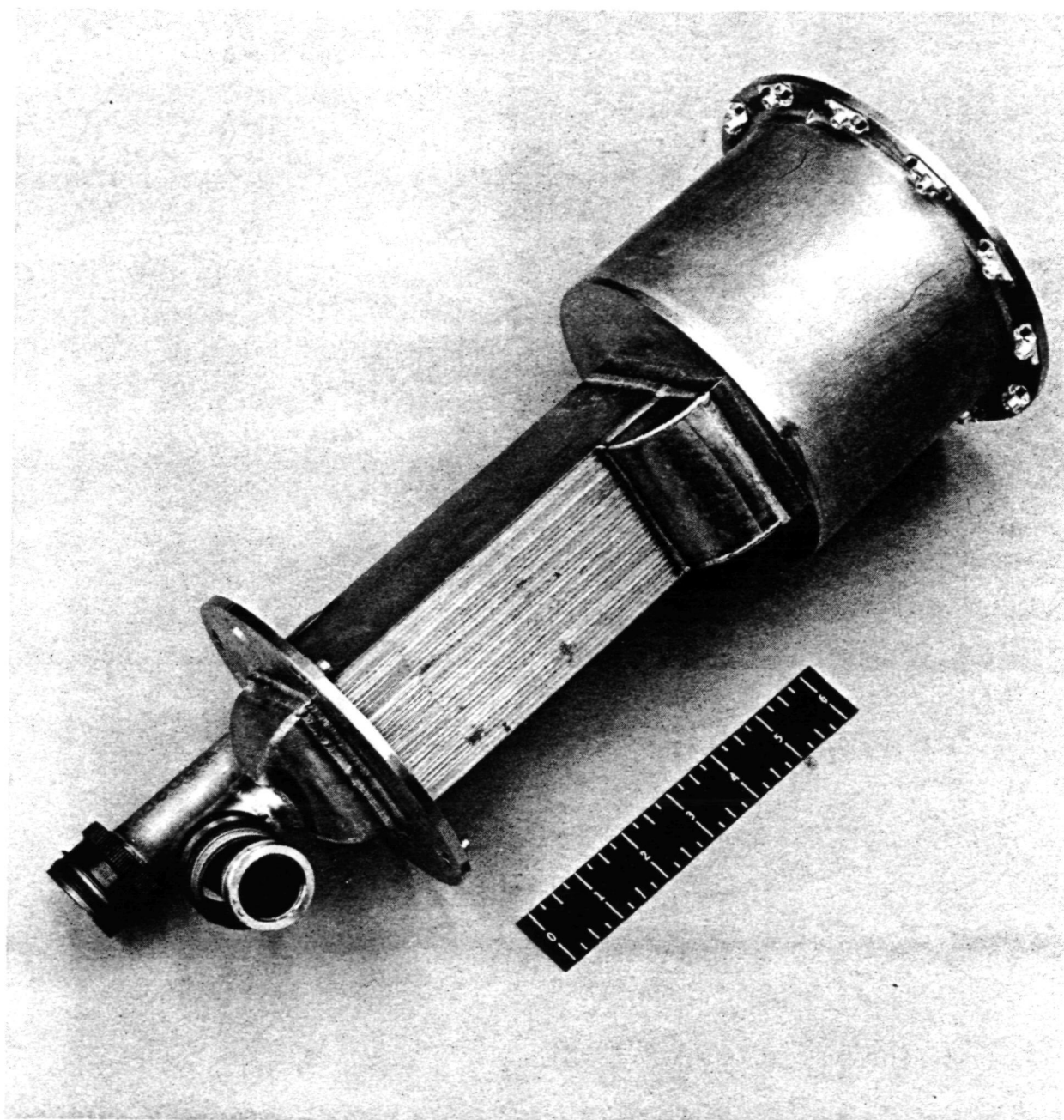


Figure 29 Heat Exchanger

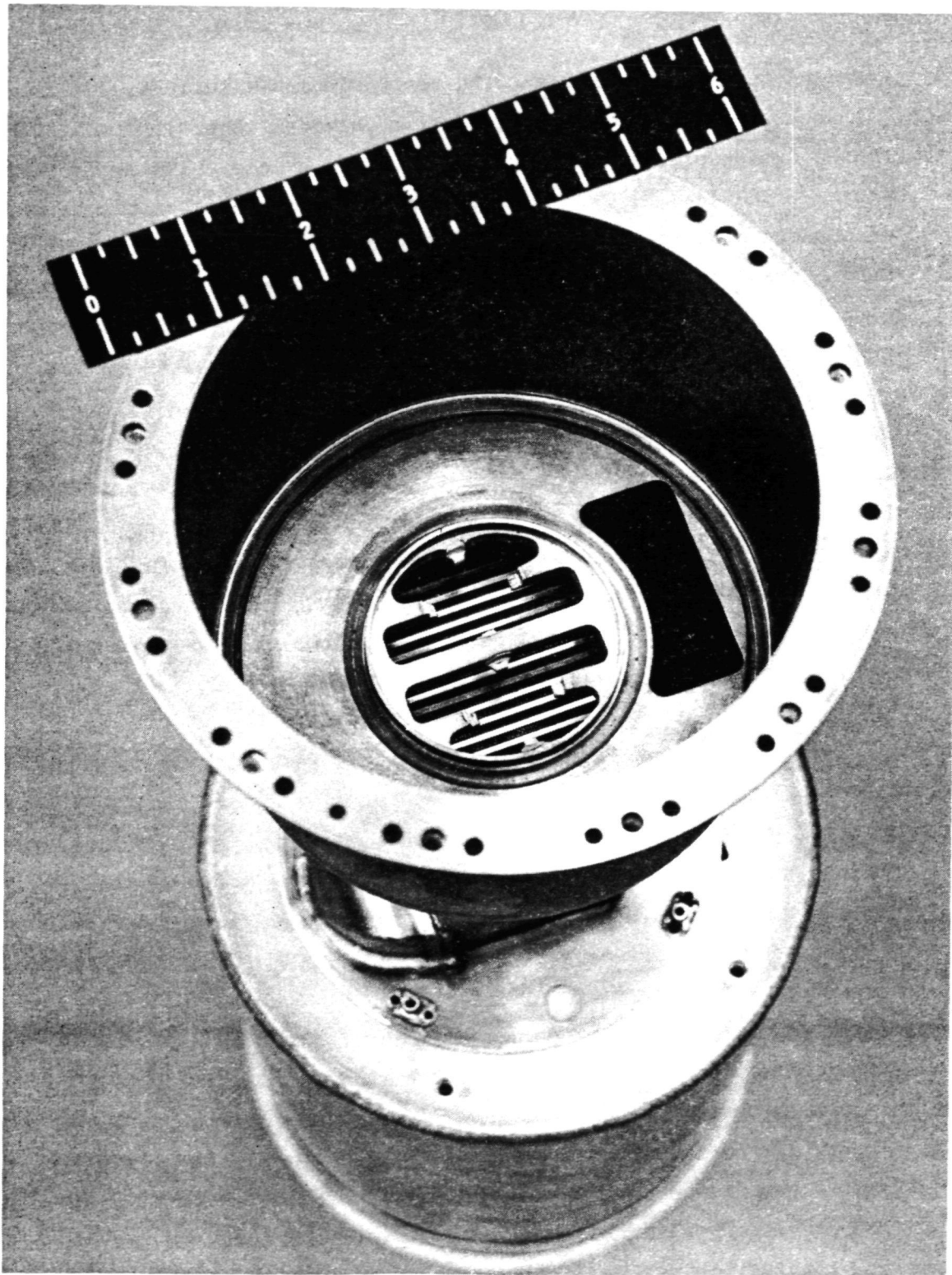


Figure 30 Heat Exchanger

The electrical heaters were designed to be physical and thermal duplicates of the plutonium isotope heaters, except that electrical power leads are required. This created design problems since the leads must be electrically insulated, must withstand 922 K (1200 F), and must penetrate the envelope of the catalytic oxidizer without permitting air leakage. These conditions were met by using multi-strand Nichrome wire leads, ceramic beads and tubing for insulation, and feed-thru via tubulations in the Inconel end plate (Ref. IMSC dwg. CC-104 in Appendix B). At the outer end of the feed-thru, air leakage is prevented by sealing with RTV silicone rubber.

When electrical heaters are used, it is possible to turn off the power during those periods when no air is being circulated thru the catalytic oxidizer. However, when the plutonium isotope heaters are installed, this is not possible and consequently the heaters reach a temperature of 922 K (1200 F) and surrounding parts get as hot as 811 K (1000 F). Accordingly, materials capable of withstanding these temperatures were selected.

The palladium catalyst on its alumina pellet substrate withstands elevated temperatures. This material is placed in a container made of nickel. Nickel was chosen because of its high thermal conductivity, its ability to withstand the temperature, and its resistance to corrosion. The shape of the catalyst bed container is consistent with the air flow path described above. It is essentially an annulus formed by a double cylinder with radial fins between the inner and outer cylinders. The catalyst fills the annulus, and is confined at one end by a fixed screen and at the other end by a removable screen with its support. When the entire catalytic oxidizer is assembled, the two heaters are side-by-side, inside of the inner cylinder of the catalyst bed container. This configuration is consistent with the air flow path described above; air flows inside the inner cylinder (around the heaters) from one end to the other. It then flows radially outward and turns in the opposite direction, flowing through the catalyst which fills the annulus (Ref. IMSC dwg. CC-102 in Appendix B). The two nickel cylinders, stationary screen, and 8 nickel fins of this assembly were designed to be self-jigging (self-aligning)

during brazing. This was accomplished by providing slots, (grooves and shoulders). The grooves are located on the outer circumference of the inner cylinder for ease of machining; it would be difficult to machine grooves on the inner surface of the outer cylinder as shown in Figure 31. The removable screen is held in place by screws which fit first into the threaded holes in the screen retainer and then into clearance holes in the container. The white coating on the outer cylinder is flame-sprayed alumina ceramic. Its purpose is to preclude any seizure or diffusion welding of the catalyst-bed container to the main body of the catalytic oxidizer (heat exchanger) which could occur at these elevated temperatures. The heater support fingers in the catalytic oxidizer body (Ref. IMSC dwg. CC-101) as well as the recesses in the end plate (Ref. IMSC dwg. CC-104) are also alumina coated to prevent bonding to the heaters.

Figure 32 is an exploded view of most of the catalytic oxidizer parts. The two heaters shown are electrically powered (Ref. IMSC dwg. CC-107). Between them and the catalyst bed container is a heater positioner bracket which supports and positions the heaters during assembly (Ref. IMSC dwg. CC-109). This bracket, containing the heaters, is slid into the catalyst bed container. Before the catalyst bed container is slid into the heat exchanger, the two large stainless steel washers (Ref. IMSC dwg. CC-105) must be placed in the heat exchanger. Their function is to prevent the internal airflow from short-circuiting without passing through the catalyst. To accomplish this presented a design problem whose requirements were:

- Withstand temperature cycling from 644 to 922 K (700 - 1200 F) with plutonium isotope heaters, or 294 - 644 K (70 - 700 F) with electric heaters.
- Withstand corrosive gases
- Provide a seal (not absolute) against small differential air pressures
- Accommodate manufacturing dimensional tolerances as well as differences in thermal expansion and contraction
- Avoid excessive loads during installation and use

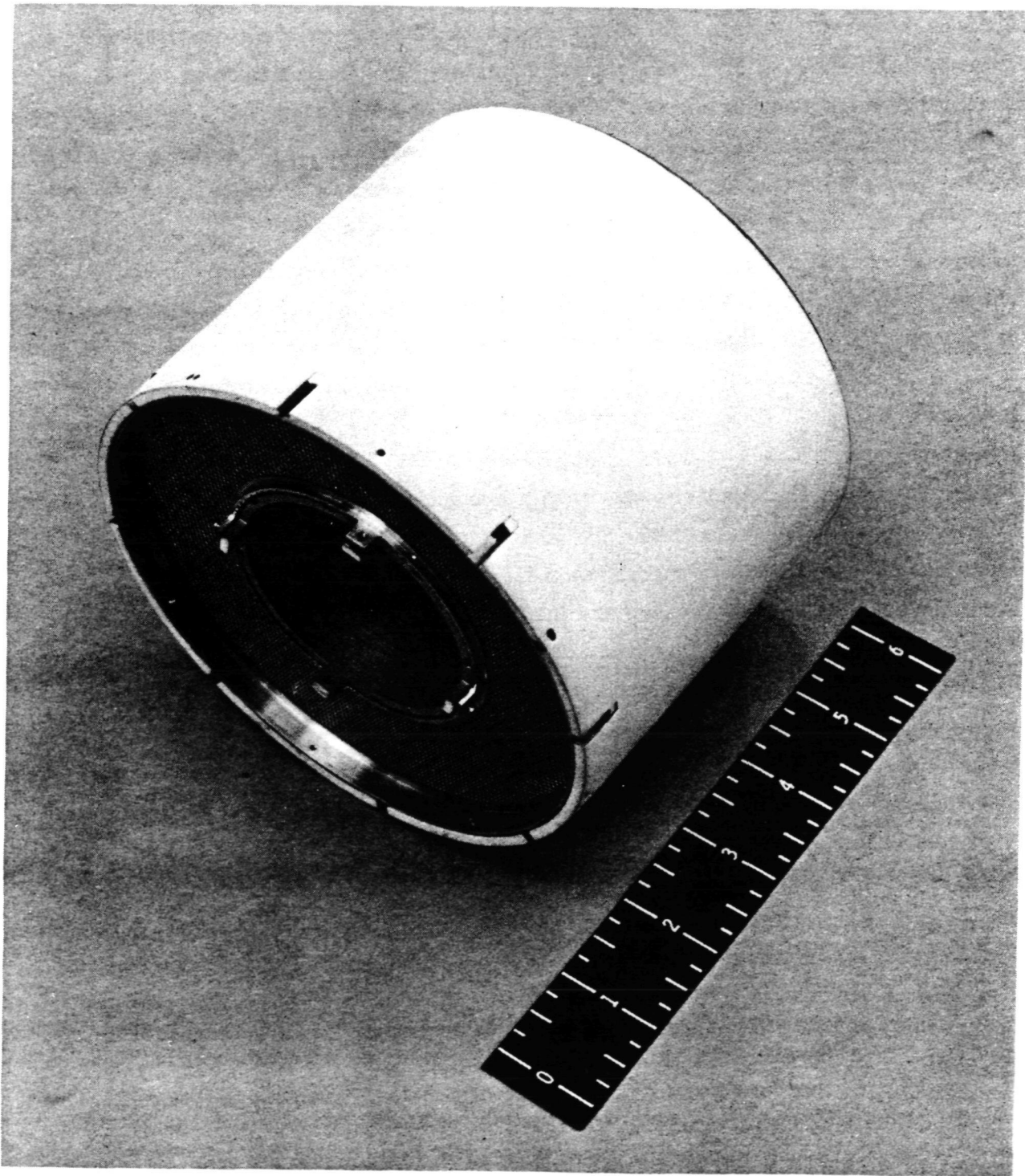


Figure 31 Catalyst Bed Container



Figure 32 Catalytic Oxidizer

The design solution of this problem consisted of machining knife-edges on the bottom of the inner and outer cylinders of the catalyst bed container (Ref. IMSC dwg. CC-102), machining V grooves into the catalytic oxidizer body (i.e. heat exchanger, Ref. IMSC dwg. CC-101) and placing stainless washers between the knife edges and the V grooves. As the cover plate is tightened down with 12 bolts, the knife edges, which are at the center of the width of each washer, cause the washer to deflect in the shape of a shallow V, since the outer and inner edge of the washer are supported by the V grooves.

Another design problem arose in providing an inside-to-outside seal around the periphery of the end plate (which can be seen just to the right of the heaters). The solution was use of a Haskel K ring made of Inconel X750 with gold plating. This provides a positive, solid stop when the cover bolts are tight, yet neither of the two facing flanges has to be grooved (one flange would have needed a precision groove if a metal O-ring seal had been used). This K ring seal also requires far less compression force than a metal O-ring. The K ring is not shown in the photo.

The heat exchanger's bolts are all screwed into floating nut plates rather than into tapped holes. If the screw threads seize or become pressure welded at the elevated temperatures involved, it is possible to machine the nut plates away.

The heat exchanger, heaters, catalyst bed container, end plate and associated parts require very effective thermal insulation to maintain the high catalyst temperatures. The most effective insulating material obtainable was used: Johns Manville Min-K 1301. This is a hard gray material having a thermal conductivity of approximately $0.12 \text{ k joules/m}^2 \text{ hr, F}$ ($0.02 \text{ BTU/ft, hr, F}$). An average thickness of 2.54 cm (1 in) was used. As shown in Figure 32 it is configured as a series of C shaped pieces to fill the space between the heat exchanger assembly and an outer aluminum case.

The duct end of the heat exchanger has a flange which is fastened to one end of the aluminum case with four bolts. The other end of the case (Ref. IMSC dwg. CC-103) is covered by a cap which is secured by a Marman clamp. The aluminum case is fitted with a tapped hole into which a spring-loaded, sheathed thermocouple is screwed. This thermocouple penetrates the Min-K insulation and bears against the outer surface of the heat exchanger so that its temperature can be monitored. The outside of the aluminum case is covered with flexible Min-K blanket, which is retained by Velcro edge binding.

7.3 COMPONENT DATA SHEETS

The following section presents data sheets for all of the system components. Included with the data sheets for the purchased parts are figures depicting these parts. Pictures of the IMSC manufactured parts are presented in the previous section.

Component: Fixed Bed
Item Designation: FB
Manufacturer: IMSC
Function: Charcoal bed for adsorption of high molar volume contaminants in cabin air, charcoal impregnated with phosphoric acid for specific control of NH_3 .
Description:
Sorbent Bed Length: 38.1 cm (15 in)
Sorbent Bed Diameter: 33.0 cm (13 in)
Sorbent: 21.8 kg (48 lb) 4x6 mesh Barnebey Cheney BD charcoal impregnated with 2 millimoles/gram of phosphoric acid
Outlet Filter: Fiberglas Mat
Flow: 991 l/min (35 SCFM) original value
1130 l/min (40 SCFM)
Differential Pressure: 623 N/m^2 (2.5 in water)
Inlet and Outlet Duct Diameter: 7.62 cm (3 in)
Inlet Debris Trap: Coarse Screen
Weight: 30.4 kg (67 lb)

Component: Regenerable Bed
Item Designation: RB
Manufacturer: IMSC
Function: Charcoal bed for adsorption of low molar volume contaminants in cabin air with periodic desorption of bed by reducing total pressure below vapor pressure of adsorbate
Description:
Sorbent Bed Length: 40.6 cm (16 in)
Sorbent Bed Diameter: 19.7 cm (7.75 in)
Sorbent: 6.13 kg (13.5 lb) 14 x 20 mesh Barnebey Cheney BD charcoal
Desorption Heater Power: 360 watts during heat up, 120 watts during guard operation, approximately 2.5 cm (1 in) insulation.
Inlet Temperature: 311 K (100 F)
Flow: 4.5 SCFM
Differential Pressure: 697 N/m² (2.8 in water)
Inlet and Outlet Duct Diameter: 2.54 cm (1 in)
Weight: 16.3 kg (36 lb)

Component: Pre-Sorbent Bed
Item Designation: S1
Manufacturer: IMSC
Function: Lithium hydroxide sorbent to remove acid
gasses, potential catalyst poisons, from
air stream prior to entering catalytic
oxidizer
Description:
Sorbent: Lithium hydroxide 6 x 8 mesh
Quantity: 0.91 kg (2.0 lb)
Length: 15.2 cm (6.00 in)
Diameter: 12.7 cm (5.00 in)
Flow: 127 l/min (4.5 SCFM)
Differential Pressure: 237 N/m² (0.95 in water)
Weight: 1.59 kg (3.5 lb)

Component: Post-Sorbent Bed
Item Designation: S2
Function: Lithium hydroxide to remove potential undesirable products of oxidation from air stream leaving catalytic oxidizer
Description:
Sorbent: Lithium hydroxide 6 x 8 mesh
Quantity: 1.36 kg (3 lb)
Length: 2.22 cm (8.75 in)
Diameter: 12.7 cm (5.00 in)
Flow 127 l/min (4.5 SCFM)
Differential Pressure 386 N/m² (1.55 in water)
Weight 2.04 kg (4.5 lb)

Component:	Catalytic Oxidizer
Item Designation:	CO
Manufacturer:	IMSC
Function:	Oxidize trace contaminant not removed by charcoal beds by passing air over 1/2% Pd catalyst heated to an operating temperature of 683 K (770 F)
Description:	
Catalyst Bed Length:	9.14 cm (3.6 in)
Catalyst Volume:	0.893 l (54.5 in ³)
Flow:	127 l/min (4.5 SCFM)
Differential Pressure:	1.49 kN/m ² (6 in water)
Catalyst:	Englehard 1/2% Pd on Alumina
Isotope Power:	Two 71.4 watt sources
Insulation:	Approximately 2.5 cm (1 in) of Min-K 1301 plus an outer shield
Catalyst Operating Temperature:*	683 K (770 F)
Catalyst Temperature During Shutdown:*	811 K (1000 F)
Heat Exchanger:	Plate fin, effectiveness approximately 90%, size approximately 5.1 x 7.6 x 15.2 cm (2 x 3 x 6 in)
Weight:	Approximately 14.1 kg (31 lb)
Special Requirements:	Alternate heat source: electrical Orientation to minimize radiation toward front of TCCS.

*Radioisotope capsule energy source mode of operation.

Component: Fixed Bed Fan
Item Designation: F1
Manufacturer: Dynamic Air Engrg. M3192A-1A
Function: Draw cabin air over the fixed charcoal
bed at rate of 991 l/min (35 SCFM)
Original design value = 1130 l/min (40 SCFM)
Description:
Flow: 991 l/min (35 SCFM)
Differential Pressure: 672 N/m^2 (2.7 in water) Original design
value - 847 N/m^2 (3.4 in water)
Type: Vane Axial, 2 stage
Length: 14.6 cm (5.75 in)
Diameter: 11.4 cm (4.5 in)
RPM: 11,500
Power: 55 watts
Weight: 1.35 kg (2.97 lb)

Ref. Figure 33

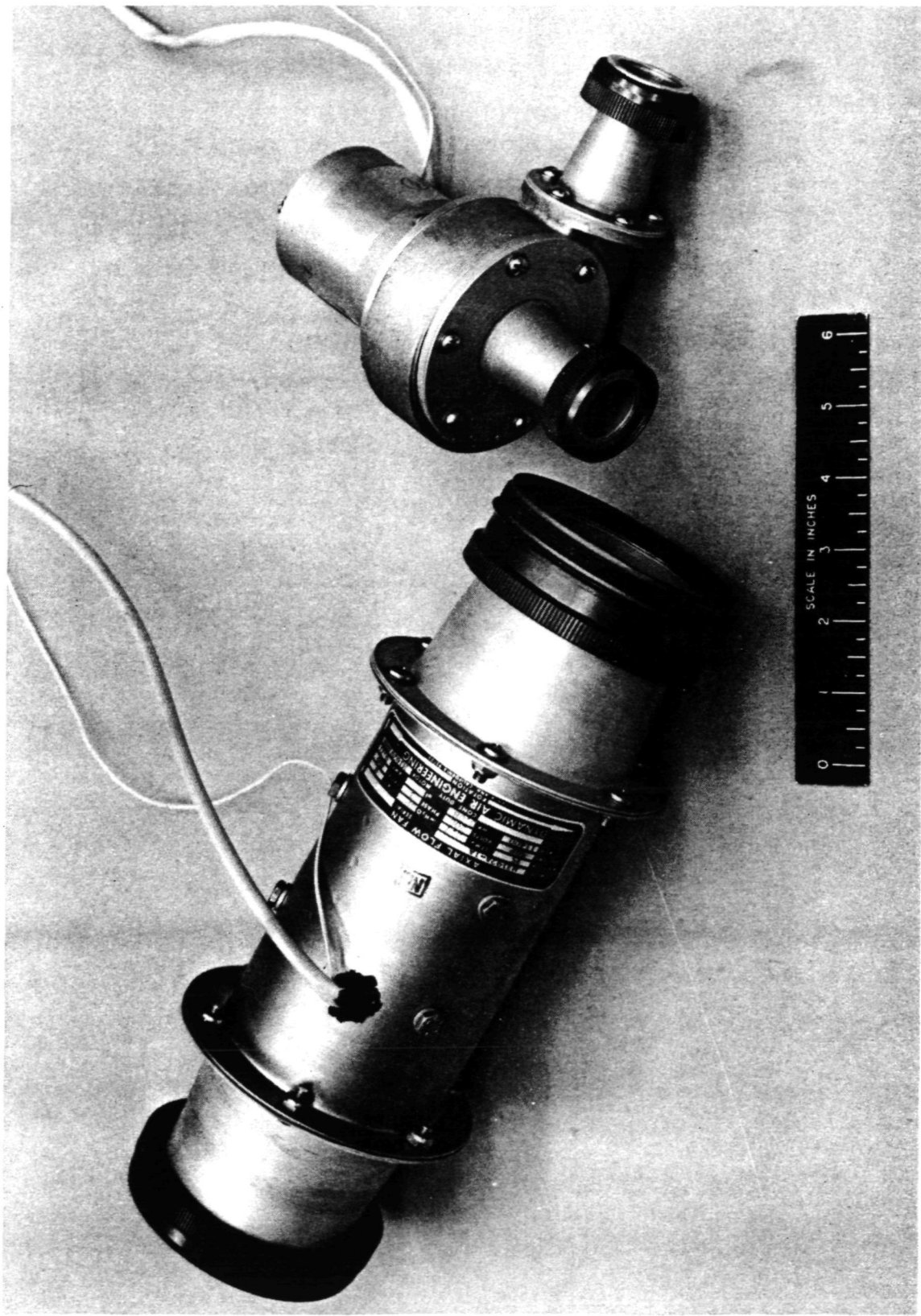


Figure 33 Fixed Bed Vane Axial Fan and Regenerable Bed Centrifugal Blower

Component: Regenerable Bed Blower
Item Designation: F2
Manufacturer: Dynamic Air Engrg. CO50K
Function: Draw air from the fixed bed fan outlet at
254 l/min (9 SCFM) half of which flows through
the regenerable bed and catalytic
oxidizer
Description:
Flow Rate: 254 l/min (9 SCFM)
Differential Pressure 4.23 kN/m² (17 in water)
Type: Centrifugal
RPM: 22,500
Power: 90 watts
Weight: 1.02 kg (2.25 lb)

Ref. Figure 33

Component: Isolation Valve 1
 Item Designation: CRV1
 Manufacturer: VACCO Industries V1D10237 per IMSC-DD 112
 Remote shut-off of air at regenerable
 bed inlet, isolates cabin air from vacuum
 source.
 Description:
 Port size 2.54 in (1 in)
 C_v 12
 Min. Differential Press. 0 kN/m^2 (0 psi)
 Max. Differential Press. 103 kN/m^2 (15 psi)
 Vacuum Range to $1.3 \times 10^{-4} \text{ N/m}^2$ (10^{-6} torr)
 Operator Solenoid, normally open
 Power 190 watts at 100 VDC
 Body Material Aluminum
 Weight 3.86 kg (8.5 lb)
 Special Feature Position indicator switch

Ref. Figure 34

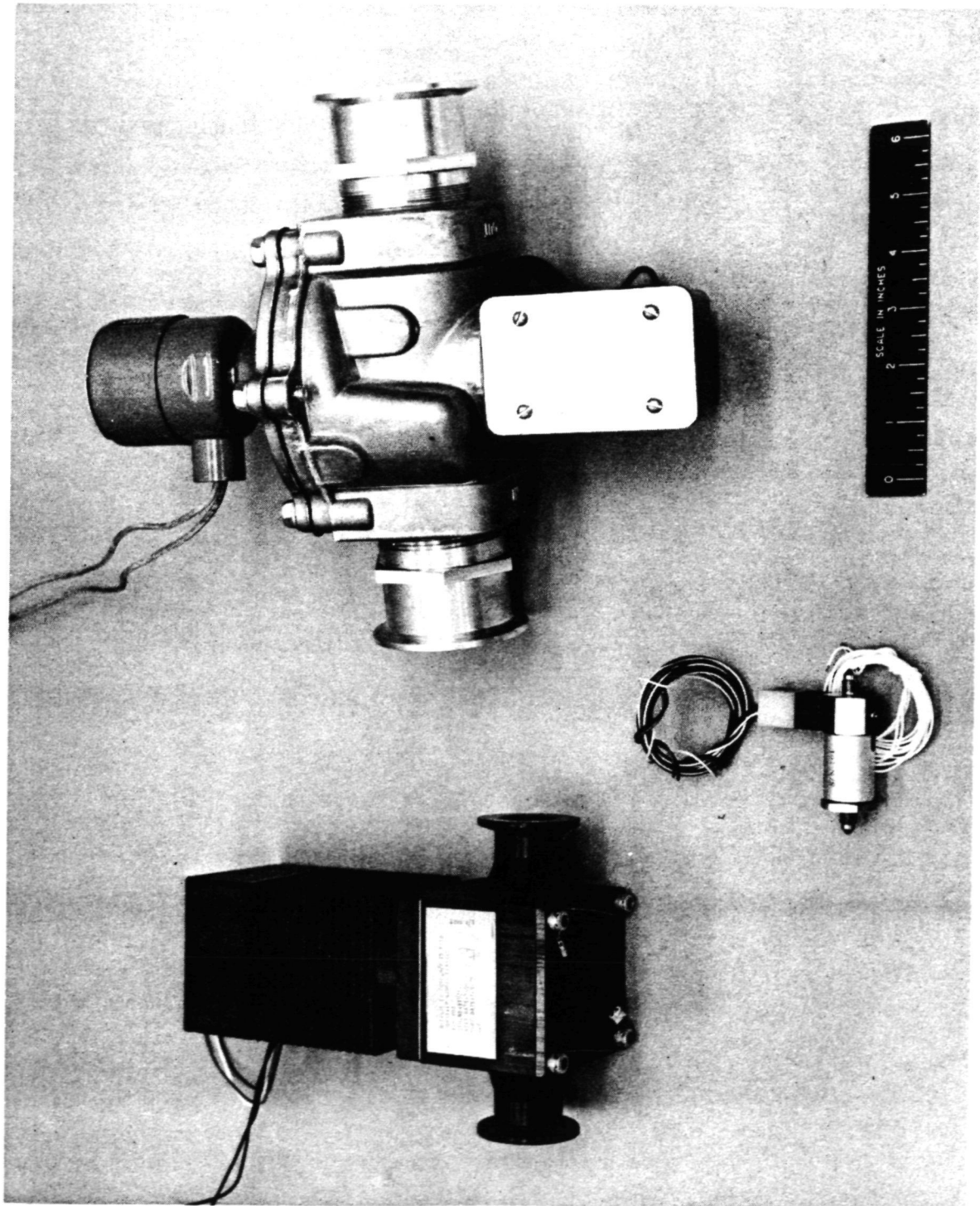


Figure 34 Solenoid Valves. 1 Inch Isolation Valve, 2 Inch Vacuum Valve, 1/8 Inch Bleed Valve

Component:	Isolation Valve 2
Item Designation:	CRV2
Manufacturer:	VACCO Industries VID 10237 per IMSC-CC112
Function:	Remote shut-off of air at regenerable bed outlet, isolates cabin air from vacuum source
Description:	
Port Size:	2.54 cm (1 in)
C_v	12
Min. Differential Pressure	0 kN/m ² (0 psig)
Vacuum Range	to 1.3×10^{-4} N/m ² (10 ⁻⁶ torr)
Operator	Solenoid, normally open
Power	190 watts at 100 VDC
Body material	Aluminum
Weight	3.86 kg (8.5 lb)
Special Feature	Position indicator switch

Ref. Figure 34

Component: Vacuum Valve
Designation: CRV3
Manufacturer: ASCO P/N HT 8215A80 VH-SW
Function: Remote shut-off of vacuum source from the trace contaminant control system
Description:
Port size: 5.08 cm (2 in)
 C_v : 50
Minimum Diff. Pressure: 0 kN/m^2 (0 psi)
Maximum Diff. Pressure: 172 kN/m^2 (25 psi)
Vacuum Range: to $1.3 \times 10^{-4} \text{ N/m}^2$ (10^{-6} torr)
Operator: Solenoid, normally closed
Power: 15.4 watts at 100 VDC
Body Material: Aluminum
Weight: 3.04 kg (6.7 lb)
Special Feature: Position indicator switch

Ref. Figure 34

Component: Vacuum Bleed Valve
Designation: CRV⁴
Manufacturer: SIEBELAIR 2814 A
Function: With flow control valves and vacuum valve closed, enables the pressure in the regenerable bed to be gradually bled to vacuum before the vacuum valve is opened.
Description:
Port Size: 0.318 cm (1/8 in)
 C_v : 0.34
Min. Diff. Pressure: 0 kN/m² (0 psi)
Max. Diff. Pressure: 172 lN/m² (25 psi)
Vacuum Range: to 1.3×10^{-4} N/m² (10^{-6} torr)
Operator: Solenoid, normally closed
Power: 12 watts
Body material: Steel
Weight: 0.363 kg (0.8 lb)

Ref. Figure 34

Component: Isolation Bleed Valve
Designation: CRV5
Manufacturer: SIEBELAIR 2814
Function: With flow control valves and vacuum valves closed, enables pressure in regenerable bed to be gradually raised from vacuum before the flow control valves are opened.
Description:
Port Size: 0.318 cm (1/8 in)
 C_v : 0.34
Min. Diff. Pressure: 0 kN/m^2 (0 psi)
Max. Diff. Pressure: 172 kN/m^2 (25 psi)
Vacuum Range: to $1.3 \times 10^{-4} \text{ N/m}^2$ (10^{-6} torr)
Operator: Solenoid, normally closed
Power: 12 watts
Body Material: Steel
Weight: 0.363 kg (0.8 lb)

Ref. Figure 34

Component: Fixed Bed Fan Differential Pressure
Sensor
Item Designation: P1
Manufacturer: Statham, Model PM 5TC \pm .15-350
Function: Monitor head rise of the fixed bed fan

Description:
Range: $\pm 1.03 \text{ kN/m}^2$ differential ($\pm 0.15 \text{ psid}$)
Length: 10.4 cm (4.11 in)
Diameter: 5.69 cm (2.24 in)
Weight: 0.312 kg (11 oz)

Ref. Figure 35

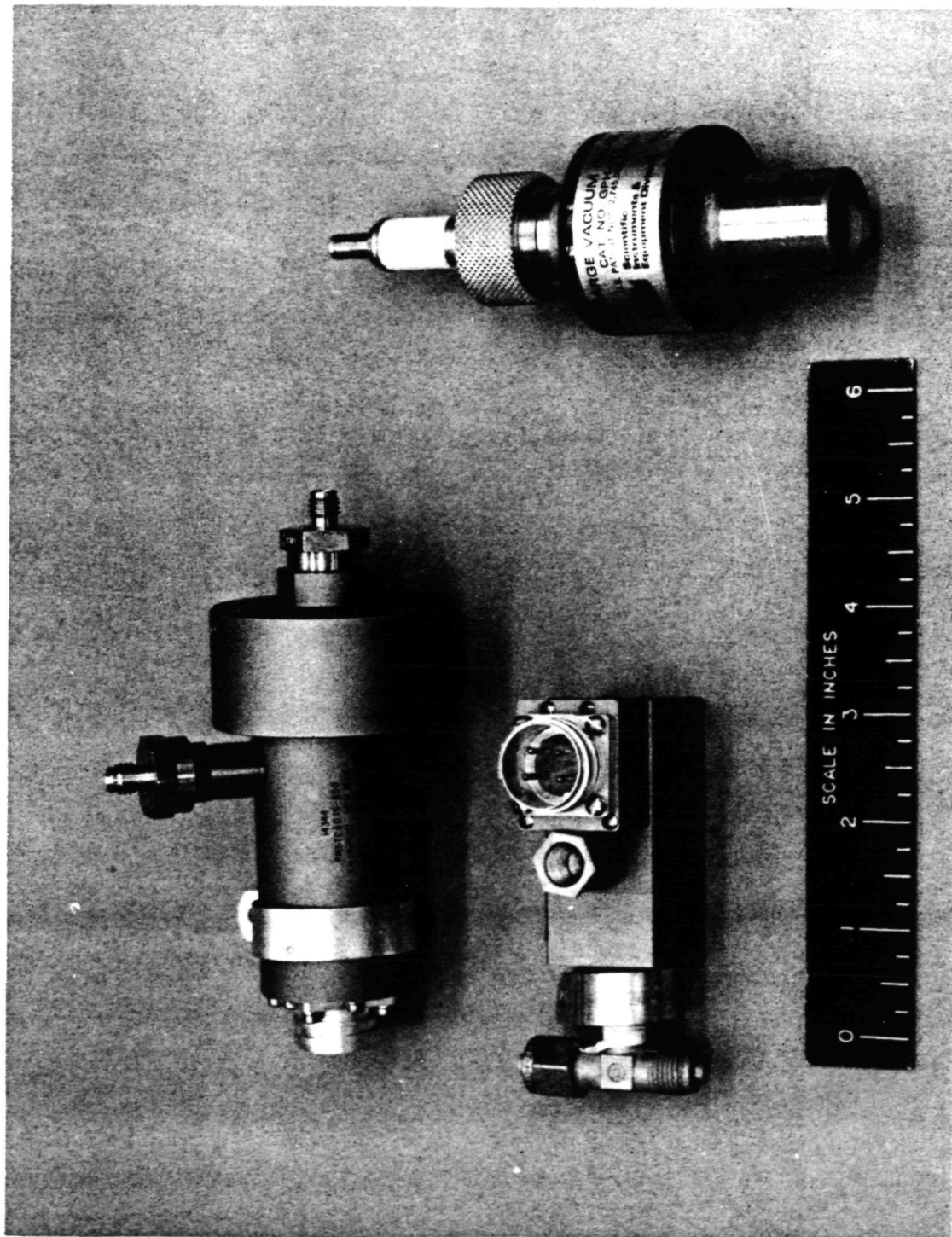


Figure 35 Fixed Bed Fan and Regenerable Bed Blower Differential Pressure Sensors and Vacuum Line Pressure Sensor

Component: Regenerable Bed Blower Differential
Pressure Sensor
Item Designation: P2
Manufacturer: Statham, Model PM 6TC
Function: Monitor head rise of the regenerable
bed fan.

Description:
Range: $\pm 6.89 \text{ kN/m}^2$ differential ($\pm 1 \text{ psid}$)
Length: 7.32 cm (2.88 in)
Width: 2.87 cm (1.13 in)
Weight: 0.170 kg (6 oz)

Ref. Figure 35

Component: Vacuum Line Pressure Sensor
Item: P3
Manufacturer: Bendix Scientific Instruments & Equip. Div.
Function: Monitor vacuum in the vacuum manifold

Description:
Sensor Length: 14.7 cm (5.78 in)
Sensor Diameter: 6.35 cm (2.5 in)
Range: 1.3×10^{-5} to 3.33 N/m^2 (1×10^{-7} to 25×10^{-3} torr)

Ref. Figure 35

Section 8

FABRICATION

The following section describes the fabrication techniques used for the IMSC manufactured components in the Trace Contaminant Control System.

8.1 GENERAL

The captive fasteners used to secure the components to their supports, and the side panels to the frame are Deutsch screws and floating plate nuts. Both are flared into an (optionally countersunk) hole using a special installation tool. The advantage of a Deutsch plate nut over a conventional plate nut is that two rivets and two rivet holes are not required.

Lettering on the control panel is engraved and filled, to provide the most durable kind of legend.

Wherever available space would permit, ducting elbows were fabricated by tube bending rather than by miter-cut and weld, for minimum pressure drop.

8.2 FIXED BED

The cylindrical part of this canister was fabricated by rolling sheet aluminum and welding a longitudinal seam. Similarly the two end cones were rolled from flat sheet and seam welded. All canister parts were then welded together.

8.3 REGENERABLE BED

Since 20.3 cm (8 in) OD by 0.318 cm (1/8 in) wall thickness 6061 aluminum tubing is commercially available, this material was used for the canister cylinder. The regenerable bed contains 18 internal heating fins. These are equally spaced in a radial array around the inside of the canister. In order to obtain adequate heat conduction, the flange of each of these fins must be bonded to the canister

throughout its entire length. This was accomplished by first tack-welding each fin to the canister cylinder; after all fins were in place the assembly was dip-brazed.

8.4 PRE-SORBENT AND POST-SORBENT BEDS

Since these canisters were fabricated from stainless steel sheet only 0.0635 cm (0.025 in) thick, there were two potential welding problems: burn-through and warping. To overcome these problems at the cylinder-to-end cone joints, the end cone was flared out to a reverse curl to enable doing a standing edge flange weld.

8.5 CATALYTIC OXIDIZER

Since the heat exchanger for this unit required highly specialized fabrication equipment and techniques, IMSC formulated requirements and sent them to four companies in this field; requesting their quotations. Two of these companies submitted bids and the one selected was Garrett Airesearch. The heat exchanger proper was designed by them to meet IMSC performance requirements, but the remainder of the body was built by them per the IMSC design drawing CC-101. This unit was fabricated of stainless steel, brazed and welded.

The Min-K 1301 insulation presented a difficult machining task because of the following characteristics of this material; (a) it is extremely brittle, and weak in tension, (b) it is abrasive, (c) the dust generated during machining should not be inhaled since it contains asbestos fibers.

An alternative method of fabricating solid Min-K would have been for Johns Manville to produce molds and cast each part to its final shape. However because of the varying shapes of the pieces, six different molds would have been required. Since only one piece of each shape was needed for this project, this would have been a very expensive method.

Fortunately, a vendor was found who had the capability of machining these Min-K parts at a reasonable cost: Foundry Service and Supply Co. of Torrance, California. This company did a remarkable job of producing parts which were dimensionally accurate and free of cracks or damage.

Another highly specialized process was the ceramic coating applied to certain areas of the heat exchanger body, the catalyst bed container and the end plate. Upon the advice of a representative of Metco, Inc., a primer coat of flame-sprayed Nickel Aluminide was applied to obtain good adhesion of the flame-sprayed pure aluminum oxide.

Fabrication of the seal washers (CC-105) presented a problem because the stainless steel is so thin. For production quantities punch-and-die tooling would have been used, but for our small quantities such tooling was not warranted. Consequently a sandwich stack of alternate stainless steel washer material and aluminum sheets was clamped onto the faceplate of a lathe, and the washers were produced using a cutting tool fed in perpendicular to the faceplate.

The cylindrical portions of the aluminum outer case are made of aluminum tubing. To prevent warping which would have resulted from welding on the Aeroquip-Marman sheet metal flanges, they were attached with rivets. See Dwg. CC-103 in Appendix B.

Section 9

TESTING

Testing of the Trace Contaminant Control System was accomplished in two phases, component level testing and system level testing. The component level tests were designed to establish functional performance to minimize problems at the system level. The system level testing was designed to demonstrate operational capability for the full mission duration and to evaluate the design methodology. The following sections of this report discuss these test activities.

9.1 COMPONENT TESTING

The purpose of testing the major components individually was to compare actual performance with design predictions and specifications. Wherever feasible, test conditions were similar to those which would be encountered in the assembled operating TCCS so that the performance of each component in its actual use environment could be simulated.

9.1.1 Fixed Bed, Fan, and ΔP Sensor Test

The purpose of this test was to establish the pressure drop and flow rate characteristics of the fixed bed and fixed bed fan. Figure 36 is a diagram of the bench test apparatus used in this test. Three Trace Contaminant Control System components were involved: the Fixed Bed (CC-117) the Fixed Bed Fan (Dynamic Air Engrg. M3192A-1A) and the Fixed Bed Fan Differential Pressure Sensor (Statham PM5 TC \pm .15-350). There were also several pieces of test equipment: draft gages to measure the pressure drops across the Fixed Bed and the Fan, a variable inlet restriction to adjust the flow rate; and a Hastings Raydist L-100 mass flowmeter to measure the flow rate.

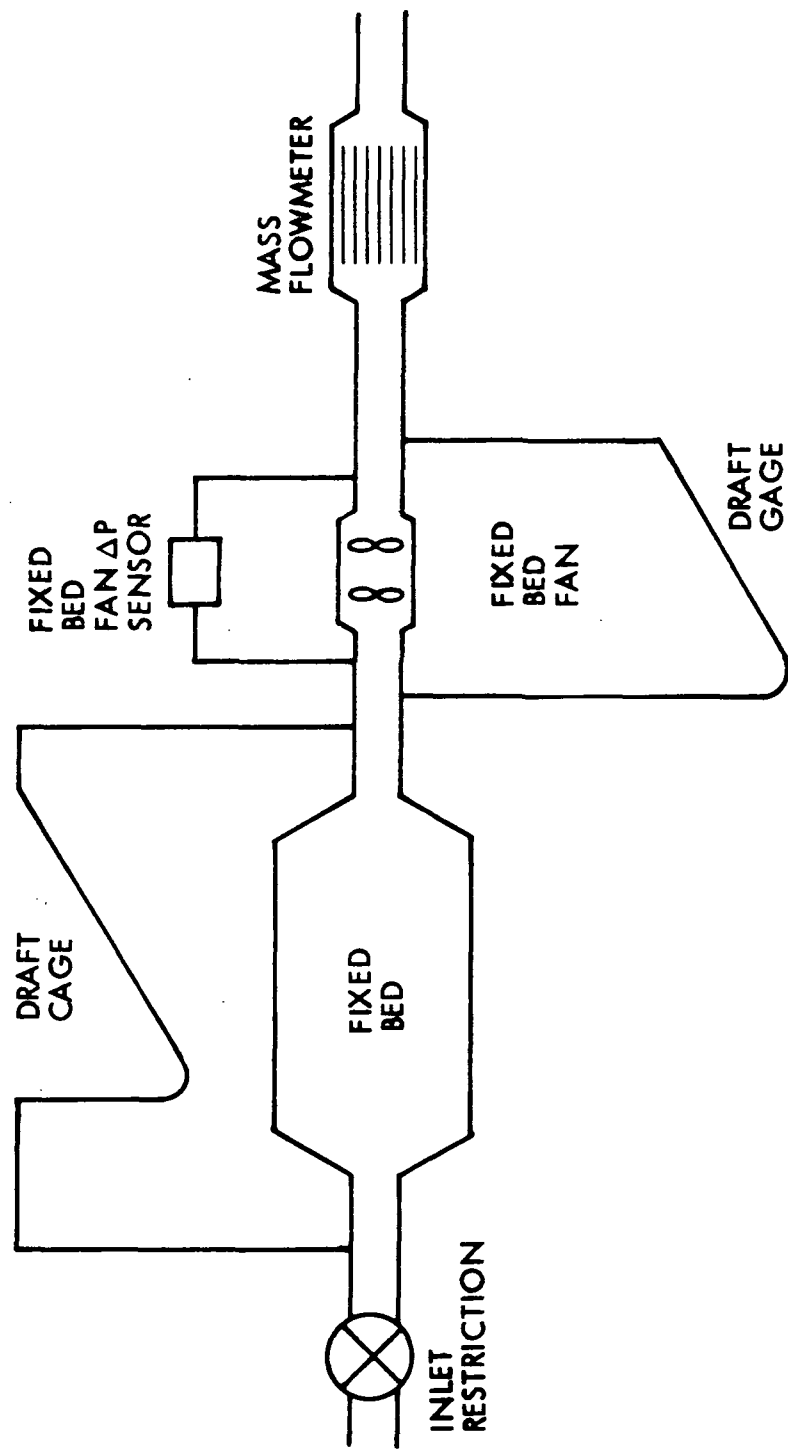


Figure 36 Equipment Arrangement for Fixed Bed and Blower Test

The test results are shown graphically on Figure 37. The characteristics of fan head rise vs flow rate are different from those given by the manufacturer, Dynamic Air Engrg. Co. However both curves happen to coincide at the actual operating point (i.e. - where they cross the system head loss vs flow rate curve).

The Statham sensor for measuring ΔP across the fan proved to be very insensitive to changes of flow rate in the measured range of 255 to 736 l/min (9 to 26 CFM). The readout on the Trace Contaminant Control System control panel is therefore useful principally to indicate whether or not the blower is operating.

9.1.2 Pre- and Post-Sorbent Beds

The purpose of this test was to establish the pressure drop characteristics of the pre and post-sorbent beds. Figure 38 shows the test arrangement schematically. A laboratory blower (Rotron SL 2 EA 2 AB) with means of adjusting the flow rate was used to provide the air flow, and a Hastings Raydist flowmeter was employed to measure the flow rate. A draft gage was connected across the bed to measure pressure drop. Results are shown graphically in Figure 39.

9.1.3 Regenerable Bed Blower and ΔP Sensor Test

The purpose of the regenerable bed blower testing was to establish the pressure drop and flow characteristics of the regenerable bed blower. A schematic diagram of the test equipment is shown in Figure 40. The inlet and outlet temperatures were taken using thermocouples, a Magnahelic meter measured the differential pressure, and two flowmeters were used: Cox (RAC 38021) and Hastings Raydist (L-109). The regenerable bed blower was a Dynamic Air Engineering Co. model C050K and the regenerable bed blower differential pressure sensor was a Statham model FM 6 TC \pm 7 psid.

Results of this test are shown graphically in Figure 41. Several of the findings are particularly noteworthy:

- o The pressure head was found to be lower than the manufacturer's data. However 4.31 kN/m^2 (17.3 in water) were adequate for this application.

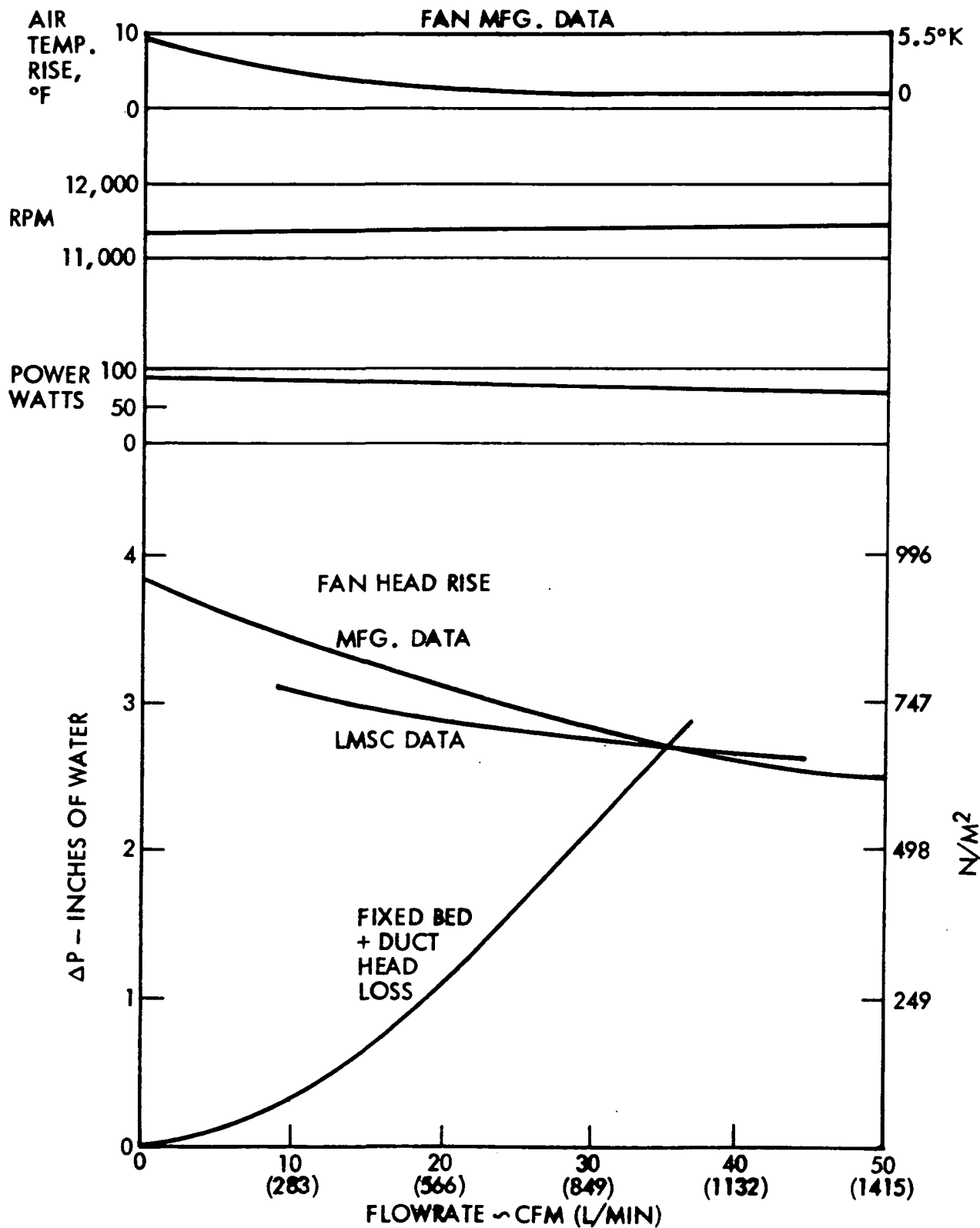


Figure 37 Fixed Bed and Fan Characteristics Fan:
Dynamic Air Engineering. M3192A-1A

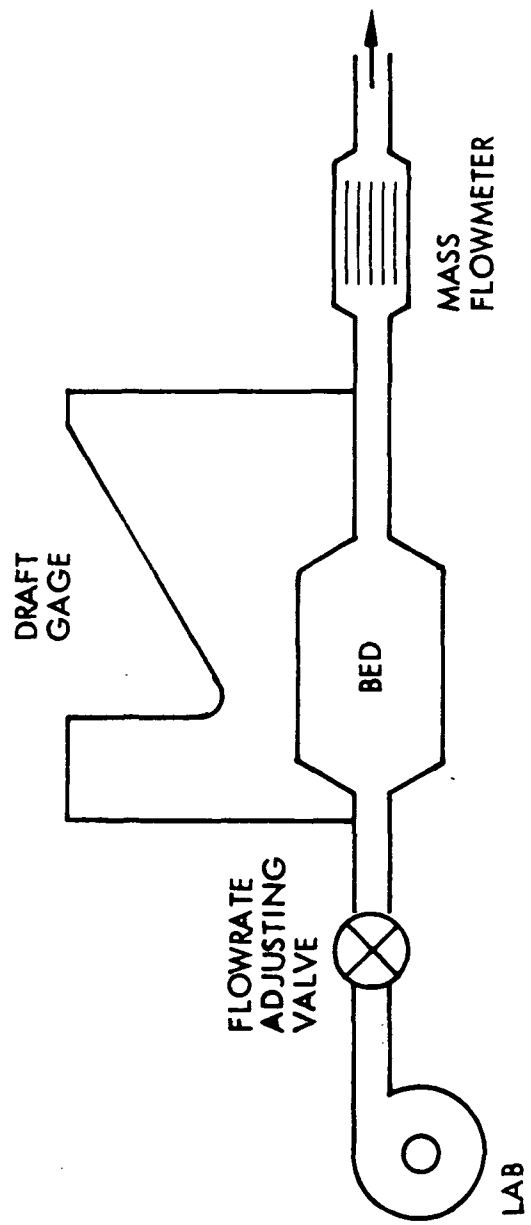


Figure 38 Equipment Arrangement for Pre and Post-Sorbent Bed Tests

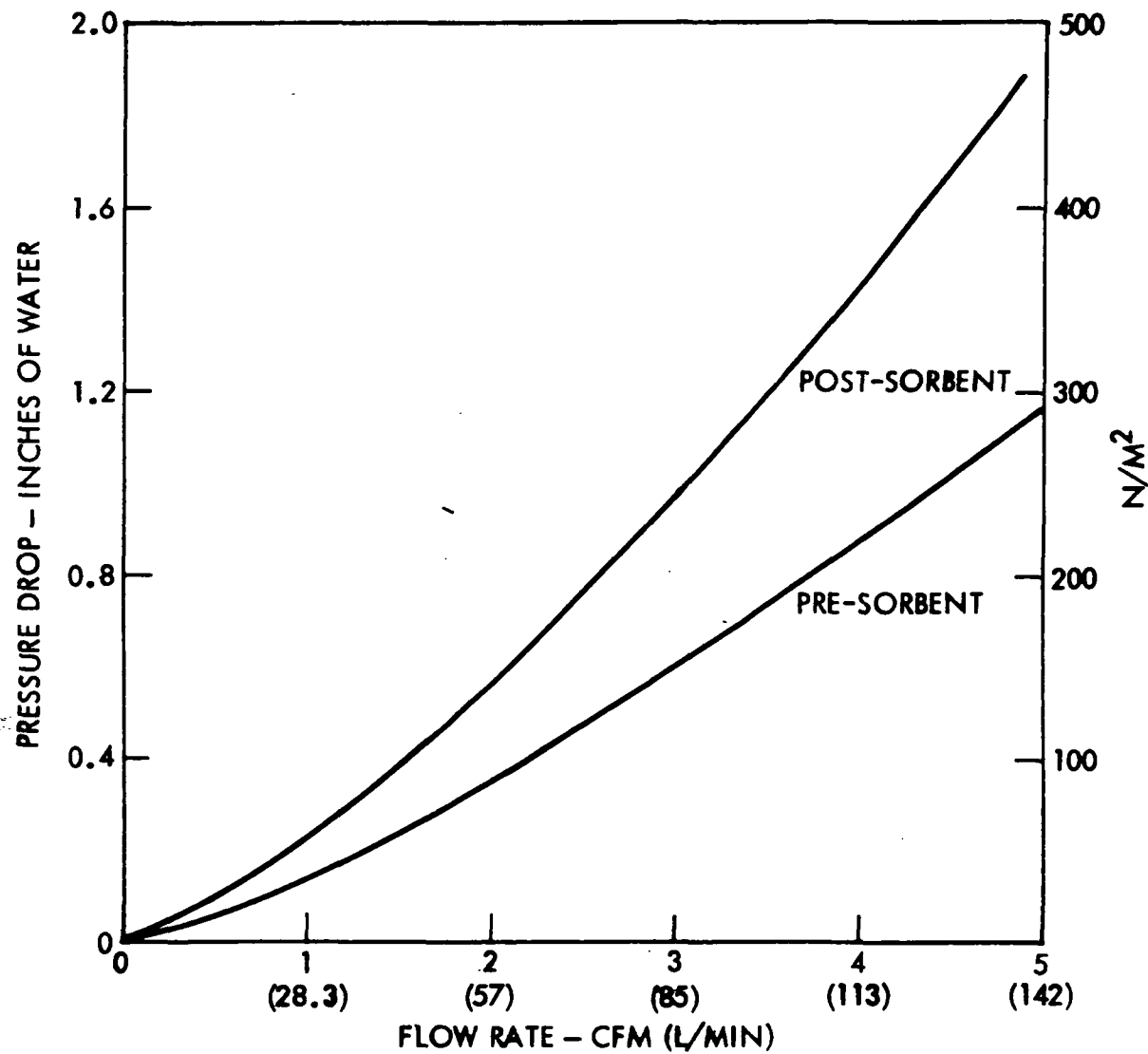


Figure 39 Pre and Post-Sorbent Canister Pressure Drop Characteristics

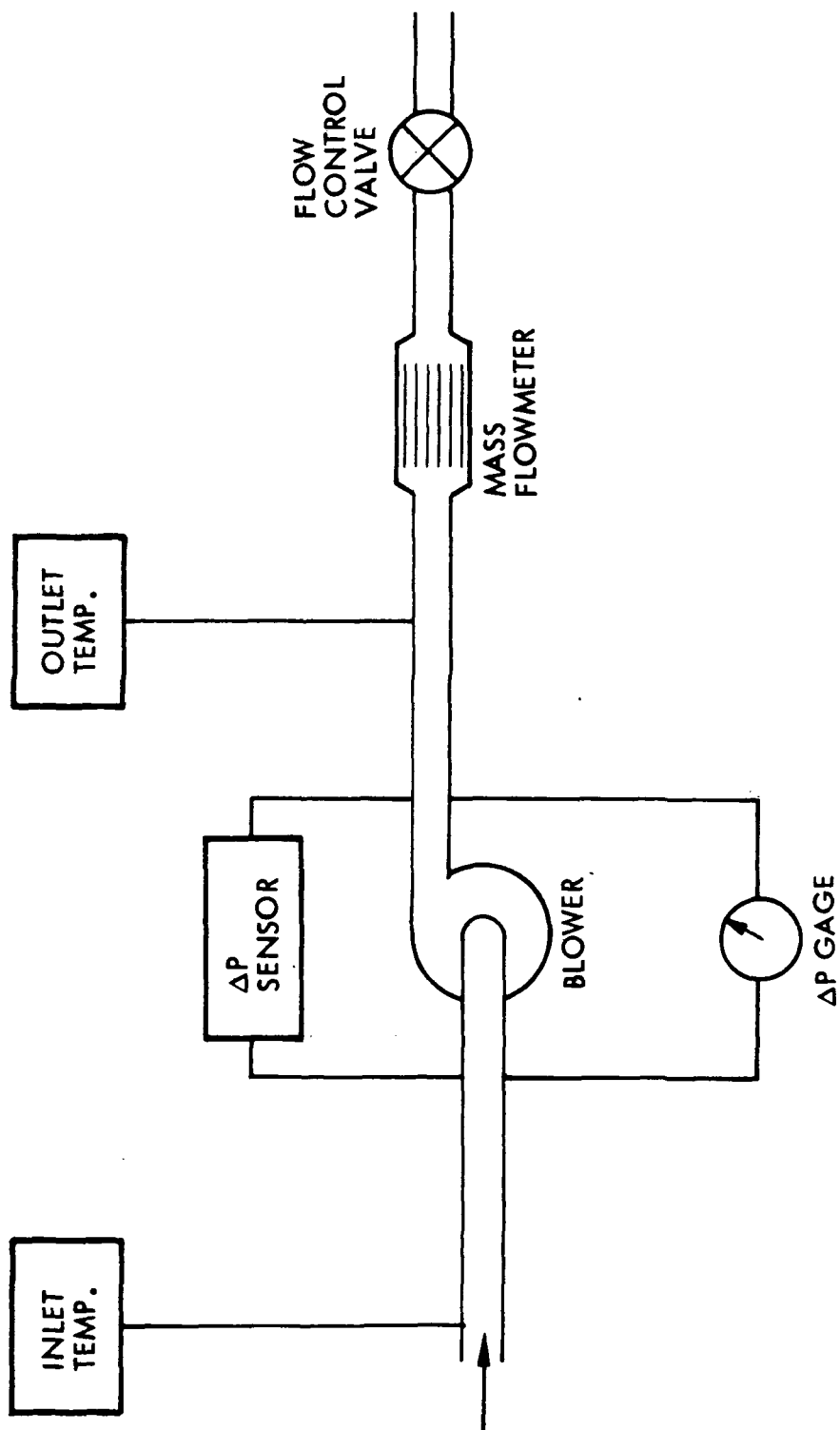


Figure 40 Regenerable Bed Blower and Pressure Drop Sensor Test

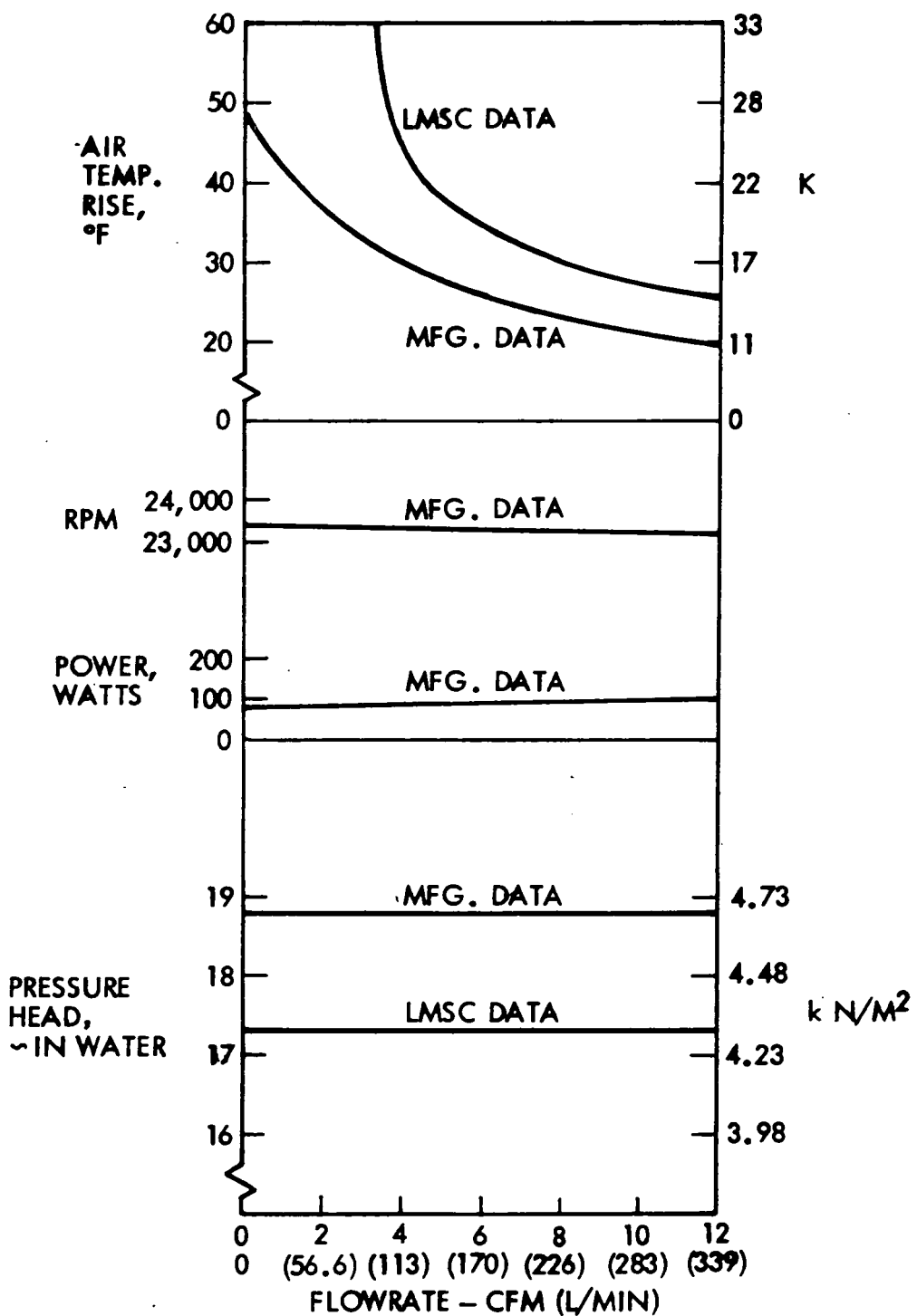


Figure 41 Regenerable Bed Blower Performance MFGR:
Dynamic Air Engineering. CO50K

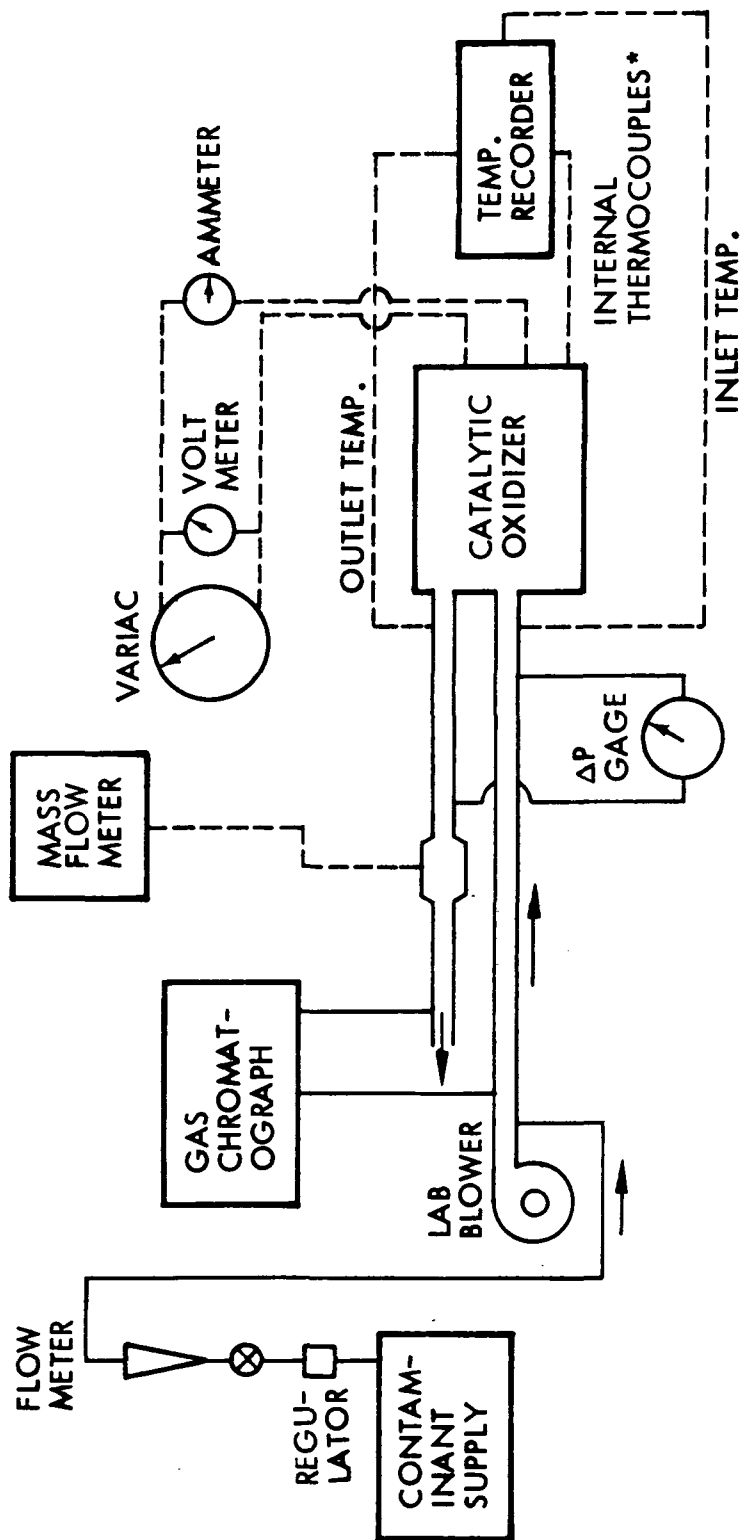
- The temperature rise was found to be higher than the manufacturer reported. At a flow rate of 127 l/min (4.5 CFM) the rise was 22 K (40 F). This would have resulted in an unacceptably high air temperature entering the regenerable bed. This dilemma was overcome by providing a bypass duct in the Trace Contaminant Control System, enabling the fan to deliver twice as much flow; approximately 254 l/min (9 CFM). This reduced the air temperature rise to about 16 K (28 F), which was acceptable. Because of the flat characteristic of pressure head vs flow rate, doubling the flow had no effect on pressure.
- Since the pressure head of the blower does not vary with flow rate in the 0 to 340 l/min (0 to 12 CFM) range the Differential Pressure Sensor output also remains constant as the flow rate varies. Therefore the differential pressure readout on the Control Panel serves only to indicate whether or not the blower is running.

9.1.4 Catalytic Oxidizer

Testing of the catalytic oxidizer was initially accomplished at IMSC with electric heaters. The unit was then shipped to the Mound Research Laboratory (operated for the U.S. AEC) where it was tested with both electrical and isotope heaters. The unit was then returned to IMSC where it was tested with isotope heaters.

9.1.4.1 Initial Tests With Electric Heaters - The initial tests of this component was performed to confirm design calculations, to define the exact performance expected from the isotope heat sources, and to determine the appropriate power level for electrical heaters that will produce acceptable temperatures when variations in vehicle power are considered. Pressure drop variations with flow rate and temperature, and preliminary contaminant removal capabilities were also to be determined.

Figure 42 is a schematic diagram of the test apparatus. The blower was a Rotron laboratory test unit, the mass flowmeter was a Hastings-Raydist instrument, the ΔP gage was manufactured by Magnahelic and the thermocouples were chromel-alumel.



*INTERNAL THERMOCOUPLES FOR TEMPERATURE MONITORING OF
HEATER SURFACE (2), CATALYST BED, GAS, & CATALYST CANISTER

Figure 4-2 Electrically Heated Catalytic Oxidizer Component Test

Tests were performed at various air flow rates and at various electric heater power levels. Tabulated results are given in Table 26. Variations of temperature with power and flow rate are shown in Figure 42, it should be noted that each of the two electric heaters received equal power input.

Since the catalyst air temperature with design air flow was only 632 K (678 F) at a total power input of 121 watts (equivalent to one Pu isotope heater of 72 and one of 49 watt rating) and since it was desired to reach a catalyst air temperature in excess of 672 K (750 F), it was decided to employ two 72 watt isotope heaters. This resulted in a heater temperature at the no flow condition of less than 922 K (1200 F) which is below the limit established for the isotopes. Figure 44 shows the effect of temperature in the oxidation of methane. Similar tests on CO showed 100% conversion.

9.1.4.2 Testing at the AEC-Mount Lab - The purpose of these tests were (1) to replicate the results of the IMSC test using electric heaters (2) to determine the handling procedures for, and radiation levels of, the isotope heated unit and (3) to measure the thermal performance of the catalytic oxidizer with isotope heaters.

Figure 49 is a diagram of the test apparatus. It is similar to that of the preceding test except that no contaminants were introduced, but instruments for measuring gamma radiation and neutron flux were added.

The thermal results of these tests are shown in Table 27. The values for the electric heat source are comparable to those obtained in the previous tests at IMSC. Also, it can be seen that the isotope heaters gave results comparable to those obtained with the electric heaters.

Radiation levels around the catalytic oxidizer when it contains two 71.4 watt Pu isotope heaters is shown in Table 28. To meet AEC standards for safe human exposure (2.5 mrem/hour - 20 mrem/day = 100 mrem/week = 1.3 rem/quarter year) one must remain at least 210 cm away from the unit, if one works at that distance 40 hours each week.

Table 26

Catalytic Oxidizer Component Test Results with Electric Heater at IMSC

Power (watts)	121	121	121	112	148	148	145	136	137	118	145	136
Flow 1/gpm (cm3/s)	380 (4.25)	0 (1)	0 (2)	120 (4.25)	117 (4.15)	0 (1)	0 (2)	120 (4.25)	85 (3.0)	95 (3.0)	139 (4.9)	139 (4.9)
Pressure Drop in/s (in water)	1.5 (6)	0	0	1.5 (6)	1.6 (6.3)	0	0	1.5 (6)	1.0 (4)	1.0 (4)	1.7 (7)	1.7 (7)
Inlet Air Temp K (°F)	304 (90)	300 (80)	307 (98)	31 (100)	311 (100)	390 (95)	306 (90)	310 (98)	314 (105)	315 (106)	316 (107)	312 (102)
Outlet Air Temp K (°F)	333 (140)	303 (85)	309 (95)	336 (145)	344 (160)	309 (95)	306 (90)	341 (153)	347 (165)	344 (160)	342 (155)	341 (152)
Catalyzer Catalyst Temp K (°F)	963 (590)	601 (582)	700 (800)	572 (570)	650 (710)	667 (740)	738 (905)	606 (630)	636 (689)	611 (640)	625 (665)	607 (632)
Catalyzer Delta Air Temp K (°F)	632 (676)	667 (740)	754 (898)	619 (655)	708 (815)	744 (880)	814 (1005)	677 (758)	689 (780)	658 (725)	678 (760)	656 (725)
Lower Heater Temp K (°F)	728 (690)	814 (1005)	861 (1090)	710 (880)	816 (1010)	878 (1120)	917 (1190)	775 (935)	794 (970)	750 (890)	777 (936)	751 (900)
Upper Heater Temp K (°F)	733 (695)	839 (1050)	880 (1126)	736 (865)	814 (1005)	878 (1120)	917 (1190)	778 (935)	794 (990)	769 (925)	774 (932)	751 (892)
¹	91.5	-	-	92	91.5	-	-	92.5	91	91.5	92	92

(1) No-flow shutdown 2 hrs. after steady state with flow.

(2) Steady state no flow shutdown.

ORIGINAL PAGE IS
OF POOR QUALITY

TABLE 27

CATALYTIC OXIDIZER COMPONENT TEST RESULTS WITH ELECTRIC HEATER &
 ISOTOPE HEAT SOURCES AT MONSANTO-MOUND LAB

Heater Type	Electric	Isotope (1)	Isotope
Power (watts)	147.8	143	143
Flow l/min (CFM)	113 (4.0)	0	117 (4.15)
Pressure Drop kN/m ² (in water)	1.5 6	-	1.6 (6.6)
Inlet Air Temp K (F)	306 (90)	-	309 (95)
Outlet Air Temp K (F)	332 (137)	-	334 (142)
Catalyst Canister Temp K (F)	637 (687)	767 (920)	633 (680)
Catalyst Inlet Air Temp K (F)	713 (823)	-	-
Lower Heater Temp K (F)	798 (977)	-	-
Upper Heater Temp K (F)	794 (970)	-	-

(1) Steady State no-flow shutdown.

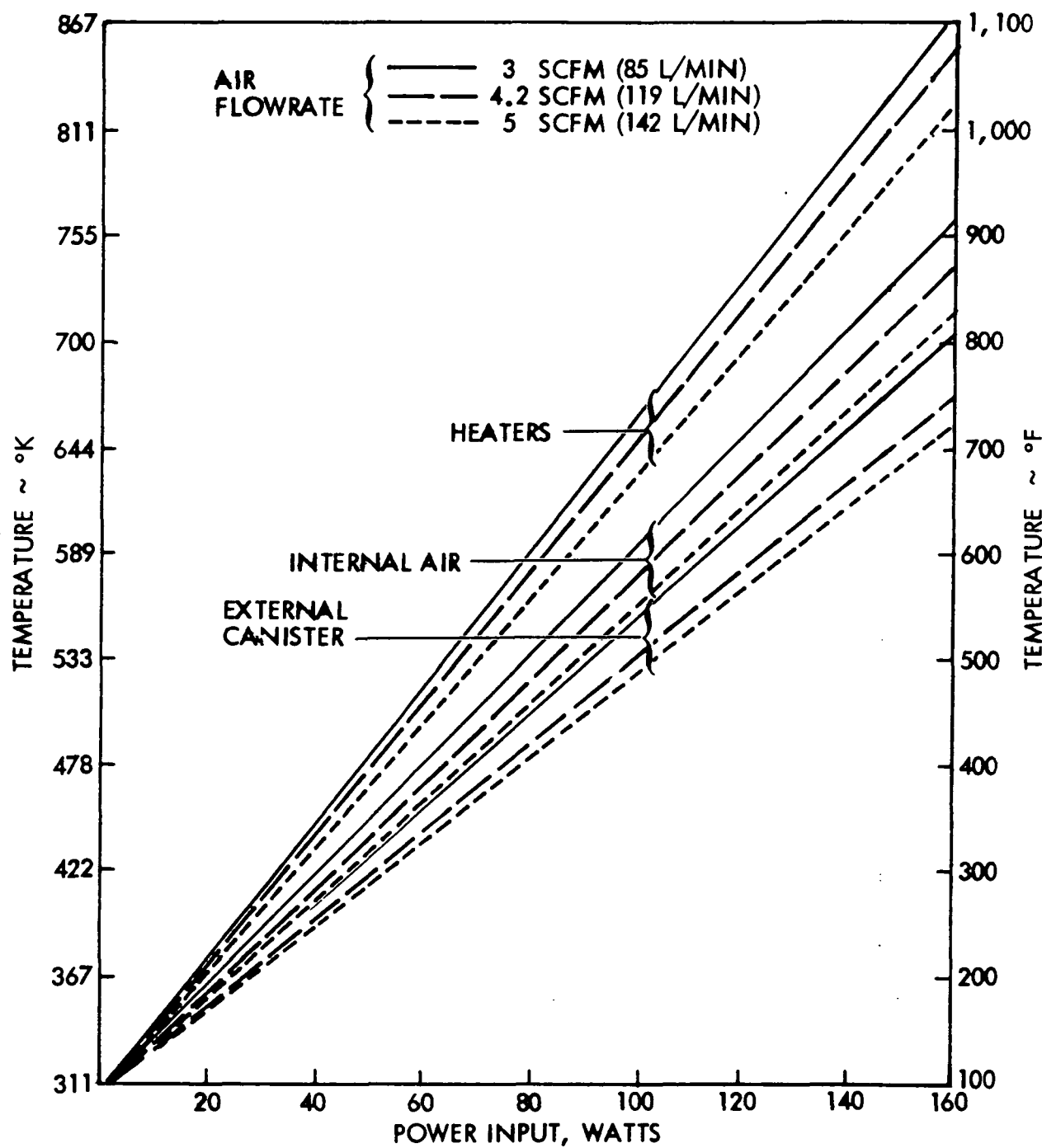


Figure 43 Catalytic Oxidizer Temperatures

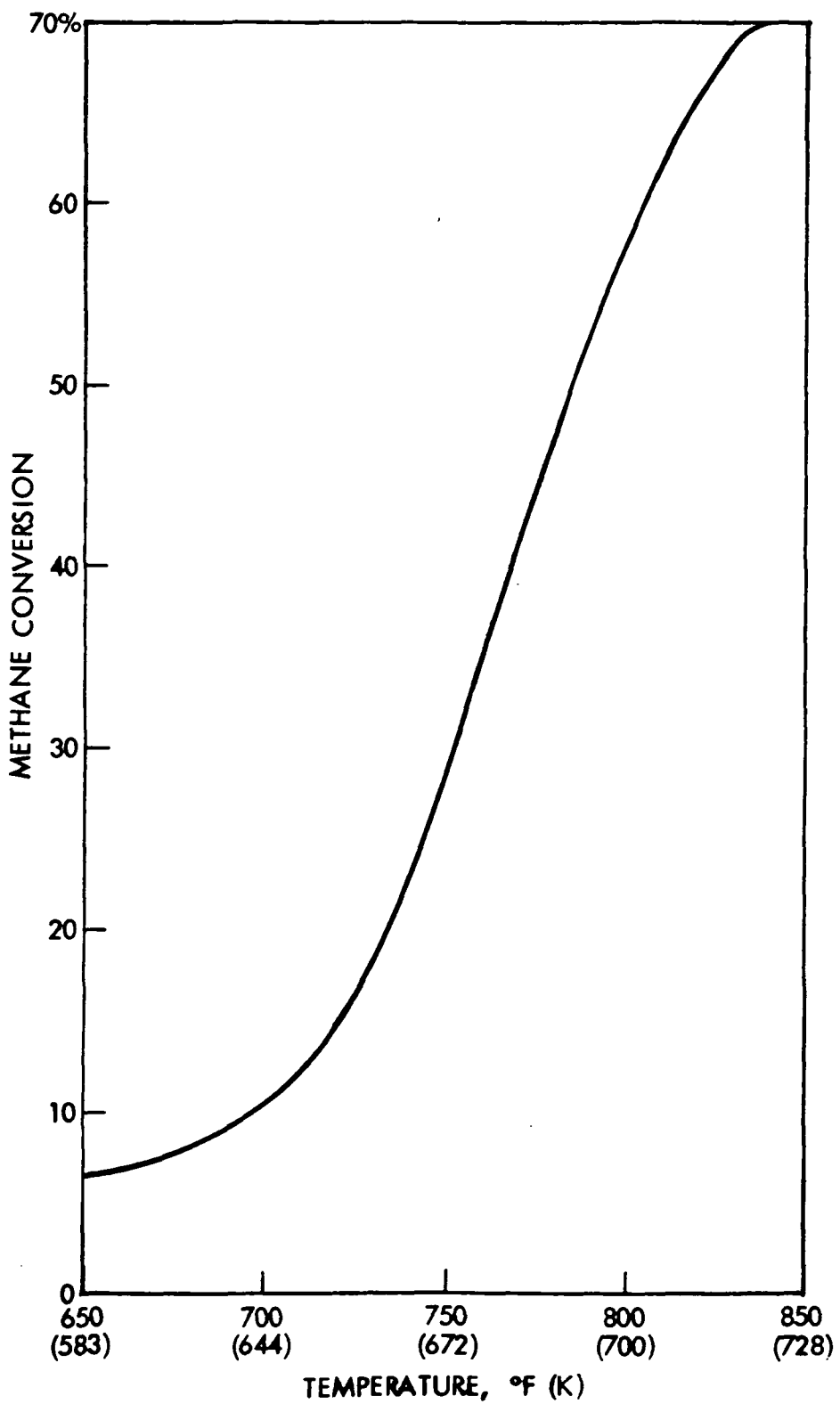


Figure 44 Catalytic Oxidizer Methane Conversion Performance

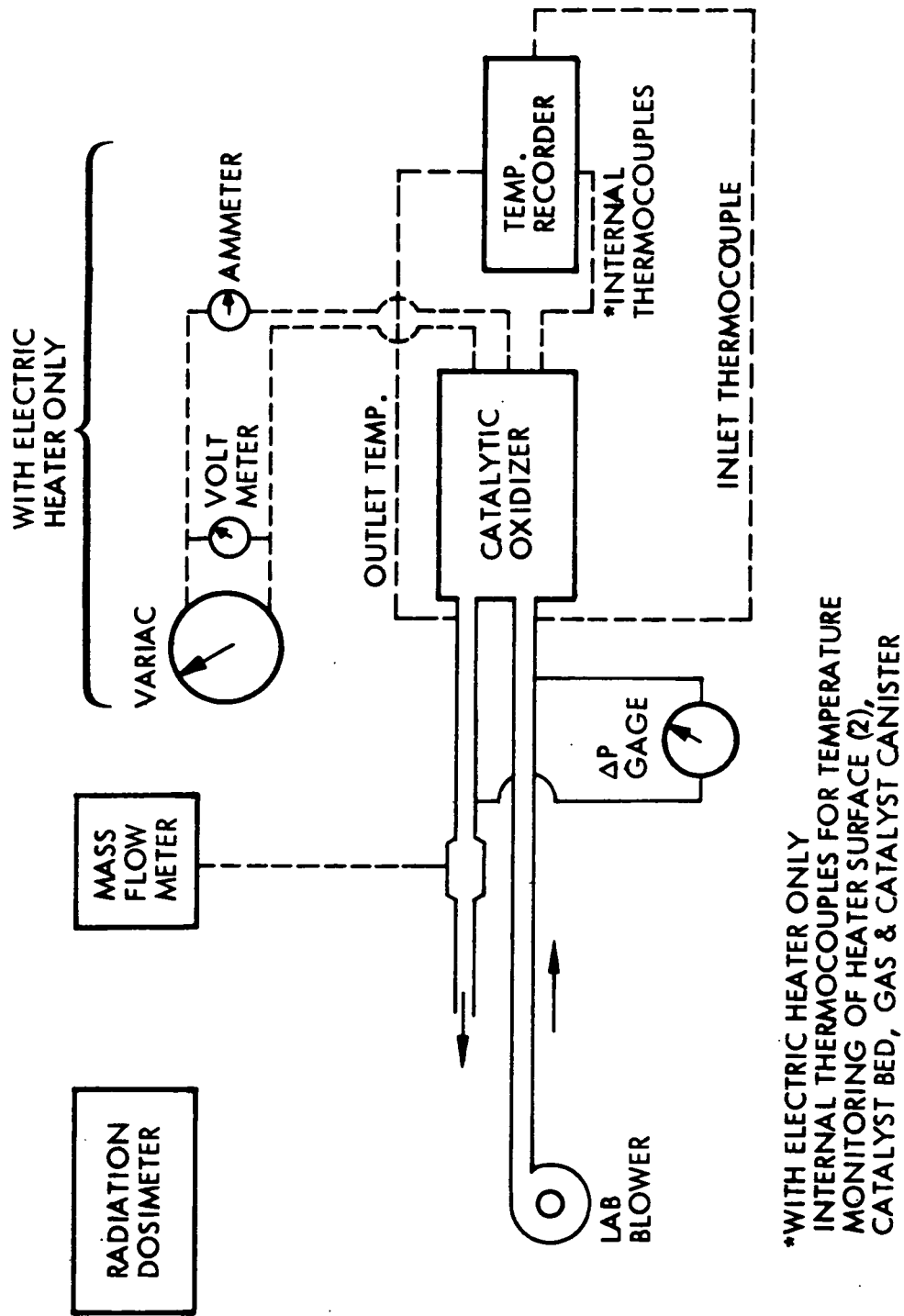


Figure 45 Catalytic Oxidizer Component Test Apparatus at AEC Mound Laboratory

9.1.4.3 Tests at IMSC with Isotope Heaters - After the tests at the AEC-Mound Lab, the isotope heaters were removed and shipped in a special container to IMSC, where they were re-installed in the catalytic oxidizer. Tests were then performed; they verified the thermal, radiation and contaminant removal performance previously obtained. The test apparatus is shown in Figure 46; it is similar to that of the preceding tests.

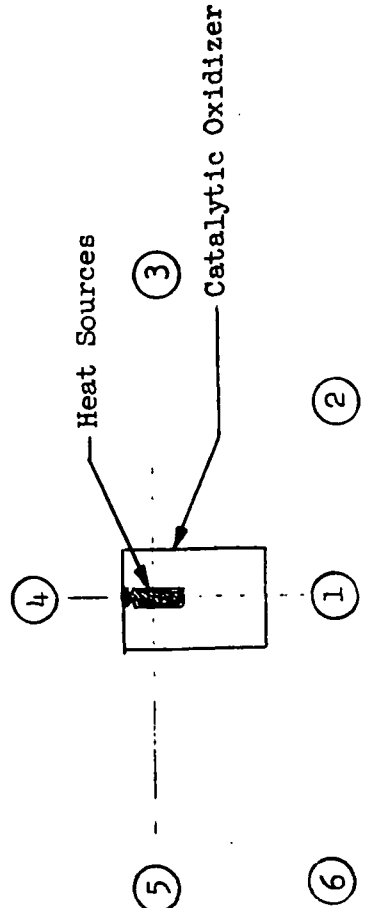
9.1.5 Regenerable Bed, Isotope Valves, Vacuum Valve and Bleed Valves Since the regenerable bed is operated on a 24 hour cycle including the application of vacuum and heating, the component level testing was performed with the subject items installed in the Trace Contaminant Control System, plus the necessary test equipment (see Figure 47). Preliminary leak tests had already been performed on the regenerable bed and the isolation valves to demonstrate that they were vacuum tight, and pressure tight.

The first attempts at desorption showed that the design bed temperature of 373 K (212 F) could not be reached within the required time (approximately one hour). Upon analysis the reason for this became obvious; the actual hardware was more than twice as heavy as the weight which had been estimated when the maximum heater power was originally calculated at 150 watts. It was found that sufficiently fast heating could be achieved with a power input of 360 watts. Temporarily the original heaters were run at this higher-than-rated power levels; meanwhile new heaters were ordered.

Adsorption testing of the regenerable bed was also conducted. The results of those tests revealed that initial break-thru of Freon 11 and Freon 12 occurred with a removal efficiency of approximately 50% per pass. In addition it was observed that the pressure drop of the regenerable bed was approximately 100 N/m^2 (0.4 in water), whereas the predicted value was in excess of 249 N/m^2 (1 in water), indicating a possible bypass. It was postulated that the large wetted area of the internal fins could have caused channeling due to the greater open area where charcoal is in contact with the metal surfaces of the canister. It was decided to use a finer mesh charcoal (increasing the pressure drop of the regenerable bed) to reduce any channeling effects which might be

TABLE 28
GAMMA & NEUTRON LEVELS AT VARIOUS LOCATIONS
FROM THE CATALYTIC OXIDIZER

Location	Distance (cm)	Gamma (mrem/hr)	Neutron (mrem/hr)	Total (mrem/hr)
1	100	0.7	5.2	5.9
2	110	1.2	7.3	8.5
3	200	0.5	3.1	3.6
4	50	5.6	33.6	39.2
5	50	7.0	38.4	45.4
6	140	0.3	2.7	3.0



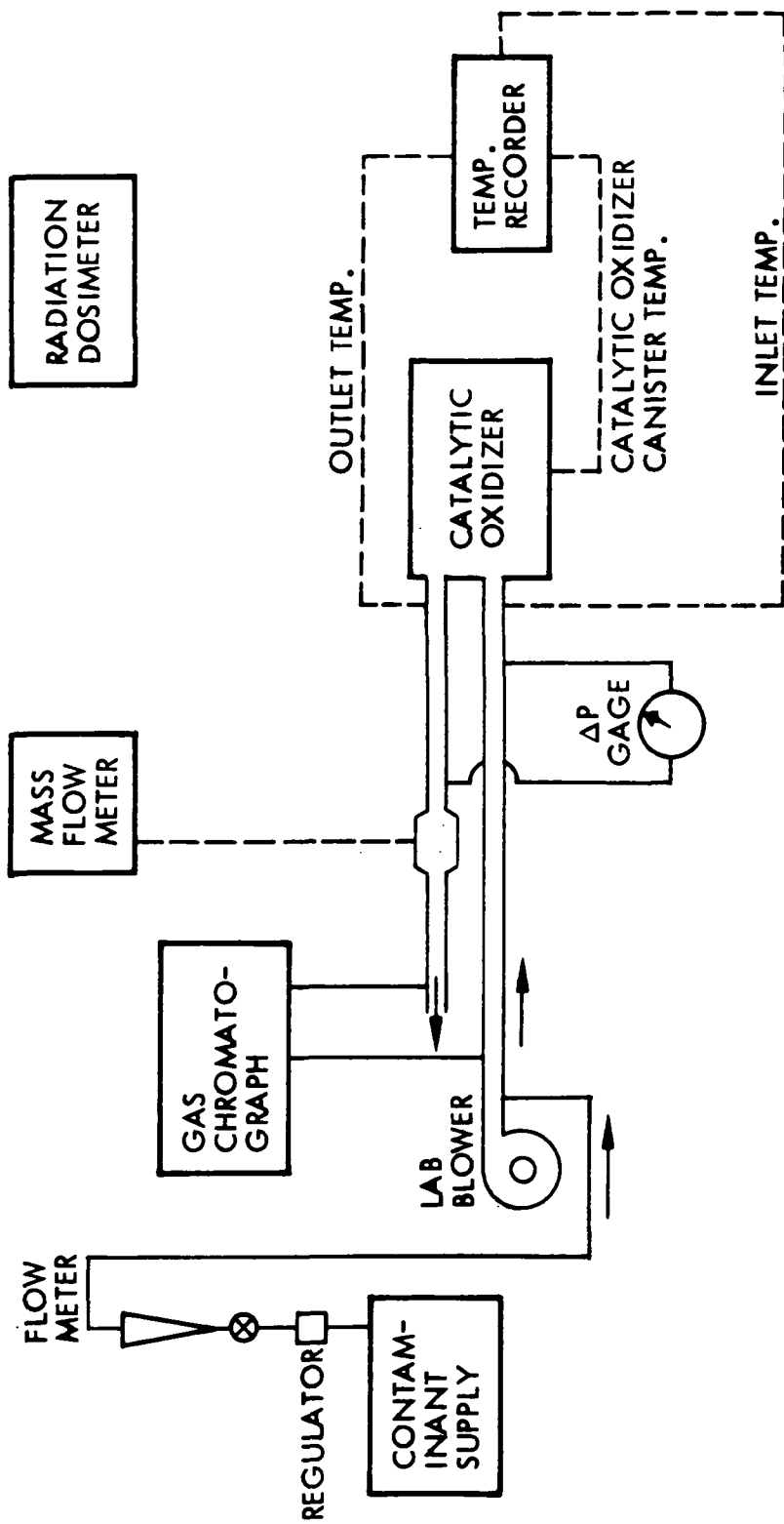


Figure 46 Catalytic Oxidizer Component Test Apparatus at LMSC
with the Isotope Heat Source

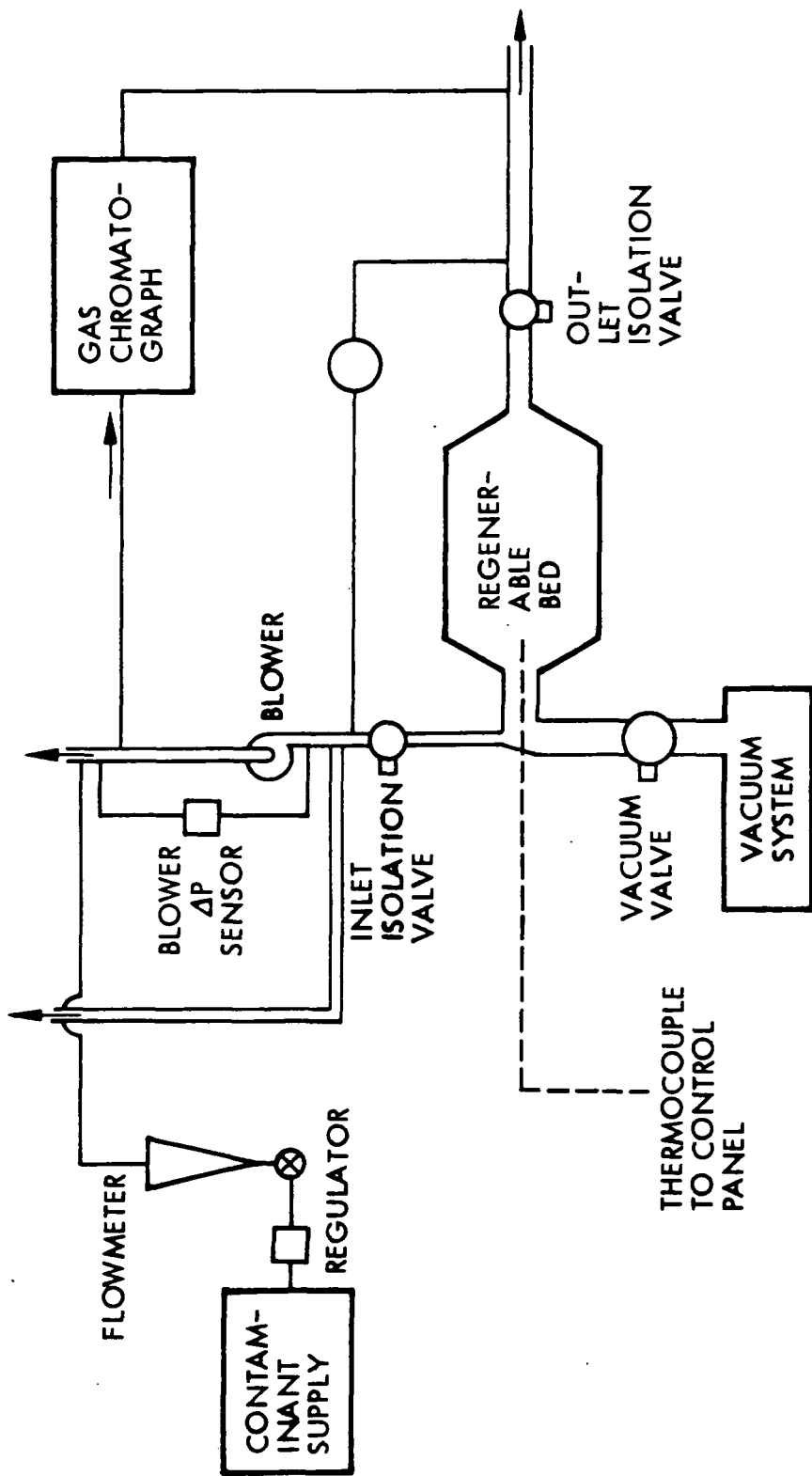


Figure 47 Equipment Arrangement for Testing of Regenerable Bed Components

present. Since the original system pressure drop calculations were somewhat conservative the head rise of the regenerable bed fan was about 1.2 kN/m^2 (5 in water) greater than required. It was decided to raise the regenerable bed pressure drop by changing from an 8×14 mesh charcoal to a 14×20 mesh charcoal except for a 3.81 cm (1.5 in) layer at each end to prevent passing through the screens. A mechanical vibrator was also used to reload the bed to further minimize potential channeling.

The pressure drop of the regenerable bed with the finer mesh charcoal was determined to be 739 N/m^2 (2.97 in of water) at 127 l/min (4.5 CFM) as shown in Figure 48. After establishing the pressure drop, the bed was operated for two days through two complete desorption cycles. After the second desorption cycle the unit was operated through a full desorption cycle with Freon 11 and Freon 12 being introduced at the inlet of the regenerable bed. The regenerable bed was being operated in an open-loop configuration and inlet Freon concentrations close to those anticipated for the final test were maintained. The results of this test are presented below.

Time After Start of Adsorption Cycle Hrs.	Freon 11		Freon 12	
	Conc. mg/m^3		Conc. mg/m^3	
	Inlet	Outlet	Inlet	Outlet
0	13.3	0	13.1	0
5 1/2	15.7	0	15.4	0
23 1/2	14.0	0	14.0	0

As can be seen from this data the removal efficiency of the regenerable bed for these compounds was 100% throughout the entire adsorption cycle. During the component testing the final desorption cycle was developed which resulted in a regenerable bed temperature of approximately 367 K (200 F) and a regenerable bed pressure of approximately 0.13 N/m^2 (1×10^{-3} torr) at the end of the desorption cycle. The bed temperature and vacuum line pressure during a desorption cycle are presented in Table 29. The ionization gauge pressure data are considered to be more accurate than the thermocouple gauge data. The final desorption is as follows:

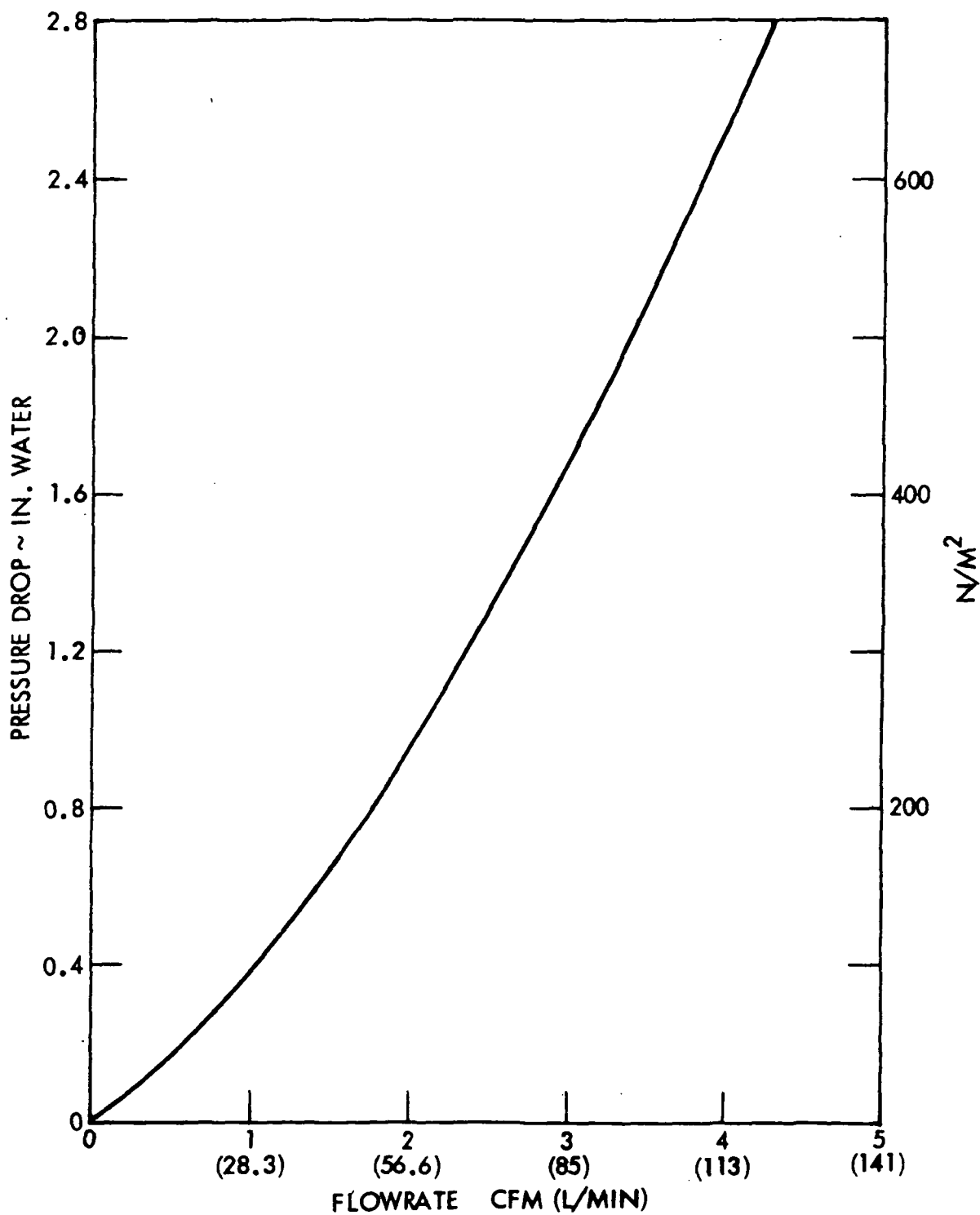


Figure 48 Pressure Drop of Regenerable Bed With 14 x 20 Mesh Charcoal (Except for 1 1/2 Inch (3.8 cm) Layer of 8 x 14 Mesh at Each End).

Regenerable Bed Desorption Cycle

<u>TIME</u>	<u>FUNCTION</u>
+ 1 minute	Isolation valve closed Heater on high current Vacuum bleed valve open Regenerable bed fan OFF
+30 minutes	Vacuum bleed valve closed Vacuum valve open
+54 minutes	Heater on low current
+ 3 hrs. 15 minutes	Vacuum valve closed Heater off
+ 3 hrs. 15 minutes 1 sec.	Isolation bleed valve open
+ 3 hrs. 20 minutes	Isolation bleed valve closed Isolation valves open Regenerable bed fan on

TABLE 29
REGENERABLE BED DESORPTION CHARACTERISTICS

Elapsed Time (min)	K	Bed Temp. (F)	N/m ²	Vacuum Line Pressure (micron)	Comment
0	309	(97)		Atm ⁽¹⁾	
1	309	(97)			Start desorption cycle
10	312	(102)			
20	328	(130)			
30	340	(152)			Close vacuum bleed, open vacuum valve
40	334	(142)			
50	350	(170)			
54		-			Switch from high heat to low heat
60	360	(188)			
70	364	(195)	127	(950)	
80	366	(198)	100	(750)	
90	368	(202)	83	(620)	
100	369	(205)	67	(500)	
110	371	(208)	61	(460)	
120	372	(210)	55	(410)	
130	373	(211)	52	(390)	Switch to diffusion pump
140	375	(215)	45	(340)	
150	377	(218)	35	(260)	
160	378	(220)	26	(195)	
170	378	(221)	14	(105)	
180	379	(222)	0.80	(6 ²)	
190	381	(225)	0.40	(3)	
195	382	(227)	0.26	(2)	Close vacuum valve open pressure bleed
200	383	(230)	0.13	(1)	End desorption cycle

(1) Thermocouple gauge pressure data available only below 1000 microns

(2) Ionization gauge data available below 10 microns.

9.2 INTEGRATED SYSTEM TESTING

Following preliminary testing of the individual system components, the components were assembled into an integrated system. The integrated system was then tested for a period of about 240 days to demonstrate its operational capability for the duration of a full mission and evaluate the design methodology. In the following sections the test apparatus and procedures, test results and analysis of the results are described.

9.2.1 Apparatus and Procedures

In this section the selection of test contaminants, the integration of the system with the support equipment, and the analytical procedures and schedule are discussed.

9.2.1.1 Selection of Contaminants - An analysis was made of the design basis for each of the Trace Contaminant Control System components to access its limits of performance. In addition previous tests were reviewed to define contaminants used to monitor system performance. The result of this study is the test system contaminant level specified in Table 30. During the test, Freon 22 and propylene were added during the low-introduction-rate phase of the test and propane during the high-introduction-rate phase of the test to gather more data on the regenerable bed performance. The contaminants were introduced at the high rates initially; then at the long-term (lower rates) for the bulk of the test days, and then 23 days before terminating the test, most contaminants were introduced at the high rates for a final verification of removal effectiveness.

9.2.1.2 Supporting Test Equipment - The integrated trace contaminant control system requires both electrical power and vacuum for its operation. In addition, testing in a closed loop required hookup with a simulated cabin volume, contaminant feed controls, and a gas sampling system.

The design of the Trace Contaminant Control System is such that the only power required for its operation is 400 cycle, 208 volt, 3 phase power. A laboratory power supply provided the power for system operation.

Table 30
Contaminants Used in the System Level Test

	High Introduction Phase		Low Introduction Phase		
	Intro.	Rate gm/day	Intro.	Rate gm/day	Comments
<u>Fixed Bed</u>					
Pyruvic Acid	1.26		1.26		Sets fixed bed flow and quantity.
Ammonia	4.0		1.75		Sets H_2PO_4^- loading
Toluene	2.5		0.25		Representative of well adsorbed contaminant
Benzene	0.9		0.09		Also set fixed bed quantity
<u>Pre-Sorbent Bed</u>					
SO_2	0.25		0.025		Typical acid gas
<u>Regenerable Bed</u>					
Methyl Alcohol	2.51		0.26		Sets regenerative bed flow and quantity (1)
Freon 11	2.5		0.25		Fixed bed breakthru monitoring and used in previous tests
Freon 12	2.5		0.25		Used in previous tests
Acetone	10.2		1.02		Used in previous tests
Methyl Acetate	2.5		0.25		Fixed bed breakthru monitoring
Methyl Ethyl Ketone	2.5		0.25		Fixed bed breakthru monitoring
Freon 22(2)	-		.025		Gather additional data on performance
Propylene(2)	-		.25		Gather additional data on performance
Propane(2)	2.5		-		Gather additional data on performance
<u>Catalytic Oxidizer</u>					
Carbon Monoxide	2.7		0.45		Sets catalytic oxidizer flow rate.
Methane	33.1		6.55		Sets catalytic oxidizer temperature.
Acetylene	2.5		0.25		Used in previous tests
Ethylene	2.5		0.25		Used in previous tests
Ethane	2.5		0.25		Used in previous tests

(1) Quantity set by tetrofluoroethylene, however, TFE too reactive for introduction.

(2) Methyl alcohol is the next contaminant in order relative to capacity.

(2) These contaminants added after test in progress.

The activated carbon regenerable bed requires vacuum for regeneration. During the regeneration cycle vacuum was provided by one of two vacuum systems. Initially, when the major portion of the water load is discharged, a heavily ballasted Kinny KTC-21 pump provided vacuum. When the pressure dropped below 150 microns a valve to a 10 cm (4 in) CVC diffusion pump with a Welsh Model 1397 roughing pump was opened. Control of the valving was automatic. This system allowed a rapid removal of water, followed by high capacity diffusion pump capability to achieve the desired desorption pressure levels.

The simulated cabin used in the closed system test was an aluminum tank which had a diameter of 1.52 m (5 ft) and was 2.44 m (8 ft) high giving a total volume of 4446 l (157 ft³). The inlet line to the TCSS was a 7.62 cm (3 in) aluminum duct 142 cm (56 in) long and 122 cm (48 in) above the base of the tank. The exit duct was also 7.62 cm (3 in) in diameter. It had a total length of 416 cm (164 in). The last run of the return duct was downward into the top of the simulated cabin. The contaminants were fed into the circulating gas stream in this last section of the return duct.

For convenience in feeding contaminants they were grouped together to minimize the number of feed systems. The groupings are summarized below:

- o A liquid feed stream consisting of benzene and toluene
- o A liquid feed stream consisting of a 5 percent solution of pyruvic acid in water
- o A liquid feed stream consisting of methyl alcohol, acetone, methyl acetate, methyl ethyl ketone, and water
- o A gas feed stream of ammonia
- o A gas feed stream of sulfur dioxide and air
- o A gas feed stream of Freon 11, Freon 12, and air
- o A gas feed stream of Freon 22, propylene, and air
- o A gas feed stream of carbon monoxide, methane, acetylene, ethylene, and ethane
- o A gas feed stream of propane and nitrogen

The benzene-toluene stream feed rate was controlled with a motorized syringe. The other liquid feed rates were maintained with a Manostat multichannel peristaltic cassette pump. Two methods were used to establish the gas introduction rates. These were low flow micrometer control valves with fixed inlet pressure; and calibrated orifices combined with inlet pressure control. The valves were used for the high introduction rate, and the calibrated orifices were used for the low introduction rate.

In all cases introduction rate controls were calibrated. Liquid rates were established by measured quantities collected over an extended period of time. Gas flow calibrations were made using precision wet test meters and bubble flow meters.

In order to implement analysis of the circulating gas in the Trace Contaminant Control System, a gas pumping and sampling manifold was built which permitted the delivery of gas from the following sources to each of the analysis stations or collection points.

- o System inlet
- o Fixed bed outlet
- o Regenerable bed outlet
- o Presorbent outlet
- o Catalytic oxidizer outlet
- o Post-sorbent outlet
- o System outlet

Provision was made to monitor gas sample flow rate and quantity as desired.

9.2.1.3 Analytical Procedures - Throughout the integrated system test, chemical analysis were performed to define the concentration of the contaminants fed into the system at each system location. A variety of analytical techniques were used including gas chromatography, colorimetric, and specific ion electrode methods. Table 31 presents a listing of the analytical techniques used to monitor each of the contaminants. In addition, several special tests were run

Table 31
Analytical Techniques Used⁽¹⁾

Ammonia	Colorimetry
Pyruvic Acid	7620 G.C., Poropak Q Column, FID ⁽²⁾
Toluene	7620 G.C., Polyphenylether Column, FID
Benzene	7620 G.C., Polyphenylether Column, FID
Methyl Ethyl Ketone	7620 G.C., Poropak Q Column, FID
Methyl Acetate	7620 G.C. Poropak Q Column, FID
Freon 11	810 G.C., SE 30 Column, EC ⁽³⁾
Acetone	7620 G.C., Poropak Q Column, FID
Freon 12	810 G.C., SE 30 Column, EC
Propylene	7620 G.C. Poropak S Column, FID
Freon 22	7620 G.C. Poropak S. Column, FID
Methyl Alcohol	7620 G.C., Poropak Q Column, FID
Carbon Monoxide	1609 G.C. Mol. Sieve Column, FID
Methane	1609 G.C. Mol. Sieve Column, FID
Acetylene	810 G.C. Mol. Sieve Column, FID
Ethylene	810 G.C. Mol. Sieve Column, FID
Ethane	810 G.C. Mol. Sieve Column, FID
Propane	7620 G.C. Poropak Q Column, FID
HF	Specific Ion Electrode & Colorimetric
HCl	Specific Ion Electrode & Colorimetric
Sulphur Dioxide	Colorimetry

(1) See Table 32 for gas chromatograph details

(2) FID = Flame Ionization Detector

(3) EC = Electronic Capture Detector

to search for unexpected contaminants. The special tests are described in Section 9.2.2 of this report.

The majority of contaminants were monitored using gas chromatography. Table 32 shows the instruments used, and the operational parameters for these contaminants.

9.2.2 Test Results

The contaminant control system components discussed in previous sections were tested in an integrated system. This section presents the results of that testing, including some preliminary discussions of the results. In the next session, the results are analyzed in detail to assess necessary changes in the design procedure. The test started on October 10, 1973 and ended on June 7, 1974. During this test period of 241 total days, the operation of the system was essentially continuous except for brief shutdowns due to minor component failures and configuration changes.

Table 33 presents a listing of the significant events which occurred throughout the duration of the test program. Other than the initial system shutdown on day 9, which was to solve a problem of fixed bed channeling, it can be seen that most of these events either are related to planned changes or are due to breakdowns in the supporting test equipment. The only failures attributed to the trace contaminant control system during the test were two relay failures which are:

- o Regenerable bed heater control relay on day 30
- o Catalytic oxidizer heater relay on day 201

During the test, chemical and analysis were made to determine the system performance. Data were taken on a regular schedule for each contaminant introduced to provide long term performance characteristics. In addition several special tests were run to investigate reaction products due to interaction between the contaminants and the system components. The data on contaminants introduced resulting from this testing are presented in Figure 49 through 62. Table 34 presents an index of this data for convenience purposes.

Table 32
Gas Chromatograph Operational Parameters

Selected Chromatograph (1)

Operational Parameters	F/M 1609 FID	F/M 810 EC	F/M 810 FID	FID	Hewlett Packard 7620
Column	10 ft x 1/8 in SS 90% 13X & 10% 5A Molecular Sieve	15 ft x 1/8 in SS 20% SE-30 on Chromosorb W 60/80 Mesh	15 ft x 1/8 in SS 90% 13X and 10% 5A Molecular Sieve	6 ft x 1/8 in SS Poropak Q 50/ 80 Mesh	6 ft x 1/8 in SS Poropak Q 50/ 80 Mesh
Column Oven Condition	Ambient	Ambient	Programmed at 10°C/min from 110°C to 260°C	Programmed at 85°C, 4°C/min program to 125°C, and hold	4 mins. iso- thermal at 85°C, 4°C/min
Detector Temp	Ambient	190°C	230°C	200°C	128°C
Injection Port Temp.	Ambient	150°C	150°C	100°C	100°C
Carrier Gas & Flow Rate	Hydrogen/ 50 cc/min	Helium/ 30 cc/min	Helium/ 50 cc/min	Helium/ 30 cc/min	Helium/ 25 cc/min
Type of Flame	H ₂ /Air	10% methane (2) 90% Argon	H ₂ /Air	H ₂ /Oxygen	H ₂ /Oxygen
Contam- inants Analyzed	Methane Carbon Monoxide	Freon 12 Freon 11	Ethane Ethylene Acetylene	Propane Methyl Alcohol Acetone	Propylene Freon 22
				Methyl Acetate Methyl Ethyl Ketone	Benzene Toluene

(1) Notes FID = Flame Ionization Detector; EC = Electron Capture Detector
(2) Detector Purge Gas

IMSC-D462467

Table 33
 Trace Contaminant Control System
 Design Verification Test Significant Events

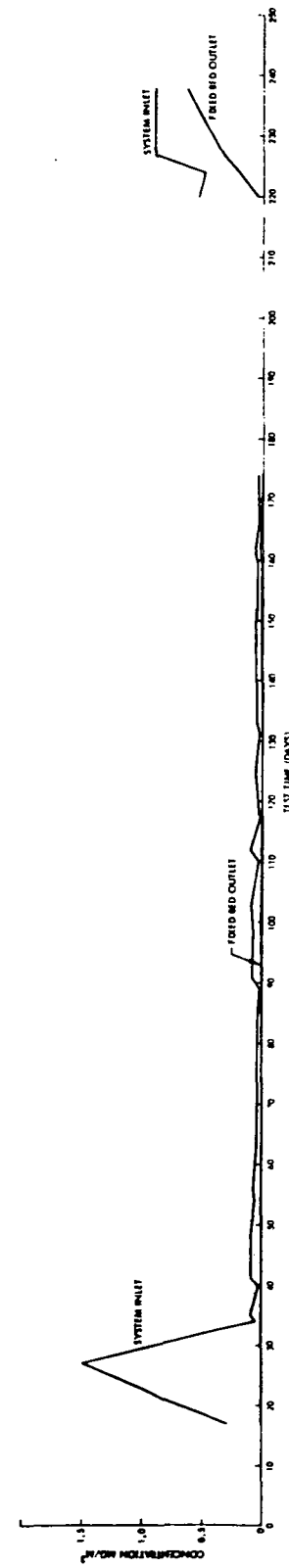
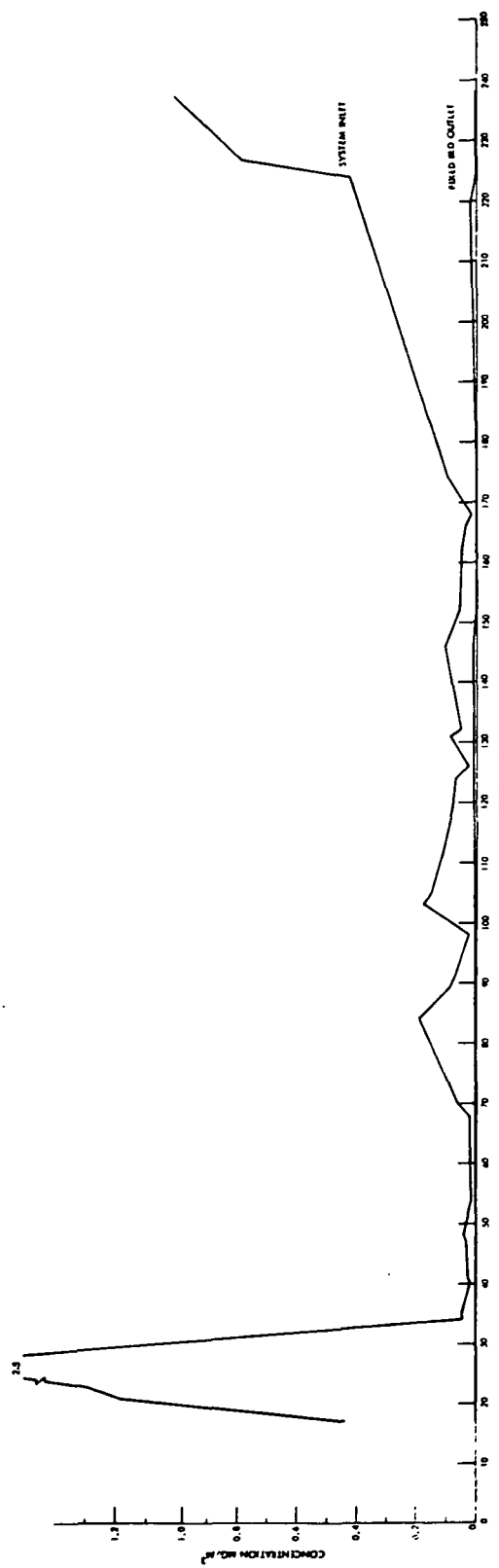
Day	Event
(Oct. 10, 1973)	
0	Initiated system operation
1	Pyruvic acid introduction initiated
4	Methyl alcohol, methyl acetate, methyl ethyl Ketone, acetone introduction initiated
5	Catalytic oxidizer contaminants introduction initiated
6	Freons introduction initiated
7	All contaminants introduced
9	Test Terminated due to poor NH ₃ removal performance fixed bed reloaded using mechanical vibrator
13	Testing resumed NH ₃ introduced
14	All contaminants introduced
25	Automatic system shutdown due to blown fuse in laboratory power supply caused by excessive ambient temperature. Room ventilation modified
26	Testing resumed; all contaminants introduced
29	Contaminant introduction switched to long term production rates
30	Automatic system shutdown due to a relay failure in the Regenerative Bed Heater Circuit. Circuit modified and new relay installed
31	Testing resumed; all contaminants introduced at the Long Term Rate
46	Automatic system shutdown due to blown fuse in laboratory power supply caused by excessive ambient temperature because IMSC initiated shutdown of building ventilation on weekends - procedure changed to leave building ventilation on continuously
47	Testing resumed all contaminants introduced at the Long Term Rate

Table 33 (continued)

Day	Event
60	Automatic system shutdown due to blown fuse in laboratory power supply - power supply was refurbished and reinstalled.
62	Testing resumed all contaminants introduced at the long term rate.
135	Automatic system shutdown due to failed laboratory power supply - power supply was repaired and reinstalled.
138	Testing resumed all contaminants introduced at the long term rate.
154	Automatic system shutdown due to poor wave form from laboratory power supply. Power supply ground modified and problem corrected.
155	Testing resumed all contaminants introduced at the long term rate.
159	Propylene, and Freon 22 added to contaminant load.
185	NH_3 breakthru fixed bed, NO observed at catalytic oxidizer outlet. NH_3 introduction terminated.
190	Initiation of desorption cycle switched from 5:00 AM to 5:00 PM.
196	Test terminated and isotope heat sources removed.
197	Installation of electric heaters initiated.
198	Installation of electric heaters completed.
199	Testing resumed with electric heaters all contaminants introduced at the long term rate with the exception of NH_3 and SO_2
201	Automatic system shutdown due to failed relay in catalytic oxidizer heater control circuit.
202	Relay replaced and system operation resumed.
206	Regenerable and catalytic oxidizer contaminants turned off, long term (2 days) desorption initiated.
208	Automatic system shutdown due to power supply failure.
211	Power supply repaired (rectifier bridge replaced) system operation resumed. All contaminants introduced with the exception of SO_2 and NH_3 .
218	All contaminants except catalytic oxidizer contaminants increased to high rates. The catalytic oxidizer contaminants increased to one-half of the high rates.
220	Catalytic oxidizer contaminants introduced at the high rate.
232	Deactivate regenerable bed desorption cycle controls.
233	Shut-off Freon feed
241	System shut-down

Table 34
Location of Data by Contaminant

Contaminant	Figure or Table Number	Page
Toluene	Figure 49	225
Benzene	50	225
Ammonia	51	226
Methyl Ethyl Ketone	52	226
Methyl Acetate	53	227
Freon 11	54	227
Acetone	55	228
Freon 12	56	228
Propylene	57	229
Propane	58	230
Freon 22	59	231
Methyl Alcohol	60	232
Acetylene	61	233
Carbon Monoxide	62	233
Ethane	63	233
Ethylene	64	234
Methane	65	234
Sulfur Dioxide	66	235
Hydrogen Chloride	Table 36	249
Hydrogen Fluoride	Table 36	249



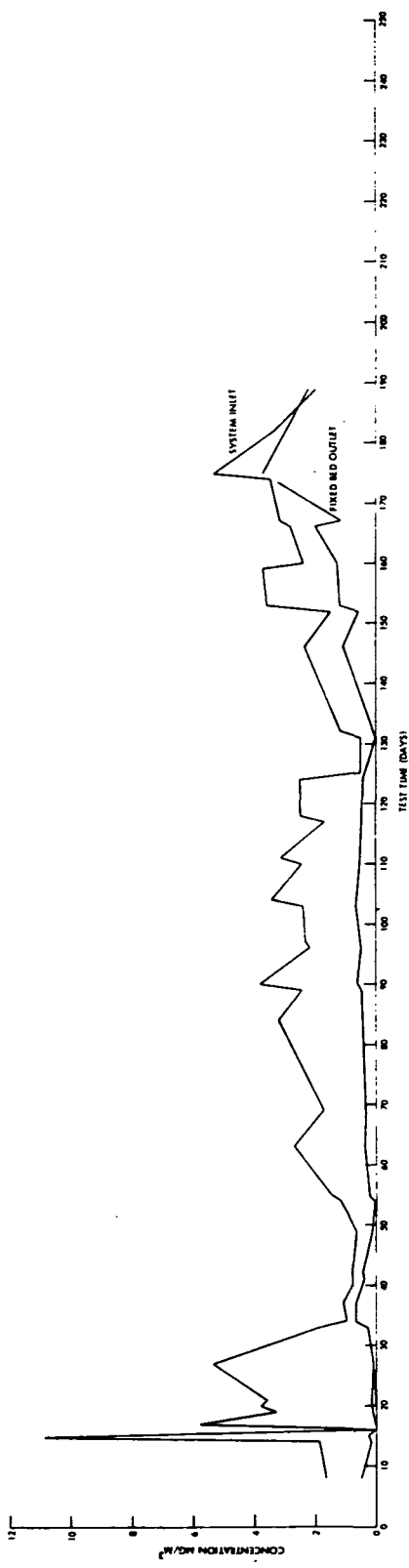


Figure 51 Ammonia - Daily Concentration Data

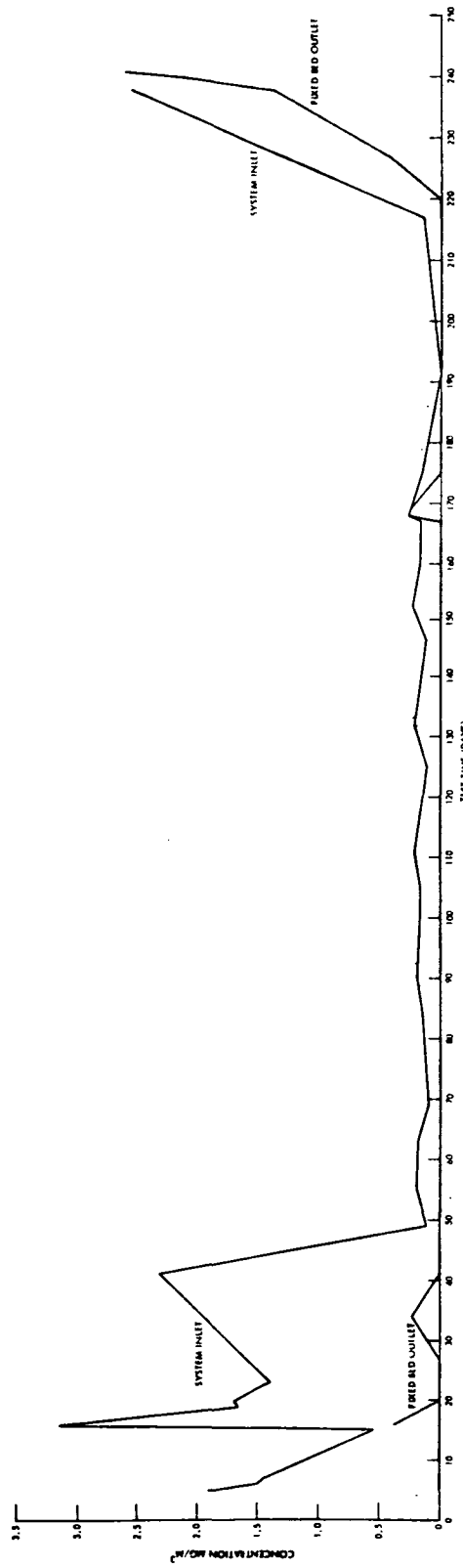


Figure 52 Methyl Ethyl Ketone - Daily Concentration Data

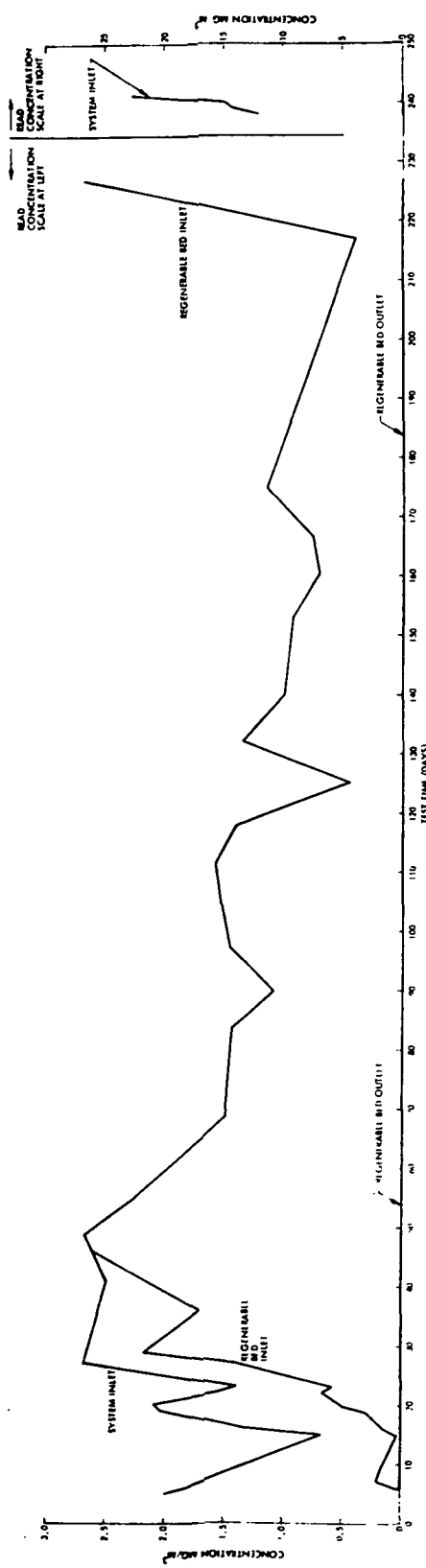


Figure 53 Methyl Acetate - Daily Concentration Data

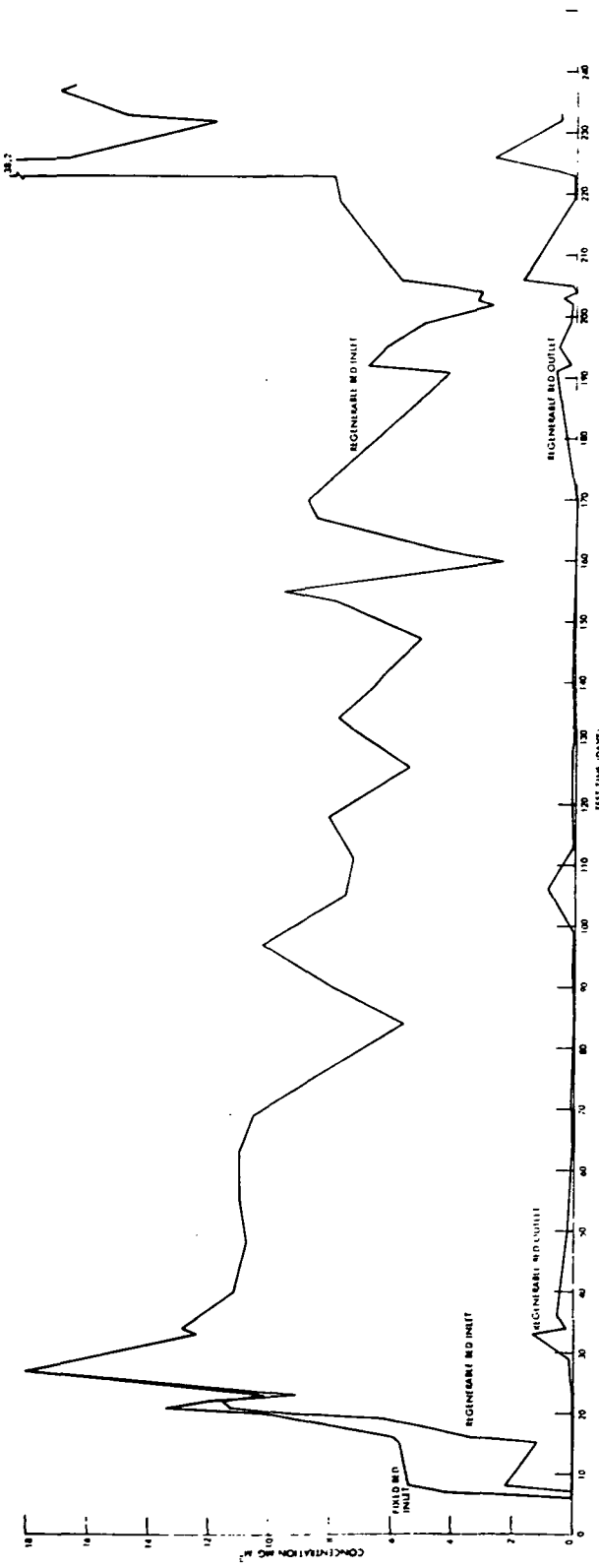


Figure 54 Freon 11 - Daily Concentration Data

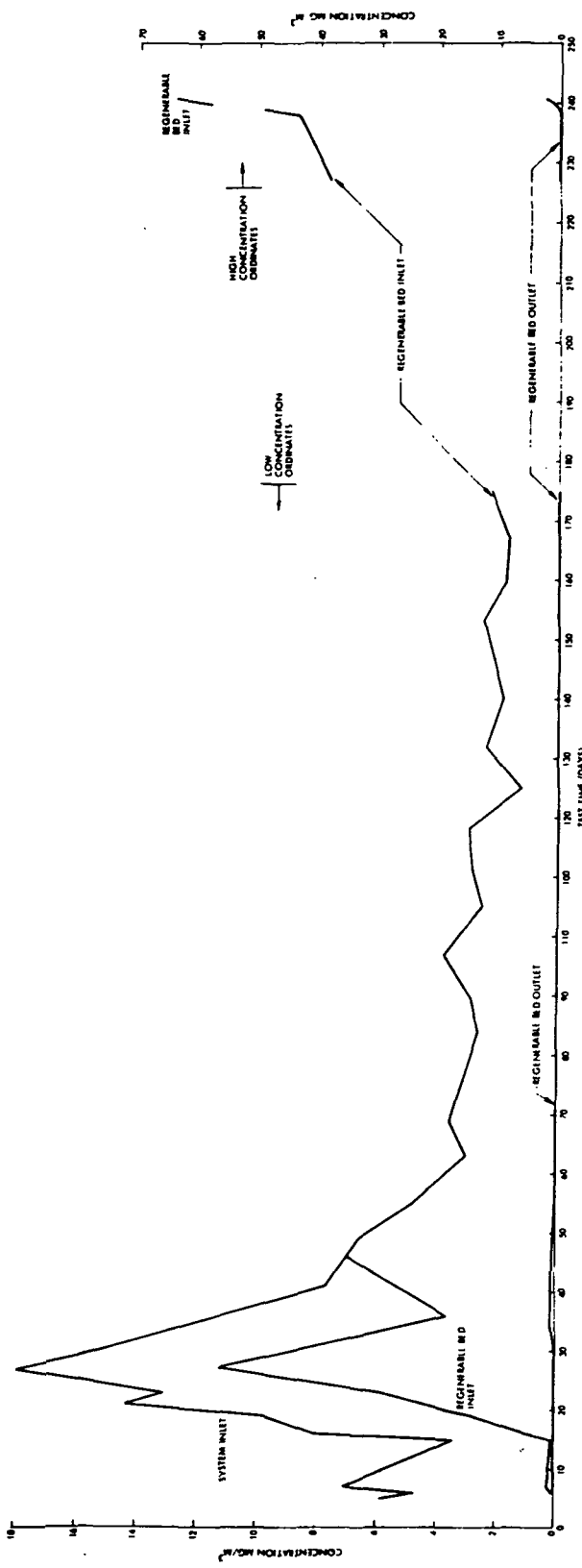


Figure 55 Acetone - Daily Concentration Data

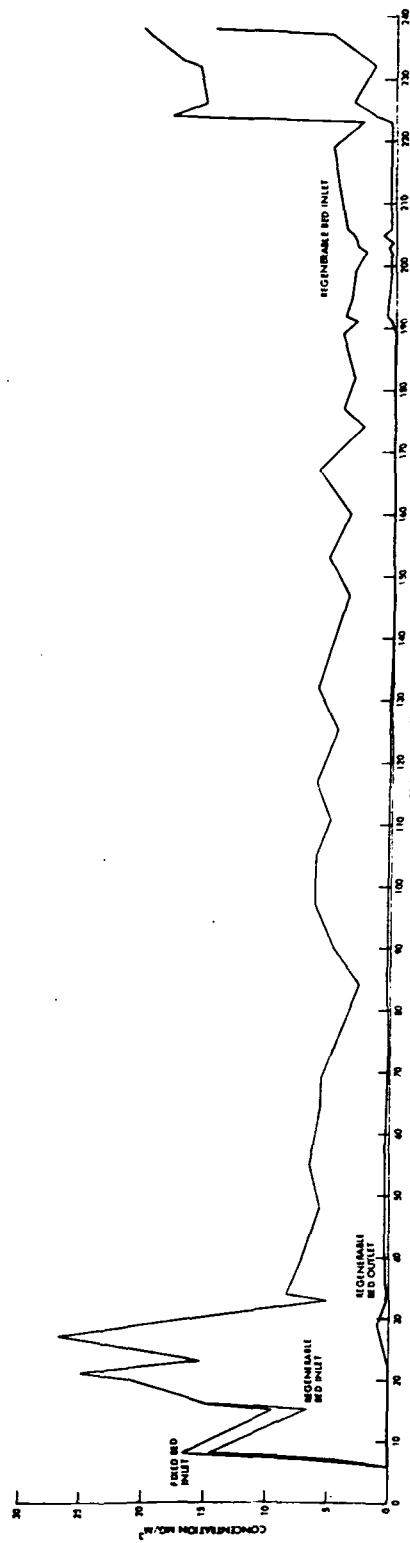


Figure 56 Freon 12 - Daily Concentration Data

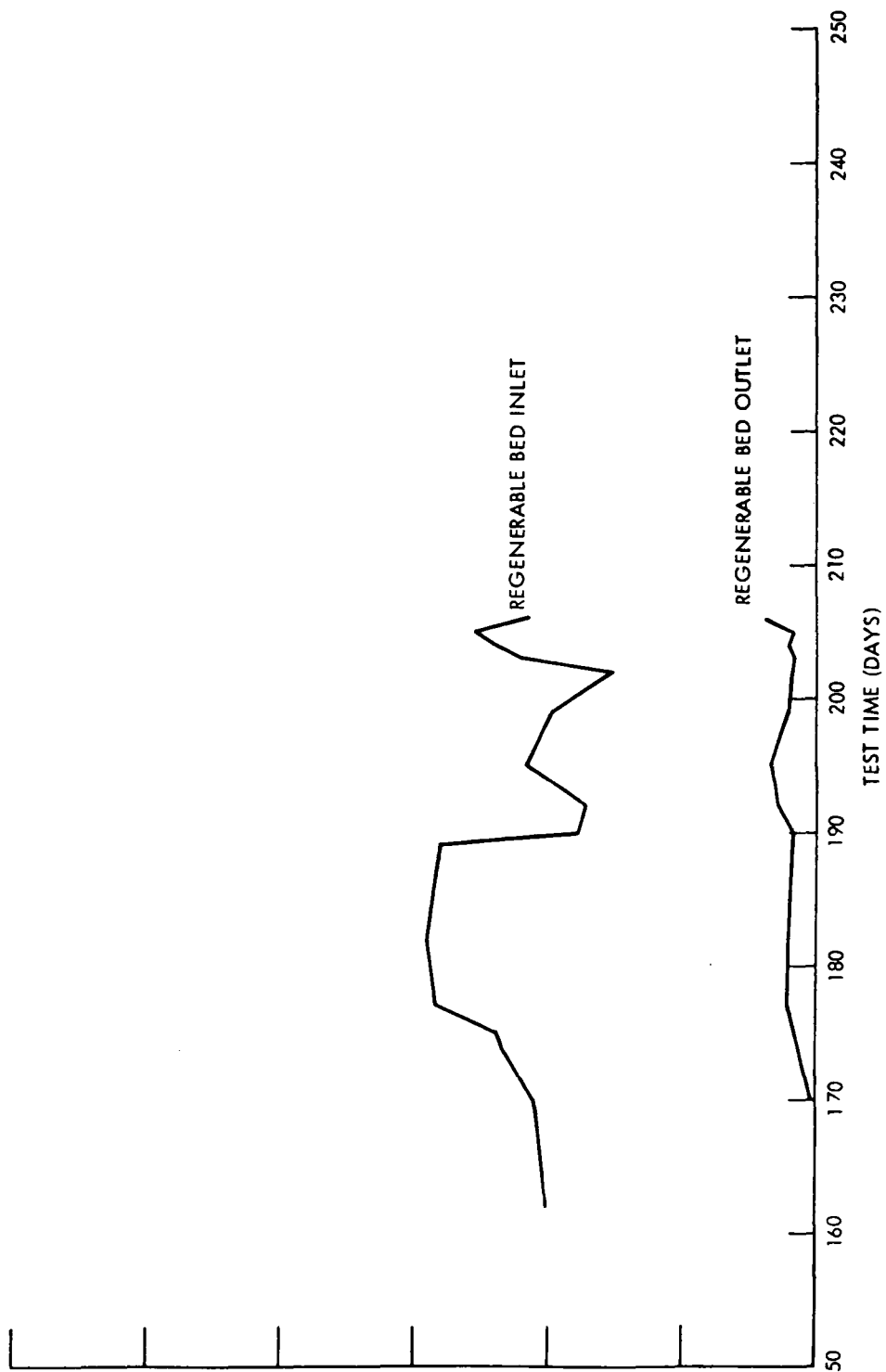


Figure 57 Propylene - Daily Concentration Data

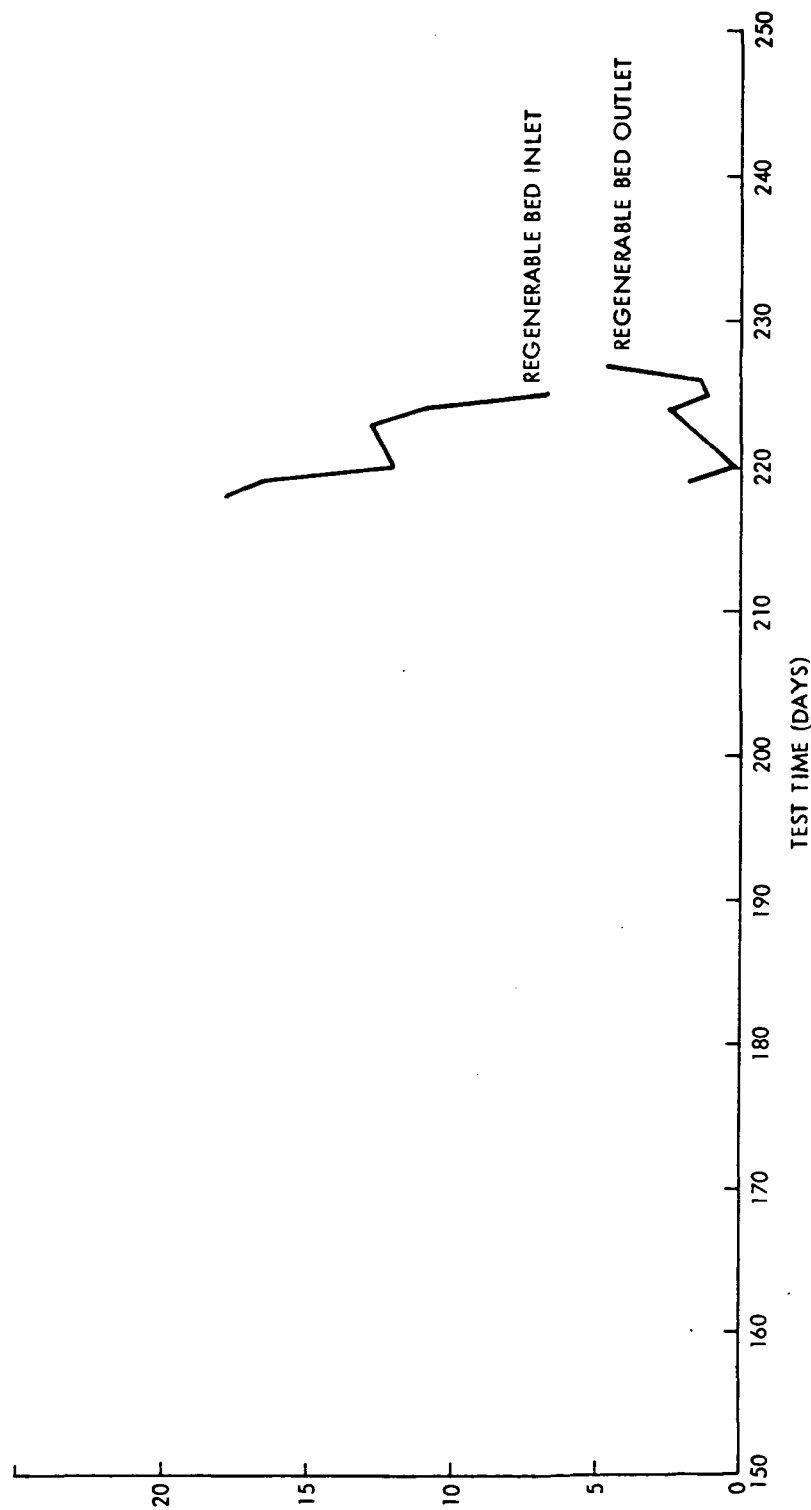


Figure 58 Propane - Daily Concentration Data

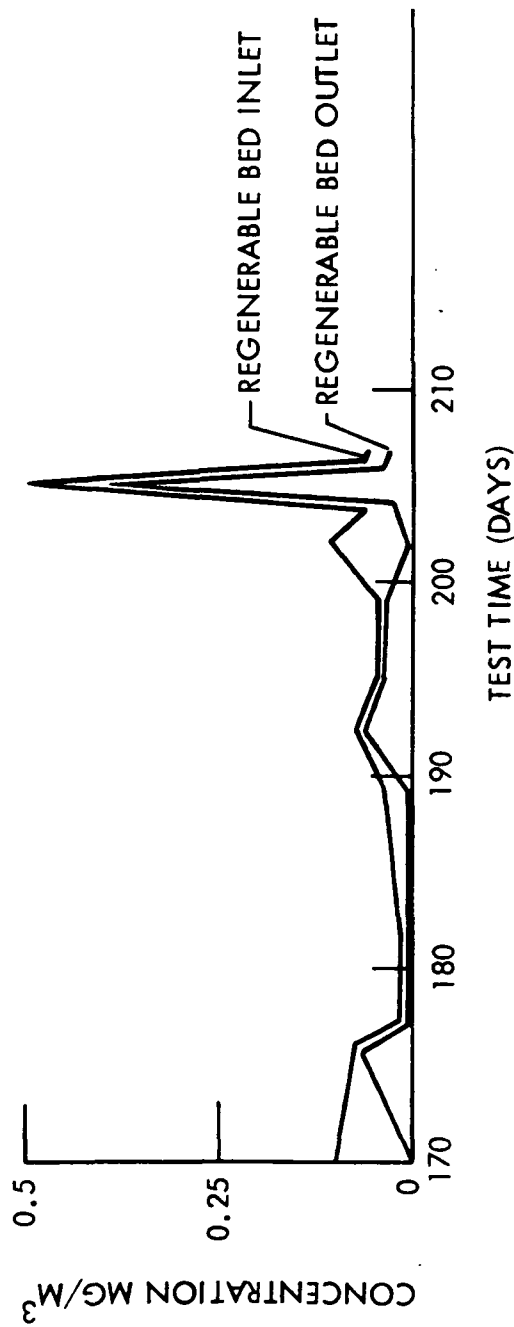


Figure 59 Freon 22 - Daily Concentration Data

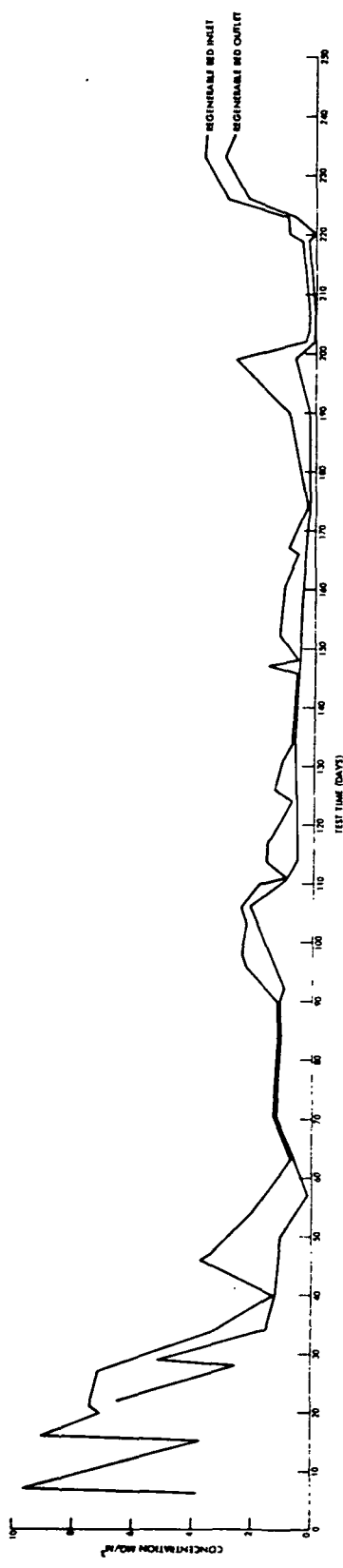


Figure 60 Methyl Alcohol - Daily Concentration Data

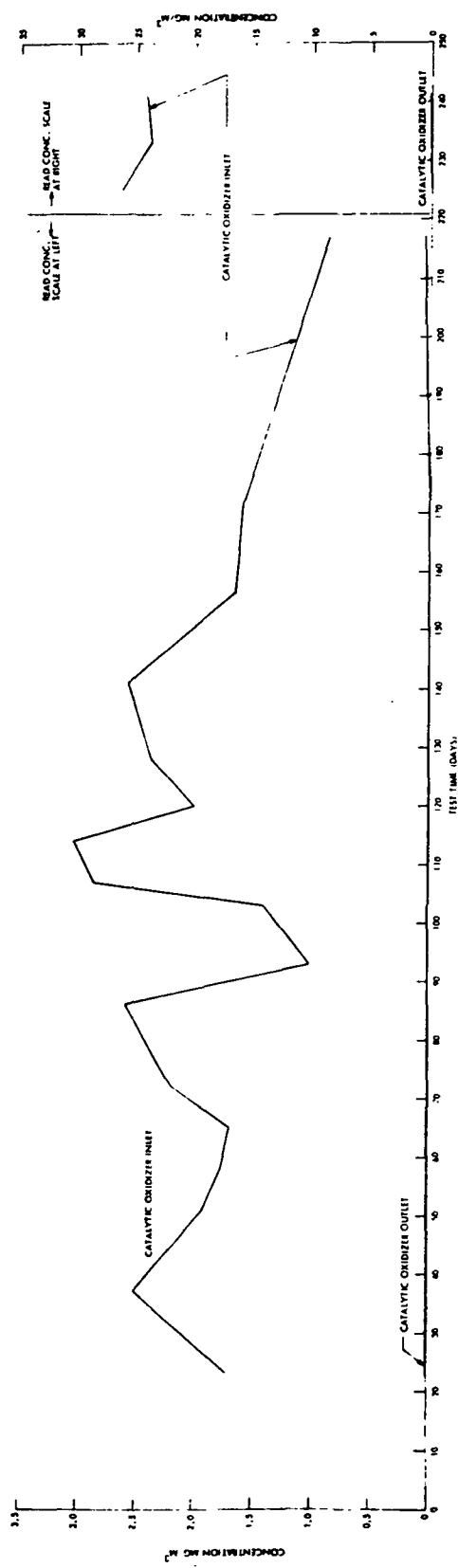


Figure 61 Acetylene - Daily Concentration Data

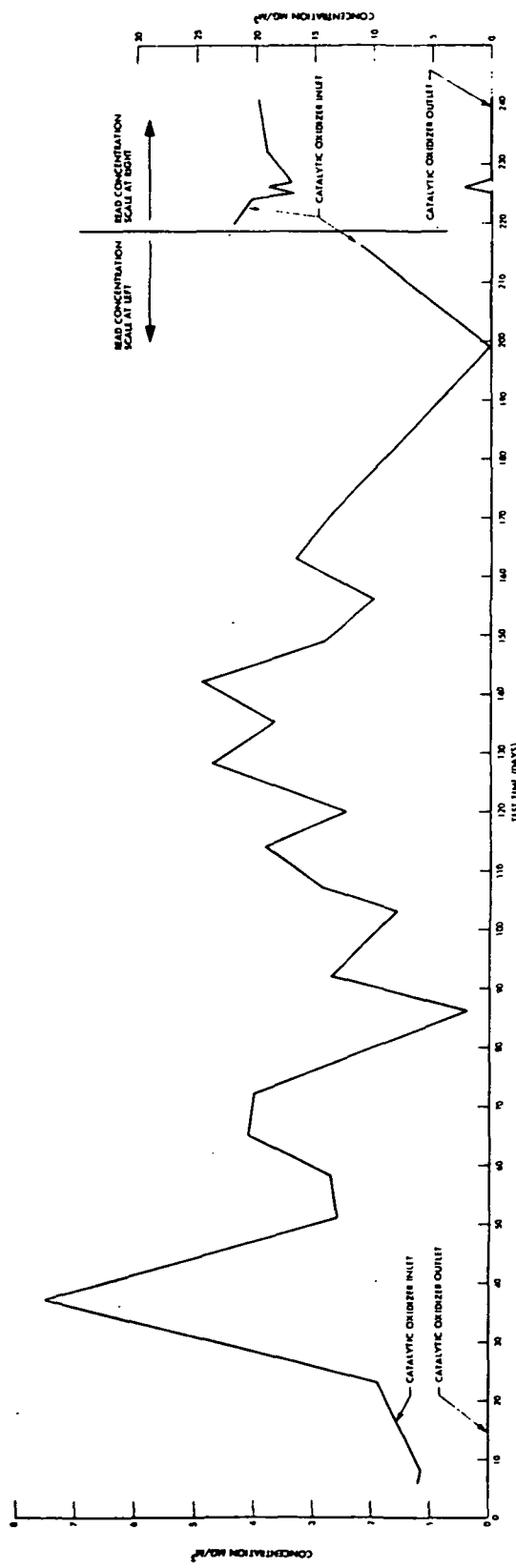


Figure 62 Carbon Monoxide - Daily Concentration Data

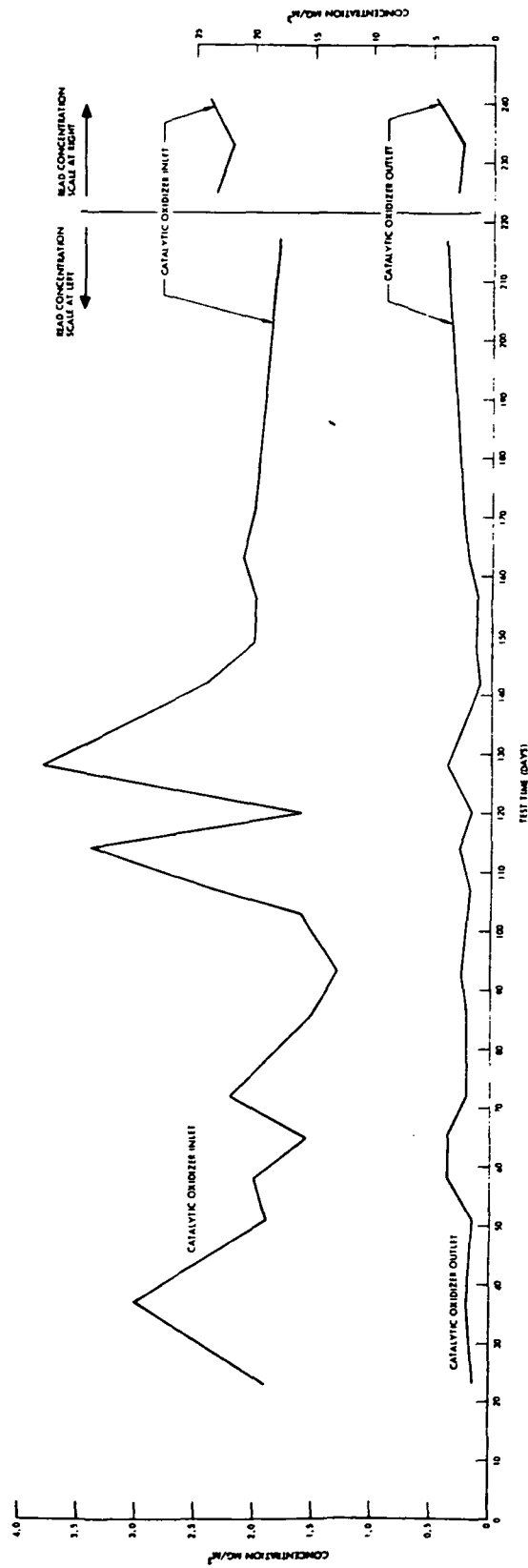


Figure 63 Ethane - Daily Concentration Data

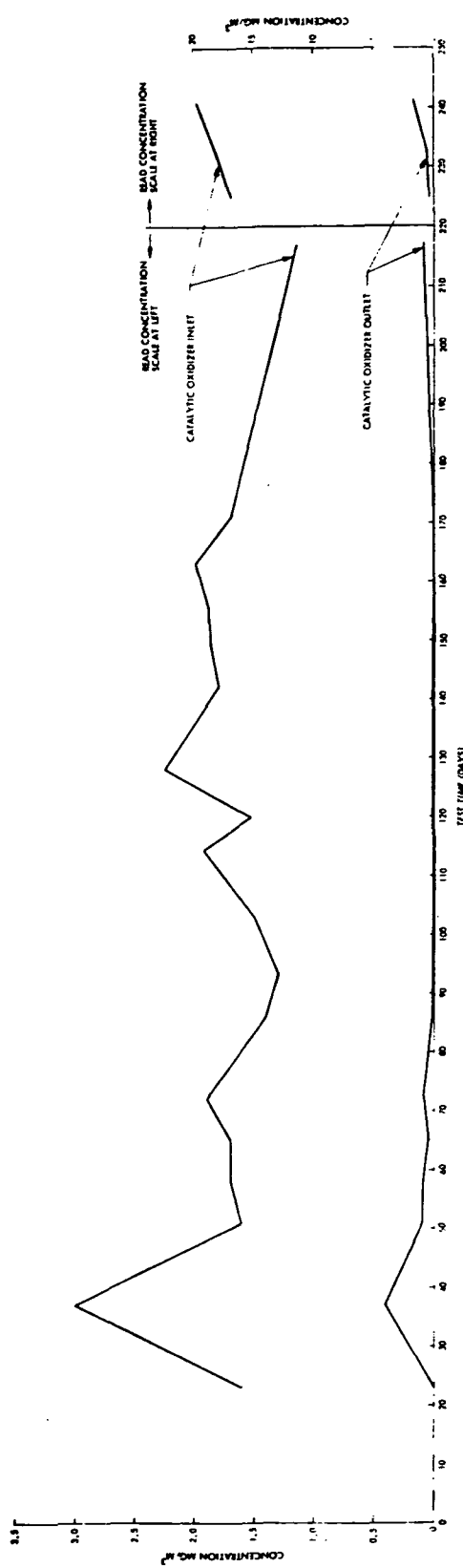


Figure 64 Ethylene - Daily Concentration Data

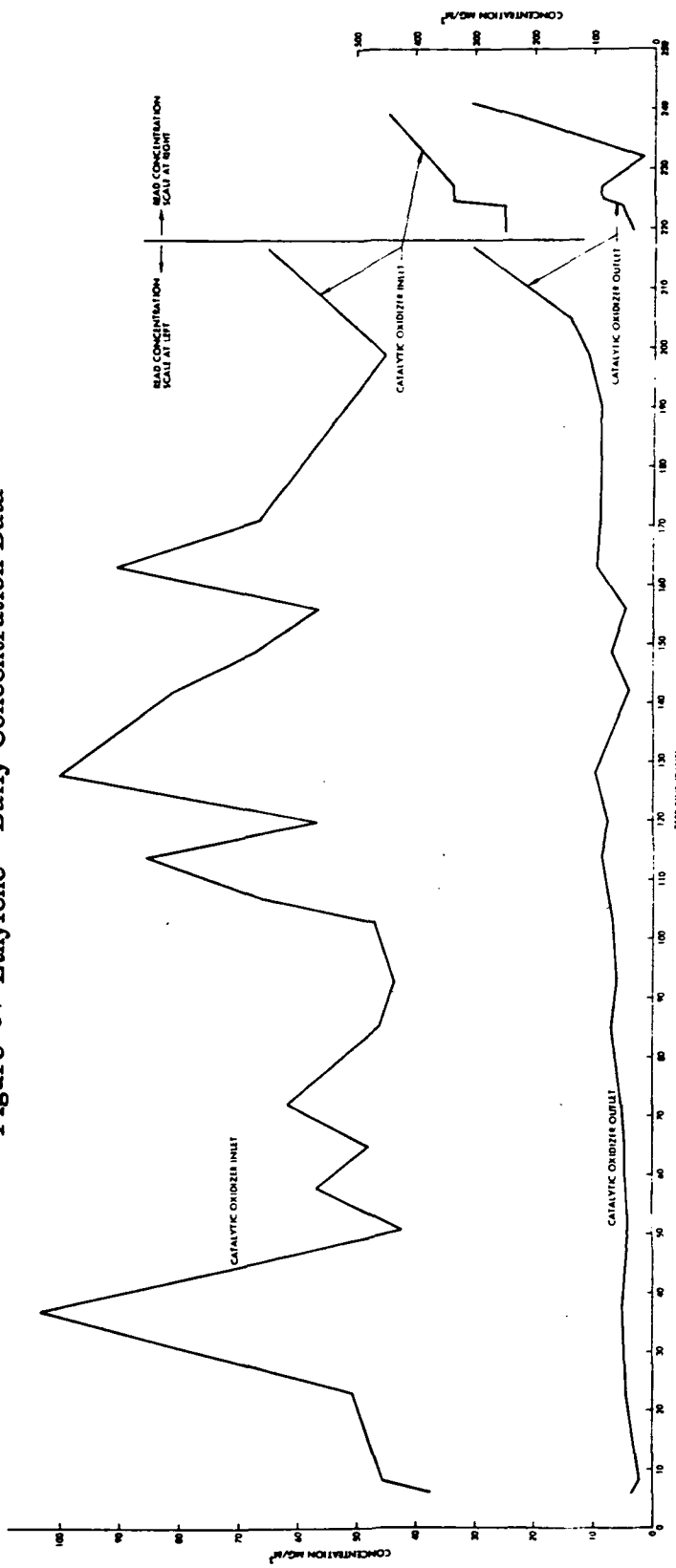


Figure 65 Methane - Daily Concentration Data

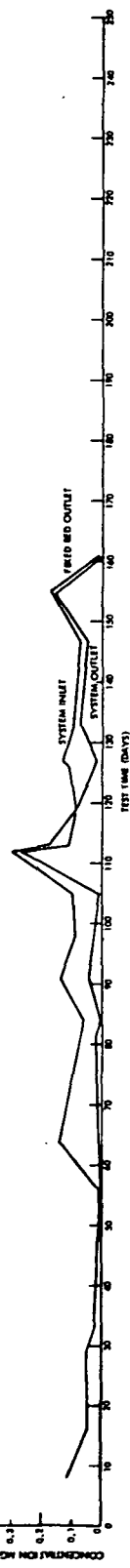


Figure 66 Sulfur Dioxide - Daily Concentration Data

The data for each of the contaminants reflect the change in concentration level across that system component to provide control. In the case of the regenerable bed contaminants, the data for control by the fixed charcoal bed, until breakthrough, are presented until a clear breakthrough is evident. This period varies depending upon the particular contaminant.

Since the flow in the low-flow loop was cyclic due to the charcoal regeneration, the concentration levels varied during the day. Daily fluctuations in the data are attributed to variations in sample time. Data taken over a 24 hour period for methane and carbon dioxide which appears in Figure 67 and 68, demonstrates this variation.

In order to confirm contaminant feed rates, Table 35 was generated to show a comparison of the calculated equilibrium levels of each contaminant with the test levels. The calculated levels are based on the inlet introduction rates, measured removal efficiency, and component flow rates. During the early portion of the test, equilibrium was not achieved at the high introduction rates. The values listed at the high rates were taken at the end of the test period. This table confirms the introduction rates except for a few cases where there are notable deviations. Pyruvic acid, although introduced, was not detected. Toluene was lower and Freon 11 and 12 values were higher than predicted. These deviations were probably caused by problems in introduction. The liquids, pyruvic acid and toluene do not readily vaporize into the circulating gas stream. The Freons were added together and the rate was probably on the high side.

Evidence of the high Freon rate at the low introduction rate phase of the test is the good agreement at the high introduction rates. At the high rate greater accuracy of feed was possible.

In addition to the plots of contaminant data, the cabin relative humidity and temperature plots are shown in Figures 69 and 67. In cyclic operation, the regenerable charcoal bed removes moisture from the system. Toward the end of

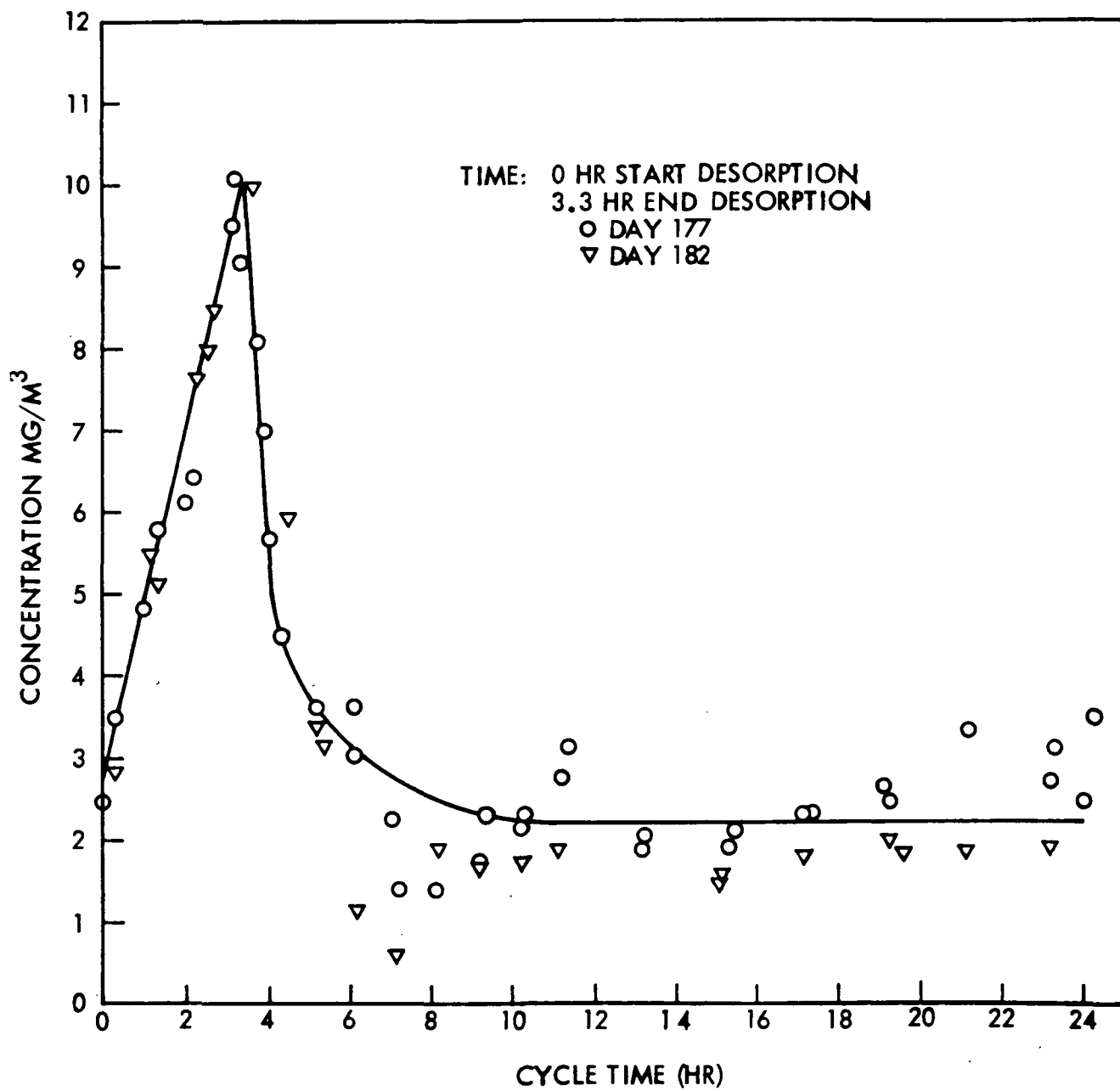


Figure 67 Cabin Methane Concentration ~ Complete Cycle Performance

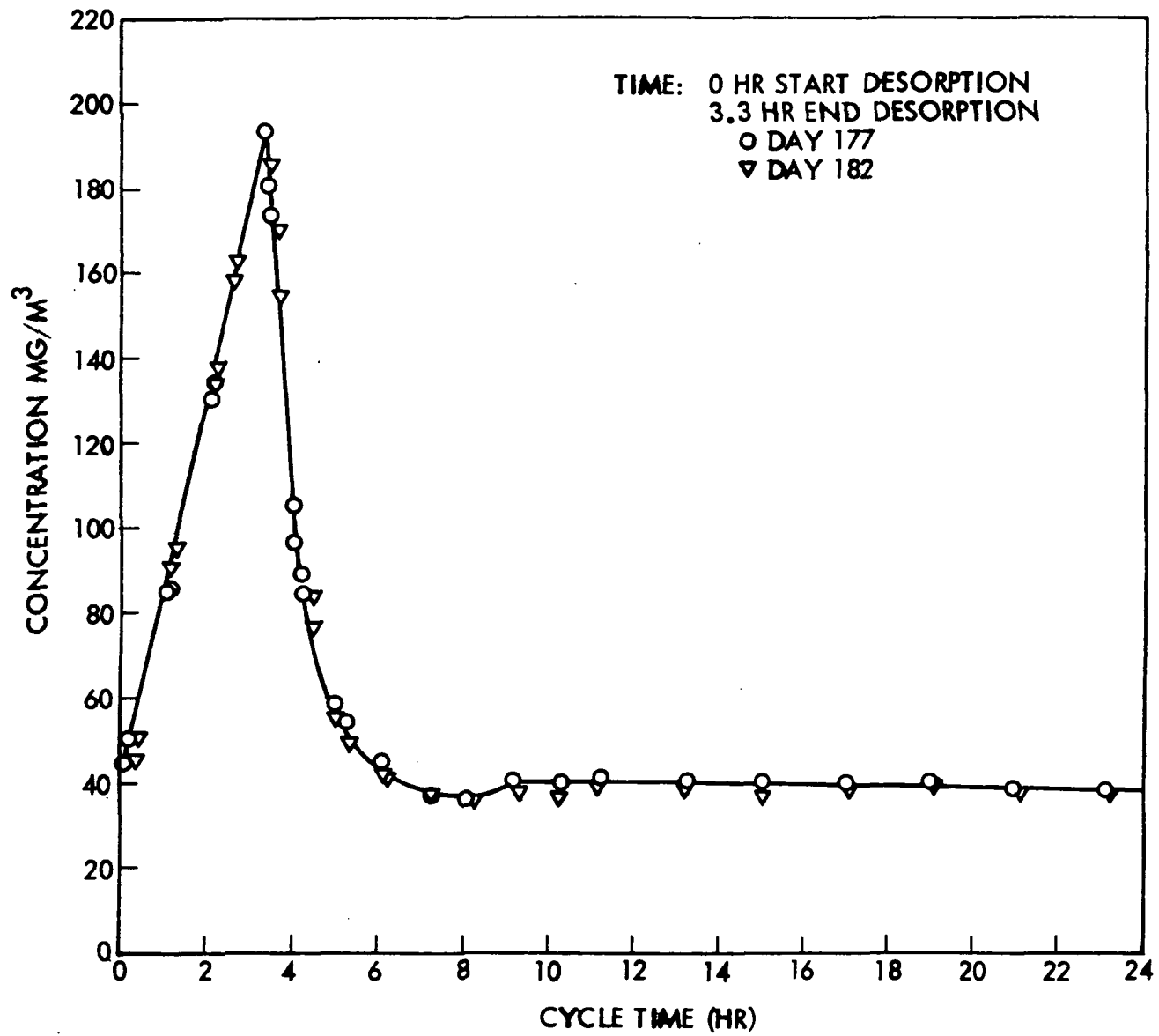


Figure 68 Cabin Carbon Monoxide Concentration ~ Complete Cycle Performance

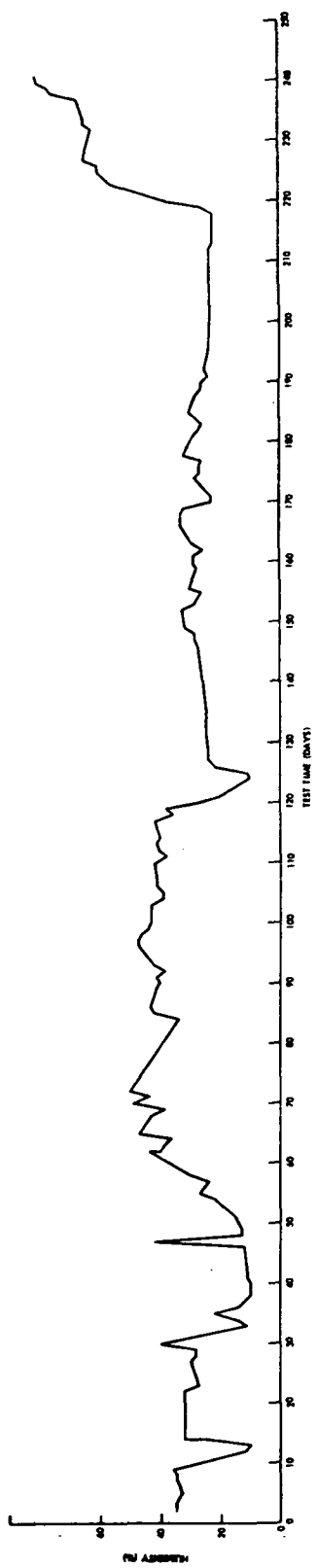


Figure 69 Daily Humidity

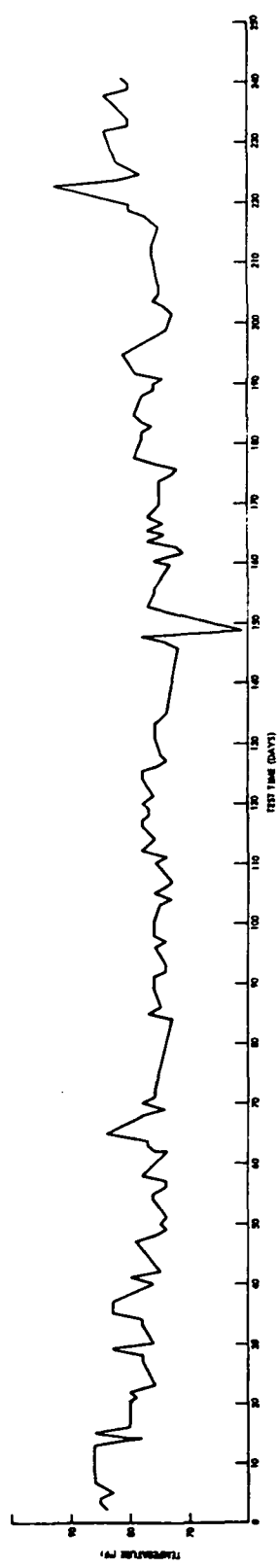


Figure 70 Daily Temperature

Table 35

Comparison of Calculated and Experimental Contaminant Equilibrium Levels

Contaminant	High Introduction Rates			Low Introduction Rate		
	Intro. Rate gm/day	Calculated Concentra- tion mg/m ³	Measured Concentra- tion mg/m ³	Intro Rate gm/day	Calculated Concentra- tion mg/m ³	Measured Concentra- tion mg/m ³
<u>Fixed Bed</u>						
Toluene	2.5	1.75	2.5	.25	.175	.05
Benzene	.9	0.55	2*	.09	.063	.075
Ammonia	4.0	3.46	5	1.75	1.51	2.6
<u>Regenerable Bed</u>						
Methyl ethyl ketone	2.5	15.3(1.75**)53*(1.75**)		.25	.175	.2
Methyl Acetate	2.5	17.8	15	.25	1.77	1.4
Freon 11	2.5	17.8	17	.25	1.77	6
Acetone	2.5	17.8	18	.25	1.77	2
Freon 12	2.5	17.8	16.5	.25	1.97	4
Propylene	-	-	-	.25	1.77	1.3
Propane	2.5	17.8	13	-	-	-
Freon 22	-	-	-	.025	.177	.05
<u>Catalytic Oxidizer</u>						
Methyl Alcohol	2.51	17.8	15	.26	1.91	1.0
Acetylene	2.5	20.3	24	.25	2.03	2.0
Ethylene	2.5	20.3	20	.25	2.03	1.5
Ethane	2.5	22.5	22.5	.25	2.25	2.0
Methane	33.1	313	350	6.55	54.7	60
Carbon monoxide	2.7	19.1	19	.45	3.2	2.0

Basis of calculated values

Fixed Bed - 991 l/min (35 CFM), continuous flow, 90 percent removal

Regenerable Bed - 113 l/min (4.0 CFM), 24 hr cycle/3.3 hr desorption, 90 percent removal

Catalytic oxidizer - 113 l/min (4.0 CFM), 24 hr cycle/3.3 hr shutdown, 100 percent removal

*Not Steady State

**Values in parenthesis taken during initial high introduction rate test phase

the test, day 232, the daily regeneration cycle was ended, causing a sharp rise in relative humidity with the steady water addition.

In the following sections, the control achieved by each system component is discussed. Discussions are organized on a contaminant basis. Lastly, special tests to identify unknown contaminants and the resultant data are presented.

9.2.2.1 Fixed Bed. The purpose of the fixed charcoal bed is the control of contaminants requiring a high gas flow rate for control. These contaminants also have low potential parameters which make them more difficult to desorb. Their removal in the fixed bed allows a lower desorption temperature for the regenerable bed. In addition, ammonia is controlled by the phosphoric acid deposited on the fixed bed charcoal. During the extent test, the fixed bed controlling all contaminants expected and in addition methyl ethyl ketone, thus confirming the expected capacity. Ammonia broke through earlier than expected; however, an initial rate which was higher than desired used some of the capacity. Breakthrough of the regenerable bed contaminants was sooner than expected, probably because of the coarser mesh used than originally planned. The following is a discussion of the performance for each of the contaminants controlled by the fixed bed.

Toluene. The behavior of toluene was similar to that of benzene. The short term rate resulted in higher than expected levels. However, when the contaminant introduction rate was reduced, the level dropped and held steady for the duration. No breakthrough was detected.

Pyruvic Acid. Pyruvic acid was introduced into the system throughout the test. However, none was detected at the inlet to the Trace Contaminant Control System. As a result no levels for pyruvic acid were determined. At the completion of the test the tank was opened and examined. A dark brown liquid was observed on the bottom of the tank. Analysis showed this liquid to be primarily pyruvic acid. Apparently the low vapor pressure of pyruvic acid prevented its evaporation into the circulating gas stream. Thus, none was detected in the gas samples.

Benzene. During the short term introduction phase the level of benzene was higher than expected. However, no breakthrough was detected at the bed outlet. No explanation exists for this high level except possibly a higher than desired contaminant feed rate. After the contaminant feed rate was changed to the long term values, benzene concentration dropped to near the anticipated levels and remained there throughout the test. No breakthrough was observed during this period. Fixed bed breakthrough was observed seven days after the resumption of the short term (higher) rates (day 225).

Ammonia. The initial breakthrough of ammonia served as an indication of channeling of the fixed bed. The bed was examined and poor packing was confirmed. After repacking on day 13 ammonia control was satisfactory. The initial concentration level was higher than anticipated. The experimental flow meter calibration was checked against the flow meter performance based on its predictability equations and was found to be in error. The cause of the error was probably due to ammonia being adsorbed by the liquid being displaced during the experimental calibration. The introduction rate was set at the value indicated by the predictability equations on day 17 and the ammonia level returned to a value nearer the anticipated level.

The concentration stayed at this level with minor fluctuations until day 152 when the first sign of breakthrough was evident. By day 175 breakthrough was nearly complete. On day 185 an analysis of the catalytic oxidizer outlet showed formation of nitric oxide from ammonia. On day 185 the ammonia contaminant feed was shut off.

The early breakthrough of ammonia is due in part to the initial abnormally high introduction rate, which existed before the flow was adjusted in accordance with the predictability equations. The amount of excess ammonia fed cannot be quantified thus, the impact on early breakthrough is not possible to assess. The only conclusion possible is that breakthrough would likely have taken longer to occur, and possibly have required 180 days.

Methyl Ethyl Ketone. Although methyl ethyl ketone was introduced as a regenerable bed contaminant it was controlled by the fixed bed throughout the test. During the period when introduction rates were high, the concentration level was higher than expected. However, when the long term rates were initiated, the level dropped and held steady until the end. Fixed bed breakthrough was observed after 10 days when introduction at the high rate was resumed.

9.2.2.2 Regenerable Bed. The primary objective of the regenerable bed is the control of potential catalyst poisons. The design is based on the removal of halogenated hydrocarbons having a high potential parameter ("A" value). A review of the computer analysis revealed that methyl alcohol was an effective measure of bed performance. Thus, it was selected as the contaminant to provide the maximum stress on the bed. Later, an error in the design program input data for methyl alcohol was discovered. New calculations showed removal of this contaminant should have occurred in the catalytic oxidizer and not the regenerable bed.

During the test, after breakthrough of methyl alcohol was observed, Freon 22 and propylene were added to the contaminant load on day 159 to determine the limits of bed performance.

The propylene data shows control and the Freon 22 data indicates partial control. As the catalytic oxidizer also provides control of regenerable bed contaminants, breakthrough is not evident from inlet concentration levels. Thus, all data observations must be made on the basis of inlet and outlet concentration levels across the bed.

In summary, the regenerable bed controlled all the test contaminants except Freon 22 and methyl alcohol. Analysis of the data, in the next section, shows that this component is undersized by about a factor of two. The following is a brief discussion of each contaminant controlled by the regenerable bed. In some cases control was accomplished by the fixed bed early in the test program.

Methyl Acetate: Breakthrough of the fixed bed for methyl acetate occurred about 7 to 11 days after introduction and partial control was evident until about day 45. Complete removal was provided by the regenerable bed. The inlet concentration rose sharply just before termination of the high introduction rates due to the fixed bed breakthrough, then dropped to a steady level of about 1.4 mg/m^3 as the regenerable bed controlled. The regenerable bed continued to provide complete control during the final period at high introduction rates.

Freon 11: Breakthrough of Freon 11 through the fixed bed occurred 2 days following introduction. The regenerable bed outlet analysis showed slight fluctuations at a very low level indicating in excess of 90 percent removal. The increase in bed outlet level on day 190 is attributed to a change in sample time from about 02:00 hrs to 20:00 hours cycle time. During the high introduction rate period, the Freon 11 level remained below the level predicted from regenerable bed performance calculations, due to partial control by the fixed bed. After day 28, the level dropped due to the lowered contaminant introduction rates. The final concentration level at the long-term rate was about 6 mg/m^3 which is higher than expected. However, no explanation exists as introduction rate and analytical standards were both checked.

During the final short term high rate period the regenerable bed removal efficiency remained at about 90%. In addition the concentration was near the expected value. This indicates that the chemical analysis was correct and that the introduction rate was probably to be in error at the low introduction rates. This is likely as the low flows are hard to set and the high flows are easily readable on the flowmeters.

Acetone: The data shows complete control of acetone by the fixed bed until day 15 at which time initial breakthrough occurred. However, significant control remained until about day 45. No acetone was detected at the outlet of the regenerable bed throughout the test. The inlet data shows an early concentration plateau at the high introduction rates while the fixed bed controls, and the concentration then increases as partial breakthrough occurs. The level

then dropped to a steady value of about 2 mg/m^3 for the duration of the low rate phase. This level indicates partial control by the fixed bed, as it is below the equilibrium level expected for regenerable bed control. During the final high rate phase the concentration levels were as expected.

Freon 12: Freon 12 broke through the fixed bed almost immediately and partial control existed only until about day 15. Throughout the test, the regenerable bed outlet was less than 0.015 mg/m^3 which indicates a removal efficiency of greater than 90 percent. The system inlet shows a buildup to anticipated levels during the high introduction period and a drop in level to about 4 mg/m^3 at the end of the test. This level is higher than expected but the removal is satisfactory. The regenerable bed removal efficiency for Freon 12 then remained at approximately 90%.

Propylene: Propylene was added along with Freon 22 on day 159 to provide additional data on the performance of the regenerable bed and detect its limits of performance. The inlet concentration rapidly rose to a steady level and then held. The regenerable bed outlet data shows a removal efficiency in excess of 90 percent throughout the cycle. Propylene is not part of the short term rate model and hence introduction was terminated on test day 218.

Freon 22: Freon 22 was added to the contaminant load on day 159 to provide more data on the regenerable bed performance after the methyl alcohol breakthrough confirmation. The test data shows that control is provided early in the adsorption cycle and that breakthrough occurs toward the end of the cycle. Freon 22 is not part of the short term rate contaminant model and hence introduction was terminated on test day 218.

Propane: Propane was added to the contaminant list on day 218 of the test. This material provides the design stress for the regenerable bed during the high introduction rate phase. A stable equilibrium level for propane was not achieved with this contaminant. However, the limited data shows control but indications are that its control is at the limit of the regenerable bed performance.

Methyl Alcohol: Methyl alcohol broke through the fixed bed immediately. Measurements on the regenerable bed indicate partial control early in the cycle with nearly complete breakthrough toward the end of the cycle. Most data was taken early in the cycle thus indicating better than actual average performance. The system inlet level is steady as methyl alcohol is oxidized in the catalytic oxidizer. During the final period at high introduction rates, the regenerable bed was providing 30% removal of methyl alcohol.

9.2.2.3 Catalytic Oxidizer - The catalytic oxidizer provides control of hydrogen, carbon monoxide, and all hydrocarbon material not removed by the charcoal beds. During the test with the isotope heat source, the contaminant introductions were maintained at their low introduction rates throughout the test to prevent a possible overheating of the unit. Since the catalyst bed temperature was slightly higher than the design value, the removal efficiencies were good. The sensitivity to sample time is evident in the daily fluctuations observed. The steady concentration levels were near those predicted, indicating accurate feed rates. In addition to the data on the oxidizer contaminants, limited data was also taken which demonstrates the destruction of Freons and the oxidation of ammonia to nitrogen oxide.

Even though some Freons and sulfur dioxide entered the oxidizer, there was no evidence of catalyst poisoning at the low inlet levels. The following is a brief discussion of each of the catalytic oxidizer contaminants.

Acetylene: Acetylene removal efficiency remained at 100 percent throughout the test.

Carbon Monoxide: Carbon monoxide removal efficiency remained at 100 percent through the test.

Ethane: Ethane removal efficiency remained at about 90 percent through the test.

Ethylene: Ethylene removal efficiency remained at 100 percent throughout the test.

Methane: The performance of the catalytic oxidizer is best characterized by methane. A gradual increase is noted in both the system inlet and catalytic oxidizer outlet concentrations during the test period. Initially the removal efficiency was about 90 percent. After 180 days of operation, the performance had dropped to about 85 percent. This decrease, although slight seems definite even when data scatter due to sample time is considered. See Section 10.1 for a further discussion of methane removal.

In addition to these basic contaminant tests, several other tests were performed on the catalytic oxidizer. These are discussed below.

Ammonia Oxidation: No evidence of oxides of nitrogen were observed until day 184. This occurred shortly after ammonia breakthrough from the fixed bed. On day 185, the ammonia feed was shutoff following confirmation of nitrogen oxide. The data on NO and NO_x is presented in Table 37. The results show a decrease in ammonia concentration from about 4 to 0.3 mg/m^3 . They simultaneously showed an increase in nitric oxide from 1 to 9 giving a positive indication ppm of the oxidation of ammonia. As the concentration performance seems to exhibit a step increase about day 154, which corresponds to ammonia breakthrough, this step could be a result of ammonia influence on oxidizer performance.

It is noted that in the previous contact, reported in NASA CR 2027, nitrous oxide was the product of ammonia oxidation. In this test nitric oxide was formed. This is likely a result of the higher oxidation temperature in this test.

Freon Degradation: Measurements of changes in the concentration level of Freon 11 and 12 across the catalytic oxidizer show the destruction of Freon at slightly less than 100 percent efficiency. This confirms destruction of low inlet concentrations of Freon without poisoning.

Daily Cycles: Two 24 hour tests were performed to track the system inlet concentration of methane and carbon monoxide with time. Plots of this data were presented in Figure 67 and 68. The data shows a sharp increase in concentration

as flow is stopped and desorption of the regenerable bed started at 05:00. The peak occurs at 08:00 where desorption ends and the flow restarts. Decay in contaminant level is rapid, with equilibrium being reached shortly after 10:00. The magnitude of the peak results from the small system volume and would be lower in a real situation with a large cabin volume. Unfortunately much of the sampling of contaminants removed in this loop was done during this decay time period.

9.2.2.4 Pre- and Post-Sorbent Beds - The purpose of the pre- and post-sorbent beds is the control of acid gases. The pre-sorbent prevents them from entering the catalytic oxidizer as they may poison the catalyst. The post-sorbent bed removes any acid gases which may be found in the catalyst oxidizer due to small quantities of halogenated hydrocarbons or mercaptans entering it.

Hydrogen Fluoride and Hydrogen Chloride: The data on hydrogen fluoride and hydrogen chloride all indicated very low concentration levels. These low levels required the processing of a large quantity of gas to collect an adequate sample to allow measurement. The collection of sample from large quantities of gas and the low levels result in considerable data scatter which is evident from the results presented in Table 36. Although the data scatter is large, three things are evident.

- o Freons are decomposing to HCl and HF in the catalytic oxidizer as this is the only source of those materials.
- o The lack of a build-up indicates control by the Trace Contaminant Control System.
- o The data shows generally moderate removal of HF and poor control of HCl across the post-sorbent bed.

Sulfur Dioxide: Data on sulfur dioxide shows a definite concentration drop across the system. However, the system outlet and catalyst oxidizer inlet values are similar. This indicates that this contaminant is being controlled elsewhere, possibly by the moisture in the fixed bed. The concentration level is consistent with fixed bed control.

Further work on pre- and post-sorbent beds is reported in Section 10.1

Table 36
Post-Sorbent Bed Performance Data for Hydrogen Chloride and Hydrogen Fluoride

Test Day	Hydrogen Chloride		Hydrogen Fluoride	
	In Concentration mg/m ³	Out Concentration mg/m ³	In Concentration mg/m ³	Out Concentration mg/m ³
37	.02	.02	.1	.1
51	.02		.3	
58		.11		.014
65	.02	.02	.005	.005
71			.001	.001
86		.20	.018	.011
92	.27	.26	.005	.005
99	.17	.12	.021	.015
106	.10	.06	.009	.004
114	.09	.09	.011	.001
120	.14	.14	.008	.005
128	.02	.02	.001	.000
134	.02	.02	.005	.005
142	.30	.21	.017	.023
149	.36	.25	.0001	.027
162	.12	.16	.035	.018
171	.14	.05	.010	.005

Note: Freon 22 added to contaminant list on day 159

9.2.2.5 Contaminants Not Introduced - Besides the standard monitoring of contaminants which were introduced into the test system, periodic analysis were made for other contaminants. These could result from contamination of contaminant feed streams or from conversion within the system components such as in the catalytic oxidizer. A variety of analytical techniques were used in these tests, including mass spectrometric, infrared spectrophotometric, gas chromatographic, and specific ion electrode methods. These special techniques and the results of the analysis are presented below. The discussions are organized by instrument analyses techniques used.

Contaminant Identification by Infrared Spectrophotometry: To further understand the test, samples were collected at different sampling locations and analyzed with a Perkin-Elmer Model 521 dual beam infrared spectrophotometer equipped with a ten-meter folded path infrared cell. Scans were made from 4000-250 cm^{-1} and observed for any changes or differences in absorption bands to identify contaminants present other than those routinely analyzed. Tables 37 summarizes the results obtained.

Contaminant Identification by Mass Spectrometry: Approximately twenty liters of the atmospheric gas were passed through 12 x 28 BD charcoal packed into an 8 cm x 0.64 cm. OD stainless steel tube at the rate of 200 cc/min. The charcoal was packed to a depth of 6 cm and then the tube ends were plugged with glass wool. The charcoal and glass wool were prepared for use by degassing at $1.3 \times 10^{-4} \text{ N/m}^2$ (1×10^{-6} torr) pressure at approximately 493 K (220 C) for eight hours and thereafter, mass spectrometry analysis was carried out to determine if any residual offgassing products remained.

The charcoal with the "sorbed" contaminants was transferred from the stainless steel tube into a solid sampling glass bulb. This bulb was attached to the mass spectrometer sampling inlet system (Hitachi/Perkin Elmer RMU-6D) and the "sorbed" contaminants were introduced into the instrument by increasing the temperature in the sub-oven surrounding the bulb holding the charcoal. Intermittent scans were made at increasing temperatures, of the contaminants outgassed from the charcoal, at approximately 1.3×10^{-3} to $1.3 \times 10^{-4} \text{ N/m}^2$ (1×10^{-5} to 1×10^{-6} torr) pressures.

Table 37

Identification by Infrared Spectrophotometric, Mass Spectrometric and Other Analyses Methods of Contaminants Species Other Than Those Routinely Analyzed

Day	Location	Method	Results (mg/m ³)
2	System Inlet	IR (Infrared)	N.D.
2	System Outlet	"	N.D.
6	Fixed Bed Outlet	"	N.D.
7	Fixed Bed Outlet	"	N.D.
7	System Inlet	"	N.D.
8	Regenerative Bed Outlet	"	N.D.
16	System Inlet	"	N.D.
54	Regenerative Bed Inlet	"	N.D.
54	Fixed Bed Outlet	"	N.D.
57	Cat. Oxidizer Inlet	"	N.D.
57	Cat. Oxidizer Outlet	"	N.D.
64	Cat. Oxidizer Outlet	MS (Mass Spec)	N.D.
110	Cat. Oxidizer Inlet	IR	N.D.
175	Post Sorbent Outlet	MS (Conc. by Charcoal)	See Table 38
176	Post Sorbent Outlet	MS	See Table 38
176	Post Sorbent Outlet	IR	N.D.
176	Post Sorbent Outlet	Colorimetric	<.01 Formaldehyde
182	Catalytic Oxidizer Inlet	MS (Conc. by Charcoal)	See Table 38
183	System Outlet	MS	See Table 38
184	System Inlet	MS (Conc. by Charcoal)	See Table 38
184	Post Sorbent Outlet	Chemiluminescence	NO: 12 *NO _x : 20
184	System Outlet	Chemiluminescence	NO: 7 NO _x : 20
185	Catalytic Oxidizer Inlet	Chemiluminescence	NO: 1 NO _x : 16
	Catalytic Oxidizer Outlet		NO: 9 NO _x : 16
191	Post Sorbent Outlet	MS (Conc Chromosorb 101)	See Table 38

Table 37 (continued)

Day	Location	Method	Results (mg/m ³)
191	Catalytic Oxidizer Inlet	MS (Conc by Chromosorb 101)	See Table 38
191	System Outlet	MS (Conc by Chromosorb 105)	See Table 38
195	Post Sorbent Outlet	MS (Conc by Chromosorb 105)	See Table 38
195	System Inlet	" " "	See Table 38
195	Catalytic Oxidizer Inlet	" " ""	See Table 38
240	Catalytic Oxidizer Outlet	IR	N.D.
240	Catalytic Oxidizer Inlet	IR	N.D.
240	System Inlet	IR	N.D.

*Response reported from instrument calibrated against known concentration of nitric oxide in nitrogen gas.

Additionally, samples were absorbed on Chromosorb 101 and 105 at ambient conditions. The technique used was similar to the procedure discussed by Mieure and Dietrich (Ref. 6). Samples were obtained similar to the charcoal method, except Chromosorb 101 and 105 was used in place of charcoal. The sample collected on the Chromosorb 101 and 105 columns were connected ahead and in series of the gas chromatographic (GC) column in the injection port of a F/M 810 gas chromatograph. The contaminants in the sample were separated on the GC column and identified by mass spectrometry whereby the GC column exit was coupled in tandem with the mass spectrometer inlet system glass frit concentrating device.

The compounds identified besides the ones known to be introduced into the system are listed in Table 38. No concentration levels can be established for these contaminants, but they are present at levels less than their anticipated parent contaminant or that of the contaminants introduced for those cases in which the new contaminants may exist as impurities that were introduced into the system along with the major contaminants.

Besides the analysis techniques discussed, mass spectrometric analyses on batch samples were made on the catalytic oxidizer outlet stream on day 64. Samples were obtained in evacuated 125 cc volume Pyrex bottles and were analyzed by scanning from 1-300 m/e units.

Contaminants Unidentified on Gas Chromatograms Obtained from Routine Analysis of Major Trace Contaminants Introduced in the System: . Besides the major trace contaminants that appeared on the gas chromatograms, some unidentified peaks occurred. These peaks were not analyzed but some predictions were made as to identity and quantity present by comparing them with the existing analysis of the contaminants routinely analyzed. The results of these analysis are presented in Table 39. Although these contaminants were present during the long term rate test phase so that maximum response could be obtained.

Table 38

Identification by Mass Spectrometry of Contaminants
Other Then Those Known to be Introduced into the System

Post-Sorbent Bed Outlet

C_2 - Trichloro-trifluoro compound(s)

Unknown compounds II and III

Nitrous Oxide

Nitric Oxide (Tentative)

Nitrogen Dioxide (Tentative)

Catalytic Oxidizer Inlet

C_2 - Trichloro-trifluoro compound(s)

Unknown compound I (mol. wt. 108)

C_2 - Dichloro compound (unsaturated)

Dichloromethane

Nitrous Oxide

Acetic Acid (Tentative)

System Outlet

C_2 - Trichloro-trifluoro compound(s)

Unknown compound I (mol. wt. 108)

Nitrous Oxide

Acetic Acid (Tentative)

System Inlet

Methyl Chloride

Chlorodifluoromethane

1,1,1 Trichloroethane

Nitrous Oxide

Table 39

Contaminants Unidentified on Gas Chromatograms Obtained from
Routine Analysis of Major Trace Contaminants Introduced Into the System

Day	Location	Instrument	Predicted Contaminant	Estimated Quantity (mg/m ³)*
240	System Inlet	HP 7620/FID Poropak Q	C_2	5
"		"	$> C_2$ (400°C B.P.)	50
"		"	C_2-C_5 (<100°C B.P.)	10
"		FM 810/EC SE 30	C_1-C_2 (~30°C B.P.)	5
"		" "	C_1-C_3 (25-50°C B.P.)	3
"		System Out	C_1-C_2 (~30°C B.P.)	2
"		" "	C_1-C_3 (25-50°C B.P.)	1

*Analysis conducted at short-term (high) introduction rates.
Estimated concentration at long-term rates is about a factor of ten lower.

Colorimetric Analysis Method for Formaldehyde: On day 176 the post-sorbent bed outlet was analyzed for the presence of formaldehyde by colorimetric methods using the standard chromotropic acid techniques. (Ref. 7) The results showed less than 0.01 mg/m³ formaldehyde concentration.

Chemiluminescence Analysis of Oxides of Nitrogen Contaminants: A Thermoelectron Model 12A chemiluminescence NO/NO_x analyzer was used for monitoring the oxides of nitrogen. Primarily the catalytic oxidizer outlet and inlet were monitored to determine buildup of these contaminant species in relation to ammonia breakthrough of the fixed bed. Although there is some partial response to ammonia in the NO_x mode of analysis, no ammonia interference occurs in the NO mode. The instrument measures directly for nitric oxide.

9.2.3 Analysis of Results

The results presented in Section 9.2.2 were carefully reviewed to determine the effectiveness of the design techniques and modifications to these techniques, if any, which are required. In this section discussions of the following subjects are presented:

- o The charcoal bed analysis procedure
- o The performance of the fixed charcoal bed
- o The performance of the regenerable charcoal bed
- o The performance of the catalytic oxidizer
- o The performance of other system components

In these sections modifications to the charcoal computer design program are presented along with changes in the potential plot data.

9.2.3.1 Charcoal Bed Analysis. In the design of the activated charcoal bed two distinct zones along the length of the bed are considered. These zones are the saturated zone, and the adsorption zone. For purposes of calculation, all of the contaminant load is considered to be adsorbed in the saturated zone. The only purpose assumed for the adsorption zone is to provide for a quantity

of charcoal in which mass transfer takes place. In this zone, the contaminant in the circulating gas stream drops from the inlet concentration level to the outlet concentration level. No contaminants are considered to be adsorbed in this zone. In fact, depending upon the actual operating conditions, the contaminants adsorbed in this zone may be as much as one third the saturated capacity. Thus, the assumption of all contaminants being adsorbed within the saturated zone is conservative.

Once the total bed design is specified, as will be the case in the proposed program, its performance can be calculated for each contaminant. The adsorption zone size is calculated for the selected contaminant. The saturated zone size for that contaminant is then calculated from the difference between the total bed size and the adsorption zone size. The time to breakthrough is then derived from rate of charcoal utilization and the saturated zone size. The details of calculation are presented in the following section. Figures 71 and 72 present typical potential plot data and adsorption zone data.

- o The capacity of charcoal for any given contaminant (q) is a function of the potential parameter for that contaminant. The potential parameter (A) is defined as

$$A = \frac{T}{V_M} \log \frac{P^0}{P_i}$$

where A = potential parameter

T = bed temperature ($^{\circ}$ K)

V_M = molecular volume (cc/gm)

P^0 = vapor pressure at T of contaminant expressed in concentration terms (mg/m^3)

P_i = inlet gas concentration (mg/m^3)

- o The capacity (q) is the cubic centimeters of liquid of a contaminant which can be adsorbed on a gram of charcoal
- o Multiple contaminants can coexist on charcoal. The degree of coexistence is defined by a critical ΔA value which is 16.

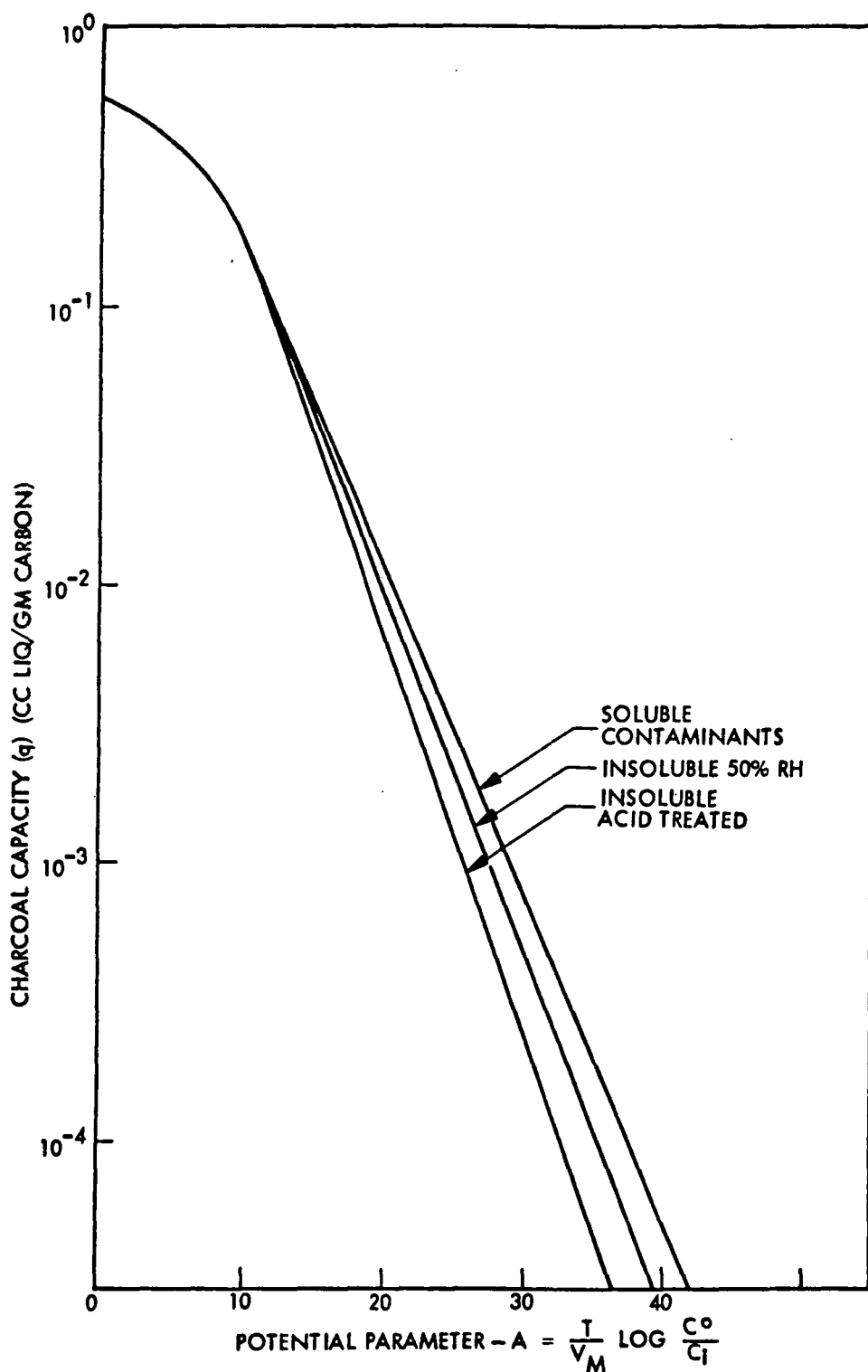


Figure 71 Potential Plot Data - Barnebey Cheney BD Charcoal

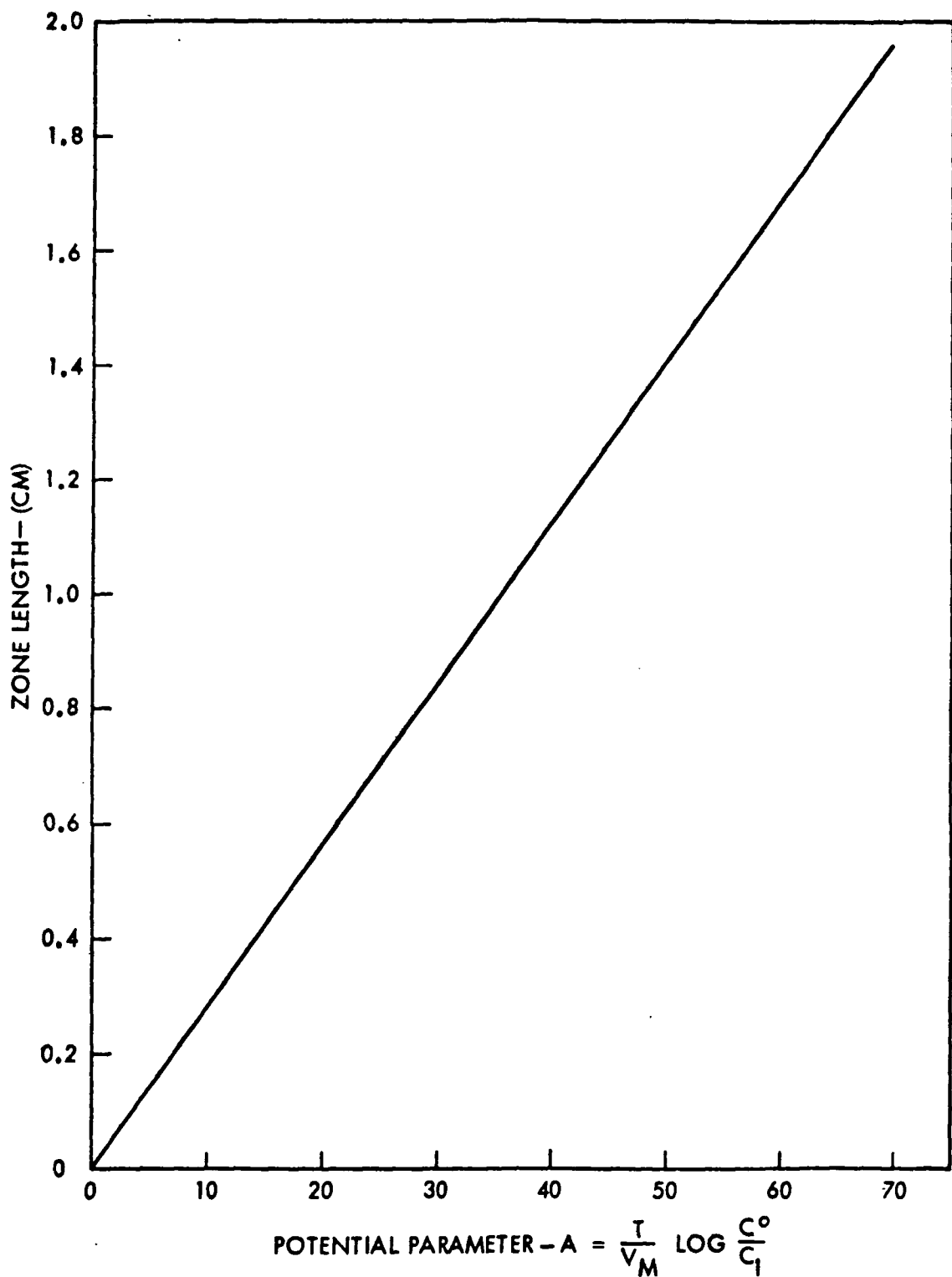


Figure 72 Adsorption Zone Length - Barnebey Cheney BD Carbon
at 39.6 cm/min (1.3 ft/min).

The sequence of calculations in determining the saturated zone size is as follows:

- 1) Calculate all values of inlet concentration

$$P_i = \frac{(24.5) (m_i)}{(Q) (\eta)}$$

where m_i = contaminant generation rate in gm/day

Q = control flow rate in CFM

η = bed removal efficiency

.8 for regenerable bed

.9 for fixed bed

P_i = inlet concentration (mg/m³)

- 2) Calculate potential parameter (A) for each contaminant

$$A = \frac{T}{V_M} \log \frac{P^0}{P_i}$$

- 3) Obtain the carbon capacity (q) for each contaminant from the potential plot. Figure 1A

- 4) Order all contaminants by A for lowest to highest value.

- 5) Calculate the quantity of each contaminant to be removed.

$$\text{MASS} = (\tau) (m_i)$$

where: MASS = quantity to be removed

τ = period of control

m_i = generation rate of that contaminant

- 6) Identify that contaminant with a MASS greater than zero which has the lowest A value and set that A value equal to Amin.

- 7) Calculate a corrected carbon capacity for each contaminant.

$$q_{\text{corr}} = q \left(1 - \frac{A - A_{\text{min}}}{16}\right)$$

Note: If $A - A_{\text{min}} > 16$ q_{corr} will be negative indicating that no co-existance exists with that contaminant and the one having the lowest A value and hence set $q_{\text{corr}} = 0$.

- 8) Calculate the quantity of charcoal required to totally control each contaminant.

$$\text{WCHAR} = \frac{\text{MASS}}{q_{\text{corr}}}$$

- 9) Determine the minimum WCHAR and note the corresponding contaminant.
- 10) Calculate the total bed size

$$WTOT = \sum WCHAR_{min}$$

Note: WTOT represents the size of bed required to control that contaminant.

- 11) Calculate the quantity of each of the other contaminants removed in the charcoal quantity WCHAR

$$MR = (q \text{ corr}) (WCHAR) \text{ min}$$

- 12) Correct the mass to be removed for each contaminant.

$$MASS = MASS - MR$$

- 13) Return to Step 6 and repeat until all MASS = 0

This procedure will result in a listing of all the contaminants in the order in which they are controlled in the saturated zone. The corresponding WTOT is the quantity of charcoal required to control that contaminant for the removal period.

The mass of the adsorption zone for any contaminant is derived from the adsorption zone length data taken at 39.6 cm/min (1.3 ft/min) as follows:

let S = Face Area of Bed (cm^2)

ρ = Charcoal Density (gm/cm^3)

Q = Gas-flow (cm^3/min)

The velocity through the bed can now be calculated as:

$$V = \frac{Q}{S}$$

Data on the adsorption zone length L was taken as a function of the potential parameter (A) at a superficial bed velocity of 39.62 cm/min (1.3 ft/min). Further we know from the previous studies, that the zone length varies directly with velocity.

Thus, the length of the adsorption zone is:

$$L_{AD} = \frac{VL}{39.62}$$

Substituting we get

$$L_{AD} = \frac{QL}{39.62 S}$$

The mass of the adsorption zone:

$$WCHAR_{AD} = (L_{AD})(S) = (L) \left(\frac{Q}{S} \right) \left(\frac{S}{39.62} \right) \epsilon$$

$$WCHAR_{AD} = (L) \left(\frac{Q \epsilon}{39.62} \right)$$

Thus, we note that the size of the adsorption zone is only a function of the gas flow rate, charcoal density, and determining contaminant.

The adsorption zone mass can then be calculated.

- 1) Note the potential parameter (A) of the cutoff contaminant.
- 2) Obtain the adsorption zone length from Figure 72.
- 3) Calculate the mass of the adsorption zone:

$$W = (L) \left(\frac{Q \epsilon}{39.62} \right)$$

The total bed mass is now calculated as the sum of the saturated zone of the design contaminant and the adsorption zone for the design contaminant.

Once the bed design is established the expected performance for individual contaminants can be calculated. The procedure to establish the performance consists of calculating the adsorption zone size and then obtaining the saturated zone size by subtracting the adsorption zone from the total bed size.

Using much the same technique as the previously described procedure,

- 1) Calculate P_i and A for the contaminant.
- 2) Obtain L from Figure 72.
- 3) Calculate the mass of the adsorption zone.
- 4) Calculate the mass of the saturated zone for the contaminant being evaluated.

$$WCHAR_{sat\ zone} = WCHAR_{total} - WCHAR_{AD}$$

Now, referring to the capacity calculations, we obtain the data for saturated zone requirements which leads to breakthrough time.

- 5) Obtain the WTOT which corresponds to the contaminant being evaluated.

6) Determine the charcoal requirements for an increment of time.

$$W = \frac{W_{TOT}}{t}$$

7) Calculate the time to breakthrough

$$\text{BREAKTHROUGH-TIME} = \text{MASS sat zone}/W$$

This procedure for evaluating the performance of a bed also applies to different contaminant specifications. However, in this case a new saturated zone list must be generated prior to step 5 above.

9.2.3.2 Fixed Bed Test Data Analysis. The design of the fixed bed is based primarily on a requirement for control of pyruvic acid for a 180 day mission. The details of this design are presented in a previous section. The following is the specified bed configuration:

ID	33 cm (13 in)
Length	38.1 cm (15 in)
Charcoal	6.44 kg (14.2 lb) sat zone
	<u>6.99 kg (15.4 lb)</u> ads zone
	15.43 kg (34.0 lb) total (with 15% safety factor)

The bed used in the IMSC test had the same dimensions as the specified bed. However, the charcoal had a higher than anticipated bulk density which resulted in a charcoal load of 18.5 kg (40.8 lb). In addition, the charcoal was treated with 3.7 kg (8.16 lb) of phosphoric acid giving a total charcoal weight of 22.2 kg (49 lb). Assuming that the calculated size of the adsorption zone is correct, the test bed has a saturated zone of 11.5 kg (25.44 lb). This represents a safety factor of about 80 percent.

During the test program, the regenerable bed contaminants introduced were removed by the fixed bed for a limited period of time. This time to breakthrough has been calculated, and compared with the measured breakthrough times

of the test. This data is presented in Table 40. The basis for the calculated data is taken from the test program which consists of 19 days at the high introduction rates for the hydrocarbon liquids, and 17 days as the high introduction rates for the Freons. The balance of the test time up to day 195, exclusive of shutdowns, is at the low introduction rates. The system was then returned to the short term rates for the duration of the test.

The actual quantity of charcoal was used in developing the calculated values. Table 40 includes four columns of computed breakthrough times. The first column presents the anticipated values as calculated from the data for contaminants and charcoal performance used in the original design program (See Ref. 2). The linear potential plot interpolation routine was used in the computer runs for these calculations.

During the test, no pyruvic acid was observed, and methyl ethyl ketone performance exceeded expectations. Thus, three additional calculated columns were included in an attempt to explain the difference in performance. In these cases the new program, just described was used. The second column presents results using the same data base as in column 1. The differences are a result of the improved semilog interpolation of the potential plot. The final two calculated columns of data illustrate the effects of additional runs with the new program by first eliminating pyruvic acid (which was not found in the actual test) and second changing the solubility code of methyl ethyl ketone and methyl acetate to soluble from insoluble. This was done for comparison purposes as both these contaminants are slightly soluble. In the generation of the basic contaminant data block, only totally soluble contaminants were assigned a soluble code. The actual data for these contaminants would be expected to lie between the extremes of the two solubility codes.

The final column of data presents the actual test data. Examination of the breakthrough data shows that the time to breakthrough was earlier than anticipated for those contaminants which are removed by the regenerable bed. The following is a discussion of the data by contaminant.

Table 40
Fixed Bed Time to Breakthrough (Days)

Contaminant	Original ¹ Program	Calculated vs Test Results			Test Results ⁵
		New Program ² Original Contaminant Load	New Program ³ Without Pyruvic Acid	New Program ^{3,4} Without Pyruvic Acid Solubility Code Changes	
Toluene	1240	1277	1277	1277	ND
Pyruvic Acid	332	314	-	-	-
Benzene	207	247	294	294	202(265)
Methyl Ethyl Ketone	166	194	187	346	205(295)
Methyl Acetate	40	41	19	66	7-11
Freon 11	13	13.5	13.5	13.7	2
Acetone	9	10.1	10.1	10.2	7
Freon 12	1.1	1.2	1.2	1.1	1

Note: All data based upon 18.2 kg (40 lb) charcoal bed, 1130 l/min (40 CFM), and an initial 19 days at the high introduction rate; with the balance at the low introduction rates. When breakthrough occurs before 19 days results are for the high introduction rate.

- 1) The original program used linear interpolation of the potential plot.
- 2) The new program uses semilog interpolation of the potential plot.
- 3) As pyruvic acid was not found in the actual test, the analysis was carried out without pyruvic acid as an input.
- 4) The contaminant data block is based upon insoluble code for methyl ethyl ketone and methyl acetate. Both are slightly soluble. The run investigates the effect of a soluble code.
- 5) Estimates made from the test data plots.
- 6) Values in parenthesis allow 10 days at the low rate for 1 day at the high rate at the end of the test.

Toluene: The bed is oversized for control of toluene. The anticipated breakthrough would be at 1277 days on a schedule of 19 days high rate and 1258 days of low rate. No breakthrough was expected or observed.

Pyruvic Acid: No pyruvic acid was detected during the test at the system inlet. The method of pyruvic acid addition was to dilute with water to a five percent acid mixture and feed at a steady rate. After completion of the test, the simulated cabin tank was opened and examined. A dark brown liquid material was found on the bottom of the tank. Analysis showed this material to be primarily pyruvic acid. Most of the water had evaporated from the water/acid mixture. It appears that the low vapor pressure of pyruvic acid prevented it from entering the circulating gas stream. Other analysis presumed initial partial breakdown of the pyruvic acid. However, the extent of breakdown seems low and as a result no conclusions can be drawn on removal of this contaminant. As it was not detected, the computed results which do not include pyruvic acid are likely the most valid.

Benzene: The calculations show an anticipated breakthrough after 19 days of high rate and 275 days of low rate. The test schedule showed no breakthrough after 19 days of high rate and 176 days of low rate. After an additional 7 days of high rate at the end of the test breakthrough was noted. The quantity of contaminant bed during these 7 days is equivalent to 70 days at the low rate. Thus, a total time to breakthrough of 19 days high rate and 246 equivalent day at low rate or 265 days is inferred. This is good agreement with the 294 expected.

Methyl Ethyl Ketone: The calculations showed an anticipated breakthrough after 19 days of high rate and between 168 and 327 days of low rate depending upon the solubility code selected. The test data shows breakthrough after 19 days of high rate, 176 days of low rate and an additional 10 days of high rate. As in the case of benzene the mass of contaminant fed during the 10 days at the high rate is equivalent to 100 days at the low rate. The resultant 19 days of high rate and 276 equivalent days of low rate for a total of 295 days falls between the predictions of the two solubility codes slightly toward the soluble code indicated.

Methyl Acetate, Freon-11, Freon-12, and Acetone: Each of these contaminants exhibited breakthrough somewhat earlier than anticipated.

In order to explain the early breakthrough of the regenerable bed contaminants through the fixed bed, the calculational procedure and adsorption dynamics must be examined in more detail.

The calculational procedure was presented in previous section. This procedure was applied to the fixed bed to predict performance as follows.

$$\begin{aligned}
 \text{Total test charcoal bed size} &= 40.8 \text{ lbs} = 18,525 \text{ gm} \\
 \text{Bed volume} &= 1.152 \text{ ft}^3 = 32,627 \text{ cc} \\
 \text{Charcoal density} &= 0.5678 \text{ gm/cc} \\
 \text{Gas flow} &40 \text{ CFM} = 1.13 \times 10^6 \text{ cc/min} \\
 \text{Saturated zone size} &= \text{Total size} - \text{Adsorption zone} \\
 \text{Adsorption zone} &= QPL/39.62 \\
 \text{Saturated zone size} &= 18,525 - 16,230 \text{ (L)}
 \end{aligned}$$

Using the equation for saturated zone size, Table 41 can be generated from the computer data and the adsorption zone data at 39.62 cm/min (1.3 ft/min).

Table 41
SHORT TERM RATE CALCULATIONS

Contaminant	Potential Parameter "A"	Charcoal Required \dot{m} (gm/day)	Saturated Zone Size WTOT (gm)	Breakthrough Time BT (days)
Toluene	12.3	38	12,844	338
Benzene	17.8	95.8	10,329	108
Methyl Ethyl Ketone	16.2	144	11,059	77
Methyl Acetate	19.6	434	9,517	22
Freon 11	21.9	629	8,462	13.5
Acetone	19.2	969	9,761	10.1
Freon 12	28.3	4,757	5,622	1.2

In Table 41, A is the potential parameter and m is the mass of charcoal required per day of operation. Both of these parameters are calculated from the program. The adsorption zone length data is then obtained from Figure 72. Then, using the equation for the saturated zone size the mass (WTOT) is calculated. The time to breakthrough if short term rates are maintained, is then calculated from the saturated zone size divided by the mass of charcoal required. This calculation sequence was carried out for each contaminant.

During the test, 19 days were spent at the short term rates for the hydrocarbons and 17 days for the Freons. The total size of the saturated zone at the end of the short term phase was then obtained by multiplying the number of days at the high introduction rates by the mass of charcoal required per day. This quantity of charcoal is unavailable for contaminant control at the low introduction rates as it is already saturated. Now, a table similar to Table 41 was generated for the long duration low introduction rate portion of the test. In this case, a new total bed size is first calculated for each contaminant. This is the initial size of 18,525 grams less the size of the short term high introduction rate saturated zone.

The terms and calculations of Table 42 are identical to those of Table 41 except that the initial bed size of 18,525 grams used in the equation for saturated zone size is replaced by the charcoal available after the short term rate period. Contaminants which show a breakthrough during the short term phase, i.e. Freon 11, acetone, and Freon 12 are omitted from this table. Further, the negative saturated zone size shown for methyl acetate indicates an adsorption zone size greater than the total quantity of available charcoal. Thus, immediate breakthrough is expected.

In order to obtain the total breakthrough time for any given contaminant, the duration at the short term rates is added to the long term breakthrough data.

Table 42
Long Term Rate Calculations

Contaminant	Charcoal Available After Short Term Rate Feed (gm)	Potential Parameter "A"	Charcoal Required (gm/day)	Saturated Zone Size WTOT(gm)	Breakthru Time BT(days)
Toluene	17,803	14.8	8.73	10,986	1258
Benzene	16,705	20.85	26.5	7,210	275
Methyl Ethyl Ketone	15,789	19.2	39.45	7,025	178
Methyl Acetate	10,279	23.1	134.7	-350*	0

*The shift in A with the step change in production rate resulted in an immediate prediction of breakthrough.

A factor which must be considered in these calculations is that the adsorption zone length data is for 6 x 14 mesh carbon. The fixed bed is composed of a 4 x 6 mesh carbon. Reviewing the equation for the adsorption zone according to Klotz Ref. 8 we see that the superficial area of the carbon and the particle size are of importance in defining the adsorption zone length.

$$L = L_t + L_r$$

$$L_t = \frac{230}{a} \left[\frac{D_p U_m}{\mu} \right]^{.41} \left[\frac{\mu}{\rho D_v} \right]^{.67} \log \frac{C_i}{C_b}$$

$$L_r = k U_m \log \frac{C_i}{C_b}$$

where a = particle superficial area, (cm^2/cm^3)

D_p = mean particle diameter (cm)

U_m = linear velocity (cm/sec)

ρ = gas density (gm/cm^3)

μ = gas viscosity, mixture (poise)

D_v = adsorbate vapor diffusion coefficient (cm^2/sec)

C_i = influent concentration

C_b = penetration concentration

k = charcoal constant, function of particle size

As the split between the L_t and L_r are not separately defined in the experimental data and values of a , D_p and k are not well defined for the charcoal, a calculated effect of differing mesh sizes is not possible using the currently existing data. However, it is noted that the coarser mesh of the fixed bed will tend to increase this zone length. For those contaminants having the greatest adsorption zone length, mainly methyl acetate, Freon-11, Freon-12, and acetone this shift will have the greatest impact. The result is to shorten the breakthrough time. This is observed in the data.

Another qualitative effect is also important in these considerations. Starting with a bed initially saturated with water, the contaminants must displace water to occupy an adsorption site. For water soluble contaminants this is accomplished through solution then displacement. This occurs readily and thus the more favorable potential plot curve occurs. For insoluble materials, displacement is more difficult and does not take place completely. This is reflected in a lower capacity curve on the potential plot and most probably some shift in the adsorption zone curve due to dynamic effects of displacement. This can be seen in the data as acetone, totally soluble, most closely approaches its anticipated breakthrough time of all the regenerable bed contaminants.

In summary, we see that the fixed bed design procedure is valid for those contaminants which normally establish its design point. However, if the adsorption zone section of the bed becomes a significant portion of the total bed, the breakthrough times will tend to be shallower than anticipated. The error will be the greatest for insoluble contaminants. This shift is possible due to the dynamics of water displacement and the mean charcoal particle size being greater than 6×14 mesh, for which the adsorption zone length curve was derived. An additional safety factor must be allowed if the design contaminants have a relatively long adsorption zone.

9.2.3.3 Regenerable Bed - The results of the regenerable bed tests showed that the unit did not perform as well as expected. Possible explanations for the deficient performance include long-term degradation, incomplete desorption or errors in the potential plot or adsorption zone data. The following section investigates these explanations and develops the conclusion that the potential plot data requires revision. The revised potential plot data is also presented. Using this corrected potential plot data and the design procedure which is presented in a previous section an accurate prediction of charcoal requirements can be made.

The primary function of the regenerable bed in the Trace Contaminant Control System (TCCS) is the control of potential catalyst poisons. These materials include halogenated hydrocarbons, and a variety of compounds containing sulfur and nitrogen. In the design of the regenerable bed, a listing was prepared of bed size as a function of those contaminants controlled. This listing shows a sharp increase in bed size beyond a size which was defined by tetrafluoroethylene. Examination of those potential poisons not controlled by a bed sized to control tetrafluoroethylene showed a small number of contaminants. Those contaminants could easily be controlled at their source or by elimination from the spacecraft by inclusion in the nonacceptable materials list. Thus, a regenerable bed size defined by tetrafluoroethylene was selected.

In the analysis which leads to bed size, two segments were considered. These are the saturated zone mass and adsorption zone mass. The latter is derived from experimental data of adsorption zone length, the potential parameter, charcoal density, and gas flow rate.

The key to the saturated zone size analysis is the coexistence of contaminants in the zone when concentration levels are low. The extent to which a contaminant is controlled within a zone is a function of its potential parameter (A), and the degree of displacement by more readily adsorbed contaminants. The size of this zone was calculated by an IMSC computer program which includes these displacement effects and is based on data for the potential parameter versus carbon capacity for Barnebey Cheney BD charcoal.

Recognizing this design procedure, a test plan was established which, using a limited number of contaminants, simulates the specified design load. A limit on the number of test contaminants was set by practical test and analytical considerations. The selected contaminants for loading the regenerable bed included those which would have a high degree of adsorption and contribute to displacement, and those which are difficult to remove and determine the final bed size. Further, to gather comparative experience with previous tests, several contaminants were selected which were used in those tests. Table 35 presented a list of the selected contaminants.

The introduction and analysis of tetrafluoroethylene, the regenerable bed design contaminant, is difficult. Thus, a decision was made to substitute methyl alcohol as the contaminant which provides the maximum stress on the regenerable bed. The design calculations showed that methyl alcohol would stress the bed to within five percent (5%) of its rated capacity.

Early in the test, methyl alcohol breakthrough was observed. Thus, additional contaminants, propylene and Freon 22, were introduced on day 154 to generate further data on bed capacity. After 180 days of testing, additional parameters that affected the bed design were investigated; these were multiple desorptions, completeness of desorption, and possible errors in the potential plot and adsorption zone design data.

The test results indicated that though methyl alcohol was not controlled by the regenerable bed, propylene was adequately controlled. Further, these results indicated that the cause for the reduced capacity was an error in the potential plot data. Based on the fact that propylene was controlled, a revised potential plot was generated. Table 43 presents a comparison of computer analysis of the regenerable bed saturated zone charcoal requirements for three different situations. The first case is based on the original computer program, the second case is based on the revised computer program just described and the third column is based on the revised computer program with the corrected potential plot. As can be seen from the table, there is no major difference between the original computer program results and the revised computer program results with the exception of methyl alcohol. The reason for the large differences in methyl alcohol is due to an error in methyl alcohol vapor pressure in the original computer program. This error was corrected at the time the revised program was run. The corrected data indicates that methyl alcohol is not a candidate to demonstrate control by the regenerable bed. It is, however, well removed by the catalytic oxidizer. In observing the quantities of charcoal required in the saturated layer by the more difficult to control contaminants, propylene and Freon 22, it can be seen that the corrected potential plot results in nearly twice as much charcoal in the saturated zone as the original potential plot. This agrees with the test results in that propylene was at the limit

Table 43
Regenerable Bed - Comparison of Computed Results

Original (1) Computer Program	Revised VP Data (2) & Computer Program			Revised Computer (3) Program Corrected Potential Plot		
	High Intro Rate	High Intro Rate		High Intro Rate	Low Intro Rate	
		Low Intro Rate	Low Intro Rate		Low Intro Rate	Low Intro Rate
Methyl Acetate	114.3 (16.2)	36.97 (19.9)	107.3 (15.8)	35.6 (19.5)	116.5 (15.8)	41.2 (15.8)
Acetylene	422.3 (16.4)	152 (20.4)	428.8 (15.9)	143.1 (20.0)	398 (15.9)	124.6 (15.9)
Freon 11	239.8 (19.7)	58 (23.3)	297.1 (20.1)	84.37 23.7	356.8 (20.1)	113.3 (20.1)
Propane (4)	2604 (25.3)	--	2648 (25.4)	--	3764 (25.4)	--
Freon 12	1622 (26.0)	468.6 (30.1)	1672 (26.5)	541.6 (30.6)	2383 (26.5)	850.5 (30.6)
Propylene (5)	--	1796 (33.0)	--	2493 (33.2)	--	4462 (33.2)
Methyl Alcohol	3863 27.8	3957 (35.3)	9614 (6) (32.2)	7455 (6) (39.6)	10080 (6) (32.2)	8286 (6) (39.6)
Freon 22 (5)	--	3206 (42.5)	--	3761 (43.1)	--	8350 (6) (43.1)

NOTE: Data in parenthesis is the potential parameter, other data is calculated saturated zone size in grams.

- 1) Original Program bed design specification basis 122 l/min (4.3 CFM) and 295K (70 F) vapor pressure data.
- 2) New Program 311 K (100 F) vapor pressure data, new calculation procedure
- 3) New Program Same as 2 except potential plot brought into agreement with test data (propylene saturated zone size agrees with test bed).
- 4) Propane introduced at high rate only.
- 5) Propylene and Freon 22 introduced at low rate only.
- 6) Contaminants with a required saturated zone size greater than 4462 grams are not controlled.

of control. The original potential plot indicated that approximately sixty percent (60%) of the bed was required for control of propylene. The more readily adsorbed contaminants are not as strongly affected by the new potential plot.

The following sections describe the analyses leading to the new potential plot.

Data Analysis - The performance data for each contaminant is presented in the results section of this report. Two effects are important in the interpretation of these data. These are the removal of contaminants by the catalytic oxidizer and the sample time. An analysis of the data shows all contaminants passing through the regenerable bed are oxidized to some extent in the catalytic oxidizer. Thus, if the regenerable bed is not functioning at the desired removal efficiency level, the cabin concentration levels will not climb because of control in the oxidizer.

An analysis of the daily cycle shows that the start of the desorption cycle was at 0500 and the end of the cycle at 0800 during the first 190 days of the test. At 0800, the regenerable bed temperature is near 367 K (200 F) at which temperature control of contaminants is poor even though the bed is mostly desorbed. Further, contaminant levels are at their highest at 0800 due to addition of contaminants during the desorption period, during which time no removal occurs. This effect is seen in Figures 67 and 68 which show the daily variation of carbon monoxide and methane with time. The catalytic oxidizer which controls these materials is shut off during the desorption cycle, giving rise to this characteristic.

When flow is initiated at 0800, the contaminant levels start to drop to the steady state levels. The greatest part of the approach curve is complete by 1200. During this approach period, bed performance will rapidly improve from poor removal at the high temperature when flow is reinitiated, to complete control as the temperature lowers and the bed loading is still low early in the cycle. Bed performance should be at its best by 10:00 as the temperature is near 311 K (100 F) the design temperature level and minimum level, at this

time. The system contaminant levels are still dropping at this time. A review of the regenerable bed data show early in the test that most samples were obtained between 0900 and 1100 and with inlet and outlet points taken at differing times. Thus, accurate definition of bed removal efficiency is difficult with the changing inlet and outlet concentration levels. Further, equilibrium levels are of little value in determining regenerable bed performance due to the interaction of the catalytic oxidizer which removes residual material passing through the regenerable bed.

Toward the end of the test, the cycle was changed to start the desorption cycle at 1700. Samples were then taken at 2200 hours at which time the contaminant decay curve is complete and efficiency is not sensitive to sample time. The following table presents data taken on five regenerable bed contaminants at different points in the cycle.

Table 44

Variation in Regenerable Bed Removal Efficiency with Cycle Time

Contaminant	Time (Hours)				
	2	5	8	22	22*
Freon 11	100%	98%	-	98%	95%
Freon 12	-	92%	-	87%	82%
Freon 22	100%	-	-	0	0
Methyl Alcohol	-	51%	68%	0	44%
Propylene	92%	98%	90%	84%	-

*Data for adsorption cycle following two desorptions on same day.

A trend is observed in Table 44 which shows efficiency high at the beginning of the cycle and declining toward the end. Further, difficult-to-control contaminants show the greatest loss in efficiency.

Effects of Desorption - Particular note is made of the two columns of data at 22 hours. The switch in desorption time at about 190 days resulted in a short adsorption cycle. Results at 22 hours following this switch showed better performance than after several cycles of the normal 20.67 hours adsorption. This suggested the desire of a more complete desorption. Therefore, near the end of the test, an extended desorption of greater than 24 hours was carried out. Figure 73 presents the variation of propylene effluent concentration with time on successive days following this extended desorption. The curves show little change between day 1 and day 2. As a long desorption preceded day 1 and a standard desorption preceded day 2, the conclusion is drawn that the desorption time of 3.3 hours used during the test resulted in essentially complete regeneration. This test demonstrated that the desorption period is adequate and that the earlier 22 hour data did not signify the need for additional desorption.

Effects of Adsorption Zone - Another possible explanation for the poor performance of the regenerable bed is a possible error in the adsorption zone length data. This seems improbable since the adsorption zone length data is based upon 6 x 12 mesh carbon while the regenerable bed is composed of finer, 14 x 20 mesh carbon. The length of the adsorption zone is a function of both superficial area and particle size. With the decreased particle size in the test bed, a resulting decrease in adsorption zone length would be expected.

Effect of Potential Plot - A review of the literature shows a variation in performance of the same type of charcoal when data is taken on different batches. This indicates either the use of a considerable safety factor or basing designs on data taken on the charcoal batch from which the final beds will be assembled.

Previous data taken on charcoal shows Barnebey Cheney BD charcoal has the greatest capacity of those charcoals tested for contaminants having a high A value. These high A value contaminants establish the design of the regenerable bed. Thus, variations will have the most pronounced effects.

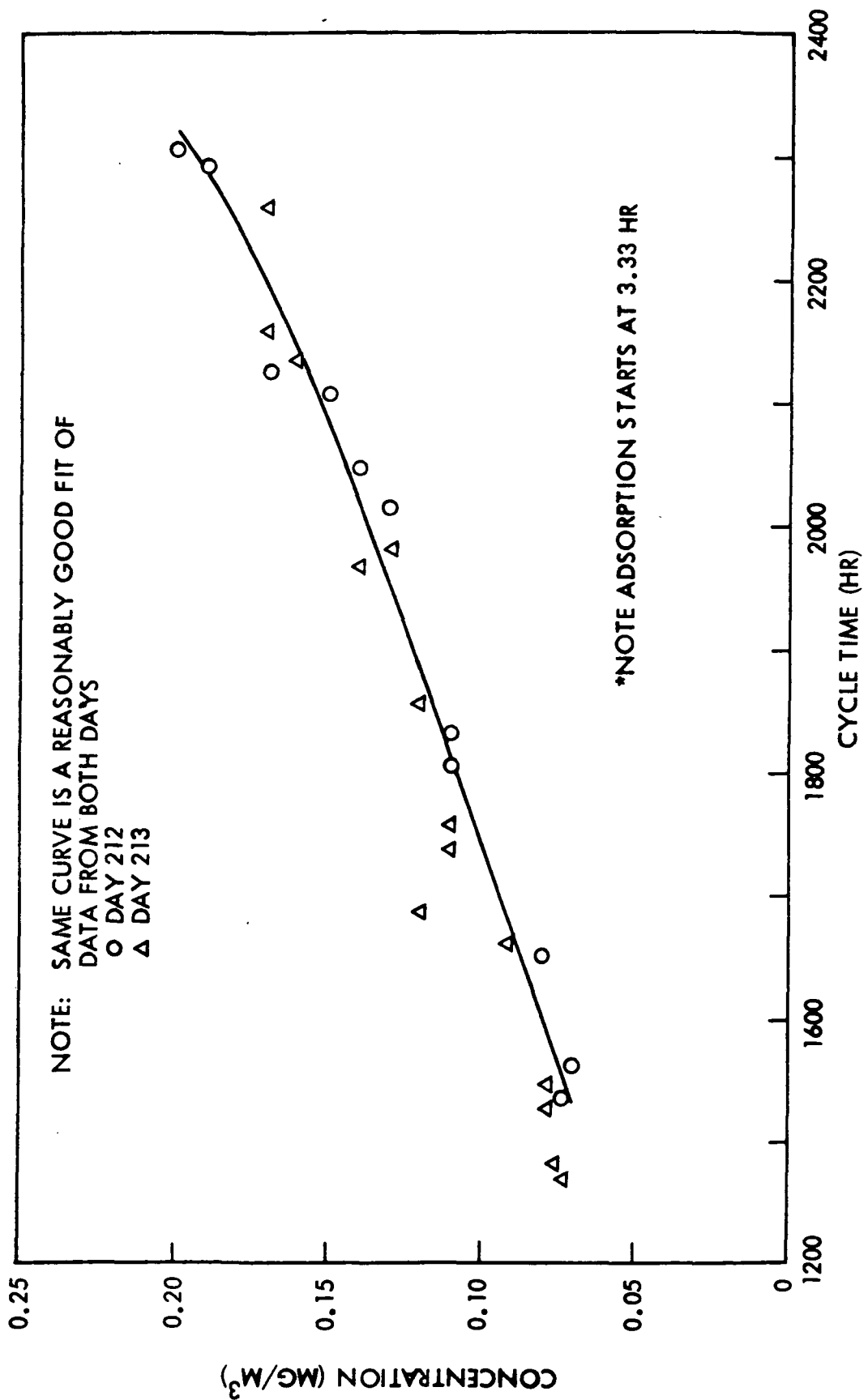


Figure 73 Effect of Long Term Desorption - Propylene Control

The test data indicates lack of regenerable bed control for methyl alcohol over the complete cycle and only partial control for Freon 22. Further, the removal efficiency data for Freon 12 and propylene suggests these contaminants are approaching their limits of adsorption, and that the potential plot is likely to be in error.

In view of a likely error in the potential plot, a new plot was developed based on successful control of propylene which seems to be at the limit of capacity for the regenerable bed.

Corrected Potential Plot - The new potential plot was based on the actual regenerable bed configuration and control of propylene.

The following parameters were used in defining the new potential plot.

o Regenerable Bed Size	6124 grams
o Bed Length	40.6 cm (16 in)
o Face Area	284 cm ² (44 in ²)
o Flow Rate	113 l/min (4 CFM)
o Propylene Removal Efficiency	90%

The selection of 113 l/min (4 CFM) for calculations is based upon measurements taken on flow rate during the test. The design flow of 127 l/min (4.5 CFM) was initially set. As the pressure loss across the pre-sorbent bed increased during the test due to the take up of moisture, the flow decreased. A measurement of flow, based on pre-sorbent pressure losses at the end of the test showed a flow of between 93 and 108 l/min (3.3 and 3.8 CFM). The selected flow of the 113 l/min (4 CFM) represents a mean flow between the pre- and post-test values.

This data for propylene results in a potential parameter of 33.2 and a capacity (q) of 0.93×10^{-6} cc/gm compared with the original design capacity of 1.75×10^{-6} cc/gram.

The new potential plot for insoluble contaminants was drawn through $A = 10$ and $q = 0.18$ and $A = 33.2$ and $q = .93 \times 10^{-6}$ cc/gm. This yields a bed which removes propylene and not Freon 22. It will be conservative as propylene is controlled with some excess capacity. The impact of this new curve is slight on a fixed bed which is treated with acid and whose design is set by low A value contaminants. However, the regenerable bed size will likely increase about two-fold. The new potential plot is presented in Figure 74. As a general rule, the uncertainties in potential plot data at high A values of the potential parameter and the variation in charcoal requirements for an acid treated bed will be slightly greater than for an untreated bed.

9.2.3.4 Catalytic Oxidizer - The catalytic oxidizer controlled all oxidizable contaminants in the test to within the allowable limits. Control was achieved with both the isotope heat source and the electrical heater. No evidence of catalyst poisoning was observed during the test period. Table 45 presents a summary of the catalytic oxidizer performance during the test.

Table 45
Catalytic Oxidizer Removal Efficiency

Contaminant	High Rate Introduction	Low Rate Introduction
Acetylene	100%	100%
Carbon Monoxide	100%	100%
Ethane	90%	90%
Ethylene	90%	100%
Methane	74%	85%

The design of the oxidizer specified a catalyst volume of 0.74 l (45 in³) and an operating temperature of 633 K (680 F). The actual test unit had 0.9 l (55 in³) of catalyst and an operating temperature of about 767 K (920 F) during the long-term portion of the test. The 767 K (920 F) is derived from Figure 45 and the daily log data which shows an external canister temperature of 694 K (790 K). Data taken on the unit with the catalyst used in the test, Figure 44, showed the methane removal efficiency was only nine percent (%) at 633 K (680 F),

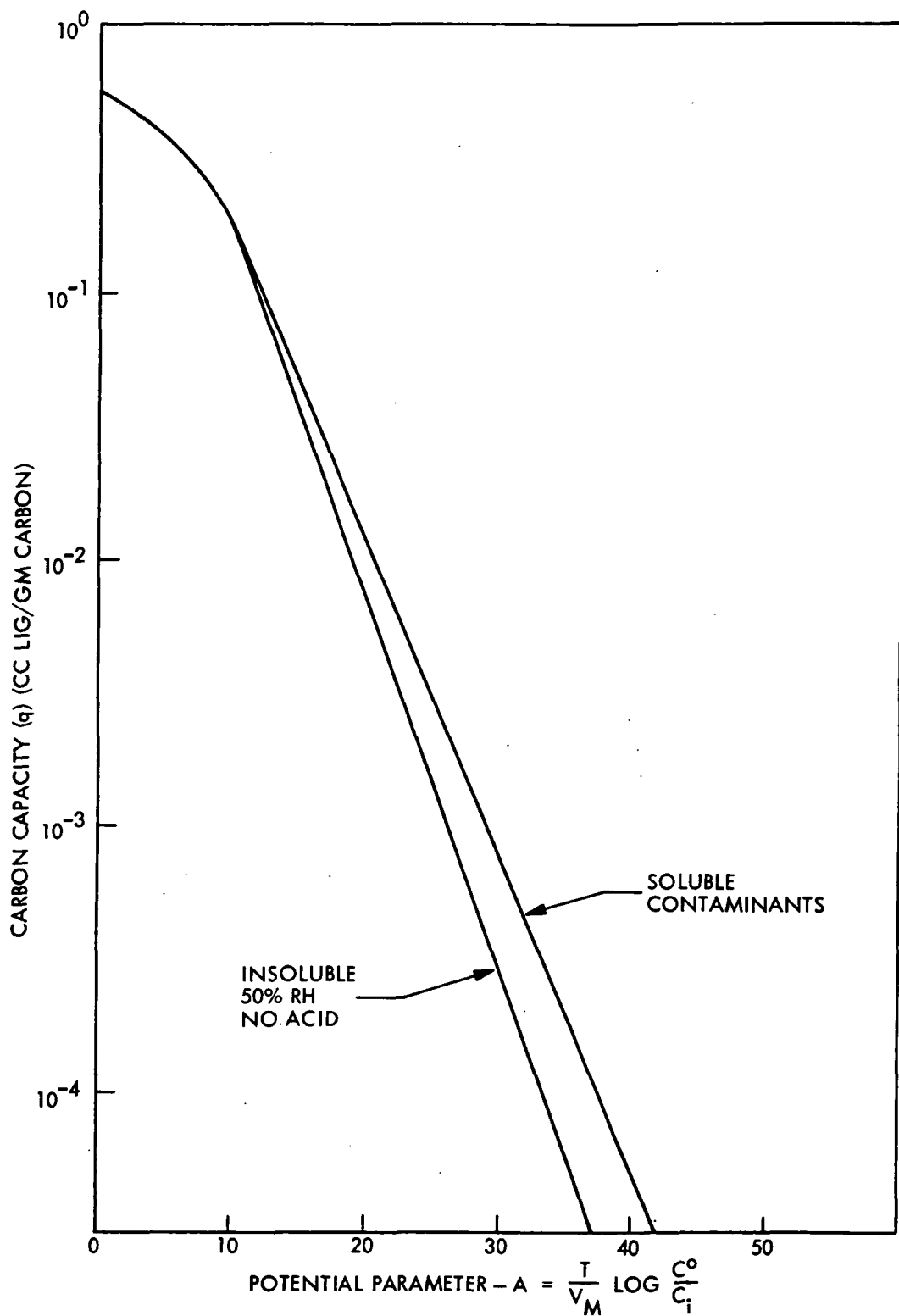


Figure 74 Corrected Potential Plot - Barnebey Cheney BD Carbon

the design temperature. At 767 F (920 F), the removal efficiency exceeds seventy percent (70%). Because of the high operating temperature, it is not surprising that the removal efficiency was good.

During the test period, three special measurements were run on the catalytic oxidizer. These are:

- o Continuous monitoring of CO and CH_4 over a 24 hour cycle
- o Continuous monitoring of temperature over a 24 hour cycle
- o Decomposition of Freons

The data on cyclic variation of carbon monoxide and methane was presented in Figures 67 and 68. The data shows a build-up in concentration at the start of the desorption cycle. This is due to the cessation of contaminant control flow and the continued contaminant feed. The build-up is at a constant rate and the slope is a function of a cabin volume. In the test situation, a large build-up was observed due to the relatively small simulated cabin volume. When the flow is reinitiated after the 3.3 hour desorption period, the concentration rapidly falls to the steady state level. The rate of decay is primarily a function of the generation rate, process flow rate, and concentration level. In a full scale spacecraft situation, the extent of build-up will be small and the concentration time curve will approach a steady state curve. The data for these two contaminants is representative of all contaminants controlled by components in the low flow loop.

A similar cyclic variation is observed in the catalytic oxidizer temperature. Data taken on the canister external surface temperature is presented in Figure 75 for two cases. The lower curve is typical for an electrically heated unit which is unheated during the desorption cycle. This allows smoothing of subsystem power as the regenerable bed desorption heaters are on at this time. The data presented are for the low contaminant generation rates. The upper curve is for a continuous heat source such as an isotope. This data was taken during a period of high contaminant rate. The true catalyst temperature is somewhat higher as seen from the data presented in Figure 75.

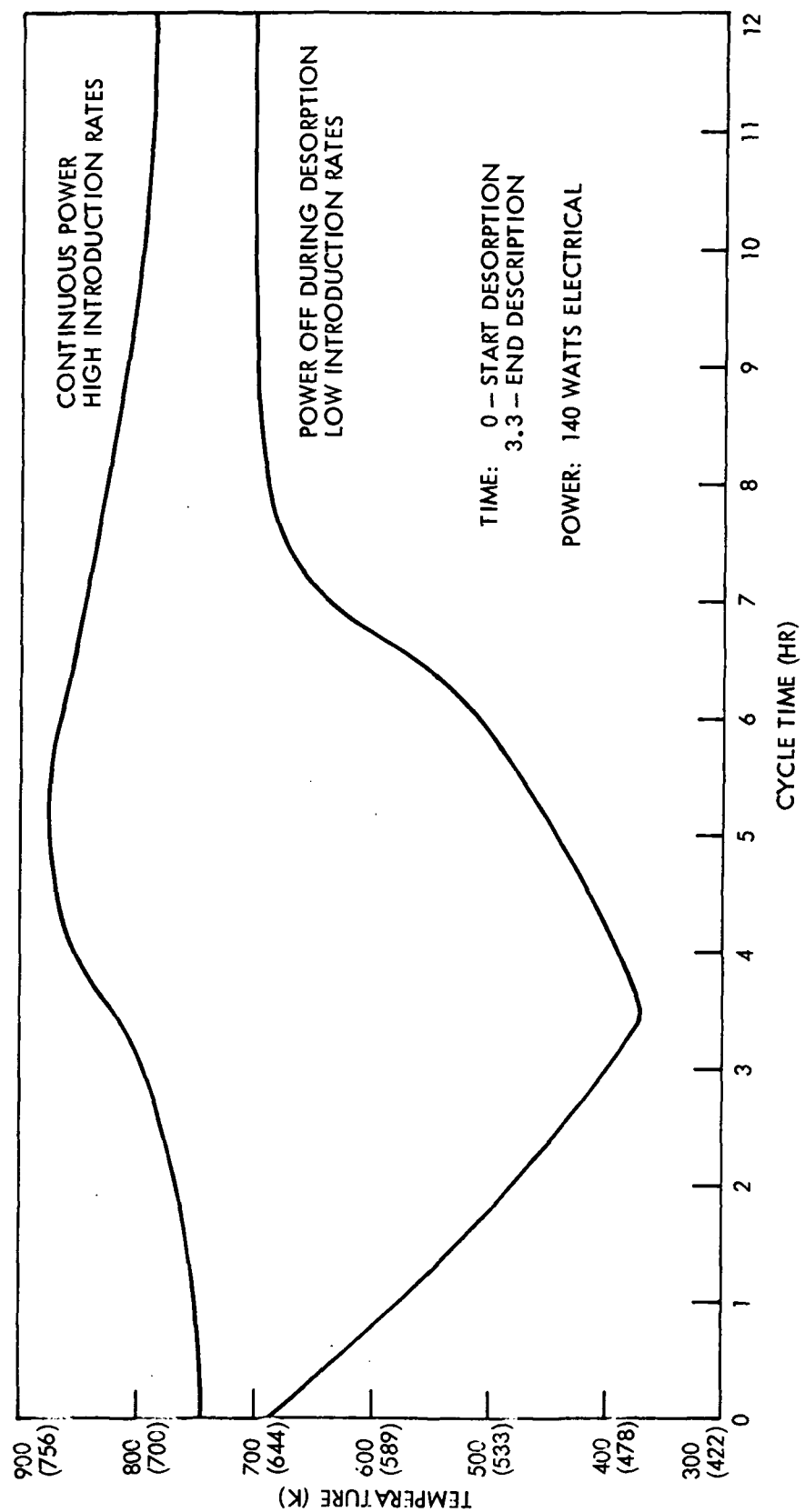


Figure 75 Catalyst Canister Temperature Profile

The shape of these curves shows either a slow cool down or heat up during the 3.3 hour desorption period. During this time the contaminants are building up as discussed in the previous section. In the operating mode where the heater is shut off during desorption, a gradual heat up is observed when flow and heater power are reinitiated. When the oxidizer temperature reaches about 533 K (500 F), the contaminants which are building up start to oxidize thus liberating energy which increases the rate of temperature rise. The curve then rolls off to the steady state temperature level. In the operating mode where the heater power is continuous, the built-up contaminants start to oxidize as soon as flow is reinitiated. This results in an increase in rate of temperature rise. As the concentration levels drop, as seen in the previous section, the energy of combustion drops, the curve turns around and the steady state temperature level is approached. In both cases, the heater power is 140 watts. The difference in steady state levels is a result of the higher average power in the continuous heater operating mode and the higher energy of combustion for the short term rates used in the development of the continuous operation data. Of particular importance is the time of build-up between the two operating modes. With continuous power, oxidation starts with flow after the 3.3 hours of desorption; with intermittent power an additional time of about two hours is required to get the unit back to operating temperature.

Referring to Figure 41, we see that a temperature of about 644 K (700 F) would be expected with an average power of 140 watts. The 689 K (780 F) steady level with continuous power corresponds to about 165 watts. The difference is the energy of combustion. Considering the peak canister temperature of 742 K (875 F) in Figure 75, a 922 K (1200 F) isotope heat source temperature is obtained from Figure 43. This is positive indication of possible over-temperature problems with an isotope heat source at high contaminant loads.

Throughout the test, a number of contaminants were introduced into the system. Each of these contaminants were controlled by some element of the Trace Contaminant Control System (TCCS). With the exception of the catalytic oxidizer, all system elements were simple adsorption devices. The oxidizer differed in operation in that it converted contaminants to alternate forms.

The major oxidizer products are water and carbon dioxide. Trace quantities of Freons and ammonia entering the unit were converted to other materials which present potential toxicity problems. The data shows a build-up of nitric oxide shortly after ammonia breakthrough. Further, both HCl and HF were detected. These likely resulted from decomposition of Freons. Other materials were found in the concentration analysis. Each of these materials were controlled within the allowable levels by other system components.

9.2.3 Post-Test Catalytic Oxidizer Examination

At the conclusion of the contaminant venting study described in the next section it was decided to conduct a post-test examination of the catalytic oxidizer. The catalytic oxidizer was disassembled. The outer blanket of Min-K and quilted Fiberglas insulation was in good condition. Only a few localized areas of the Velcro closure material had deteriorated, but the Velcro was still usable. The rigid Min-K insulation inside of the aluminum end cap had chipped and cracked each time the unit has been opened. Since this had been done a number of times (changing from electrical heaters to isotope heaters and then back to electrical heaters several times) the Min-K showed appreciable cracking because it is subject to such effects. Figures 76 and 77 show the unit.

The bolts holding the Inconel end plate onto the stainless steel heat exchanger assembly came loose after some "Liquid Wrench" solvent was applied to the threads. Both the end plate and the heat exchanger were in very good condition and could be re-used. The flange of the heat exchanger would require that before re-use the scaly coating be removed, to provide a smooth flat sealing surface. Some chips had broken off of the local alumina coatings on the heat exchanger. The Haskel K Ring used as a seal between end plate and heat exchanger was still functional but should be replaced for further use. The catalyst bed assembly was in perfect condition. Even the #0-80 screws could be unscrewed. The heater support was in good reusable condition. One of the electrical heaters had an open circuit. It was found that this was due to one nichrome lead wire having broken where it enters the heater. The wire had

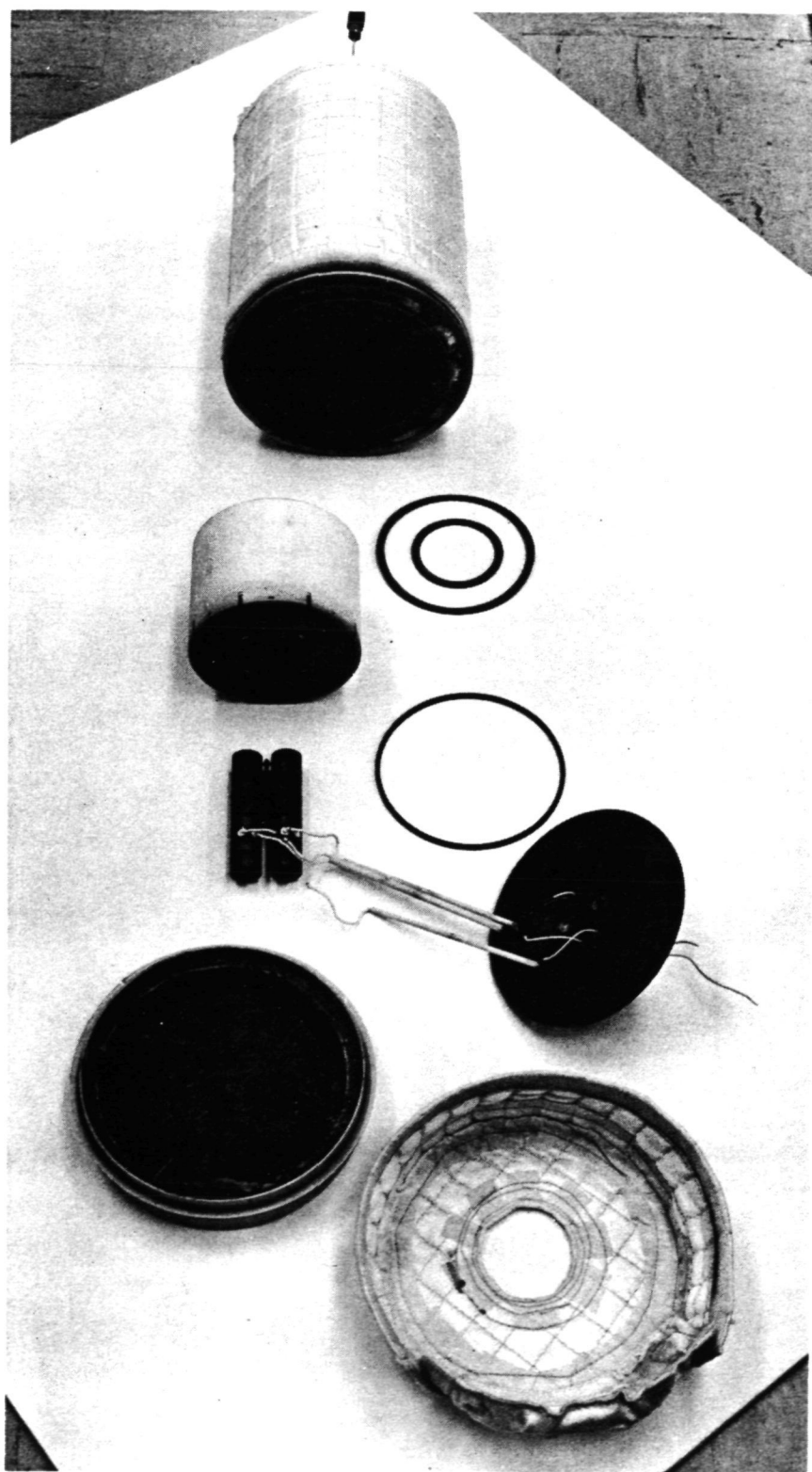


Figure 76 Catalytic Oxidizer After Completion of Test Program



Figure 77 Interior of Catalytic Oxidizer

probably been weakened by previous flexing at this point. Means of reducing the probability of such a failure can be devised for future designs. The inner and outer stainless steel seal washers were in good condition, but these items are designed to be replaced each time the unit is opened and reassembled. The two Gamah couplers used to attach the inlet and outlet ducts to the catalytic oxidizer were both in good reusable condition.

Several analyses were made of the catalyst pellets, which were originally 0.5% palladium on 1/8 inch alumina pellets. For comparison, a sample of unused pellets was analyzed along with the used ones which were taken from the catalytic oxidizer. A semi-quantitative spectroscopic analysis for metals gave these findings:

SAMPLE	MAJOR	MINOR	TRACE
New Pellets	Pd, Al		Fe, Cu, Si
Used Pellets	Pd, Al	Ag, Mo, Cr	Fe, Cu, Si

Subsequently, quantitative analyses for Pd were performed by wet chemistry and by atomic absorption with the following results:

SAMPLE	% PALLADIUM
New Pellets	0.49
Used Pellets	0.50 (Average of two locations)

Section 10
CONTAMINANT VENTING STUDY

10.1 Investigation of Non-Venting Techniques

The test series to evaluate catalyst resistance to poisoning was started on 9-3-74. The primary objectives of these tests were to identify a poison resistant catalyst and the required catalytic oxidizer operating conditions. This would be necessary if for some reason a regenerable bed could not be used to remove potential catalyst poisons. One possible reason for elimination of the regenerable bed would be contamination of spacecraft surfaces during the regeneration cycle. Four catalysts were purchased and a test plan was established for these evaluations. The test plan called for the evaluation of each catalyst at several operating temperatures. The first catalyst selected for test was the 0.5 percent palladium on alumina used in the previous test series. An initial operating temperature of 867 K (1100 F) was selected. The results of chemical analysis conducted during the test program showed that this catalyst resisted poisoning but that the post-sorbent bed was not as effective as desired in controlling the products generated in the catalytic oxidizer. As a result, the test plan was modified to continue testing of the 0.5 percent palladium catalyst at 867 K (1100 F) and to examine the performance of the post-sorbent bed in detail. Throughout the course of these tests (which ended on 9-11-75) there was no evidence of catalyst poisoning at the selected operating conditions.

During the evaluation of candidate post sorbent materials tests were conducted utilizing several candidate sorbents. These included lithium hydroxide both at room temperature and elevated temperature, charcoal impregnated with potassium hydroxide and Purafil. The results of these tests indicated that no single material was best suited for all of the compounds requiring a post sorbent for control. The products of combustion from the halogenated compounds, chloride

and fluoride, and from sulfur compounds were best controlled by either cool lithium hydroxide or the base treated charcoal. NO and NO_x however were controlled by Purafil.

These results indicate that the selected approach for a post sorbent bed would be a composite bed consisting of either lithium hydroxide or the base treated charcoal and Purafil. It is felt that the best overall performance would be obtained from the lithium hydroxide Purafil combination.

The following sections describe the results of the testing as related first to catalyst poisoning and then the performance of the post sorbent bed.

10.1.1 Catalyst Poisoning Investigation

A potential problem in eliminating the regenerable charcoal bed is that poorly absorbed compounds may "poison" the catalyst. Poisoning is defined as a reduction in catalyst oxidation efficiency. Under conditions where concentrations of halogenated compounds, organic nitrogen and sulfur compounds, and acid gases are high, oxidation catalysts may poison. During the previous testing described in Section 9.2.2 it was observed that small quantities of Freon 11, 12 and 22 along with some acid gases entered the catalytic oxidizer without degrading oxidizer efficiency. This indicated that this catalyst could be operated at conditions that would prevent poisoning and led to additional testing. Since methane is the most difficult hydrocarbon to oxidize the behavior of the catalytic oxidizer in removing methane in a background of poisons was studied during these tests.

The same catalyst used in the long-term test was used for the poisoning evaluation. This batch of 0.5% palladium had been used for 241 test days from October 10, 1973 to June 7, 1974 prior to the poisoning test. Conditions for the poisoning test are shown in Table 46:

Table 46 Catalyst Poisoning Test Conditions

Catalytic Oxidizer Flow	= 99 l/min (3.5 CFM)
Catalytic Oxidizer Temperature	= 867 K (1100 F)

Table 46 (continued)

Contaminant Feed Rates

	Short-Term* gm/day	Long Term gm/day
Methane	3.31	3.31
Ethane	.25	.25
Carbon Monoxide	.27	.27
Freon 11	2.5	.25
Freon 12	2.5	.25
Acetonitrile	.25	.025
Carbon Disulfide	.25	.025
Isopropyl alcohol	2.5	.25

*Contaminant feed rates were set at the short term values until day 21, then were changed to the long-term rates.

Contaminant inlet concentrations were about 20 mg/m^3 for methane, 2 mg/m^3 for Freon 12, and 4 mg/m^3 for Freon 11 during the test. Methane removal efficiency remained at a nearly constant level of about 80% during the 373 days of testing. Figure 78 shows the catalytic oxidizer inlet and outlet concentrations, and the removal efficiency for methane. Figures 79 and 80 show the corresponding Freon 11 and Freon 12 data.

The data indicate good control of the Freons, with about an 80% removal efficiency for Freon 12, and about an 85% removal efficiency for Freon 11. Acetonitrile was decomposed in the catalytic oxidizer, with an average removal efficiency of about 80%. Measurements of cyanide, a possible decomposition product, indicated levels near the lower limit of detectability of 0.1 mg/m^3 . Measurements of nitrogen compounds formed in the system showed more nitrogen than would be available from acetonitrile. This indicated possible formation of nitrogen compounds from nitrogen in the air.

Carbon disulfide was controlled by the catalytic oxidizer, with an average removal efficiency of about 70%. Measurements of the product SO_2 level were

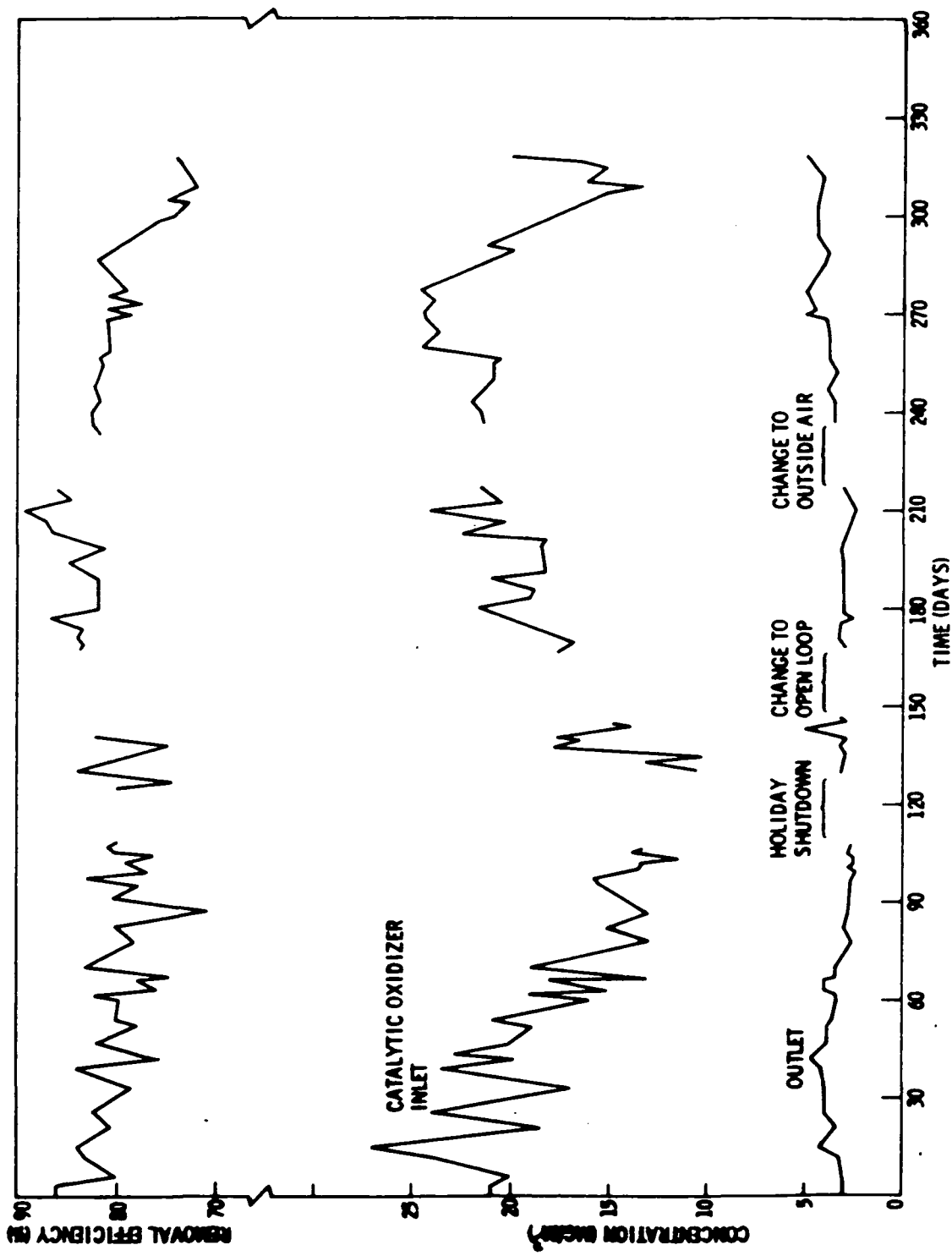


Figure 78 Methane Concentration and Conversion Efficiency vs Time

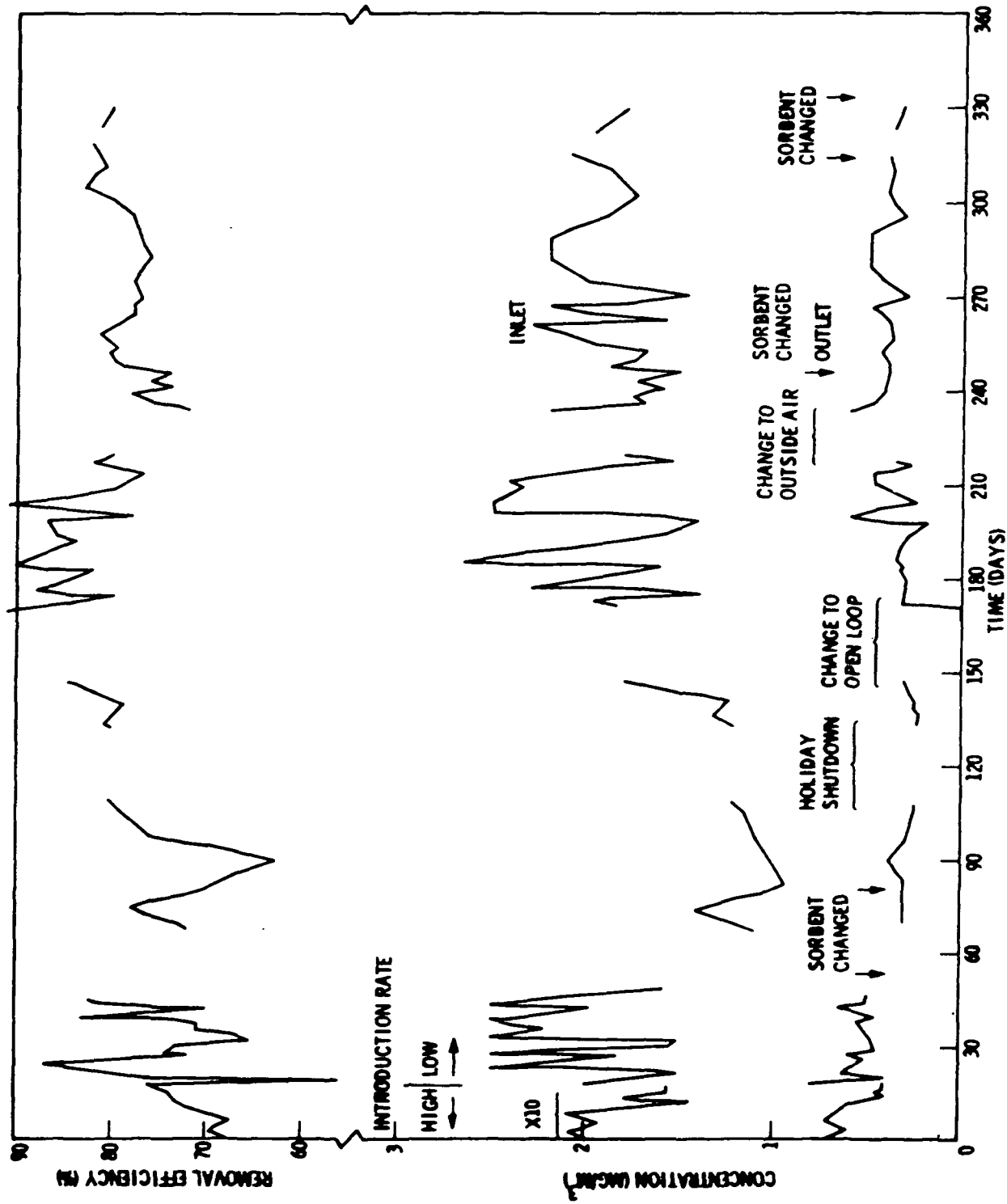


Figure 79 Freon-12 Concentration and Conversion Efficiency vs Time

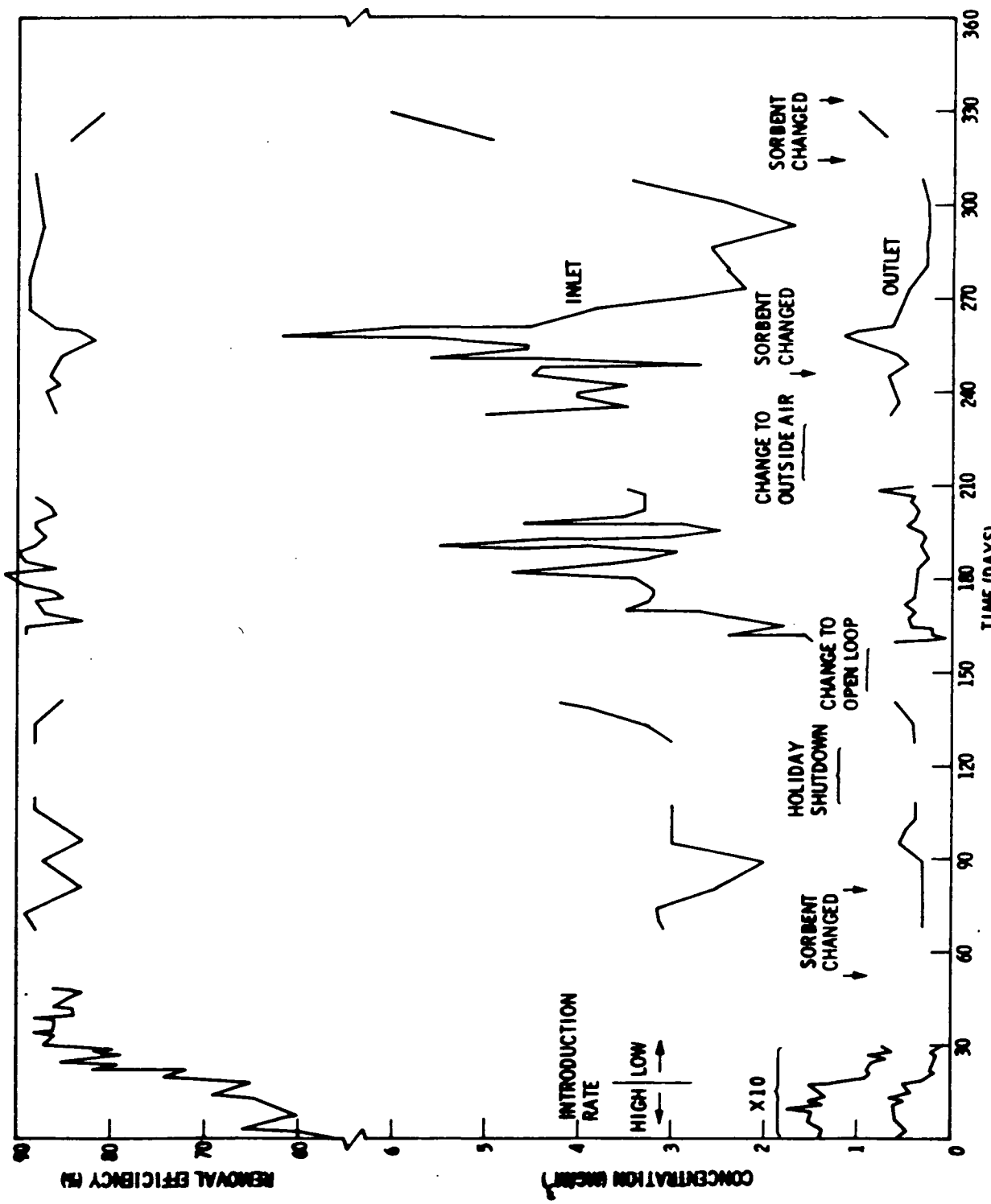


Figure 90 Freon-11 Concentration and Conversion Efficiency vs Time

below 0.05 mg/m³, or only about 20% of the possible level that could result from the carbon disulfide decomposition. Thus, the catalytic oxidizer seemed to control the product of carbon disulfide oxidation.

The test configuration was changed after the first 150 days, to an open loop configuration to allow a better assessment of the post sorbent bed performance. During this test, methane, Freon 11 and Freon 12 were introduced into a stream of 99 l/min (3.5 CFM) of air. Initially room air was used, which was changed on test day 202 to outside air to avoid contamination by Freons 21, 114, and 113 which are cleaning solvents used in the laboratory, and were contributing a variable halogenated hydrocarbon load to the catalytic oxidizer.

During no portion of the test program did the catalyst show any sign of poisoning. It was therefore concluded that the 0.5% palladium catalyst could be considered poison resistant under the conditions used in this test.

10.1.2 Post-sorbent Evaluations

Considerable testing was carried out on the post-sorbent bed to establish the best candidate material and configuration. Table 47 presents a summary of the tests conducted. Table 48 presents a detailed listing of the significant events of the test program in chronological order. The following discussions are split into two sections. The first is a description of the post-sorbent tests which includes a description of the tests carried out on each bed and a brief review of the results which led to the selection of the next bed. The second section reviews the data by chemical sorbed.

Beds 1 and 2 - Testing was started on post-sorbent bed 1, which was filled with lithium hydroxide, on 9/3/74. At that time the pre-sorbent bed was empty. On 10/25/74 the pre-sorbent bed was filled with lithium hydroxide and the test continued with both the pre- and post-sorbents beds on line, until 11/20/74. At that time both the pre- and post-sorbent beds were emptied in preparation for the testing of bed 3.

Table 47
Post-Sorbent Bed Testing

Bed Number	Chemical	Start Date	End Date	System Config.	Removal Efficiency			Comments
					Cl ⁻	F ⁻	NO _x	
1	LiOH	9-3-74	10-24	Closed	-	-	-	Both Cl ⁻ & F ⁻ levels stable indicating control. Steady NO level \sim 7.5 ppm.
2	LiOH	10-25	11-20	Closed	-	-	-	Both post-sorbent bed 1 & pre-sorbent bed on line. Both Cl ⁻ & F ⁻ levels stable indicating control. Steady level \sim 5 ppm.
3	KOH/Charcoal	11-20	1-31-75	Closed	-	-	-	Both Cl ⁻ and F ⁻ levels stable indicating control. Steady NO level \sim 1.2 ppm.
4	KOH/Charcoal	2-7 3-26	5-7	Open	82%	39%	50%	Cl ⁻ and F ⁻ analysis technique finalized on 3-26-75. Switch from room air inlet to outside air inlet 4-14-75. Tested until NO _x breakthrough.
5	KOH/Charcoal	5-7	7-18	Open	80	46%	30%	Tested until NO _x breakthrough
6	LiOH	7-21	8-1	Open	82%	-	Nil	Immediate breakthrough of NO _x . Test continued to gather limited Cl ⁻ data.
7	Purafil	8-1	9-11-75	Open	-	-	95%	NO _x outlet levels generally \sim 0.05 ppm. Heater lead failure on 9-11-75 ends testing.

Table 48
Catalyst Evaluations - Significant Events

Date	Day	Event
9-3-74	1	Test program initiated. Hydrocarbon contaminants on low introduction rate Other contaminants fed at high rate.
9-3-74	2	Hydrocarbons switched to high feed rates.
9-6-74	4	Hydrocarbons switched to low feed rates. 1000 cc/min of air introduced into system.
9-10-74	8	System 400 cycle power supply failed.
9-11-74	9	System restored with new 400 cycle power supply on line.
9-23-74	21	All contaminants set at low introduction rates.
9-30-74	28	Automatic shutdown (due to plant power interruption). System restarted.
10-1-74	29	Automatic shutdown (due to plant power interruption). System restarted.
10-25-74	53	System shutdown: LiOH pre-sorbent installed. System restarted.
11-20-74	79	System shutdown: LiOH removed from pre- and post-sorbent canisters. Pre-sorbent canister filled with KOH/charcoal.
11-21-74	80	System restarted.
12-20-74	109	System shutdown for holidays.
1-6-75	125	System restarted.
1-31-75	150	System shutdown for modifications to allow open loop testing of oxidizer.
2-7-75	157	System restarted in open loop mode. No contaminant feed.
2-24-75	174	Feed of contaminants started.
4-1-75	210	Shutdown to replace regenerable bed fan bearing; restart.
4-2-75	211	Contaminant feed restarted.
4-14-75	211	Contaminant feed stopped; outside air supply started.
4-18-75	227	Contaminant feed restarted.
5-7-75	246	Shutdown to change post-sorbent; system restarted.
5-21-75	260	Start liquid contaminants.
7-18-75	318	Shutdown to change post-sorbent bed.
7-21-75	321	System restarted; no contaminants.
7-22-75	322	Contaminant feed restarted.
8-1-75	332	Shutdown to change post-sorbent bed; system restarted.
8-4-75	334	Contaminant feed restarted.
9-11-75	373*	Shutdown due to heater failure.

*Calender days; 319 days with contaminant feed.

The testing of beds 1 and 2 was carried out using a closed-loop system. The flow through the catalytic oxidizer and pre- and post-sorbent beds was set at 99 l/min (3.5 CFM). The contaminants fed into the system are shown in Table 46. Initially, all contaminants were to be fed into the system at the high introduction rates for two weeks and then dropped to the low rates. However, on 9/6/74 analysis showed that humidity was building up and that oxygen concentration was decaying. This was attributed to the combustion of the hydrocarbon contaminants. As a result the hydrocarbon contaminant feeds were reduced to the low rates and an air inflow bleed of 1000 cc/min was established to make up for oxygen consumed by combustion. On 9/10/74 a power supply failure shut the system down. The power supply was replaced and the system was restarted on 9/11/74. Testing then continued uninterrupted, with the exception of two plant power shut downs, until 10/25/74 when the pre-sorbent bed was filled with LiOH. Testing then resumed, with both beds on-line, uninterrupted until 11/20/74.

The results of the testing on these beds are presented in Table 49 and 50. The results show that HCl, HF, SO_2 , and NO_x are found at the catalytic oxidizer outlet and thus must be controlled by a post-sorbent bed. During this period the primary emphasis was on catalyst evaluations. Thus, post-sorbent bed performance must be inferred from analysis at the inlet and outlet of the catalytic oxidizer. The absence of a significant build-up, of these contaminants, in the closed system is taken as an indication that they were being controlled. The only contaminants for which an unacceptably high level is seen are HCl and NO. The impact of adding the second LiOH bed in the pre-sorbent location is shown by the reduced levels of NO and NO_x that occurred subsequent to this.

The selection of lithium hydroxide as the initial post-sorbent bed was based on previous test data which showed that it was a good sorbent for the acid gases HCl, HF and SO_2 . Only limited experience with NO and NO_x indicated that sorption of these gases was poorer. The data taken through 10/25/74 shows that NO and HCl were considerably above the allowable levels. Due to the high catalytic oxidizer inlet levels of these compounds it was reasoned that the post-sorbent performance was lower than desired. One possible explanation was that the elevated temperature at the catalytic oxidizer outlet may reduce the sorbent kinetic reaction rate due to a lowered relative humidity.

TABLE 49
CHEMICAL ANALYSIS RESULTS - BED 1

Contaminant	Sample ⁽²⁾	Day	21	28	35	42	49
		Date	9-27	10-4	10-11	10-18	10-25
Ethane	I		3.1 ⁽¹⁾	2.8	1.5	1.2	Discontinued
	O		0.3	0.4	0.2	0.2	
Acetonitrile	I		3.7	2.9	0.41	0.77	Discontinued
	O		0.4	0.14	0.26	0.23	
Carbon Disulfide	I		2.9	7.2	4.3	.88	Discontinued
	O		1.7	1.0	0.5	.81	
Isopropyl Alcohol	I		2.4	1.3	0.36	0.23	Discontinued
	O		0.05	0.07	0.05	.01	
HF	I		9.5x 10 ⁻⁵	5.5x 10 ⁻³	8.3x 10 ⁻³	2.8x 10 ⁻²	1.4x 10 ⁻¹
	O		1.3x 10 ⁻⁴	4x 10 ⁻³	4.5x 10 ⁻³	5.1x 10 ⁻³	5.0x 10 ⁻³
HCl	I		1.8x 10 ⁻³	9.1		0.50	
	O		2.7x 10 ⁻³	7.4		0.64	
HCN	I			7.2x 10 ⁻²	1.2x 10 ⁻¹	1.1x 10 ⁻¹	9.2x 10 ⁻²
	O			6.4x 10 ⁻³	3.2x 10 ⁻²	7.7x 10 ⁻²	5.2x 10 ⁻²
SO ₂	I		.09	0.87	1.0	0.14	0.01
	O		.12	2.3	2.4	0.25	0.02
NO	I		4.2	7.4	6.7	7.5	
	O		4.6	8.4	7.3	8.6	
NO _x	I		4.6	7.5	7.0	8.1	
	O		7.0	8.9	8.1	9.4	

(1) All concentrations in mg/m³

(2) I = Catalytic Oxidizer Inlet
O = Catalytic Oxidizer Outlet

TABLE 50
CHEMICAL ANALYSIS RESULTS - BED 1 AND 2

Contaminant	Sample ⁽²⁾	Day	Week Ending 11-1								
			11-1		11-8		11-15		11-22		
			Time Period	Early	Late	Early	Late	Early	Late	Early	
HF	I					0.28 ⁽¹⁾	0.15	0.11	0.45	0.14	0.1
	O					0.25	0.70	0.08	0.43	0.16	0.1
HCl	I			0.62	0.26	0.20	0.25	0.44	0.38	0.84	0.70
	O			0.37	0.14	0.16	0.12	0.24	0.34	0.85	0.61
HCN	I			4.0x 10 ⁻²	1.5x 10 ⁻²	5.6x 10 ⁻²	3.2x 10 ⁻²	0.16	0.16	0.28	0.11
	O			2.8x 10 ⁻²	1.5x 10 ⁻²	4.1x 10 ⁻²	4.2x 10 ⁻²	0.12	0.09	0.21	0.11
SO ₂	I			0.01				0.05	0.02		0.01
	O			0.01				0.02	0.02		0.01
NO	I			4.8	5.1		4.9	4.0	5.0		5.6
	O			5.7	6.2		6.0	4.9	5.8		6.6
NO _x	I			5.0	5.2		5.2	4.4	5.2		6.0
	O			6.2	6.5		6.2	5.8	6.0		7.0

(1) All concentrations in mg/m³

(2) I = Catalytic Oxidizer Inlet
O = Catalytic Oxidizer Outlet

It was then decided to load the pre-sorbent bed, bed 2, with lithium hydroxide to assess the effect of a cooler temperature. Loading the pre-sorbent bed, with lithium hydroxide should have confirmed the cool location hypothesis of improved removal efficiency as this system location is cooler and has a higher relative humidity. The data taken through 11/20/74 when the testing of these two beds was terminated showed that two beds with the pre-sorbent bed, in its cooler location did not perform significantly better than the post-sorbent bed alone in its warmer location. As performance was not satisfactory, no attempt was made to resolve the contribution of each bed.

Bed 3 - After testing of LiOH, both beds were emptied and the post-sorbent bed filled with activated carbon treated with 2 milimoles of KOH per gram of carbon. This bed was run from 11/20/74 until 1/31/75 in the closed-loop mode. The selection of this material for test is based upon the high capacity of caustic materials for acid gases. It was felt that potassium hydroxide, the most active of the alkali hydroxides would likely have a greater affinity for moisture which would promote the sorption and reaction of acid gases. Further, suspension of potassium hydroxide on activated carbon should provide a high surface area for reaction and enhanced moisture for reaction.

Figure 81 presents the nitric oxide data taken during testing of beds 1, 2 and 3. It is evident from this figure that the KOH treated activated carbon is more effective than lithium hydroxide for control of nitric oxide. Data taken on chloride, presented in Table 51, shows equilibrium chloride levels when KOH is utilized of the same order as when lithium hydroxide is utilized as a post-sorbent.

The test program to this point was carried out in the closed-loop mode with the fixed bed and simulated cabin volume intact from the previous test. It was felt that contaminants collected in the simulated cabin volume and in the fixed bed could cloud the data on the catalytic oxidizer and post-sorbent bed performance. Furthermore, since at this point the test evaluation of post-sorbent beds was being emphasized, it was felt that open-loop operation with careful, control of feed contaminants would be the best mode of operation. Thus, testing of the KOH-treated charcoal bed in the closed-loop system was terminated.

TABLE 51
BED 3 - CHLORIDE DATA (mg/m³)

Date	Catalytic Oxidizer	
	IN	OUT
11-22	.053	.0095
	.048	
11-25	0.076	0.145
	0.069	0.066
11-26		0.100
12-2	0.83	0.83
	1.80	1.50
12-4	1.05	0.90
	0.88	2.0
12-6	1.52	
	0.35	
12-9		0.48
		0.25
12-10	0.52	0.19
	0.44	0.29
1-24	.004	.3
1-27	.013	.010
1-28	.07	.01
1-29	.004	.004

Bed 4 - Testing of the fourth post-sorbent bed was started on 2/7/75 and completed on 5/7/75. This bed was filled with KOH-treated charcoal. The system was operated in the open-loop mode with room air taken into the system and with the system discharge vented to the roof. The contaminants fed into the system during this test were restricted to hydrocarbons, carbon monoxide and Freon 11 and 12. During this test, data on the quality of room air and outside ambient air was compared. The results showed lower levels of NO_x and trace Freons in outside air. Thus, the test system was modified on 4/14/75 to take in outside air and discharge the system air to the room.

At the start of this run, data was taken with the contaminant feeds off to obtain background data. The results of this testing are presented in Table 52. On 2/24/75 the contaminant feed was started. The HCl and HF data taken is presented in Table 53. A significant change is noted in the data from 3/27/75 onward. This is due to an improved method of sampling. HCl and HF data taken before this date is considered unreliable. The results show removal efficiencies for chloride and fluoride of about 90 and 60 percent respectively.

The data on NO_x is presented in Figure 81. A nominal removal efficiency of about 60 percent is shown during testing with the room-air inlet. After changing to the outside-air inlet, breakthrough was noted. It seems reasonable that the lower inlet concentration resulted in NO_x being desorbed from the bed.

Bed 5 - Post-sorbent bed 5 was filled with KOH-treated charcoal. Testing of this bed was started on 5/7/75 and lasted until breakthrough of NO_x was noted. The test was terminated on 7/18/75.

Initially, the contaminants introduced were hydrocarbons, carbon monoxide, and Freon 11 and 12 at the low rates. On 5/21/75, addition of acetonitrile and carbon di-sulfide was also started at the low introduction rates. Those liquid contaminants were fed by motorized syringe into the inlet of the regenerable bed canister which was empty. These contaminants were not monitored as the earlier tests demonstrated their control. The purpose was to give a more accurate simulation of actual oxidizer outlet conditions.

TABLE 52
BACKGROUND CONTAMINANT DATA
OXIDIZER OUTLET

Contaminant	Analysis Date	Contaminant Concentration
NO	2-14, 2-19	.2 mg/m ³ , .22 mg/m ³
NO _x	2-14, 2-19	.4 mg/m ³ , .31 mg/m ³
HCl	2-11, 2-12	.098 mg/m ³ , .084 mg/m ³
HF	2-10, 2-11, 2-12	.002 mg/m ³
SO ₂	2-12, 2-13	.008 mg/m ³
HCN	2-12, 2-13	.001 mg/m ³

The chloride and fluoride data taken during this run is presented in Table 54. This table shows increased consistency of data which is a result of the improved analysis techniques. Removal efficiencies for chloride and fluoride are about 80 and 40 percent respectively. This is consistent with the performance of bed 4. It should be noted that this bed was not tested to breakthrough for these materials.

The data on control of NO_x is shown in Figure 81. Breakthrough of the bed was first noted on 7/8/75. Testing was continued until 7/18/75 to confirm the breakthrough data.

Data was gathered on the post-sorbent bed's ability to control sulfure dioxide from 6/2/75 through 6/25/75. This data is presented in Table 55. The table shows that SO₂ is controlled to a concentration below the allowable level.

TABLE 53
BED 4 - SUMMARY OF CHLORIDE AND FLUORIDE DATA

Date	Catalytic Oxidizer Outlet		Post-Sorbent Outlet	
	Cl ⁻	F ⁻	Cl ⁻	F ⁻
2-24	-	-	.037	-
2-25	-	.002	-	.002
2-26	-	-	.029	-
2-27	-	.002	-	.002
2-28	.003		.057	-
3-3	.004		.004	
3-4		.002		.002
3-5	.006		.006	
3-6		.003		.003
3-7	.005		.006	
3-10	.062		.076	
3-11		.004		.005
3-12	.072		.157	
3-13		.006		.006
3-14	.104		.073	
3-17	.034		.001	
3-18		.001		.001
3-19	.030		.010	
3-20		.001		.001
3-21	.053		.060	
3-24	.046		.053	
3-25 ¹	.110	.001 .048		
3-26 ²	0.9	.086		

Data in mg/m³

1 Started use of polyflow sample line close coupled to sample point.

2 Started use of polyethylene bubbler for fluoride samples.

TABLE 53 (continued)

Date	Catalytic Oxidizer Outlet		Post-Sorbent Outlet	
	Cl ⁻	F ⁻	Cl ⁻	F ⁻
4-1			0.04	
4-2	1.39	0.083		0.008
4-3	1.33	0.150		
4-4	1.33	0.203		
4-7			0.13 ⁴	0.003
4-8			0.021	0.002
4-9			0.019	
4-10			0.104	0.001
4-11			0.033	0.008
4-14				
4-17	0.162	0.18 ⁴		
4-21	0.093			
	0.150			
4-22		0.400	0.091	0.33 ⁴
4-23	0.172		0.042	
4-24		0.144		0.087
4-25	0.106		0.013	
4-28	0.71		0.17 ⁴	
4-29		0.170		.057
4-30	0.97		0.133	
5-1		0.110		0.084
5-2	0.920		0.150	
5-5	0.74		0.21	
5-6		0.18		0.095
5-7	1.07		0.05	

TABLE 54

BED 5 - SUMMARY OF CHLORIDE AND FLUORIDE DATA

Date	Cat.	Oxid.	Outlet	mg/m ³	Post-Sorb.	Outlet	mg/m ³
	Cl		F	Cl			F
5-8				0.17			0.10
5-9		0.75				0.07	
5-12		0.97*					0.15
		0.88					
5-14		0.96				0.10	
5-15				0.14			0.08
5-16		1.05				0.04	
5-19		1.90				0.19	
5-20				0.17			0.05
5-21		2.95				0.17	
5-22				0.22			0.09
5-23		3.03				0.98	
5-27		1.42				0.15	
5-28				0.16			0.11
5-29		1.32				0.25	
5-30				0.15			0.08
6-2		1.24				.15	
6-4				.15			.07
6-5		1.28				.28	
6-9		1.53				.23	
6-10				.16			.08
6-13		1.93				.30	
6-16		1.23				.30	
6-17				.11			ND
6-19		1.22				.22	
6-23		1.26				.09	

*One sample was taken - analyzed on 5-12, sample taken was analyzed 5-19.

TABLE 54 (continued)

Date	Cat. Oxid. Outlet mg/m ³		Post-Sorb. Outlet mg/m ³	
	Cl ⁻	F ⁻	Cl ⁻	F ⁻
6-24		.12		
6-27	1.04		.21	
6-30	1.43		.18	
7-1		.06		.013
7-8	1.32		.20	
7-9		.20		.14
7-11	1.18		.38	
7-14	1.51		.12	
7-15		.12		.14
7-18	1.51		.51	

TABLE 55

BED 5 - SUMMARY OF SO₂ DATA

Date	Cat. Oxid. Outlet mg/m ³	Post-Sorb. Outlet mg/m ³
6-2		.18
6-4	.15	.05
6-4	.08	.004
6-11	.005	.005
6-12	.008	
6-18	ND	
6-19		ND
6-25	.09	.06

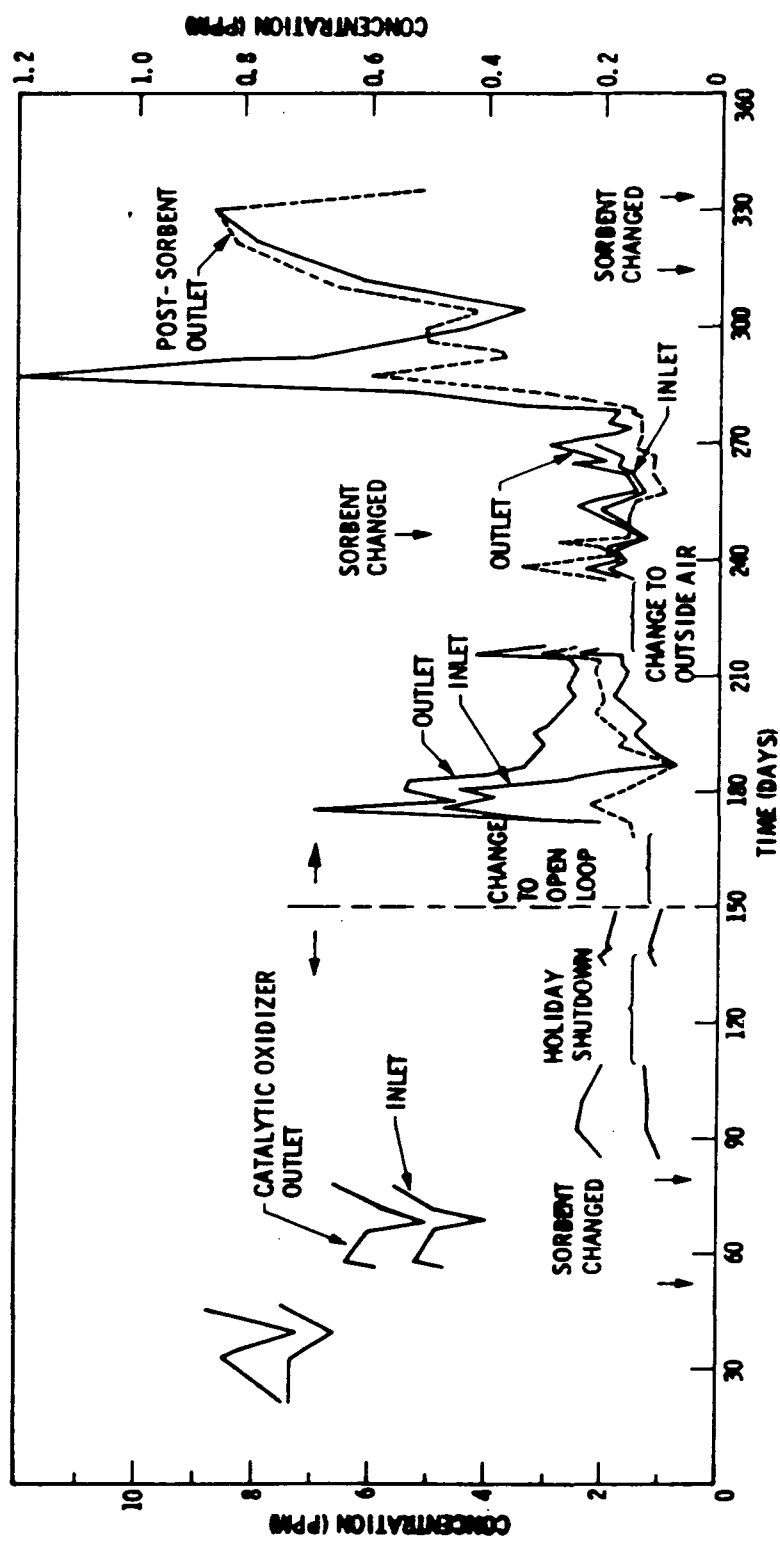


Figure 81 NO Concentration vs Time

Bed 6 - Initial tests carried out with a lithium hydroxide post-sorbent bed were in the closed loop mode and used analysis techniques for chloride and fluoride which yielded questionable results. In order to obtain improved data on the performance of lithium hydroxide, the post-sorbent bed was loaded with lithium hydroxide and a test of bed 6 was started in the open-loop mode on 7/21/75. All contaminants were introduced into the system at the low introduction rates. Breakthrough of NO_x was immediate. Thus, the test was stopped on 8/1/75 after limited gathering of data on chloride.

Table 56 presents the chloride data from this test. It shows control of chloride with an 80 percent removal efficiency. The nitrogen breakthrough is shown at the end of Figure 81.

TABLE 56
BED 6 - SUMMARY OF CHLORIDE DATA

Date	Catalytic Oxidizer Outlet (mg/m^3)	Post-Sorbent Outlet (mg/m^3)
7-28	1.25	.20
7-29	1.31	.21
7-30	1.46	.42
7-31	1.24	.15

Bed 7 - Review of the literature showed that potassium permanganate should be a good chemical for removal of NO_x . Purafil is about 5 percent permanganate on alumina. Manufacturers data on Purafil does not indicate good removal for oxides of nitrogen. However, the indicated possible use of this material from the literature resulted in the final test bed which was filled with Purafil. Bed 7 was started on 8/1/75. All contaminants were introduced at the low introduction rates. The test ended on 9/11/75 when one of the leads to the catalytic oxidizer heater failed.

The efficiency of Purafil for removal of NO_x exceeded 95 percent. No data on other contaminants was gathered due to the heater failure.

Throughout the test chemical analyses were carried out to characterize the performance of the catalytic oxidizer and post-sorbent bed. The characterization of the post-sorbent bed is based upon data for HCl, HF, NO, NO_x , SO_2 , CN. In the following section the results for each of these materials are discussed.

HCl and HF - The data taken on HCl and HF was presented in Tables 49 to 54 and 56. Initially the system was monitored only across the catalytic oxidizer inlet and outlet. However, starting with the test of bed 3, the test points were moved to include the post-sorbent bed inlet and outlet.

The analysis technique used to monitor these two materials was to bubble a measured quantity of sample gas through a measured quantity of water. The chloride and fluoride is absorbed in the water from the gas stream. The halogen content of the water is then measured and the results converted to milligram per cubic meter in the gas phase. During tests on beds 1 and 2 the gas was drawn through the gas monitoring console and the halogen content measured using the Orion specific ion electrode instrument. This operates satisfactorily at high concentrations (i.e. over 10 ppm) but is near the limit of its sensitivity at concentrations encountered in the TCCS. In January of 1975 the Orion calibration procedure was improved. This resulted in a significant drop in concentration levels. Thus, it is concluded that values reported during the tests of beds 1 through 3 are high. Further, work with a colormetric analysis technique showed better results than with the Orion. Thus at the start of testing on bed 4, the chloride analysis technique was much improved.

The data taken from 2-24-75 through 3-24-75 shows considerably less chloride at the catalytic oxidizer outlet than was anticipated based on a mass balance. Thus, the gas sampling console was eliminated and gas samples were drawn from the system through short sections of polyflow line. In addition fluoride samples were taken with polyethylene bubblers. After 3-26-75, when these changes were completed, the data became more consistent. Further, although a mass balance cannot be achieved, the results are within reason.

It can be concluded, based upon the data from 3-26-75 through the end of the test, that chloride can be removed by either a lithium hydroxide or base treated charcoal post-sorbent with greater than 80 percent efficiency.

Fluoride removal in the order of 50 percent is indicated. Due to the large capacity of the caustic beds for halogenated hydrocarbons and a desire to define a method for control of NO_x , none of the beds were tested to breakthrough for HCl or HF. However, based on chemical quantity, it is assumed that any of the chemical beds would be acceptable for an extended period.

Purafil which worked best for NO_x was not tested for halogen control as the test was aborted due to a heater failure in the catalytic oxidizer.

NO/NO_x - A major desire in the test program was the selection of an effective method of control for oxides of nitrogen generated in the catalytic oxidizer. The concentrations of these gases is well within the range of the analytical instruments and the data is considered reliable. In the testing of the lithium hydroxide post-sorbent bed in closed loop operation, a high equilibrium cabin level of NO_x is noted in Figure 81. This is a direct indication of poor control of this compound by LiOH. The addition of the second LiOH bed in the cooler location resulted in a lower NO_x level. However, the gain was small when one considers that the chemical quantity was more than doubled.

Improvement is noted when the KOH treated charcoal bed, bed 3, data is examined. In order to obtain improved data on KOH treated charcoal open-loop tests were run on beds 4 and 5. The data from bed 5 shows an NO_x removal efficiency of about 50 percent.

The tests carried out on bed 7, Purafil, showed extremely high removal efficiency however a heater failure prevented completion of this test to breakthrough.

It can be concluded that Purafil is the optimum material for NO_x control, KOH treated charcoal is effective and that LiOH should not be used. The capacity of Purafil for NO_x can be estimated based on a chemisorption of one mole of gas per mole of permanganate. Purafil has a 5 percent loading of permanganate on alumina.

Sulfur Dioxide - Initially tests on beds 1 and 2 indicated that warm lithium hydroxide was not effective for removal of SO_2 . When additional LiOH was added in the cooler location, the SO_2 level dropped to very low levels and stayed there. It can thus be concluded that either LiOH in a cool location or the KOH treated charcoal is a satisfactory SO_2 sorbent. During the tests on bed 6, SO_2 was again monitored. The results indicate control. However concentration levels were so low that an estimate of removal efficiency is not feasible.

Cyanide - CN showed a high level when the warm lithium hydroxide post-sorbent was utilized. When the cooler LiOH was added in a different location, a sharp drop was noted, followed by a subsequent climb. The cyanide level was the lowest with the base treated charcoal. These levels were below 0.07 mg/m^3 .

10.2 Vacuum Venting Analysis

The potential problem of condensation of venting contaminants on spacecraft external surfaces was investigated. The study was performed in three steps: (1) determining the rate and rate profile of the contaminants vented from the regenerable charcoal bed; (2) determining the contaminant gas exhaust flow field characteristics for the plume from the exhaust nozzle; and (3) calculating the amounts possibly deposited on spacecraft surfaces. It is concluded that venting of the regenerable bed will pose no problems related to adverse effects on spacecraft thermal control surfaces. There are no problems related to optical surfaces or external instruments if reasonable care is taken in locating the vent relative to these sensitive surfaces.

10.2.1 Contaminant Gas Vent Rate

The regenerable bed is desorbed to space vacuum periodically to vent contaminants adsorbed on the charcoal. The desorption is carried out at elevated temperatures on a regular cycle.

The program DESORB tracks the desorption cycle with time. The input data to DESORB includes the list of contaminants entering the regenerable bed at the mission time being evaluated, the saturated zone size for each contaminant as defined by CHAR, the data on contaminants including vapor pressure as a function of temperature, and the data on the desorption cycle including temperature profile, desorption time, and vacuum duct loss factors. Data on the bed design factors is also required. DESORB then calculates, in an incrementing manner with time, the quantities of each contaminant remaining on the bed and the total bed pressure as a function of time.

The calculational procedure used in ICHAR was described in Section 9.2.3.1.

The calculational procedures used in DESORB are as follows:

From the definition of the potential parameters,

$$A = \frac{T}{V_m} \log \frac{P^0}{P_i}$$

$$P_i = P^0 \cdot 10^{-(AV_m/T)}$$

Knowing P_i for each contaminant, the total properties of the gas in the bed can be defined as:

$$P = \sum P_i$$

$$MW = \sum \frac{(MW_i) (P_i)}{P}$$

As contaminants are discharged to space vacuum, we have a situation where choked flow will exist in the discharge duct. Using the equations for the Fanno line, we must solve for the mass flow in the outlet (vent) duct.

$$W = \frac{(S)(P)(MW)^{.5}}{T^{.5}} \left(\frac{k}{R} \right)^{.5} M \left(1 + \frac{k-1}{2} M^2 \right)^{.5}$$

where: S = Duct Area (ft^2)

P = Duct inlet pressure (bed pressure) psf

MW = Gas molecular weight

T = Gas temperature ($^{\circ}\text{K}$)

k = Gas C_p/C_v

R = Universal gas constant

M = Mach number

The Mach number can be defined, if equations for adiabatic constant - area flow for a perfect gas is assumed, from the following:

$$\frac{4fL}{D} = \frac{1-M^2}{kM^2} + \left(\frac{k+1}{2k} \right) \ln \frac{(k+1)M^2}{2 \left(1 + \frac{k-1}{2} M^2 \right)}$$

where $4 fL/D$ is the duct loss factor.

It can be seen that all terms required to calculate the flow out from the bed are available.

Once the vent flow W is known, the vent flow for each contaminant over a time increment can be defined as:

$$W_i = W \left(\frac{MW_i}{MW} \right) \Delta \tilde{\tau}$$

where $\tilde{\tau}$ = time increment.

The remaining mass of each contaminant after $\Delta\tau$ is:

$$WR_i = WI_i - W_i$$

where WR_i = mass remaining

WI_i = mass initial

W_i = mass vented

Assuming that the desorption of the carbon is uniform, a new q may be calculated from

$$q = \frac{WR_i}{WCi}$$

where WCi = carbon saturated zone mass for i . The new q leads to a new A and the sequence is repeated until $\sum \Delta\tau$ = Total time at vacuum.

Analytical Basis

An equilibrium exists between a contaminant adsorbed on activated carbon and that contaminant in the gas phase around the carbon. The equilibrium is described by the potential plot. This plot relates the capacity of carbon for a contaminant (q) in cc/gram to the potential parameter A .

where: $A = (T/V_m) \log P^0/P_i$

T = charcoal temperature (0K)

V_m = contaminant molecular volume (cc/gm mol)

P^0 = contaminant vapor pressure at T

P_i = contaminant partial pressure at charcoal surface

During adsorption, a contaminant enters the bed with some partial pressure, or concentration, P_i . This contaminant is adsorbed on the carbon up to a capacity q as defined by the potential plot (q vs A) for the carbon being used. Considering that the bulk of the adsorbed contaminant lies in the saturated zone we see that at the end of the desorption cycle, the carbon is loaded to a level of q , as defined by P_i , for each contaminant. Further, the quantity of carbon which is loaded to q for each contaminant is defined by the mass of the saturated

zone as calculated by the CHAR program. Additionally, it can be shown that the total mass of the contaminant adsorbed on the carbon must be the generation rate times the removal efficiency of the bed. That material passing through the bed will be destroyed in the catalytic oxidizer. With this equilibrium and initial loading as a basis, the desorption of the carbon is now considered.

During desorption the bed is isolated from the cabin, then preheated before venting is started. At that point in time where the vacuum valve is first opened we can calculate the partial pressure for each contaminant as follows.

- o q is unchanged as all conditions are the same as at the end of the desorption cycle.
- o A is unchanged as the potential plot defines it uniquely as a function of q .
- o P^0 has changed as the desorption temperature is higher than the adsorption temperature.

DESORB

In the operation of the program DESORB a list of contaminants including all contaminant data and the charcoal required to control each is generated using CHAR. This data is loaded as a block input. In addition, the charcoal A vs q data and vapor pressure equation constants are loaded as a block. The following individual inputs are requested by the program.

- o Source of contaminant data (file)
- o Source of charcoal data (file)
- o Desorption temperature ($^{\circ}$ F)
- o Bed size (lbs)
- o Removal efficiency (Decimal)
- o Charcoal treatment (phosphoric acid Yes or No)
- o Total cycle time (hrs)
- o Desorption time (minutes)
- o Duct loss factor (4 fl/D)
- o Duct area (ft^2)

The program then commences calculation. The calculations are incremental in nature. The total desorption time is divided into a number of time increments and the initial value of each contaminant adsorbed on the carbon is calculated.

$$(1) MI_i = MR_i = M(\text{gm/day}) \times (\text{efficiency}) \times T(\text{hours/cycle})$$

The parameters of each time increment are then calculated as follows:

I - For each contaminant

$$q = \frac{MR_i}{WC_i}$$

A for potential plot

P^o from vapor pressure equations and input constants

$$P_i = P^o \times 10 \exp (- A_i V_m / T)$$

II - For the total bed

$$P = \sum P_i$$

$$MW = \sum \frac{MW_i P_i}{P}$$

$$\frac{4fL}{D} = \frac{1 - M^2}{kM^2} + \left(\frac{k+1}{2k} \right) \ln \frac{(k+1)M^2}{2(1 + \frac{k-1}{2} M^2)}$$

$$W = \frac{SP(MW) \cdot 5}{T \cdot 5} \left(\frac{k}{R} \right) \cdot 5 M \left(1 + \frac{k-1}{2} M^2 \right) \cdot 5 \Delta \tau$$

III For each contaminant

$$W_i = (W) \left(\frac{MW_i}{MW} \right) \quad (\text{removed})$$

$$WR_i = WR_i - W_i \quad (\text{remaining})$$

The procedure then returns to I and continues until

$$\sum \Delta \tau = \text{desorption time}$$

In this manner all pertinent desorption parameters are developed as a function of time.

Program Limitations

The DESORB program as it currently exists incorporates some simplifying assumptions which reduce the accuracy of the results. These assumptions considerably reduced the program complexity and reduced the development time. However, the effects are second order and should not significantly alter the program results.

These assumptions are:

- o Equilibrium exists between the adsorbed and desorbed phases as defined by the potential plot.
- o Effects of pressure drop in the bed are not included.
- o There is no diffusion of contaminants to the outlet end of the bed.
- o Desorption is at a constant temperature.
- o No heat transfer effects are included.
- o Water adsorption is not included.
- o C_p/C_v is not varied with gas composition.
- o No leakage is included.

These assumptions can be conveniently grouped into three categories.

Item 1 and 2 relate to the actual dynamics of the process. It seems likely that some hysteresis exists between the adsorption and desorption of the charcoal, and that during the initial heat-up phase of desorption, some contaminant will pass through the charcoal toward the outlet end of the bed. The effect of a non-equilibrium condition will tend to depress the vapor pressure. A computer run made to check these possible effects shows that if the equilibrium vapor pressure is only 90 percent of the calculated value the desorption will proceed to within one percent of the equilibrium level. Transfer of mass to the outlet end of the bed will, with time load the entire bed to some threshold level. The result of this effect would be to cause a steady rise in outlet concentration levels during the adsorption cycle. Extended test operation demonstrates that there is no such upward trend in outlet concentration; thus, this effect is shown to be minimal.

Contaminants being desorbed from the carbon within the bed must pass out through the bed. There will be a resulting pressure loss and as a result the final equilibrium will be lower at the inlet of the bed and higher at the inside end of the saturated zone. Estimates of pressure loss in the venting process suggest that the outlet duct is the dominant factor making the assumption of a zero bed loss reasonable. The structure of the program permits including bed loss factors, if deemed necessary, at some future date.

The current program makes all desorption calculations at a constant inputed temperature. However, provision has been made for input of a temperature profile or temperature calculation by a subprogram. During the 180 day extended test, desorption temperature did not vary over a wide range and the program should give a valid indication of performance.

The effects of heat transfer and water could also be included. The heat transfer is composed of four dominant terms which are:

- o Energy input
- o Insulation
- o Thermal mass
- o Desorption energies

After the system reaches temperature during the initial heating, the power is reduced to just provide for the insulation loss. This results in a nearly steady temperature profile. As a result, little need for heat transfer calculations was seen. If a different power schedule were used a subprogram could be written for heat transfer calculations.

The major desorption thermal transient effect is due to water desorption. Most contaminants are adsorbed at a very low level. As a result the total desorption energies are trivial. Water is an exception. Early in desorption large quantities of water are lost resulting in a rapid drop in bed temperature from the final preheat level to the new steady desorption level. Equilibrium

isotherms for water on carbon and desorption energies are available and thus water could be programmed in as just another contaminant. The heat transfer calculations could include the water desorption effects. Insufficient time resulted in eliminating this feature. However, the 180 day test shows this transient period of temperature to be very short and likely to be unimportant.

A second effect of including water would be on the bed pressure. As the mass flow from the bed is directly proportional to pressure and as the quantity of a contaminant lost in time increment is directly proportional to its partial pressure fraction, it can be seen that the effect of total pressure drops out. Thus, the absence of water and leakage air is justifiable on the basis of having no effect on the desorption of contaminants.

The final assumption of constant $k (C_p/C_v)$ was checked with the program. During the desorption process, the gas composition changes with time. As a result k used in the mass flow equations will also change. A value of 1.4 is used in the program. During adsorption k may possibly vary from 1.1 to 1.4. Runs made at 1.2 and 1.4 show no difference in final equilibrium levels and only a slight difference in final pressure levels. The lower k , likely for hydrocarbons, at the end of desorption shows about a 0.5 percent lag time in desorption performance. This slight effect and great difficulty in calculating a composite k makes this assumption justifiable.

Finally no leakage effects are included. In spacecraft operation gas loss through leakage will be minimized and thus was not considered.

Program Runs

For the development of the program and initial system evaluations using the program, a contaminant list was generated. This list is based upon the low introduction rate specification used in the long-term test. The list and corresponding data is presented in Table 57. As previously discussed, data

Table 57
Contaminant Input Data

Index	Name						
Rate	MAC	RHO	VM	MW	PO	Code	
001	Benzene						
.900-01	.300+01	.870+00	.781+02	.960+02	.390+06	2	
002	Toluene						
.250+00	.750+02	.780+00	.920+02	.118+03	.142+06	2	
003	Pyruvic Acid						
.126+01	.900+00	.106+01	.881+02	.870+02	.471+05	1	
004	F11						
.250+00	.280+02	.150+01	.138+03	.880+02	.587+07	2	
005	F12						
.250+00	.300+03	.150+01	.121+03	.750+02	.284+08	2	
006	Methyl Alcohol						
.251+00	.390+01	.750+00	.320+02	.420+02	.134+06	1	
007	Acetone						
.102+01	.710 03	.750+00	.581+02	.770+02	.714+06	1	
008	Methyl Acetate						
.250+00	.300+02	.880+00	.741+02	.850+02	.414+06	2	
009	MEK						
.250+00	.590+02	.810+00	.721+02	.970+02	.370+06	2	

INDEX	A program location number
Rate (gm/day)	Contaminant generation rate
MAC (mg/m ³)	Maximum allowable concentration
RHO (gm/cc)	Liquid density
MW	Molecular weight
VM (cc/gm)	Molecular volume
PO (mg/m ³)	Vapor pressure at 100 F
CODE	Solubility Code 1 = soluble 2 = insoluble

on the saturated zone mass is required. The program CHAR was run using the list presented in Table 57 and the saturated zone masses are given in Table 58. Table 57 gives the vapor pressure of each contaminant at 311 K (100 F), the adsorption temperature. Vapor pressure at the desorption temperature was calculated using the vapor pressure constants presented in Table 59. Using the following equations:

o IF $A = 0$

$$\log P(\text{mmHg}) = A - \frac{B}{(C+t)} \quad \text{where } t \text{ is degrees C}$$

o IF $A = 0$

$$\log P(\text{mmHg}) = \frac{-52.23B}{T} + C \quad \text{where } T \text{ is degrees K}$$

An estimate of the vacuum ducting and valve pressure loss factors was made. The total loss should be in the range of $4fL/D = 0.05$ to 0.5 based on an area of 10 cm^2 (.02 ft²). The test bed had a mass of 6.15 kg (13.5 lb) and was desorbed for a period of 160 minutes over 24 hours. The charcoal was not acid treated and had a removal efficiency of 90 percent.

Using these inputs, several program runs were made to determine the effects of desorption temperature and duct loss factors on the desorption cycle, as shown below:

<u>Temperature</u>	<u>Loss Factor</u>
200°F	5
250	5
300	5
200	.5
200	.05
250	50
250	.5
250	.05

The program runs show that the desorption performance is most sensitive to temperature and, to a much lower extent, discharge duct pressure loss factors. The data shows that, for the test system, desorption is accomplished in 160 minutes and 367 K (200 F) to a satisfactory level. This was verified by the long-term test. It also shows that complications of the vacuum system

Table 58
 Saturated Zone Mass (Sum)
 Output Summary

Regenerable Bed 24 Hours Cycle 3.0 Hours Desorption
 Temp = 100 F Dacrit = 16 Bed Efficiency = .900
 Untreated Charcoal

Index	Name	Mass	Sum
002	Toluene	.4283+01	.4283+01
001	Benzene	.8123+01	.1241+02
003	Pyruvic Acid	.3990+01	.1640+02
009	MEK	.2055+01	.1845+02
008	Methyl Acetate	.1743+02	.3588+02
004	F11	.2949+02	.6537+02
007	Acetone	.7878+02	.1442+03
005	F12	.2822+03	.4263+03
006	Methyl Alcohol	.2020+04	.2446+04

NOTE: SUM (gm) Mass of charcoal required for control of a contaminant
 saturated zone size: used as an input to DESORB.

Table 59
Vapor Pressure Constants

Contaminant	Constants		
	A	B	C
Benzene	6.90565	1211.033	220.79
Toluene	6.95464	1344.80	219.482
F-11	0	.2E+8	-3019.7
F-12	0	.161895E+8	-2417.56
MeOH	7.87863	1473.11	230
Ac	7.02447	1161	224
MeAc	7.20211	1232.83	228
MEK	6.97421	1209.6	216
Prop	6.81960	785	247
F-22	0	.2427E+8	-2398.78
Propane	6.82973	813.2	248
Water	0	.52385E+9	-5029.14

If A ≠ 0

$$\log_{10} P = A - B/(C + t)$$

where $t = {}^{\circ}\text{C}$

$P = \text{mmHg}$

If A = 0

$$P = (B) (10 \exp (C/T))$$

where $T = {}^{\circ}\text{K}$

$P = \text{mmHg}$

due to interface requirements would likely require a higher desorption temperature or a longer desorption time. The condition analyzed for the vacuum venting analysis was 395 K (250 F) bed temperature and a duct loss factor of 5. Table 60 gives the results. Other program runs at k of 1.2 rather than 1.4, and at a desorption vapor pressure of 90% of that predicted by the potential plot showed that these are second order effects.

10.2.2 Contaminant Gas Exhaust Plume Analysis

The flow field produced by venting contaminants from the regenerable charcoal bed was determined using a Method-of-Characteristics analysis. The Method-of Characteristic solution predicts the inviscid jet-plume flow field. The MOC program (Ref. 8) currently in use at IMSC is a versatile computer program capable of treating two-dimensional/axisymmetric ideal or reacting gas system, as well as accommodating a variety of boundary conditions. Furthermore, the program contains options for nozzle boundary-layer and continuum to free-molecular transition considerations. In the latest version of the MOC program, a coupled two-phase plume solution is also incorporated to permit accurate predictions of gas-particle plume flow fields. The gases are vented to space through a 2 in. (5 cm) duct at the flow rates shown in Table 61. The solution is applicable to supersonic, axisymmetric continuum flow of an ideal gas with $k = 1.4$. The analyses were performed for three time intervals, 0.02 - 0.03 min., 1.04 - 1.12 min., and 145.6 - 153.6 min. The mass flow rate for each contaminant, and the equivalent gas constant and molecular weight are shown for each case on Table 61.

Mass flow rate at the start of desorption is several orders-of-magnitude larger than the average throughout the desorption period. Thus to analyze potential deposition problems, we may concentrate on the initial period, or .02 to .03 minutes. The mass flow, static pressure, Mach number and heating rate contours are shown in Figures 82 to 85 for this case. Consider the contour labeled S in Figure 82. This is the locus of points at which the mass flux is $2.6 \times 10^{-8} \text{ gm/cm}^2\text{-sec}$. Surfaces located perpendicular to this contour would be subjected to this desorption rate.

Table 60
180 Day Test System Desorption Analysis

Time	CONTAMINANTS								
	MEOH	MEAC	AC	F12	TOL	MEK	BENZ	F11	PRESS
.02	.225	.224	.915	.225	.225	.225	.081	.225	1269
.03	.223	.224	.913	.225	.224	.224	.081	.225	1261
.05	.222	.223	.910	.224	.224	.224	.081	.224	1252
.06	.221	.223	.908	.224	.223	.224	.081	.224	1244
.08	.219	.222	.905	.224	.223	.223	.081	.224	1236
.16	.213	.219	.893	.223	.220	.222	.080	.223	1196
.24	.207	.216	.881	.222	.218	.220	.080	.222	1159
.32	.200	.214	.980	.221	.215	.219	.079	.221	1125
.40	.195	.211	.859	.221	.213	.218	.079	.220	1092
.48	.189	.208	.848	.220	.211	2.16	.078	.219	1062
.56	.183	.206	.838	.219	.209	.215	.078	.218	1034
.64	.178	.203	.828	.218	.206	.213	.078	.217	1007
.72	.172	.201	.819	.217	.204	.212	.077	.217	981
.80	.167	.199	.809	.216	.202	.210	.077	.216	957
.88	.162	.196	.801	.215	.200	2.09	.077	.215	934
.96	.157	.194	.892	.215	.198	.208	.076	.214	913
1.04	.152	.192	.783	.214	.196	.206	.076	.213	892
1.12	.148	.190	.775	.213	.194	.205	.075	.212	872
1.20	.143	.188	.767	.212	.192	.204	.075	.211	853
1.28	.138	.186	.760	.211	.190	.202	.075	.211	836
1.36	.134	.184	.752	.210	.188	.201	.074	.210	818
1.44	.130	.182	.745	.210	.186	.200	.074	.209	802
1.52	.125	.180	.738	.209	.184	.198	.074	.208	786
1.60	.121	.178	.731	.208	.183	.197	.073	.207	771
9.60	.000	.074	.363	.145	.089	.109	.051	.154	169
17.60	.000	.042	.218	.100	.068	.080	.039	.123	72
25.60	.000	.032	.166	.074	.057	.066	.031	.103	41
33.60	.000	.025	.133	.060	.049	.057	.025	.088	29
41.60	.000	.019	.110	.050	.043	.049	.021	.075	22
49.60	.000	.015	.091	.043	.038	.042	.019	.064	18
57.60	.000	.013	.076	.036	.034	.037	.017	.055	15
65.60	.000	.011	.064	.031	.030	.032	.015	.049	11
73.60	.000	.010	.055	.027	.027	.029	.014	.044	8
81.60	.000	.009	.049	.023	.025	.026	.013	.040	6
89.60	.000	.008	.045	.020	.023	.024	.012	.037	5
97.60	.000	.007	.041	.018	.022	.023	.012	.035	4
105.60	.000	.007	.037	.016	.021	.021	.011	.032	4
113.60	.000	.006	.034	.015	.020	.020	.010	.030	3
121.60	.000	.005	.032	.013	.019	.019	.010	.029	3
129.60	.000	.005	.029	.012	.019	.018	.009	.027	3
137.60	.000	.005	.027	.011	.018	.017	.009	.025	2
145.60	.000	.004	.025	.011	.017	.017	.008	.024	2
153.60	.000	.004	.024	.010	.017	.016	.008	.023	2

NOTE: Time in minutes

Desorption temperature = 250

Pressure in mmHg

Duct loss factor 4 fL/D = 5

Other data residual grams

Table 61

Contaminant Gas Flow Rates

Case	Time Interval (min)	Mass Flow (gm/min)						Gas Constant (Rt 1b K)
		Methyl Alcohol	Methyl Acetate	Acetone	Freon-12	Toluene	Methyl Ethyl Ketone	
1	0.02-0.03	0.20		0.20		0.10	0.10	0.60
2	1.04-1.12	0.050	0.025	0.100	0.0125	0.0125	0.0125	23.8
3	145.6-153.6			0.000125	0.000125	0.000125	0.000125	22.0
							0.00050	18.6

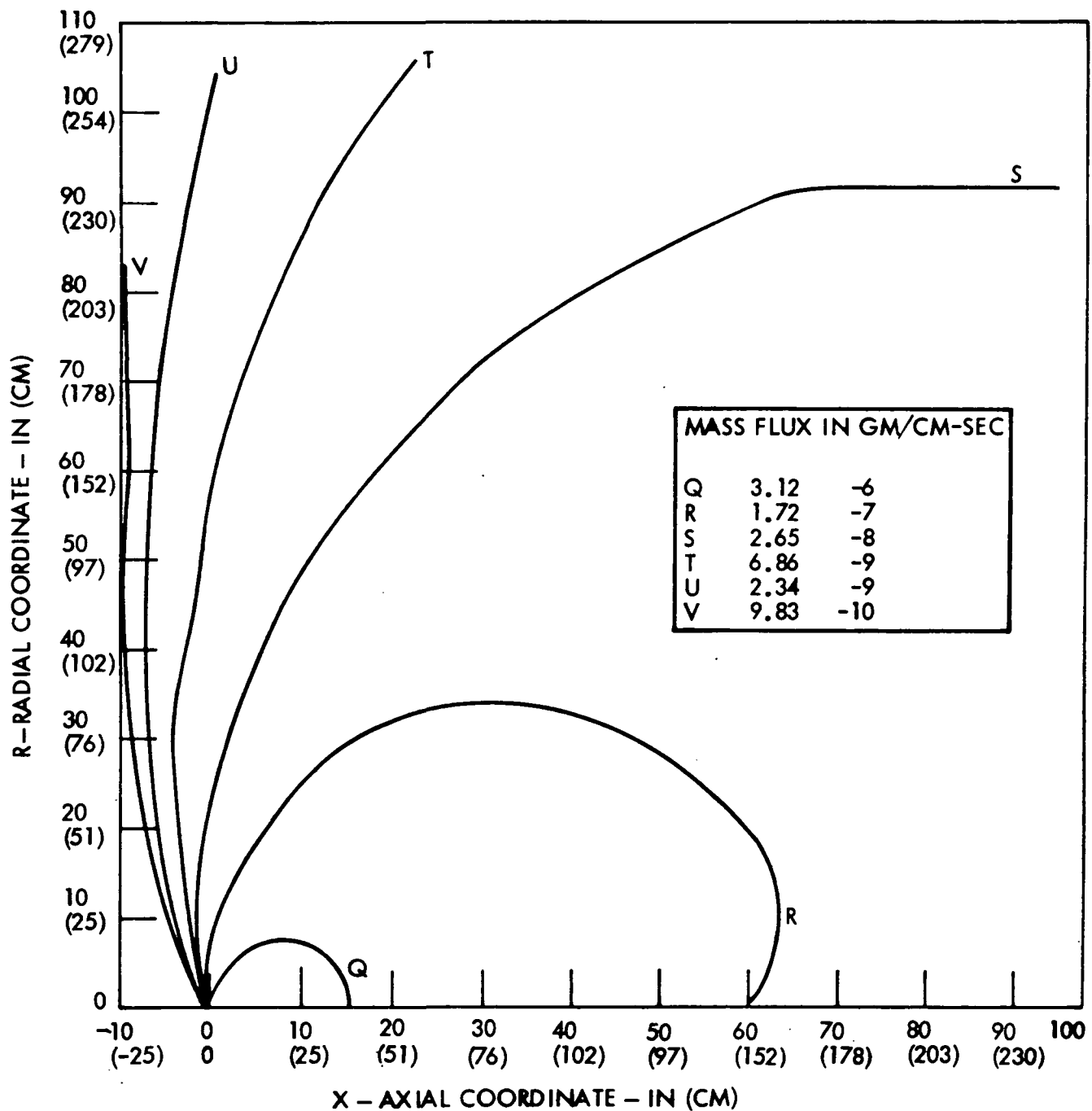


Figure 82 Contaminant Venting - Constant Mass Flux Contours

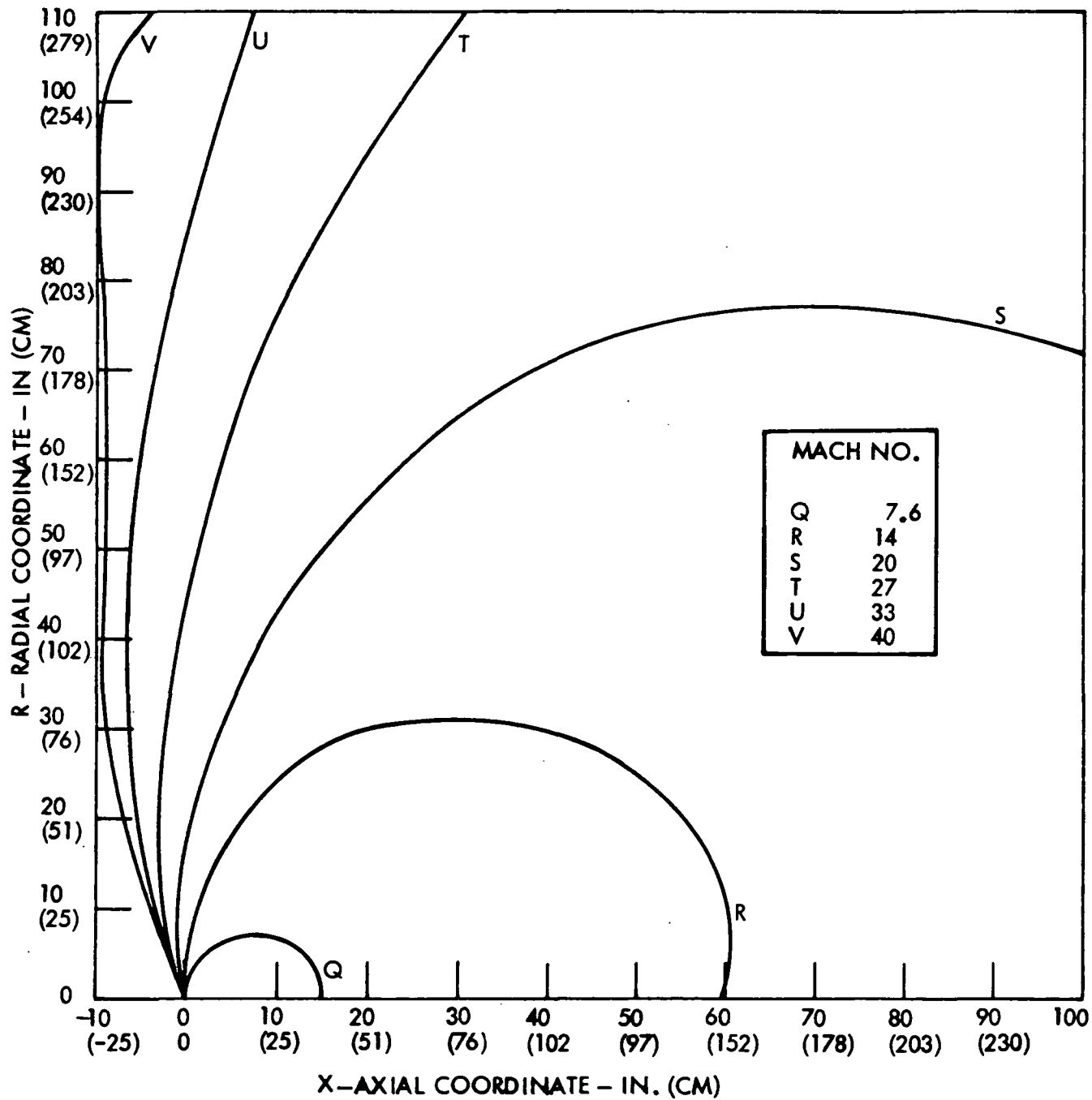


Figure 83 Contaminant Venting - Constant Mach No. Contours

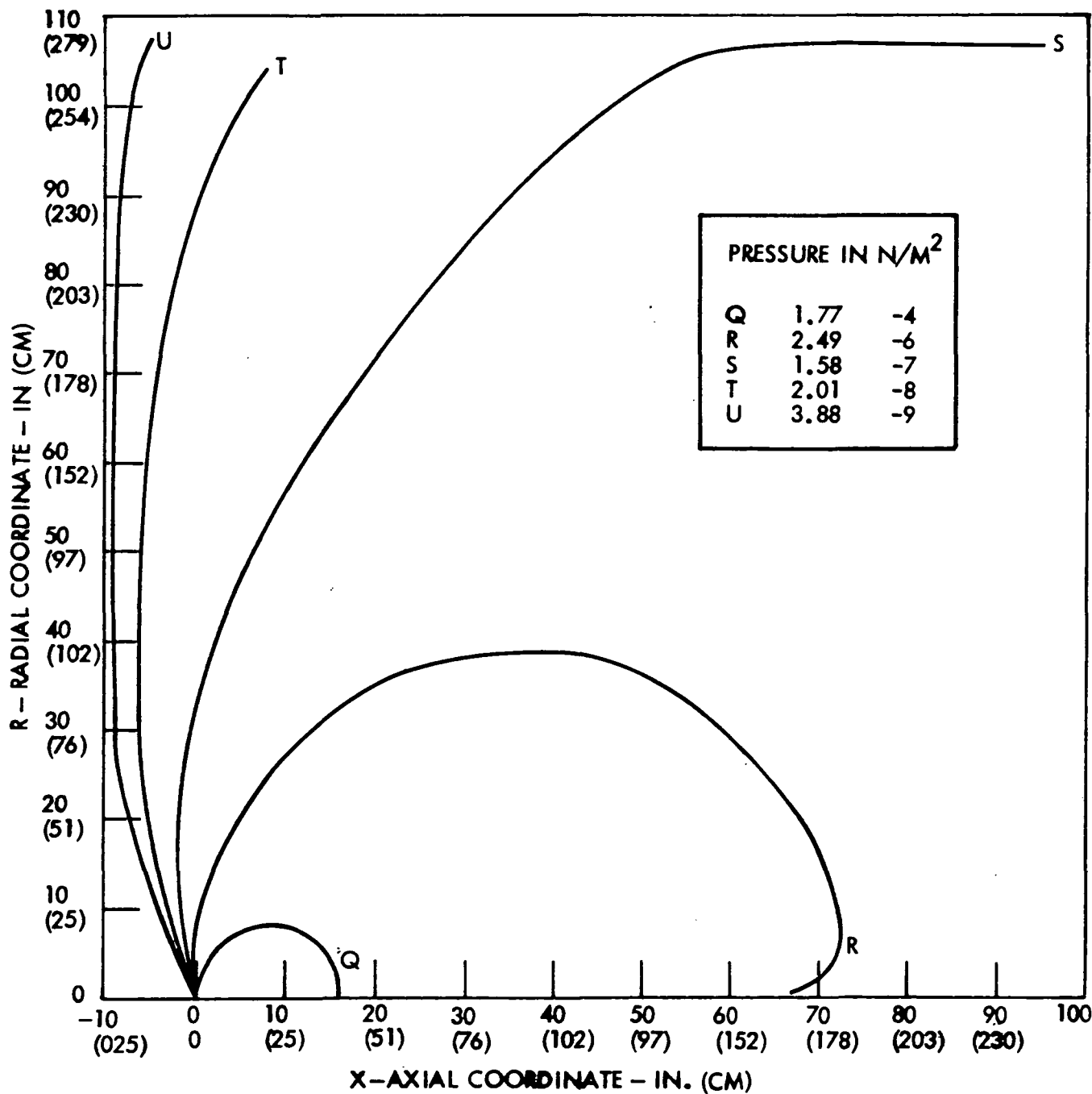


Figure 84 Contaminant Venting - Constant Pressure Contours

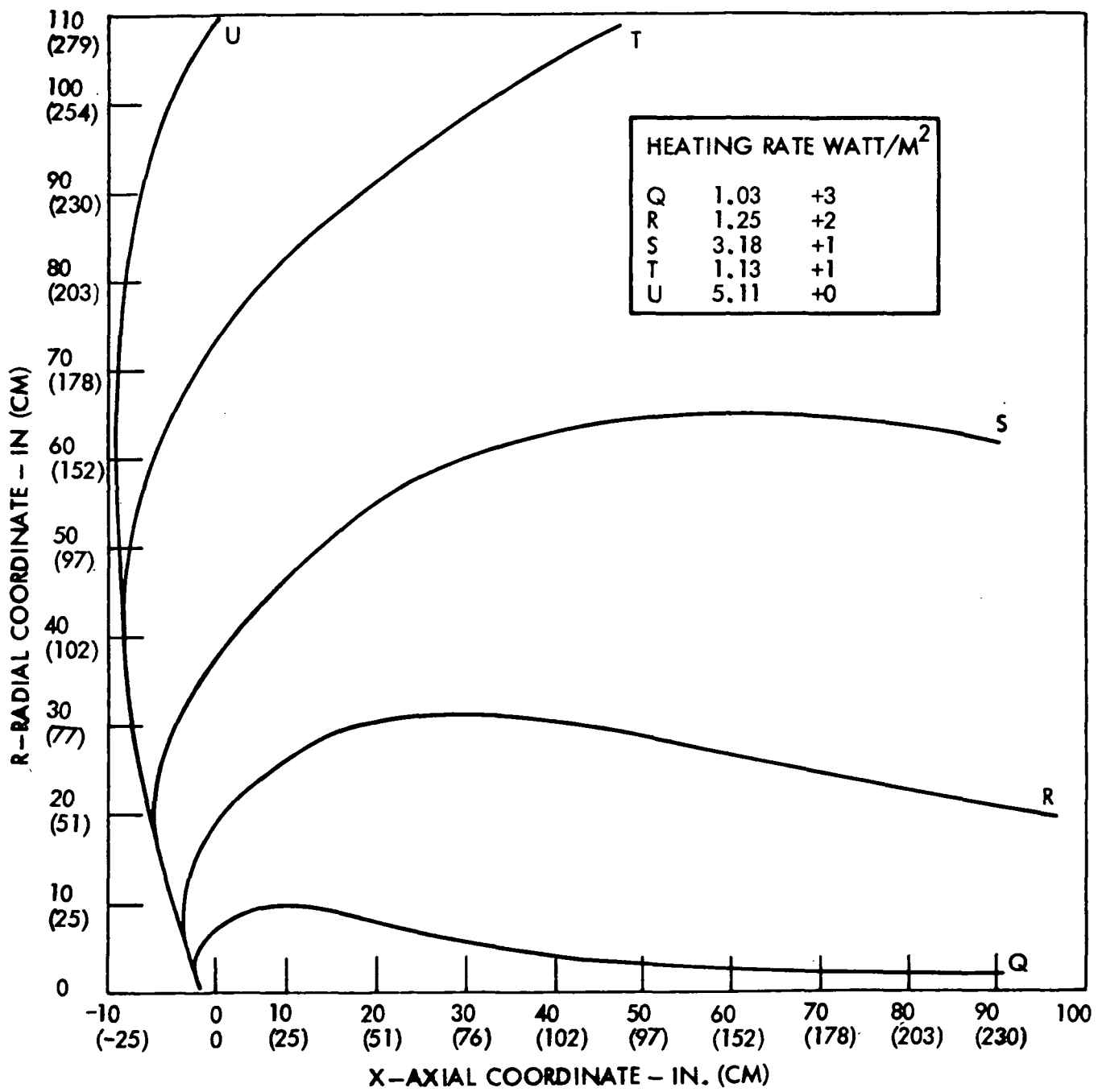


Figure 85 Contaminant Venting - Constant Heating Contours

10.2.3 Contaminant Evaporation Rate

If it is assumed that the accommodation coefficient for the contaminants is unity, the deposition rate of condensate cited above would be equivalent to about $2.6 \text{ A/cm}^2\text{-sec}$, or for the total charcoal bed desorption time, a film thickness of about 1000 A/cm^2 (ignoring evaporation). This type of film would have negligible effect on conventional spacecraft thermal control materials. Ignoring evaporation is a most unrealistic assumption.

It is more realistic to consider the evaporation rate of each contaminant as a measure of residual deposition. For free evaporation of a material into a vacuum environment, the Hertz-Langmuir-Knudson equation is applicable:

$$m = P \sqrt{\frac{MW}{2\pi RT}} = .0583P \sqrt{\frac{MW}{T}}$$

where m = Evaporation Rate, $\text{gm/cm}^2\text{-sec}$

P = Vapor Pressure, mmHg

MW = Molecular Weight

T = Temperature, K

R = Gas Constant

The evaporation rate calculated for each contaminant is presented in Table 62.

Table 62
Contaminant Evaporation Rate

Contaminant	Evaporation Rate - 300 K (80F)	Evaporation Rate 200 K (-100 F)
Toluene	$1.1 \text{ gm/cm}^2\text{-sec}$	2.7×10^{-3}
Benzene	2.7	
Methanol	2.7	
Methyl Ethyl Ketone	3.0	
Acetone	6.1	
Methyl Acetate	7.2	7.6×10^{-3}
Freon 11	33	
Freon 12	129	4

At 300 K (80 F), the evaporation rate of each constituent is many orders of magnitude larger than the deposition rate. Since the regeneration takes place over a three hour period, some of the venting may take place when the spacecraft is in eclipse, and the surface temperature may drop to near 200 K (-100 F). In this case evaporation is reduced due to the lower vapor pressure at lower temperature. Figure 86 shows the vapor pressure-temperature relationships for the eight contaminants. Toluene has the lowest vapor pressure of the contaminants, and the calculated evaporation rate for this compound is 2.7×10^{-3} gm/cm²-sec, which is still many orders of magnitude larger than any conceivable condensation rate. On the basis of this analysis, it is inconceivable that the venting process would have even a transient effect on vehicle surfaces. It is also highly unlikely that the effects of particulate or electromagnetic radiation would be relevant. It is far more likely that residual monolayers of contaminant chemisorbed on the surface would be desorbed rather than polymerized, considering the photochemical properties of these eight compounds. It is obvious that by using reasonable care in location of the vent, there would be no difficulty presented even for sensitive surfaces such as optics or instrumentation.

10.2.4 Other Vented Materials

Thus far the analysis has concerned the specific compounds vented from the regenerable charcoal bed that are unusual in that there has been no prior spacecraft experience. Water is also vented when the charcoal bed is regenerated. The water absorption isotherm of Figure 5 indicates venting of about 0.1 gm of water per gram of charcoal, or about 600 gm of water over the daily three hour regeneration period. This is small compared to the venting rate of the waste water dump system which handles urine, food and wash water, and cabin condensate at about 3.3 kg/day (6 man crew) or in comparison to the flash evaporator used to supplement the radiator heat rejection loop. Water vent rates for the flash evaporator are 8 to 40 kg/hr depending on whether the evaporator is operating as an on-orbit "top-off" unit or rejecting the ascent and decent phases heat load.

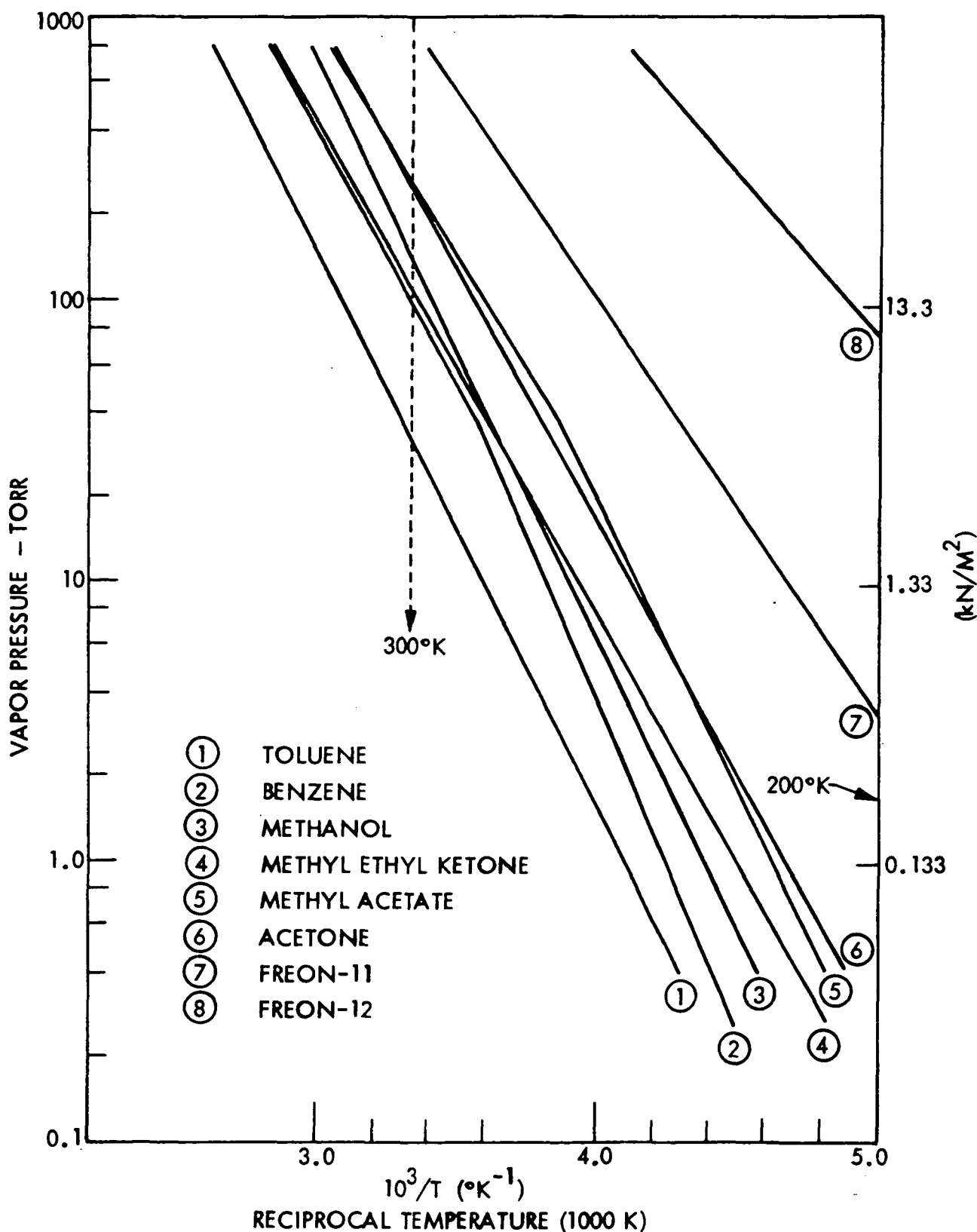


Figure 87 Vapor Pressures

There is a potential problem in fine dust from the charcoal bed. Use of a micron size filter retains any such dusts inside the regenerable bed canister. The other measure to avoid this problem is to slowly bleed the charcoal bed to a vacuum upon initiating regeneration. This is done using the vacuum bleed valve over a 30-minute period. Testing showed that these measures were effective in avoiding charcoal dusts.

Section 11
SPACE CONTAMINANT CONTROL SYSTEM CONCEPTUAL DESIGN

A preliminary analysis was made to determine the conceptual design of a contaminant control system for Spacelab. The design is based upon a modification of the contaminant load model generated for the space station prototype. A computer analysis was carried out to define the required flow rates and bed sizes. In addition, a preliminary design layout and weight and power estimate was generated. This information is presented in Table 63 and Figure 87.

11.1 Contaminant Load Model

A review was made of available data from which a contaminant load model for Spacelab could be constructed. This review revealed that insufficient information existed from which a reasonable assessment of a new contaminant load model could be estimated. The results of the ESRO phase A studies included no quantitative and very little qualitative data on contaminants. The ESRO Spacelab System Requirements Documents contain no data on trace contaminants. Attempts were made to determine whether sufficient data existed to better define the contaminant load model from a single Spacelab such as the life sciences laboratory. Preliminary data were available as to the types of equipment that might be in such a facility, however insufficient data existed as to what the off-gassing rates from this equipment might be. The Spacelab design philosophy calls for the use of commercial equipment. A contaminant off-gassing test was conducted by Beckman for four pieces of typical commercial scientific equipment. From these results it would be impossible to develop a complete load model however the conclusion can be drawn that commercial equipment appears to have higher off-gassing rates of problem contaminants than flight qualified equipment which has severe material controls. It was therefore decided to use the SSP contaminant load model for this conceptual design; however, the ratio of equipment to metabolic contaminant load was varied.

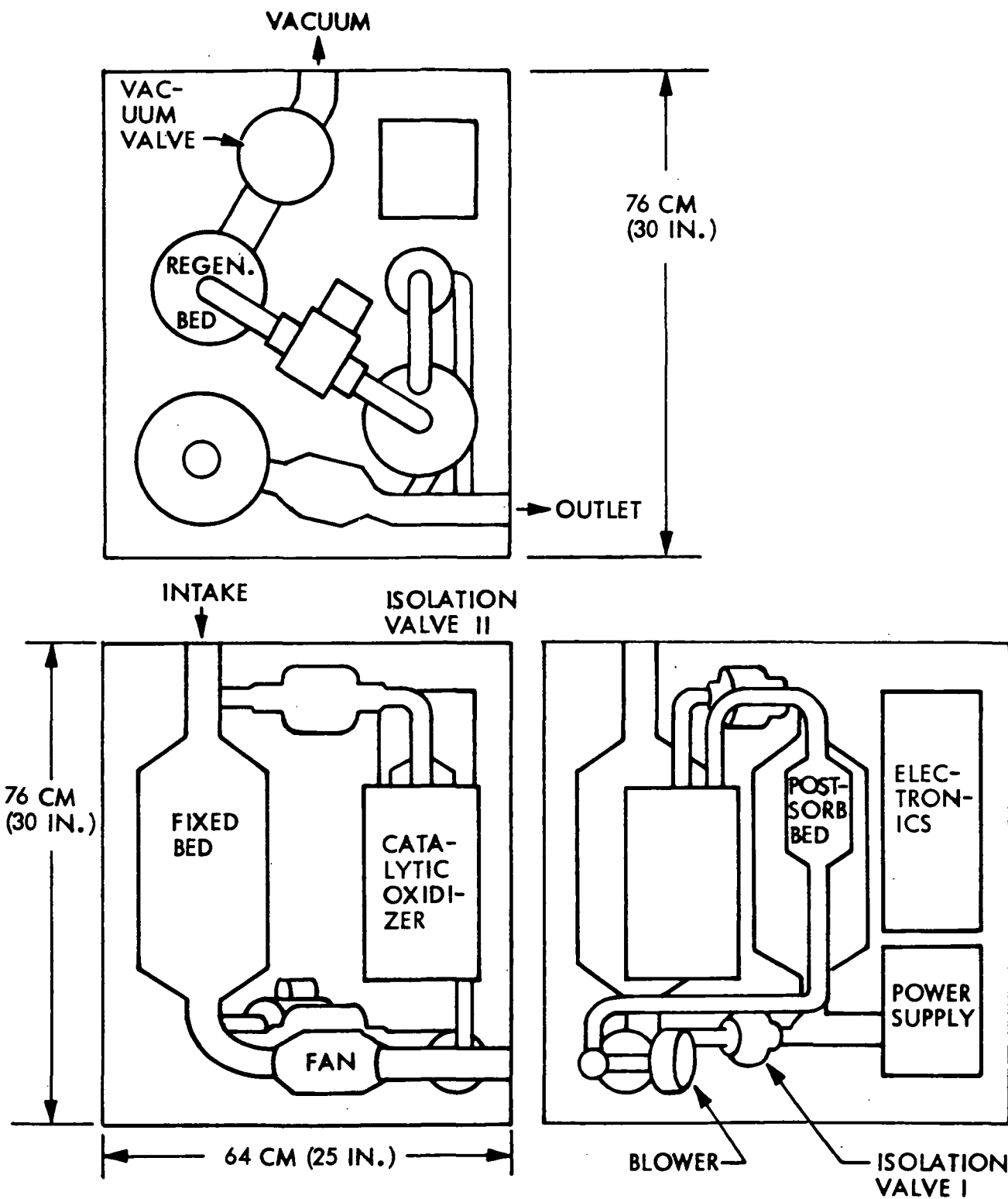


Figure 87 Spacelab Trace Contaminant Control System Layout

TABLE 63
Space Contaminant Control System/Summary Data

Item	SSP TCCS	0.5 Metabolic 0.1 Equip	0.5 Metabolic 0.2 Equip	0.5 Metabolic 0.2 Equip	0.5 Metabolic 0.5 Equip
Weight kg (lb)	109 (239)	66.3 (146)	70.8 (156)	77.2 (170)	
Envelope cm ³ (in)	76x86x86 30x34x34	64x76x76 25x30x30	64x76x76 25x30x30	94x76x76 37x30x30	
Power (watts)	435/315	125/175	170/188	315/255	
Fixed Bed Flow l/min (CFM)	1130 (40)	565 (20)	565 (20)	565 (30)	
Charcoal/Fixed Bed kg (1b)	21.8 (48)	4.5 (10)	4.5 (10)	4.5 (10)	
Oxidizer/Regenerable Bed Flow l/min (CFM)	142 (5)	28 (1)	48 (1.7)	113 (4)	
Charcoal/Regenerable Bed kg (1b)	6.4 (14)	1.1 (2.5)	1.8 (4)	4.5 (10)	
Power Summary:	(1) 55	(2) 55	(1) 30	(2) 30	(1) 30
Fixed Bed Fan					
Regenerable Bed Fan	0	90	0	30	30
Regenerable Bed Heater	360	0	75	0	0
Catalytic Oxidizer	0	150	0	100	265
Controls	20	20	20	20	0
					130
					0
					20

(1) desorption mode

(2) adsorption mode

A series of contaminant models was developed starting with the space station prototype model (SSP). The SSP model is based on a 6 man crew and a vehicle weight of about 90,800 kg (200,000 lb). The Spacelab has a crew of 3 men and a weight of about 9080 kb (20,000 lb). The contaminant models developed for the Spacelab analysis uses 0.5 of the SSP metabolic load and 0.1, 0.2, or 0.5 of the equipment load. The selection of the equipment load to be used depends upon the equipment design philosophy. If comparable design philosophies exist, an equipment load of one-tenth the level used in the SSP model seems reasonable as the Spacelab mass is one-tenth of the SSP mass. SSP data was based on specially designed equipment with careful selection and control of materials. The Spacelab will use modified commercial equipment in many cases. Thus, an equipment load of a higher level seems in order. For the purposes of this study equipment contaminant loads of 0.1, 0.2, and 0.5 times the SSP values were considered.

11.2 Design Analysis

In the design analysis of the trace contaminant control system a shortened contaminant list was used. This list includes both equipment and metabolically generated contaminants which were selected on the basis of providing the maximum stress in the system components. A computer analysis was run on the Spacelab system to define component sizes. The resultant control flow rates, component sizes, and power requirements are shown in Table 63.

In the operation of the system, incoming air first passes through the fixed charcoal bed. A portion of this air then passes through the regenerable bed, catalytic oxidizer and post sorbent bed. During this time the catalytic oxidizer is maintained at temperature by an electric heater. Once every 24 hours, the regenerable bed is heated and desorbed to space. At this time the low flow loop fan and catalytic oxidizer heater is shut down and the regenerable bed heater is activated. The power numbers in Table 63 reflect these two operating modes.

Section 12
CONCLUSIONS

The program for the design, fabrication and test of a trace contaminant control system resulted in the successful demonstration of a six man sized system, which included an isotope heated catalytic oxidizer and regenerable charcoal bed. The design verification test indicated that the system design was capable of controlling a contaminant load that might be anticipated to occur in a space station.

The hardware, which was designed for the SSP (Space Station Prototype) demonstrated high reliability. Four equipment malfunctions occurred in 460 days of testing. Two of these were relay failures which probably could have been avoided through the use of spacecraft qualified electronics. One was the failure of the regenerative charcoal bed fan blower bearing, which probably could have been avoided by the use of a bearing designed for higher reliability. An electric heater lead wire failed due evidently to assembly and disassembly of the heat source, and to the design of the electric heater which simulated the radioisotope heater.

The most significant conclusion resulting from the testing was the verification of the system design methodology. Also design information was developed in this program which allows new designs to be generated for widely differing requirements as well as for predicting the performance of existing designs.

During the course of the program additional specific conclusions were reached relative to contaminant control technology. A summary of these conclusions are presented below:

- o Pyruvic acid should be deleted from the contaminant load model since testing has indicated that it can not be present in the vapor phase at its maximum allowable concentration.
- o Potential plot data used for the design of a charcoal bed should be obtained from the specific charcoal to be used since considerable variability in charcoal characteristics has been observed between batches.
- o Catalyst performance data should also be obtained on the specific catalyst to be used since variability between lots of catalysts has also been observed.
- o Impregnating charcoal with phosphoric acid has been demonstrated to be an effective technique for control of ammonia.
- o Analyses have shown that overboard venting of contaminants from the desorption of a regenerable bed should cause no problem with contamination of spacecraft surfaces.
- o Testing has shown that regenerable bed performance does not degrade with continued regenerations.
- o The primary function of the regenerable bed is to act as a presorber for the catalytic oxidizer.
- o A lithium hydroxide presorber is not required since moisture in the fixed bed removes acid gases.
- o A system that does not provide a regenerable bed will allow potential catalyst poisons and producers of undesirable products to enter the catalytic oxidizer.
- o Testing has shown that operation of the catalytic oxidizer at higher temperatures (e.g. 1100° F) successfully prevents poisoning.
- o Allowing halogen, nitrogen or sulfur containing compounds to enter the catalytic oxidizer will cause them to be converted to undesirable products.
- o An effective post sorbent can be provided with a composite bed consisting of lithium hydroxide and Purafil.

References

1. R. M. Dora, et. al., "Monitoring the Bioeffluents of Man," Aerospace Medical Association Preprints, 36th Annual Meeting, April 1965, New York.
2. T. M. Olcott, et. al., "Development of a Sorber Trace Contaminant Control System," Lockheed Missiles and Space Company, Sunnyvale, Ca. NASA CR-2027, April 1972.
3. Monsanto Research Corporation, "Plutonium-239 Radioisotope Heat Sources," MLM-1757, 1966.
4. National Council on Radiation Protection, Biological Effects of Neutron Radiation, NCRP Report 38, 1966.
5. R. G. Rose "Radiation Constraints for Skylab, Shuttle and Space Station," 1/15/75 letter, NASA - Manned Spacecraft Center.
6. J. P. Mieure, M. W. Dietrick, J. Chromographic Science, 11, 559, 1973.

7. Bay Area Air Pollution Control District, Standard Methods, Method F-1, Formaldehyde in Air, November 20, 1970.
8. R. J. Prozan, Development of a method-of-characteristics solution for supersonic flow of an ideal, frozen, or equilibrium reactions gas mixture, IMSC/HREC A782535-A, April 1966.
9. I. M. Klotz, "The Absorption Wave", Chapter 8, Summary Technical Report, Division 10, National Defense Research Council, 1946.